THESE

Pour obtenir le grade de

DOCTEUR de l'Université de Strasbourg

Spécialité : **CHIMIE**

présentée par

Shaofeng LIU

Synthèse de complexes des métaux de transition et leurs applications en oligomérisation et polymérisation de l'éthylène

Synthesis of Transition Metal Complexes and Their Application for Ethylene Oligomerization and Polymerization

---

Soutenu le 2 juillet 2011 devant la commission d'examen

Pierre BRAUNSTEIN	Directeur de recherche CNRS à l'Université de Strasbourg, Membre de l'Académie des Sciences *Co-Directeur de Thèse*
Wen-Hua SUN	Professeur à l'Institut de Chimie, Académie des Sciences de Chine, Pékin (Chine) *Co-Directeur de Thèse*
Heinz BERKE	Professeur à l'Université de Zurich (Suisse) *Rapporteur*
Rainer GLASER	Professeur à l'Université du Missouri, Columbia (Etats-Unis) *Rapporteur*
Philippe MEUNIER	Professeur à l'Université de Bourgogne à Dijon *Examinateur*
Richard WELTER	Professeur à l'Université de Strasbourg *Examinateur*

Remerciements

Ce travail a été effectué dans le cadre d'une thèse en cotutelle au Laboratoire de Chimie de Coordination de l'Institut de Chimie (UMR 7177 du CNRS) de l'Université de Strasbourg, et à l'Institut de Chimie, Académie des Sciences de Chine, Pékin.

Je tiens tout d'abord à remercier mes directeurs de thèse le Dr. Pierre Braunstein, Directeur de Recherche au CNRS et membre de l'Académie des Sciences en France, et Dr. Wen-Hua Sun, professeur à l'Institut de Chimie, Académie des Sciences de Chine à Pékin, pour m'avoir accueilli au sein de leurs laboratoires et encadré ce travail, et l'Ambassade de France en Chine pour sa confiance et son soutien financier.

Mes remerciements vont aussi à tous ceux qui ont contribué à ce travail: Dr. Wenjuan Zhang, Dr. Weiwei Zuo, Dr. Suyun Jie, Dr. Shu Zhang, et, à Strasbourg, Dr. Riccardo Peloso et Dr. Roberto Pattacini.

Je tiens aussi à remercier les Drs. Roberto Pattacini et Lydia Brelot pour la détermination des structures cristallographiques, et Marc Mermillon-Fournier pour son aide avec les problèmes techniques.

Un grand merci aux membres du Laboratoire de Chimie de Coordination: Jacky, Soumia, Marc, Roberto, Riccardo, Weiwei, Lucie, Pierre, Mélanie, Thomas, Victor, Shuanming, Xianghao, Sabrina, Matthieu, Christophe, Paulin, Martin, Sophie. Merci aussi aux collogues à Pékin: Wenjuan Zhang, Xijie Liu, Suyun Jie, Qisong Shi, Junxian Hou, Weiwei Zuo, Shu Zhang, Katrin Wedeking, Peng Hao, Kefeng Wang, Rong Gao, Min Zhang, Yanjun Chen, Liwei Xiao, Shifang Yuan, Miao Shen, Tianpengfei Xiao, Wei Huang, Shengju Song, Liping Zhang, Jiangang Yu, Hao Liu, Yanning Zeng, Zhenghua Tang, Tianfu Liu, Xiaofei Kuang, et les autres.

Merci à mes amis, non chimistes, de Strasbourg et Pékin.

Enfin, j'adresse un merci à mes parents et ma soeur en Chine.

Table of Contents

COMPOSITION DU DOCUMENT ET ORGANISATION DE LA BIBLIOGRAPHIE

Ce document se divise en 9 chapitres qui contiennent une Introduction Générale, 7 chapitres décrivant les résultats scientifique originaux et une Conclusion Générale.

Par souci d'efficacité et de concision, le manuscrit est organisé sous forme de publications, parues ou soumises. Ainsi, les chapitres II–VIII sont rédigés en anglais mais chacun est précédé d'un résumé en français:

Le chapitre II a été publié dans le journal *J. Polym. Sci., Part A : Polym. Chem.*, **2008**, *46*, 3411-3423.
Il dispose en sa fin de sa propre bibliographie.

Le chapitre III a été publié dans le journal *J. Polym. Sci., Part A: Polym. Chem.*, **2009**, *47*, 3154-3169.
Il dispose en sa fin de sa propre bibliographie.

Le chapitre IV a été publié dans le journal *Organometallics*, **2010**, *29*, 732-741.
Il dispose en sa fin de sa propre bibliographie.

Le chapitre V a été publié dans le journal *Organometallics*, **2010**, *29*, 2459-2464.
Il dispose en sa fin de sa propre bibliographie.

Le chapitre VI a été publié dans le journal *Dalton Trans.*, **2010**, *39*, 2563-2572.
Il dispose en sa fin de sa propre bibliographie.

Le chapitre VII a été publié dans le journal *Dalton Trans.*, **2010**, *39*, 7881-7883.
Il dispose en sa fin de sa propre bibliographie.

Le chapitre VIII est sous presse à *Organometallics*, il dispose en sa fin de sa propre bibliographie.

En tête de chaque chapitre sont précisées les contributions de chacun des co-auteurs de la publication correspondante.

CHAPITRE I

General Introduction

Olefins, particularly ethylene, propylene and butenes, which are easily available, cheap and reactive, are the basic building block of the petrochemical industry.[1] Meanwhile, olefin-based polymers are by far the most important and thus the most produced synthetic polymers today.[2] Olefinic materials possess an amazingly broad range of practical applications due to their availability, cost effectiveness, low density, nontoxicity and bioacceptability. The broad-range of their material properties, such as mechanical, thermodynamic and crystalline characteristics, and outstanding resistance to weathering, oxygen, heat, ozone and chemicals are unique. Therefore, polyolefins are indispensable materials in modern life and they impact our daily lives in countless beneficial ways, including plastic shopping bags, food packages, squeeze bottles, containers, storage boxes, toys, gasoline tanks and car bumpers.[3]

The success of polyolefins is the close integration of the catalyst, progress and products. Among them, no doubt, the key driver of the entire process has been the development of new catalysts allowing process and product developments from a scientific point of view. The polymerization of ethylene was discovered in 1933 and has been in operation by the high pressure (up to 300 MPa) and high temperature (up to 300 °C) process since 1938.[4] The catalysts currently used industrially are still dominated with the multi-sited heterogeneous Ziegler-Natta catalysts based on $MgCl_2$-supported $TiCl_4$,[5] chromium-based Phillip catalysts[6] and the single-site group 4 metallocene catalysts[7] as well as constrained-geometry catalysts (CGC)[8]. The first key discovery was made by Ziegler,[5a,b] by combinaing $TiCl_4$ with alkylaluminum, which displayed high ethylene polymerization activity under mild reaction conditions as opposed to the high-pressure and high-temperature free-radical polymerization process. In conjunction with Natta's stereoregular propylene polymerization,[5c,d] the Ziegler-Natta catalysts led to the creation of high density polyethylene (HDPE) and isotactic polypropylene (*i*-PP). Unexpectedly, their market was disappointing and relegated to a small niche of commodity products in terms of volume, quality and versatility of the materials in the first 20 years. Until the late 1960s, $MgCl_2$ was used as a support for the $TiCl_4$-based catalyst systems.[5e] These $MgCl_2$-supported $TiCl_4$ catalysts exhibited activities two orders of magnitude greater than Ziegler's original catalysts, and led to continuous significant improvements in the performances of the activity, stereoselectivity, ability to control both the molecular characteristics and morphology of the resulting polymers, and they opened the way to the tremendous recent and still ongoing expansion.

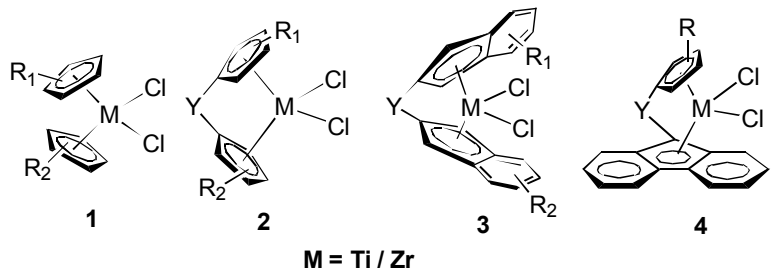

Scheme 1 Group 4 Metallocenes Catalysts

for references, see page 7

Group 4 metallocenes (**1-4**, Scheme 1) activated with alkylaluminum were first used as soluble models of Ziegler-Natta catalysts for a better understanding of the catalytic mechanism in the 1950s rather than as practical catalysts due to their poor activity.[9] In the early 1980s, Sinn and Kaminsky found that methylaluminoxane (MAO) could activate the metallocene Cp_2ZrCl_2 for olefin polymerization with a tremendous improvement in catalytic activity, rivaling $MgCl_2$-supported $TiCl_4$ catalysts.[10] Using these homogeneous and better-defined metallocenes, the products could be obtained with attractive properties, such as well defined structure, little branching and very narrow molar mass distribution.[7]

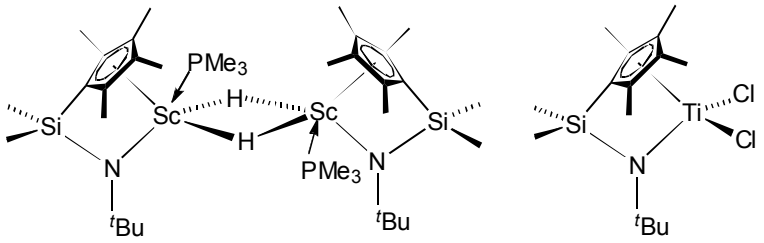

5 **6**

Scheme 2 Constrained Geometry Catalysts (CGC)

In the early 1990s, a new family of active polymerisation catalysts, namely constrained geometry catalysts (CGCs, **5** and **6**, Scheme 2), was developed by formally replacing one cyclopentadienyl ring by an amido moiety.[8] Compared to metallocenes, the CGCs exhibit superiority for the copolymerisation of ethylene and α-olefins, owing to a less crowded coordination sphere, a smaller $Cp_{centroid}$-M-N (Cp = cyclopentadienyl) bite angle and the decreased tendency of the bulk polymer chain to undergo chain transfer reactions, and thus allowing access to a wide array of polymers with unique material properties and considerable commercial value.

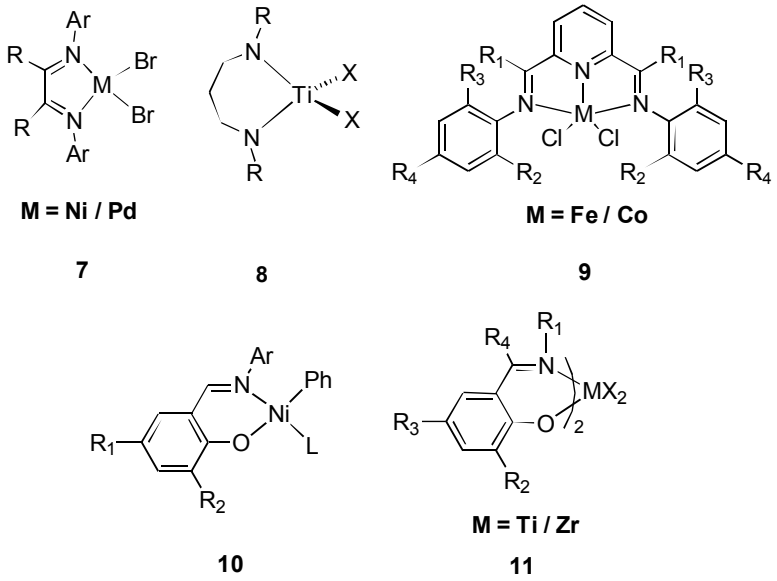

M = Ni / Pd **M = Fe / Co** **M = Ti / Zr**

7 **8** **9** **10** **11**

Scheme 3 Transition Metal Complexes Catalysts

for references, see page 7

Stimulated by related developments in other fields of catalysis, homogeneous organometallic compounds were introduced as suitable model systems for ethylene polymerization.[11] During the first half of the 1990s, the development of new generations "post-metallocene" catalysts to harness the potential of other metals to polymerize ethylene and thus avoid the growing patent minefield in Group 4 cyclopentadienyl systems has raised considerable interest. The discovery of highly active (α-diimine) nickel and palladium catalysts (**7**, Scheme 3) for ethylene polymerization to either linear or highly branched polyethylene (PE), depending on the ligand backbone and reaction conditions, dramatically demonstrated these possibilities.[12] This discovery was viewed as the resurrection of late-transition-metal catalysts and accelerated the research on post-metallocene catalysts. In 1996, McConville reported that titanium complexes bearing diamide ligands (**8**, Scheme 3) displayed high catalytic properties towards higher α-olefin polymerizations.[13] In 1998, extremely active bis(imino)pyridyl iron and cobalt (**9**, Scheme 3) catalysts for the linear polymerization of ethylene were reported independently by Brookhart[14] and Gibson.[15] Subsequently, nickel[16] (**10**, Scheme 3) and group 4 transition metal complexes[17] (**11**, Scheme 3) with phenoxy-imine ligands were reported as high performance olefin polymerization catalysts. As a result of a tremendous amount of academic and industrial research, a diverse number of new and highly potent catalysts based on both early and late transition metals have now been discovered.[18] Through catalyst design, these transition metal complex catalysts have created numerous polymers with controlled molecular weight and molecular weight distribution, specific tacticity, better comonomer distribution and content. Moreover, these catalysts have enjoyed success in the production of high added-value polymers, such as linear low density polyethylenes (LLDPE), isotactic and syndiotactic polypropylenes (*i*-PPs and *s*-PPs), syndiotactic polystyrenes (*s*-PSs) and ethylene/1-butene amorphous copolymers.

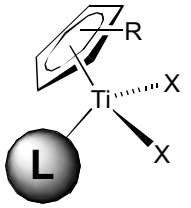

12

Scheme 4 Non-bridged Half-metallocene Catalysts

Attempts to combine the merits of the individual metallocenes and transition metal complex catalysts have led to the successful development of a series of non-bridged half-metallocene catalysts, Cp′M(**L**)X_n (M = Ti, Zr, Hf; **L** = anionic ligand; X = halogen or alkyl; **12**, Scheme 4),[19] which exhibited promising catalytic behavior and overcame the synthetic and patent problems associated with metallocenes[7] and/or CGC[8] catalysts.

As our work aimed at designing metal complexes as catalysts for ethylene reactivity,[20] numerous late-transition complexes[21] bearing heterocyclic multidentate ligands along with titanium complexes bearing bis(imino-indolide)[22] and 6-benzimidazolylpyridyl-2-carboximidate[23] were designed and used

for references, see page 7

for the synthesis of practical catalysts. As far as these two kinds of titanium complexes are concerned, the former showed good ability for copolymerization of ethylene with norbronene or ester, while the latter exhibited extremely high activity for ethylene homopolymerization. As an extension, titanium complexes ligated by 6-benzimidazolylpyridyl-2-carboximidate,[24] *N*-((benzimidazol-2-yl)quinolin-8-yl) benzamide,[25] 2-benzimidazolyl-*N*-phenylquinoline-8-carboxamide[26] and *N*-(2-methyl quinolin-8-yl)benzamide[27] have been synthesized and their catalytic behavior in olefin polymerization was studied in detail.

The synthesis and coordination chemistry of heterotopic ligands bearing phosphorus and nitrogen donor atoms represents an increasingly active field of research owing to the properties that such ligands confer to their metal complexes in stoichiometric or catalytic reactions.[28] The significantly different electronic and hard-soft properties of the donor functions largely influence their metal coordination behaviour and account for the observation of monodentate *P*- or *N*-coordination and static or dynamic (hemilabile) *P,N*-chelation.[28c] In the course of studies on *P,N*-ligands in which the P donor function is of the phosphine, phosphonite or phosphinite-type and the N donor belongs to a pyridine or an oxazoline heterocycle, it was observed that some of their mononuclear complexes of Ru(II),[29] Ni(II),[28f,30] Co(II)[31] and Pd(II)[32] or Fe-Cu[33] and Fe-Co[34] bimetallic complexes led to active pre-catalysts for a number of reactions. As an extension to *N,P,N*-tridentate ligands containing oxazoline heterocycles, the bonding behaviour of the bis(oxazoline)phenylphosphine and bis(oxazoline)phenylphosphonite ligands was compared.[30a,35] As far as bis(oxazoline)phosphine ligands are concerned, only *P,N*- or *N,P,N*-coordination modes have been observed in Pd(II) complexes. We wished to extend these studies to *N,P,N*-ligands where N represents a pyridine donor and compare its coordination properties with those of bis(oxazoline)phenylphosphine, in particular towards Pd(II) complexes. For this purpose, the ligand selected was bis(2-picolyl)phenylphosphine ($N_{py}PN_{py}$), a flexible, symmetric and neutral *N,P,N*-ligand containing two pyridine arms and a phosphine-type P donor.[36] We will report the synthesis and the characterization of Pd(II) complexes bearing the neutral bis(2-picolyl)phenylphosphine ($N_{py}PN_{py}$) ligand, and their structures in the solid state and their hemilability in the solution have been analyzed by X-ray diffraction and NMR experiments, respectively.[37]

Furthermore, the oligomerization of ethylene leading to the production of linear α-olefins (C_4-C_{20}), which are today a source of comonomers (C_4-C_8), lubricants (C_{10}), surfactants (C_{12}-C_{20}), biodegradable detergents, new kinds of polymers and many other industrially useful chemicals, has become a topic of considerable interest in both academia and industry.[1,28f,38] In particular, more and more interest has been focused on the selective trimerization[39] or tetramerization[40] of ethylene by Cr-based catalysts, producing 1-hexene or 1-octene as comonomers for the production of linear low-density polyethylene (LLDPE). In contrast to the conventional Cossee-Arlman linear growth mechanism,[41] the mechanism of highly selective trimerization or tetramerization of ethylene is believed to involve a series of metallacycles, which was first proposed by Manyik et al.[42] in 1977 and expanded by Briggs[43]. Jolly

for references, see page 7

isolated well-characterized chromacyclopentane and chromacycloheptane complexes and confirmed that the latter readily liberated 1-hexene.[44] Conclusive experimental evidences with deuterated ethylene provided by Bercaw are consistent with the metallacyclic mechanism, in which no H/D scrambling occurs in contrast to conventional oligomerization involving an insertion/β-elimination mechanism.[45] More recently, deuterium labeling studies conducted by Gibson[46] and McGuinness[47] further supported this mechanism for nonselective oligomerization and polymerization. However, Müller and Rosenthal have suggested an alternative mechanistic concept of binuclear metallacycles for ethylene tetramerization.[48] Despite these intensive studies, there remains considerable debate on the initiation step of the catalytic cycle, the chromium oxidation state in the active species, the chain growth, transfer and termination mechanisms, as well as the relationship of these factors with the catalytic activity and selectivity. It is, therefore, not surprising that much attention has been paid on isolating active intermediates of the catalytic cycle. For this purpose, the chemistry of chromium with aluminium activators (e.g., MAO, AlR_3, Et_2AlCl, $EtAlCl_2$ and $AlMe_2Cl$) has been investigated and a series of chromium alkyl and bimetallic Cr-Al complexes have been reported.[49] To gain a better insight into the catalytic properties and coordination chemistry of such Cr(III) complexes, we have recently embarked on a project aimed at isolating compounds formed by reaction between $[Cr(N_{py}PN_{py})Cl_3]$ and Al-based activators and study their performances as ethylene oligomerization catalysts or pre-catalysts.

for references, see page 7

References

1. Skupińska, J. *Chem. Rev.* **1991**, *91*, 613-648.
2. Galli, P.; Vecellio, G. *J. Polym. Sci., Part A: Polym. Chem.* **2004**, *42*, 396-415.
3. (a) Lieberman, R. B. Olefin Polymers-Polypropylene. In *Kirk-Othmer Encyclopedia of Chemical Technology*, 4th ed.; Kroschwitz, J. I., Howe-Grant, M. ed.; Wiley-Interscience: New York, **1996**; Vol. 17, p 784; (b) Kissen, Y. V. Olefin Polymers-Polyethylene. In *Kirk-Othmer Encyclopedia of Chemical Technology*, 4th ed.; Kroschwitz, J. I., Howe-Grant, M. ed.; Wiley-Interscience: New York, **1996**; Vol. 17, p 702; (c) Deutsch, C. H., Finding Flexibility in Plastics-High Technology Could Add New Life to an Old Product. *NY Times* **1997**, Sept 9, D1.
4. (a) Fawcett, E. W.; Gibson, R. U.; Perrin, M. W.; Paton, J. G.; Williams (ICI), E. G. GB 471590, **1936**; (b) Polyethylenes 1933-1983: Past, Present, Future. The Plastics and Rubber Institute, London, **1983**.
5. (a) Ziegler, K.; Holzkamp, E.; Breil, H.; Martin, H. *Angew. Chem.* **1955**, *67*, 541-547; (b) Ziegler, K.; Gellert, H. G. *Angew. Chem.* **1955**, *67*, 424-425; (c) Natta, G.; Pino, P.; Corradini, P.; Danusso, F.; Mantica, E.; Mazzanti, G.; Moraglio, G. *J. Am. Chem. Soc.* **1955**, *77*, 1708-1710; (d) Natta, G. *J. Polym. Sci.* **1955**, *16*, 143-154; (e) Kashiwa, N.; Tokumizu, T.; Fujimura, H. Mitsui Petrochemicals, Ind., US Patent 3642746, **1967**.
6. (a) Hogan, J. P.; Banks, R. L. Phillips Petroleum Co.; Belg. Pat. 530617, 1955; U.S. Pat. 2825721, 1958; (b) Hogan, J. P. *J. Polym. Sci.* **1970**, *8*, 2637-2652; (c) Karol, F. J.; Karapinka, G. L.; Wu, C.; Dow , A. W.; Johnson, R. N.; Garrick, W. L. *J. Polym. Sci.* **1972**, *10*, 2621-2637; (d) Groppo, E.; Lamberti, C.; Bordiga, S.; Spoto, G.; Zecchina, A. *Chem. Rev.* **2005**, *105*, 115-183.
7. (a) Jordan, R. F. *Adv. Organomet. Chem.* **1991**, *32*, 325-387; (b) Brintzinger, H. H.; Fischer, D.; Mülhaupt, R.; Rieger, B.; Waymouth, R. M. *Angew. Chem. Int. Ed. Engl.* **1995**, *34*, 1143-1170; (c) Kaminsky, W. *J. Chem. Sci., Dalton Trans.* **1998**, 1413-1418; (d) Alt, H. G.; Köppl, A. *Chem. Rev.* **2000**, *100*, 1205-1221.
8. (a) McKnight, A. L.; Waymouth, R. M. *Chem. Rev.* **1998**, *98*, 2587-2598; (b) Braunschweig, H.; Breitling, F. M. *Coord. Chem. Rev.* **2006**, *250*, 2691-2720.
9. Long, W. P.; Breslow, D. S. *J. Am. Chem. Soc.* **1960**, *82*, 1953-1957.
10. Sinn, H.; Kaminsky, W.; Vollmer, H. J.; Woldt, R. *Angew. Chem. Int. Ed. Engl.* **1980**, *19*, 390-392.
11. Cornils, B.; Hermann, W. A. Applied Homogeneous Catalysis with Organometallic Compounds; VCH: New York, **1996**.
12. Johnson, L. K.; Killian, C. M.; Brookhart, M. *J. Am. Chem. Soc.* **1995**, *117*, 6414-6415.
13. (a) Scollard, J. D.; McConville, D. H.; Payne, N. C.; Vittal, J. J. *Macromolecules* **1996**, *29*, 5241-5243; (b) Scollard, J. D.; McConville, D. H. *J. Am. Chem. Soc.* **1996**, *118*, 10008-10009.
14. Small, B. L.; Brookhart, M.; Bennett, A. M. A. *J. Am. Chem. Soc.* **1998**, *120*, 4049-4050.
15. Britovsek, G. J. P.; Gibson, V. C.; Kimberley, B. S.; Maddox, P. J.; McTavish, S. J.; Solan, G. A.; White, A. J. P.; Williams, D. J. *Chem. Commun.* **1998**, 849-850.
16. (a) Wang, C.; Friedrich, S.; Younkin, T. R.; Li, R. T.; Grubbs, R. H.; Bansleben, D. A.; Day, M. W. *Organometallics* **1998**, *17*, 3149-3151; (b) Younkin, T. R.; Conner, E. F.; Henderson, J. I.; Friedrich, S. K.; Grubbs, R. H.; Bansleben, D. A. *Science* **2000**, *287*, 460-462.
17. (a) Matsui, S.; Tohi, Y.; Mitani, M.; Saito, J.; Makio, H.; Tanaka, H.; Nitabaru, M.; Nakano, T.; Fujita, T. *Chem. Lett.* **1999**, 1065-1066; (b) Tian, J.; Coates, G. W. *Angew. Chem. Int. Ed.* **2000**, *39*, 3626-3629; (c) Makio, H.; Kashiwa, N.; Fujita, T. *Adv. Synth. Catal.* **2002**, *344*, 477-493.
18. (a) Britovsek, G. J. P.; Gibson, V. C.; Wass, D. F. *Angew. Chem. Int. Ed.* **1999**, *38*, 428-447; (b) Ittel, S. D.; Johnson, L. K.; Brookhart, M. *Chem. Rev.* **2000**, *100*, 1169-1203; (c) Gibson, V. C.; Spitzmesser, S. K. *Chem. Rev.* **2003**, *103*, 283-315; (d) Gibson, V. C.; Redshaw, C.; Solan, G. A. *Chem. Rev.* **2007**, *107*, 1745-1776; (e) Matsugi, T.; Fujita, T. *Chem. Soc. Rev.* **2008**, *37*, 1264-1277.
19. Nomura, K.; Liu, J.; Padmanabhan, S.; Kitiyanan, B. *J. Mol. Catal. A: Chem.* **2007**, *267*, 1-29.
20. (a) Sun, W.-H.; Zhang, D.; Zhang, S.; Jie, S.; Hou, J. *Kinet. Catal.* **2006**, *47*, 278-283; (b) Sun, W.-H.; Zhang, S.; Zuo, W. *C. R. Chim.* **2008**, *11*, 307-316.
21. (a) Sun, W.-H.; Jie, S.; Zhang, S.; Zhang, W.; Song, Y.; Ma, H. *Organometallics* **2006**, *25*, 666-677; (b) Sun, W.-H.; Wang, K.; Wedeking, K.; Zhang, D.; Zhang, S.; Cai, J.; Li, Y. *Organometallics* **2007**, *26*, 4781-4790; (c) Sun, W.-H.; Hao, P.; Zhang, S.; Shi, Q.; Zuo, W.; Tang, X.; Lu, X. *Organometallics* **2007**, *26*, 2720-2734; (d) Hao, P.; Zhang, S.; Sun, W.-H.; Shi, Q.; Adewuyi, S.; Lu, X.; Li, P. *Organometallics* **2007**, *26*, 2439-2446; (e) Shen, M.; Hao, P.; Sun, W.-H. *J. Organomet. Chem.* **2008**, *693*, 1683-1695; (f) Gao, R.; Zhang, M.; Liang, T.; Wang, F.; Sun, W.-H. *Organometallics* **2008**, *27*, 5641-5648; (g) Xiao, L.; Gao, R.; Zhang, M.; Li, Y.; Cao, X.; Sun, W.-H. *Organometallics* **2009**, *28*, 2225-2233.
22. (a) Zuo, W.; Sun, W.-H.; Zhang, S.; Hao, P.; Shiga, A. *J. Polym. Sci., Part A: Polym. Chem.* **2007**, *45*, 3415-3430; (b) Zuo, W.; Zhang, M.; Sun, W.-H. *J. Polym. Sci., Part A: Polym. Chem.* **2009**, *47*, 357-372.
23. Zuo, W.; Zhang, S.; Liu, S.; Liu, X.; Sun, W.-H. *J. Polym. Sci., Part A: Polym. Chem.* **2008**, *46*, 3396-3410.
24. Liu, S.; Zuo, W.; Zhang, S.; Hao, P.; Wang, D.; Sun, W.-H. *J. Polym. Sci., Part A: Polym. Chem.* **2008**, *46*, 3411-3423.

for references, see page 7

25. Liu, S.; Yi, J.; Zuo, W.; Wang, K.; Wang, D.; Sun, W.-H. *J. Polym. Sci., Part A: Polym. Chem*. **2009**, *47*, 3154-3169.
26. Sun, W.-H.; Liu, S.; Zhang, W.; Zeng, Y.; Wang, D.; Liang, T. *Organometallics* **2010**, *29*, 732-741.
27. Liu, S.; Sun, W.-H.; Zeng, Y.; Wang, D.; Zhang, W.; Li, Y. *Organometallics* **2010**, *29*, 2459-2464.
28. (a) Helmchen, G.; Pfaltz, A. *Acc. Chem. Res.* **2000**, *33*, 336-345; (b) Braunstein, P.; Graiff, C.; Naud, F.; Pfaltz, A.; Tiripicchio, A. *Inorg. Chem*. **2000**, *39*, 4468-4475; (c) Braunstein, P.; Naud, F. *Angew. Chem. Int. Ed.* **2001**, *40*, 680-699; (d) Rechavi, D.; Lemaire, M. *Chem. Rev.* **2002**, *102*, 3467-3493; (e) McManus, H. A.; Guiry, P. J. *Chem. Rev.* **2004**, *104*, 4151-4202; (f) Speiser, F.; Braunstein, P.; Saussine, W. *Acc. Chem. Res.* **2005**, *38*, 784-793; (g) Hou, J.; Sun, W.-H.; Zhang, S.; Ma, H.; Deng, Y.; Lu, X. *Organometallics* **2006**, *25*, 236-244; (h) Desimoni, G.; Faita, G.; Jørgensen, K. A. *Chem. Rev.* **2006**, *106*, 3561-3651; (i) Maggini, S. *Coord. Chem. Rev.* **2009**, *253*, 1793-1832.
29. Braunstein, P.; Fryzuk, M. D.; Naud, F.; Rettig, S. J. *J. Chem. Sci., Dalton Trans*. **1999**, 589-594.
30. (a) Kermagoret, A.; Tomicki, F.; Braunstein, P. *Dalton Trans.* **2008**, 2945-2955; (b) Kermagoret, A.; Braunstein, P. *Organometallics* **2008**, *27*, 88-99.
31. Jie, S.; Agostinho, M.; Kermagoret, A.; Cazin, C. S. J.; Braunstein, P. *Dalton Trans.* **2007**, 4472-4482.
32. (a) Braunstein, P.; Fryzuk, M. D.; Le Dall, M.; Naud, F.; Rettig, S. J.; Speiser, F. *J. Chem. Sci., Dalton Trans.* **2000**, 1067-1074; (b) Agostinho, M.; Braunstein, P.; Welter, R. *Dalton Trans*. **2007**, 759-770.
33. Braunstein, P.; Clerc, G.; Morise, X. *New J. Chem*. **2003**, *27*, 68-72.
34. Braunstein, P.; Clerc, G.; Morise, X.; Welter, R.; Mantovani, G. *Dalton Trans.* **2003**, 1601-1605.
35. Kermagoret, A.; Braunstein, P. *Dalton Trans.* **2008**, 585-587.
36. (a) Lindner, E.; Rauleder, H.; Hiller, W. *Z. Naturforsch., B: Anorg. Chem., Org. Chem*. **1983**, *38B*, 417-425; (b) Hung-Low, F.; Renz, A.; Klausmeyer, K. K. *Eur. J. Inorg. Chem.* **2009**, 2994-3002.
37. Liu, S.; Peloso, R.; Braunstein, P. *Dalton Trans*. **2010**, *39*, 2563-2572.
38. (a) Lappin, G. R.; Sauer, J. D. Alphaolefins Applications Handbook; Marcel Decker Inc.: Berkeley, CA, **1989**; (b) Vogt, D. Oligomerisation of Ethylene to Higher Linear α-Olefins, in *Applied Homogeneous Catalysis with Organometallic Compounds*; Cornils, B., Hermann, W. A. ed.; VCH: New York, **1996**; Vol. 1, pp 245-258.
39. (a) Dixon, J. T.; Green, M. J.; Hess, F. M.; Morgan, D. H. *J. Organomet. Chem*. **2004**, *689*, 3641-3668; (b) Wass, D. F. *Dalton Trans.* **2007**, 816-819.
40. Bollmann, A.; Blann, K.; Dixon, J. T.; Hess, F. M.; Killian, E.; Maumela, H.; McGuinness, D. S.; Morgan, D. H.; Neveling, A.; Otto, S.; Overett, M.; Slawin, A. M. Z.; Wasserscheid, P.; Kuhlmann, S. *J. Am. Chem. Soc*. **2004**, *126*, 14712-14713.
41. (a) Cossee, P. J. *J. Catal.* **1964**, *3*, 80-88; (b) Arlamn, E. J.; Cossee, P. J. *J. Catal.* **1964**, *3*, 99-104.
42. Manyik, R. M.; Walker, W. E.; Wilson, T. P. *J. Catal.* **1977**, *47*, 197-209.
43. Briggs, J. R. *J. Chem. Soc., Chem. Commun.* **1989**, 674-675.
44. Emrich, R.; Heinemann, O.; Jolly, P. W.; Krüger, C.; Verhovnik, G. P. J. *Organometallics* **1997**, *16*, 1511-1513.
45. (a) Agapie, T.; Schofer, S. J.; Labinger, J. A.; Bercaw, J. E. *J. Am. Chem. Soc.* **2004**, *126*, 1304-1305; (b) Agapie, T.; Labinger, J. A.; Bercaw, J. E. *J. Am. Chem. Soc.* **2007**, *129*, 14281-14295.
46. Tomov, A. K.; Chirinos, J. J.; Jones, D. J.; Long, R. J.; Gibson, V. C. *J. Am. Chem. Soc.* **2005**, *127*, 10166-10167.
47. McGuinness, D. S.; Suttil, J. A.; Gardiner, M. G.; Davies, N. W. *Organometallics* **2008**, *27*, 4238-4247.
48. Peitz, S.; Aluri, B. R.; Peulecke, N.; Müller, B. H.; Wöhl, A.; Müller, W.; Al-Hazmi, M. H.; Mosa, F. M.; Rosenthal, U. *Chem. Eur. J.* **2010**, *16*, 7670-7676.
49. (a) Gibson, V. C.; Newton, C.; Redshaw, C.; Solan, G. A.; White, A. J. P.; Williams, D. J. *J. Chem. Soc., Dalton Trans*. **2002**, 4017-4023; (b) Vidyaratne, I.; Scott, J.; Gambarotta, S.; Duchateau, R. *Organometallics* **2007**, *26*, 3201-3211; (c) Temple, C.; Jabri, A.; Crewdson, P.; Gambarotta, S.; Korobkov, I.; Duchateau, R. *Angew. Chem. Int. Ed.* **2006**, *45*, 7050-7053; (d) Jabri, A.; Temple, C.; Crewdson, P.; Gambarotta, S.; Korobkov, I.; Duchateau, R. *J. Am. Chem. Soc.* **2006**, *128*, 9238-9247; (e) Jabri, A.; Mason, C. B.; Sim, Y.; Gambarotta, S.; Burchell, T. J.; Duchateau, R. *Angew. Chem. Int. Ed.* **2008**, *47*, 9717-9721; (f) Zhang, J.; Li, A.; Hor, T. S. A. *Organometallics* **2009**, *28*, 2935-2937; (g) Vidyaratne, I.; Nikiforov, G. B.; Gorelsky, S. I.; Gambarotta, S.; Duchateau, R.; Korobkov, I. *Angew. Chem. Int. Ed.* **2009**, *48*, 6552-6556.

for references, see page 7

CHAPITRE II

Bis(2-(6-methylpyridin-2-yl)-benzimidazolyl)titanium dichloride and Titanium Bis(6-benzimidazolylpyridine-2-carboxylimidate): Synthesis, Characterization and Their Catalytic Behaviors for Ethylene Polymerization

SHAOFENG LIU,[†] WEIWEI ZUO,[†] SHU ZHANG,[†] PENG HAO,[†] DELIGEER WANG,[†,‡] WEN-HUA SUN[*,†]

[†]*Key Laboratory of Engineering Plastics and Beijing National Laboratory for Molecular Sciences, Institute of Chemistry, Chinese Academy of Sciences, Beijing 100080, China*
[‡]*Department of Chemistry, Inner Mongolia Normal University, Hohhot 010022, China*

This Chapter has been published in *J. Polym. Sci., Part A : Polym. Chem.*, **2008**, *46*, 3411-3423.

Contributions from the various co-authors: Dr. WEIWEI ZUO was involved in the synthesis and catalysis assistance, Dr. SHU ZHANG performed the X-ray structure analyses, Dr. PENG HAO assisted in the synthesis, professors DELIGEER WANG and WEN-HUA SUN supervised the work and are responsible for giving directions and providing discussions. I am most grateful to all of them.

Résumé du Chapitre II

Une série de ligands du type 6-(benzimidazol-2-yl)-*N*-organylpyridine-2-carboxamide a été synthétisée et transformée en ligands tridentes dianioniques du type 6-benzimidazolylpyridine-2-carboxylimidate. Les compexes bis(2-(6-methylpyridin-2-yl)-benzimidazolyl)titane dichlorure (**C1**) and bis(6-benzimidazolylpyridine-2-carboxylimidate) de titane (**C2**-**C8**) ont été obtenues avec des rendements acceptables. Ces complexes furent caractérisés par analyse élémentaire et RMN. Les études cristallographiques par diffraction des rayons X ont révélé dans les cas de **C1** et **C4** une géométrie de coordination octaédrique déformée autour du titane. En utilisant le MAO (méthylalumoxane) comme cocatalyseur, tous les complexes ont montré une activité catalytique de bonne à élevée pour la polymérisation de l'éthylène. Le complexe neutre bis(6-benzimidazolylpyridine-2-carboxylimidate)titane (**C2**-**C8**) a montré une forte activité catalytique et une bonne stabilité pour une durée de réaction prolongée à température élevée. Par contre, **C1** a une durée de vie plus courte et une très faible activité catalytique est notée après 5 min. Un accroissement de la température de réaction augmente la productivité en polyéthylènes de faibles poids moléculaires alors qu'une augmentation de la pression d'éthylène conduit à une meilleure activité catalytique et à une productivité plus élevée en polyéthylènes de hauts poids moléculaires. Lorsque le rapport MAO /

titane est augmenté, une plus grande activité catalytique est observée et des polyéthylènes de faibles poids moléculaires sont formés.

2.1 Abstract of Chapter II

A series of 6-(benzimidazol-2-yl)-*N*-organylpyridine-2-carboxamide were synthesized and transformed into 6-benzimidazolylpyridine-2-carboxylimidate as dianionic tridentate ligands. Bis(2-(6-methylpyridin-2-yl)-benzimidazolyl)titanium dichloride (**C1**) and titanium bis(6-benzimidazolylpyridine-2-carboxylimidate) (**C2-C8**) were synthesized in acceptable yields. These complexes were systematically characterized by elemental and NMR analyses. Crystallographic analysis revealed the distorted octahedral geometry around titanium in both complexes **C1** and **C4**. Using MAO as cocatalyst, all complexes exhibited from good to high catalytic activities for ethylene polymerization. The neutral bis(6-benzimidazolylpyridine-2-carboxylimidate)titanium (**C2-C8**) showed high catalytic activities and good stability for prolonged reaction time and elevated reaction temperature; however, **C1** showed a short lifetime in catalysis as being observed very low activity after 5 min. The elevated reaction temperature enhanced the productivity of polyethylenes with low molecular weights, while the reaction with higher ethylene pressure resulted in better catalytic activity and resultant polyethylenes with higher molecular weights. At higher ratio of MAO to titanium precursor, the catalytic system generated better activity with producing polyethylenes with lower molecular weights.

2.2 Introduction

Driven by billions-dollar polyolefins market and expecting the advanced properties of polyolefins to be finely controlled in molecular weights and distributions as well as co-monomer distributions in polymerization processes, much effort is focused on designing and synthesizing metal complexes as catalyst precursors for olefin polymerization. These metal complex catalysts could be divided into early- and late-transition metal complexes. The late-transition metal complex catalysts mostly involve iron, cobalt, nickel and palladium and have been well documented in recent review articles,[1] and some promising research has been scaled-up for industrial processes. However, the catalysts currently used in industrial processes are still dominated by early-transition metal catalysts, such as titanium in Ziegler-Natta catalyst,[2] zirconium in metallocene catalyst[3] and chromium in Phillips catalysts.[4] Indicated by metallocene catalyst as well-defined complex catalysts with the advantages in polyolefins, the complex catalysts could provide the anticipated species to tailor the microstructures of desired polyolefins with advanced properties. Synthetic problems blocked the general large-scale application of metallocene catalysts; fortunately the half-metallocene complexes as constrained geometry catalysts (CGC) were developed and commercialized by Dow chemicals.[5] Following the works of CGC catalysts, the half-titanocene catalysts are well developed and reviewed.[6]

for references, see page 26

Inspired by the fast-development of coordination and organometallic chemistry, numerous transition-metal complexes have been designed and investigated for olefin polymerization. For example, the group IVB complexes ligated by phenoxyimines (named as FI catalyst) were found with extremely high activity for ethylene polymerization by Fujita group in late 1990s,[7] while the phenoxyimino nickel complexes showed high activity for norbornene polymerization affording soluble polynorbornenes.[8] With these, it is not difficult to realize that some ligands could be shared in designing complex catalysts for both early- and late-transition metal for olefin polymerization. Another model of well-known group IVB complex catalysts (PI catalyst) highly active for living polymerization of ethylene and copolymerization of ethylene with norbornene, was also initially developed with pyrrolide-imino ligands by Mitsui Chemicals.[9] As our extensive research of nickel imino-indolide catalyst for ethylene oligomerization progress,[10] the titanium analogues showed high activity toward ethylene polymerization and copolymerization with norbornene.[11] Recently, there are some reports dealing with dianionic tridentate and trianionic ligands, and their group IVB complexes showed interesting catalytic behaviors.[12] Beyond the scope of olefin polymerization, the hemilability of multi-dentate ligands[13] became attractive because of their mixing bonding characteristics which enhanced the stability and reactivity of complexes with incoming substrates.[14] In both models of FI and PI catalysts, the group IVB metal core was coordinated with two ligands of anionic bidentate. Combining two bidentate models into one model gave us the idea to design dianionic tridentate ligands for group IVB complexes as catalysts for olefin polymerization. On the basis of our recent achievements in late-transition metal complexes bearing benzimidazolylpyridine ligands,[15] we designed and synthesized derivatives of 6-(benzimidazol-2-yl)-*N*-organylpyridine-2-carboxamide for the purpose as dianionic tridentate ligands in reaction with titanium tetrachloride and half-titanocene trichloride. Their half-titanocene complexes showed high catalytic activities for ethylene polymerization, and another paper will fully discuss their results.[16] The titanium complexes ligated with two ligands, bis(2-(6-methylpyridin-2-yl)-benzimidazolyl)titanium dichloride (**C1**) and titanium bis(6-benzimidazolylpyridine-2-carboxylimidate) (**C2**-**C8**), were synthesized and carefully characterized. Both kinds of titanium complexes showed high activities toward ethylene polymerization when activated by MAO, and **C2**-**C8** showed good thermal stability and a long lifetime in catalytic system. Herein, we describe the synthesis and characterization for the title titanium complexes as well as their catalytic behaviors of ethylene polymerization.

2.3 Experimental Section

2.3.1 General Considerations

All manipulations of air and/or moisture-sensitive compounds were performed under nitrogen atmosphere using standard Schlenk techniques. Methylaluminoxane (MAO, 1.46 M in toluene) was purchased from Albemarle and other reagents were purchased from Aldrich or Acros Chemicals. Sodium hydride (NaH), purchased from Beijing Regent Chemicals, was washed with hexane before

for references, see page 26

use to remove contained mineral oil. Tetrahydrofuran (THF), toluene and hexane were refluxed over sodium and benzophenone, distilled, and then stored under nitrogen atmosphere. Dichloromethane (CH_2Cl_2) was refluxed over calcium hydride, distilled, and then stored under nitrogen atmosphere. IR spectra were recorded on a Perkin Elmer FT-IR 2000 spectrometer using KBr disc in the range of 4000-400 cm^{-1}. Elemental analysis was performed on a Flash EA 1112 microanalyzer. ^1H NMR and ^{13}C NMR spectra were recorded on a Bruker DMX 300 MHz instrument at ambient temperature using TMS as an internal standard.

2.3.2 Synthesis of 6-benzimidazolylpyridine-2-carboxylimidic Derivatives

6-(1H-benzimidazol-2-yl)-N-(2,6-dimethylphenyl)pyridine-2-carboxamide

According to literature method,[17] methylmagnesium chloride (CH_3MgCl) THF solution (22 wt%, 1 mL, 3 mmol) was dropwise added to a 2,6-dimethylbenzenamine (0.435 g, 3.6 mmol) THF solution at 0 °C, and the mixture was further stirred for additional 15 min. At 0 °C, ethyl 6-(1*H*-benzimidazol-2-yl)pyridine-2-carboxylate (0.801 g, 3 mmol) in 5 mL THF was added over 30 min into the above solution. The mixture was further stirred for additional 30 min, and the solvent THF was removed under reduced pressure. Water (50 mL) was added to wash out sodium salt. The obtained residue was extracted with ethyl acetate (3 × 50 mL). The product, 6-(1*H*-benzimidazol-2-yl)-*N*-(2,6-dimethylphenyl)pyridine-2-carboxamide, was purified by column chromatography (silica gel, petroleum ether / ethyl acetate = 1:1) and obtained in 77% yield (0.792 g). ^1H NMR ($CDCl_3$, 300 MHz): δ 10.72 (s, N-H, 1H), 9.30 (s, N-H, 1H), 8.65 (d, *J* = 7.9 Hz, 1H), 8.35 (d, *J* = 7.6 Hz, 1H), 8.06 (t, *J* = 7.8 Hz, 1H), 7.87 (bs, 1H), 7.50 (bs, 1H), 7.32-7.35 (m, 2H), 7.14 (t, *J* = 6.3 Hz, 1H), 7.09 (d, *J* = 7.2 Hz, 2H), 2.22 (s, 6H). ^{13}C NMR ($CDCl_3$, 75 MHz): δ 162.8, 150.1, 150.0, 148.0, 140.5, 136.8, 130.5, 128.9, 128.1, 125.9, 124.9, 124.6, 123.7, 123.3, 120.7, 119.8, 112.8, 19.2. IR (KBr, cm^{-1}): 3324, 2967, 1655, 1596, 1515, 1453, 1317, 1278, 1223, 1153, 989, 769, 745, 649. Anal. Calcd. for $C_{21}H_{18}N_4O$: C, 73.67; H, 5.30; N, 16.36. Found: C, 73.40; H, 5.21; N, 16.73.

6-(1H-Benzimidazol-2-yl)-N-(2,6-diethylphenyl)pyridine-2-carboxamide

Using the above procedure, 2,6-diethylbenzenamine was used instead of 2,6-dimethyl benzenamine, 6-(1*H*-benzimidazol-2-yl)-*N*-(2,6-diethylphenyl)pyridine-2-carboxamide was obtained as white solid in 83% yield. ^1H NMR ($CDCl_3$, 300 MHz): δ 10.32 (s, N-H, 1H), 9.28 (s, N-H, 1H), 8.66 (d, *J* = 7.8 Hz, 1H), 8.38 (d, *J* = 7.6 Hz, 1H), 8.09 (t, *J* = 7.9 Hz, 1H), 7.88 (bs, 1H), 7.55 (bs, 1H), 7.30-7.36 (m, 2H), 7.29 (t, *J* = 7.4 Hz, 1H), 7.19 (d, *J* = 7.6 Hz, 2H), 2.67 (q, *J* = 7.6 Hz, 4H), 1.21 (t, *J* = 7.4 Hz, 6H). ^{13}C NMR ($CDCl_3$, 75 MHz): δ 162.6, 150. 6, 150.2, 148.3, 145.2, 142.1, 139.0, 135.2, 134.0, 128.2, 127.8, 124.0, 123.8, 123.0, 122.3, 120.5, 111.2, 25.8, 14.3. IR (KBr, cm^{-1}): 3294, 2967, 1657, 1596, 1514, 1459, 1317, 1277, 1228, 1146, 1074, 997, 925, 834, 745, 650. Anal. Calcd. for $C_{23}H_{22}N_4O$: C, 74.57; H, 5.99; N, 15.12. Found: C, 74.35; H, 5.87; N, 15.10.

6-(1H-Benzimidazol-2-yl)-N-(2,6-diisopropylphenyl)pyridine-2-carboxamide

Using the same procedure, 6-(1*H*-benzimidazol-2-yl)-*N*-(2,6-diisopropylphenyl)pyridine-2-

for references, see page 26

carboxamide was obtained as a white solid in 69% yield. ^{1}H NMR ($CDCl_3$, 300 MHz): δ 10.25 (s, N-H, 1H), 9.24 (s, N-H, 1H), 8.67 (d, *J* = 7.8 Hz, 1H), 8.40 (d, *J* = 7.7 Hz, 1H), 8.10 (t, *J* = 7.8 Hz, 1H), 7.89 (bs, 1H), 7.54 (bs, 1H), 7.33-7.37 (m, 3H), 7.27 (d, *J* = 7.8 Hz, 2H), 3.18 (sept, *J* = 6.8 Hz, 2H), 1.25 (d, *J* = 6.8 Hz, 12H). ^{13}C NMR ($CDCl_3$, 75 MHz): δ 163.3, 150.6, 150.2, 148.3, 145.2, 139.0, 135.1, 132. 8, 132.5, 128.2, 124.1, 123.8, 123.3, 123.1, 122.4, 120.5, 111.2, 29.2, 13.6. IR (KBr, cm^{-1}): 3348, 2963, 1684, 1595, 1503, 1453, 1378, 1317, 1275, 1136, 1051, 997, 926, 798, 746, 650. Anal. Calcd. for $C_{25}H_{26}N_4O$: C, 75.35; H, 6.58; N, 14.06. Found: C, 75.13; H, 6.48; N, 13.73.

6-(1H-Benzimidazol-2-yl)-N-(2,6-difluorophenyl)pyridine-2-carboxamide

Using the same procedure, 6-(1*H*-benzimidazol-2-yl)-*N*-(2,6-difluorophenyl)pyridine-2-carboxamide was obtained as a white solid in 84% yield. ^{1}H NMR ($CDCl_3$, 300 MHz): δ 11.21 (s, N-H, 1H), 9.79 (s, N-H, 1H), 8.55 (d, *J* = 6.5 Hz, 1H), 8.26 (t, *J* = 7.0 Hz, 1H), 8.20 (d, *J* = 6.5 Hz, 1H), 7.79 (d, *J* = 6.8 Hz, 1H), 7.66 (d, *J* = 7.2 Hz, 1H), 7.52 (m, 1H), 7.28-7.34 (m, 4H). ^{13}C NMR ($CDCl_3$, 75 MHz): δ 163.6, 150.9, 149.1, 148.2, 146.7, 140.8, 137.0, 132.3, 131.9, 125.1, 124.1, 123.9, 123.7, 123.3, 122.4, 120.5, 113.0. IR (KBr, cm^{-1}): 3258, 3053, 2967, 1680, 1597, 1522, 1452, 1369, 1319, 1242, 1014, 986, 779, 746, 687, 650. Anal. Calcd. for $C_{19}H_{12}F_2N_4O$: C, 65.14; H, 3.45; N, 15.99. Found: C, 64.67; H, 3.65; N, 15.70.

6-(1H-Benzimidazol-2-yl)-N-(2,6-dichlorophenyl)pyridine-2-carboxamide

Using the same procedure, 6-(1*H*-benzimidazol-2-yl)-*N*-(2,6-dichlorophenyl)pyridine-2-carboxamide was obtained as a white solid in 74% yield. ^{1}H NMR ($CDCl_3$, 300 MHz): δ 10.73 (s, N-H, 1H), 9.57 (s, N-H, 1H), 8.67 (d, *J* = 7.8 Hz, 1H), 8.37 (d, *J* = 7.7 Hz, 1H), 8.08 (t, *J* = 7.8 Hz, 1H), 7.88 (bs, 1H), 7.54 (bs, 1H), 7.42 (d, *J* = 8.0 Hz, 2H), 7.35 (m, 2H), 7.23 (t, *J* = 7.9 Hz, 1H). ^{13}C NMR ($CDCl_3$, 75 MHz): 163.2, 162.6, 149.8, 148.3, 146.8, 143.1, 138.9, 134.1, 132.1, 128.9, 128.1, 123.9, 123.6, 122.7, 122.4, 118.6, 112.5. IR (KBr, cm^{-1}): 3248, 3023, 2984, 1680, 1599, 1531, 1452, 1317, 1278, 1019, 957, 915, 799, 745, 687, 651. Anal. Calcd. for $C_{19}H_{12}Cl_2N_4O$: C, 59.55; H, 3.16; N, 14.62. Found: C, 59.43; H, 3.18; N, 14.50.

6-(1H-Benzimidazol-2-yl)-N-butylpyridine-2-carboxamide

According to our recent method,[18] ethyl-6-(1*H*-benzimidazol-2-yl)pyridine-2-carboxylate (0.801 g, 3 mmol) and 1-butylamine (0.219 g, 3 mmol) were mixed in 30 mL methanol, and stirred for 12 h. The product 6-(1*H*-Benzimidazol-2-yl)-*N*-buylpyridine-2-carboxamide was obtained in 92% yield (0.812 g). ^{1}H NMR ($CDCl_3$, 300 MHz): δ 11.16 (s, N-H, 1H), 8.58 (d, *J* = 7.9 Hz, 1H), 8.30 (d, *J* = 7.7 Hz, 1H), 8.21 (s, N-H, 1H), 8.00 (t, *J* = 7.7 Hz, 1H), 7.85 (bs, 1H), 7.47 (bs, 1H), 7.27-7.37 (m, 2H), 3.44 (m, 2H), 1.55 (m, 2H), 1.37 (m, 2H), 0.88 (t, *J* = 7.3 Hz, 3H). ^{13}C NMR ($CDCl_3$, 75 MHz): δ 165.6, 151.3, 150.6, 147.7, 139.8, 124.7, 124.2, 123.5, 116.3, 40.4, 32.6, 21.1, 14.1. IR (KBr, cm^{-1}): 3340, 2935, 2860, 1665, 1595, 1572, 1535, 1456, 1421, 1390, 1315, 1261, 1093, 804, 745, 650. Anal. Calcd. for $C_{17}H_{18}N_4O$: C, 69.37; H, 6.16; N, 19.03. Found: C, 69.13; H, 6.28; N, 19.13.

6-(1H-Benzimidazol-2-yl)-N-octylpyridine-2-carboxamide

Using the same procedure,[18] ethyl-6-(1*H*-benzimidazol-2-yl)pyridine-2-carboxylate (0.801 g, 3

for references, see page 26

mmol) was reacted with 1-octylamine (0.388 g, 3 mmol) in methanol to give 6-(1*H*-benzimidazol-2-yl)-*N*-octylpyridine-2-carboxamide as a white solid in 89% yield. ^{1}H NMR ($CDCl_3$, 300 MHz): δ 11.79(s, N-H, 1H), 8.59 (d, *J* = 7.8 Hz, 1H), 8.50 (s, N-H, 1H), 8.32 (d, *J* = 7.7 Hz, 1H), 7.98 (t, *J* = 7.8 Hz, 1H), 7.85 (d, *J* = 6.8 Hz, 1H), 7.36-7.26 (m, 3H), 3.33 (m, 2H), 1.42 (m, 2H), 1.25-1.12 (m, 10H), 0.81 (t, *J* = 6.7 Hz, 3H). ^{13}C NMR ($CDCl_3$, 75 MHz): δ 161.9, 147.8, 147.0, 144.2, 136.1, 120.8, 120.1, 37.3, 29.2, 27.1, 26.8, 26.6, 24.5, 20.0, 11.4. IR (KBr, cm^{-1}): 3285, 3016, 2928, 1660, 1596, 1575, 1535, 1446, 1421, 1378, 1320, 1244, 1093, 996, 821, 747, 649. Anal. Calcd. for $C_{21}H_{26}N_4O$: C, 71.97; H, 7.48; N, 15.99. Found: C, 72.13; H, 7.28; N, 16.03.

2.3.3 Synthesis of Complexes C1-C8

Bis(2-(6-methylpyridin-2-yl)-benzimidazolyl)titanium dichloride (C1)

To a 2-(6-methylpyridin-2-yl)-*1H*-benzimidazole[15c] (0.627 g, 3.00 mmol) 30 mL THF solution at -78 °C, NaH (0.072 g, 3.0 mmol) suspended in 10 mL THF was added. The mixture was allowed to warm up to room temperature and stirred for additional 2 h. The resultant solution was dried in vacuum to give a white powder, which was dissolved in freshly dried toluene (60 mL). At -78 °C, $TiCl_4$ (0.285 g, 1.5 mmol) solution in 20 mL toluene was dropwise added over 30 min. The resultant mixture was allowed to warm up to room temperature, and stirred for additional 12 h. The solvent was removed under vacuum, and the residue was extracted with dried CH_2Cl_2 (2 × 30 mL) and then filtered. The filtrate was concentrated to 15 mL, and bis(2-(6-methylpyridin-2-yl)-benzimidazolyl)titanium dichloride (**C1**) as a red solid and brown crystals (0.477 g, yield 59%) were obtained few days later by layering 30 mL hexane. ^{1}H NMR ($CDCl_3$, 300 MHz): δ 8.13 (t, *J* = 7.8 Hz, 2H), 8.05 (d, *J* = 7.8Hz, 2H), 7.91 (d, *J* = 7.8 Hz, 2H), 7.49 (d, *J* = 8.3 Hz, 2H), 6.95-7.08 (m, 4H), 6.25 (d, *J* = 7.8Hz, 2H), 2.70 (s, 6H). ^{13}C NMR ($CDCl_3$, 75 MHz): δ 151.5, 148.2, 148.0, 141.6, 138.2, 129.4, 125.5, 125.0, 122.2, 120.8, 120.0, 119.9, 16.8. Anal. Calc. for $C_{26}H_{20}Cl_2N_6Ti$: C, 58.34; H, 3.77; N, 15.70. Found: C, 58.13; H, 3.68; N, 15.63.

Titanium bis{6-(benzimidazol-2-yl)-N-(2,6-dimethylphenyl)pyridine-2-carboxamide} (C2)

To a 6-(1*H*-benzimidazol-2-yl)-*N*-(2,6-dimethylphenyl)pyridine-2-carboxamide (1.026 g, 3.00 mmol) THF solution (30 mL) at -78 °C, NaH (0.144 g, 6.0 mmol) was added. The mixture was allowed to warm up to room temperature, and stirred for additional 2 h. At -78 °C, 10 mL toluene solution of $TiCl_4$ (0.285 g, 1.5 mmol) was dropwise added over 30 min. The resultant mixture was allowed to warm up to room temperature, and stirred for additional 12 h. With the same workup procedure, titanium bis{6-(benzimidazol-2-yl)-*N*-(2,6-dimethylphenyl)pyridine-2-carboxamide} (**C2**) was obtained as dark red crystals (0.683 g, yield 63%). ^{1}H NMR ($CDCl_3$, 300 MHz): δ 8.43 (t, *J* = 7.9 Hz, 2H), 8.36 (d, *J* = 7.9 Hz, 2H), 8.32 (d, *J* = 7.9 Hz, 2H), 7.59 (d, *J* = 8.1 Hz, 2H), 7.18 (t, *J* = 7.5 Hz, 2H), 7.12 (d, *J* = 7.5 Hz, 4H), 6.85-6.93 (m, 4H), 6.16 (d, *J* = 8.1 Hz, 2H), 2.28 (s, 6H), 1.76 (s, 6H). ^{13}C NMR ($CDCl_3$, 75 MHz): δ 154.7, 152.5, 148.3, 143.3, 141.6, 139.0, 126.2, 125.4, 125.0, 124.6, 122.4, 120.8, 120.5, 119.1, 116.9, 110.7, 14.9. Anal. Calcd. for $C_{42}H_{32}N_8O_2Ti$: C, 69.23; H,

for references, see page 26

4.43; N, 15.38. Found: C, 69.13; H, 4.28; N, 15.03.

Titanium bis{6-(benzimidazol-2-yl)-N-(2,6-diethylphenyl)pyridine-2-carboxamide} (C3)

Using the same procedure as for the synthesis of **C2**, **C3** was obtained as a red solid in 73% yield. ^{1}H NMR ($CDCl_3$, 300 MHz): δ 8.45 (t, *J* = 7.6 Hz, 2H), 8.37 (d, *J* = 7.6 Hz, 2H), 8.32 (d, *J* = 7.6 Hz, 2H), 7.62 (d, *J* = 8.0 Hz, 2H), 7.31 (t, *J* = 7.7 Hz, 2H), 7.19 (d, *J* = 7.7 Hz, 4H), 6.90-7.01 (m, 4H), 6.15 (d, *J* = 8.0 Hz, 2H), 2.66 (q, *J* = 6.8 Hz, 4H), 2.07 (q, *J* = 6.8 Hz, 4H), 1.23 (t, *J* = 6.8 Hz, 6H), 0.71 (t, *J* = 6.8 Hz, 6H). ^{13}C NMR ($CDCl_3$, 300MHz): δ 156.0, 154.6, 152.3, 148.3, 143.3, 141.6, 140.3, 139.0, 138.9, 130.5, 122.6, 122.4, 121.0, 120.4, 119.1, 116.8, 110.7, 21.8, 10.5. Anal. Calcd. for $C_{46}H_{40}N_8O_2Ti$: C, 70.41; H, 5.14; N, 14.28. Found: C, 70.13; H, 5.28; N, 14.03.

Titanium bis{6-(benzimidazol-2-yl)-N-(2,6-diisopropylphenyl)pyridine-2-carboxamide} (C4)

Using the same procedure, **C4** was obtained as a red solid in 72% yield. ^{1}H NMR ($CDCl_3$, 300 MHz): δ 8.45 (t, *J* = 7.8 Hz, 2H), 8.35 (d, *J* = 7.8 Hz, 2H), 8.30 (d, *J* = 7.7 Hz, 2H), 7.61 (d, *J* = 8.0 Hz, 2H), 7.50 (t, *J* = 7.8 Hz, 2H), 6.91-6.97 (m, 8H), 6.10 (d, *J* = 8.0 Hz, 2H), 2.17 (m, 2H), 1.85 (m, 2H), 1.27 (d, *J* = 6.8 Hz, 12H), 0.88 (d, *J* = 6.8 Hz, 12H). ^{13}C NMR ($CDCl_3$, 75 MHz): δ 156.6, 154.2, 153.3, 149.7, 145.3, 143.3, 142.4, 140.5, 140.3, 137.1, 123.5, 122.3, 121.8, 121.3, 120.7, 118.4, 114.9, 112.9, 27.6, 22.1. Anal. Calcd. for $C_{50}H_{48}N_8O_2Ti$: C, 71.42; H, 5.75; N, 13.33. Found: C, 71.13; H, 5.56; N, 13.03.

Titanium bis{6-(benzimidazol-2-yl)-N-(2,6-difluorophenyl)pyridine-2-carboxamide} (C5)

Using the same procedure, **C5** was obtained as a dark red solid in 49% yield. ^{1}H NMR ($CDCl_3$, 300 MHz): δ 8.64 (t, *J* = 7.9 Hz, 2H), 8.56 (d, *J* = 7.9 Hz, 2H), 8.47 (d, *J* = 7.9 Hz, 2H), 7.85 (d, *J* = 8.0 Hz, 2H), 7.61 (t, *J* = 7.8 Hz, 2H), 6.89-7.25 (m, 8H), 6.38 (d, *J* = 8.0 Hz, 2H). ^{13}C NMR ($CDCl_3$, 75 MHz): δ 156.0, 155.0, 154.5, 152.5, 148.2, 146.5, 143.3, 141.5, 125.3, 124.9, 124.5, 122.4, 120.4, 119.0, 116.7, 111.9, 110.6. Anal. Calcd. for $C_{38}H_{20}F_4N_8O_2Ti$: C, 61.31; H, 2.71; N, 15.05. Found: C, 61.03; H, 2.56; N, 14.97.

Titanium bis{6-(benzimidazol-2-yl)-N-(2,6-dichlorophenyl)pyridine-2-carboxamide} (C6)

Using the same procedure, **C6** was obtained as a dark red solid in 52% yield. ^{1}H NMR ($CDCl_3$, 300 MHz): δ 8.42 (t, *J* = 7.7 Hz, 2H), 8.38 (d, *J* = 7.7 Hz, 2H), 8.31 (d, *J* = 7.7 Hz, 2H), 7.52 (d, *J* = 8.1 Hz, 2H), 7.25 (t, *J* = 7.8 Hz, 2H), 7.11 (d, *J* = 7.8 Hz, 4H), 6.88-6.95 (m, 4H), 6.19 (d, *J* = 8.0 Hz, 2H). ^{13}C NMR ($CDCl_3$, 75 MHz): δ 156.4, 150.4, 146.3, 145.2, 144.2, 142.1, 139.1, 134.7, 132.8, 127.8, 126.6, 125.5, 124.8, 123.6, 122.4, 119.6, 114.0. Anal. Calcd. for $C_{38}H_{20}Cl_4N_8O_2Ti$: C, 56.33; H, 2.49; N, 13.83. Found: C, 56.27; H, 2.45; N, 13.79.

Titanium bis{6-(benzimidazol-2-yl)-N-buylpyridine-2-carboxamide} (C7)

Using the same procedure, **C7** was obtained as a dark red solid in 71% yield. ^{1}H NMR ($CDCl_3$, 300 MHz): δ 8.43 (t, *J* = 7.8 Hz, 2H), 8.36 (d, *J* = 7.8 Hz, 2H), 8.30 (d, *J* = 7.9 Hz, 2H), 7.61 (d, *J* = 8.0 Hz, 2H), 6.91-7.07 (m, 4H), 6.21 (d, *J* = 7.8 Hz, 2H), 3.75 (t, *J* = 6.7 Hz, 4H), 1.6 (m, 4H), 1.3 (m, 4H), 0.9 (t, *J* = 6.6 Hz, 6H). ^{13}C NMR ($CDCl_3$, 75 MHz): δ 158.2, 150.4, 146.2, 137.7, 134.3, 132.0, 129.0, 127.1, 126.1, 125.5, 124.3, 122.9, 112.2, 28.5, 22.5, 19.8, 12.2. Anal. Calcd. for $C_{34}H_{32}N_8O_2Ti$:

for references, see page 26

C, 64.56; H, 5.10; N, 17.71. Found: C, 64.78; H, 5.41; N, 17.89.

Titanium bis{6-(benzimidazol-2-yl)-N-octylpyridine-2-carboxamide} (C8)

Using the same procedure, **C8** was obtained as a dark red solid in 59% yield. ^{1}H NMR ($CDCl_3$, 300 MHz): δ 8.49 (t, *J* = 7.9 Hz, 2H), 8.41 (d, *J* = 7.9 Hz, 2H), 8.29 (d, *J* = 7.8 Hz, 2H), 7.58 (d, *J* = 8.0 Hz, 2H), 6.85-6.94 (m, 4H), 6.19 (d, *J* = 7.8 Hz, 2H), 3.36 (t, *J* = 6.8 Hz, 4H), 1.86 (m, 4H), 1.04-1.26 (m, 20H), 0.75 (t, *J* = 6.6 Hz, 6H). ^{13}C NMR ($CDCl_3$, 75 MHz): δ 154.6, 152.3, 148.2, 143.2, 141.7, 140.3, 137.9, 130.5, 122.6, 120.9, 120.4, 119.1, 110.7, 31.3, 29.2, 27.1, 26.8, 26.6, 24.8, 21.8, 11.4. Anal. Calcd. for $C_{42}H_{48}N_8O_2Ti$: C, 67.73; H, 6.50; N, 15.05. Found: C, 67.78; H, 6.59; N, 14.99.

2.3.4 Procedures for Ethylene Polymerization

A 250-mL autoclave stainless steel reactor equipped with a mechanical stirrer and a temperature controller was heated in vacuum for at least 2 h over 80 °C, allowed to cool to the required reaction temperature under ethylene atmosphere, and then charged with toluene, the desired amount of co-catalyst and a toluene solution of the precursor. The total volume was 100 mL. After reaching the desired reaction temperature, the reactor was stirred and pressurized to 10 atm or 30 atm of ethylene pressure, and the ethylene pressure was kept with feeding of ethylene. After the reaction mixture was stirred for the desired period of time, the reaction was stopped without ethylene input. The pressure was released, and the polymerization reaction was quenched by addition of acidic ethanol. The precipitated polymer was washed with ethanol several times and dried in vacuum.

2.3.5 X-ray Structure Determinations

Single crystals of **C1** suitable for X-ray diffraction were obtained by re-crystallization of its toluene/benzene solution at -30 °C. Crystals of **C4** suitable for single-crystal X-ray analysis were obtained by slowly layering hexane on CH_2Cl_2 solutions of complex **C4**. Single-crystal X-ray diffraction for complex **C1** was carried out on a Rigaku R-AXIS Rapid IP diffractometer with graphite-monochromated Mo-Kα radiation (λ = 0.71073 Å) at 293(2) K, while intensity data of complex **C4** were collected on a Bruker Smart 1000 CCD diffractometer with graphite-monochromated Mo Kα radiation (λ = 0.71073 Å) at 293(2) K. Cell parameters were obtained by global refinement of the positions of all collected reflections. Intensities were corrected for Lorentz and polarization effects and empirical absorption. The structures were solved by direct methods and refined by full-matrix least-squares on *F*2. All non-hydrogen atoms were refined anisotropically. Structure solution and refinement were performed by using the SHELXL-97 package.[19] Crystal data collection and refinement details for **C1** and **C4** are given in Table 1. CCDC-658019 (**C1**) and -658020 (**C14**) contain the supplementary crystallographic data for this paper, which could be obtained free of charge from the Cambridge Crystallographic Data Centre via www.ccdc.cam.ac.uk/data_request/cif.

for references, see page 26

Table 1. Crystallographic Data and Refinement Details for **C1** and **C4**

	C1	**C4**
Formula	$C_{36}H_{31}Cl_2N_6Ti$	$C_{52}H_{52}Cl_4N_8O_2Ti$
Formula wt	666.47	1010.72
T (K)	293(2)	293(2)
wavelength (Å)	0.71073	0.71073
cryst syst	triclinic	monoclinic
space group	P-1	$P2_1/c$
a (Å)	11.275(2)	12.7966(9)
b (Å)	12.418(3)	20.7014(1)
c (Å)	14.040(3)	20.2989(1)
α (deg)	109.51(3)	90.00
β (deg)	99.43(3)	105.687(2)
γ (deg)	107.06(3)	90.00
V (Å^3)	1695.0(6)	5177.0(6)
Z	2	4
D_{calcd} (g cm^{-3})	1.306	1.297
μ (mm^{-1})	0.444	0.419
F (000)	690	2104
θ range (deg)	1.61-25.01	1.43-28.33
limiting indices	$0\leq h\leq 13$ $-14\leq k\leq 14$ $-16\leq l\leq 16$	$-15\leq h\leq 17$ $-27\leq k\leq 27$ $-27\leq l\leq 26$
no. of rflns collected	13734	41556
no. of unique rflns	7211	12877
Completeness to θ (%)	94.8 (θ = 25.01°)	99.8 (θ = 28.33°)
abs correction	empirical	empirical
no. of params	379	604
goodness of fit on F^2	1.046	0.991
final R indices ($I > 2\sigma(I)$)	R1 = 0.0734 wR2 = 0.2171	R1 = 0.0880 wR2= 0.2478
R indices (all data)	R1 = 0.0961 wR2 = 0.2383	R1 = 0.2111 wR2= 0.3183
Largest diff peak, hole (e Å^{-3})	1.164, -0.450	0.916, -0.788

2.4 Results and Discussion

2.4.1 Synthesis and Characterization of 6-(benzimidazol-2-yl)-*N*-organylpyridine-2-carboxamide Derivatives

Due to different reactivity of alkylamines and arylamines with ester compounds, the direct reactions of 1-butylamine or 1-octylamine with ethyl 6-(benzimidazol-2-yl) pyridine-2-carboxylate formed the 6-(benzimidazol-2-yl)-*N*-butylpyridine-2-carboxamide or 6-(benzimidazol-2-yl)-*N*-octylpyridine-2-carboxamide (Scheme 1). However, it is necessary to transform arylamine into anionic arylamino-magnesium chloride[17] in order for the compound to easily react with the ethyl pyridine-2-carboxylate to form various arylcarboxamide compounds, 6-(benzimidazol-2-yl)-*N*-arylpyridine-2-carboxamide derivatives (Scheme 1). These organic compounds were routinely characterized and confirmed with elemental, IR spectroscopic and NMR analyses.

for references, see page 26

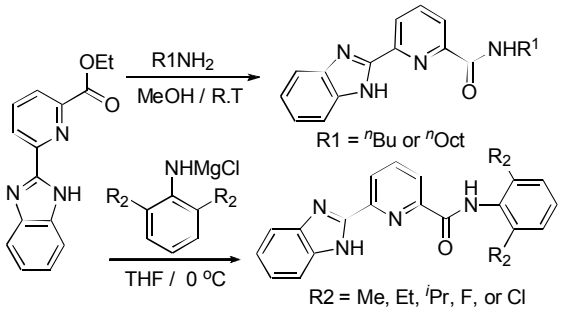

Scheme 1. Synthesis of the ligands

2.4.2 Synthesis and Characterization of Titanium Complexes

According to the synthetic procedure of bis(imino-indolide)titanium dichloride,[11] the complex **C1** was synthesized (Scheme 2). 2-(6-Methylpyridin-2-yl)-benzimidazole was first deprotonated using sodium hydride in tetrahydrofuran solution, then the solution was treated with 0.5 eq of titanium tetrachloride in toluene at -78 °C. The resultant mixture was stirred for additional 12 h at room temperature. The solvents were removed under vacuum, and the product residents were extracted with CH_2Cl_2 and filtered. Its CH_2Cl_2 solution was concentrated and layered with hexane to give a red solid in yield of 59.4%, bis(2-(6-methylpyridin-2-yl)-benzimidazolyl)titanium dichloride (**C1**). Considering 6-(benzimidazol-2-yl)-*N*-organylpyridine-2-carboxamide, the carboxamides should be transformed into their 2-carboxylimidic forms by employing the pretreatment with one equivalent of NaH.[20] Due to incorporation of the benzimidazole, the current 6-(benzimidazol-2-yl)-*N*-organylpyridine-2-carboxamides would consume two equivalents of NaH to form dianionic sodium intermediates in THF at -78 °C. To the solution at -78 °C, 0.5 eq. of $TiCl_4$ in toluene was added dropwise, and the resultant mixture was slowly warmed up to room temperature followed by stirring for additional 12 h. Similar workup procedure was used to get the pure complexes, titanium bis(6-benzimidazolylpyridine-2-carboxylimidate) **C2-C8** (Scheme 2). All the complexes were carefully characterized and confirmed with elemental and NMR analyses. In addition, complexes **C1** and **C4** were further characterized by single-crystal X-ray diffraction.

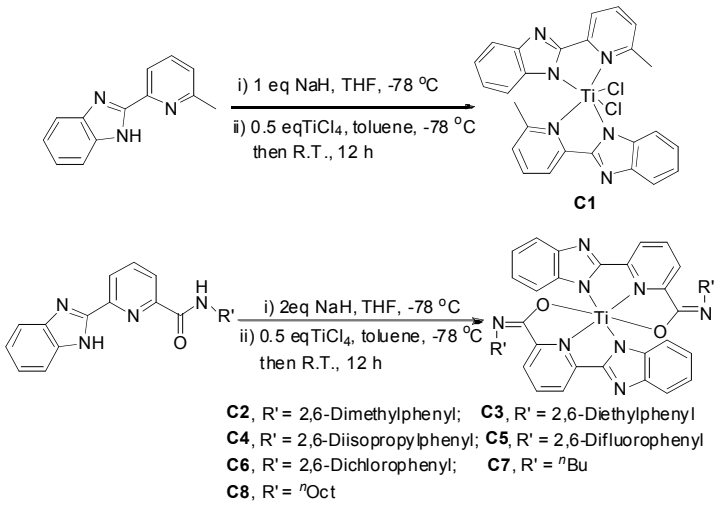

Scheme 2. Synthesis of Complexes **C1-C8**

for references, see page 26

Crystals of **C1** suitable for single-crystal X-ray analysis were obtained by re-crystallization of **C1** in its toluene/benzene solution at -30 °C. The molecular structure of **C1** was shown in Figure 1, and its selected bond lengths and angles were collected in Table 2. In the solid state, the toluene and benzene molecules were incorporated; however, there were no direct interactions with the metal center. Complex **C1** containing two ligands and two chlorides around the titanium centre, adopted a distorted octahedral geometry. Two chelating ligands afforded four N atoms to coordinate to the Ti (IV) center, with two benzimidazole-N atoms *trans* oriented (N2-Ti-N5 = 159.22(2)°; Ti-N2 = 2.017(3) Å; Ti-N5 = 2.027(3) Å) and two pyridine-N atoms *cis*-located with N1-Ti1-N4 = 77.59(1)° along with Ti-N1 = 2.299(3) Å and Ti-N4 = 2.298(3) Å. The two chloride ligands are located in *cis*-positions with an approximate angle (Cl1-Ti-Cl2 = 98.74(6)°) and nearly identical bond lengths (Ti-Cl1 = 2.235(1) Å; Ti-Cl2 = 2.243(1) Å). The Ti-N and Ti-Cl bonds were similar to those observed in PI catalytic model.[9] The dihedral angle defined by the two chelating rings (Ti-N2-C7-C6-N1; Ti-N5-C20-C19-N4) was 63.0°, and the dihedral angle between the benzimidazole-ring and the pyridine-ring was 15.9°, respectively.

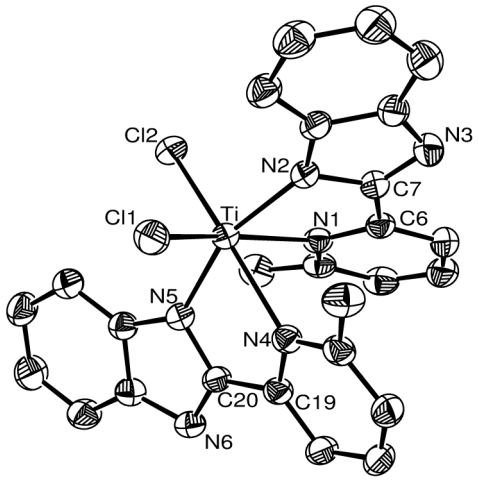

Figure 1. Molecular structure of complex **C1**. Thermal ellipsoids are shown at 30% probability. Hydrogen atoms and solvent molecules have been omitted for clarity.

Table 2. Selected bond lengths (Å) and angles (°) for Complex **C1**

Bond lengths (Å)			
Ti-N1	2.299(3)	Ti-N2	2.017(3)
Ti-N4	2.298(3)	Ti-N5	2.027(3)
Ti-Cl1	2.235(1)	Ti-Cl2	2.243(1)
Bond angles (°)			
N1-Ti-N2	74.96(1)	N4-Ti-N5	74.83(1)
Cl1-Ti-Cl2	98.74(6)	N2-Ti-N5	159.22(1)
N2-Ti-Cl1	95.23(1)	N5-Ti-Cl1	98.56(1)
N2-Ti-Cl2	97.99(1)	N5-Ti-Cl2	95.31(1)
N2-Ti-N4	89.06(1)	N5-Ti-N1	88.51(1)
Cl1-Ti-N4	92.39(1)	Cl2-Ti-N4	166.23(1)
Cl1-Ti-N1	165.84(1)	Cl2-Ti-N1	92.82(1)
N4-Ti-N1	77.54(1)		

for references, see page 26

Crystals of **C4** (Figure 2) suitable for single-crystal X-ray analysis were obtained by laying hexane on its CH_2Cl_2 solution. The selected bond lengths and angles were collected in Table 3. In the solid state, two molecules of dichloromethane were incorporated. It can be found from Figure 2 that the titanium was coordinated with two dianionic tridentate ligands and adopted a distorted octahedral geometry, in which two deprotonated benzimidazole-N atoms was *cis*-situated (N1-Ti1-N5 = 94.10(1)°), two pyridine-N atoms *trans* oriented (N3-Ti1-N7 = 170.06(1)°) and two deprotonated amide-O atoms *cis*-located (O1-Ti1-O2 = 96.71(1)°). The two ligands were structurally similar and situated approximately perpendicular to each other with the dihedral angle of 89°. The benzimidazole and pyridine planes of each ligand fragment were coplanar with the largest deviation of 0.0428 Å. The two chelating rings (Ti1-N1-C7-C8-N3; Ti1-N3-C12-C13-O1) were almost in the same plane with a dihedral angle of 1.3°. The angles N1-Ti1-N3 and N3-Ti1-O1 are equal to 73.16(1)° and 74.55(1)° with a sum of 147.71(1)°, which is equal to the bite angle N1-Ti1-O1. This value is higher than that found in half-metallocenes which may be due to the more steric hindrance between the two ligand fragments.[16] The two types of Ti-N bonds (Ti1-N1 = 2.064(4) Å, Ti1-N5 = 2.063(4) Å; Ti1-N3 = 2.122(4) Å, Ti1-N7 = 2.135(4) Å) were in the usual range for titanium complexes, but slightly different due to their different chemical environments. Unlike the common N,O chelating motif,[21] the 2-carboxylimidate group was bonded through O-atom to the titanium center. The C-N bond lengths (C13-N4 = 1.278(5) Å, C38-N8 = 1.271(6) Å) were shorter than typically C-N single bond, displaying the double bond character, while the C-O bond length (C13-O1 = 1.327(5) Å, C38-O2 = 1.339(5) Å) lay in the range between the single and double bonds. The structural data indicated delocalized character of the electron in the amide group due to chelating rings (Ti1-N3-Cl2-Cl3-O1, Ti1-N7-C37-C38-O2). Similar phenomenon was also observed in titanium and zirconium biaryl amidate complexes.[7e] The isopropyl-substituted phenyl groups were situated far away from the titanium center and were orientated perpendicularly to the chelating rings (Ti1-O1-Cl3-Cl2-N3, Ti1-N7-C37-C38), with dihedral angles of 99.2° and 77.2°.

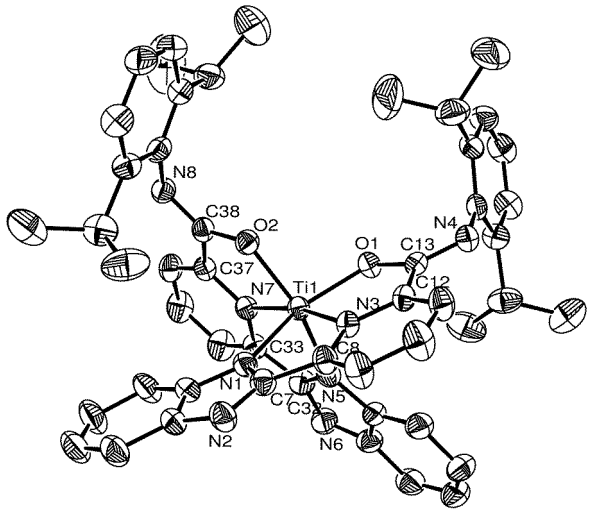

Figure 2. Molecular structure of complex **C4**, showing 30% probability thermal ellipsoids for all non-hydrogen atoms. Hydrogen atoms and solvent molecules have been omitted for clarity.

for references, see page 26

Table 3. Selected bond lengths (Å) and angles (°) for Complex **C4**

Bond lengths (Å)			
Ti1-O1	1.888(3)	Ti1-O2	1.889(3)
Ti1-N1	2.064(4)	Ti1-N5	2.063(4)
Ti1-N3	2.299(3)	Ti1-N7	2.064(4)
C13-O1	1.327(5)	C13-N4	1.278(5)
C38-O2	1.339(5)	C38-N8	1.271(6)
Bond angles (°)			
O1-Ti1-N1	147.71(1)	O2-Ti1-N5	147.64(2)
N3-Ti1-N7	170.06(1)	N1-Ti1-N3	73.16(1)
O1-Ti1-N3	74.55(1)	N5-Ti1-N1	94.10(1)
O2-Ti1-N7	74.37(1)	N5-Ti1-N7	73.49(1)
O1-Ti1-O2	96.71(1)	O2-Ti1-N1	94.13(1)
O1-Ti1-N5	92.80(1)	O1-Ti1-N7	113.90(1)
N1-Ti1-N7	98.30(1)		

Compared the structures of **C1** and **C4**, ligand containing carboxylimidate group resulted in a more crowded coordination environment around titanium (**C4**), meanwhile the dihedral angles between the two chelating ligands had increased from 63.0° (Ti-N1-N3; Ti-N5-N7) in **C1** to 89.5° (Ti1-N1-N3-O1; Ti1-N5-N7-O2) in **C4**. All these structural differences between complex **C1** and **C4** would be responsible for their different catalytic behaviors in ethylene polymerization.

2.4.3 Catalytic Behavior of Complex C1

Ethylene polymerization using **C1**/MAO system was conducted to investigate the influences of polymerization conditions such as Al/Ti molar ratio, reaction temperature and time factors on the catalytic behaviors. The results were illustrated in Table 4. The increasing Al/Ti molar ratio resulted in higher catalytic activity. When 10000 equivalents of MAO were applied to the catalytic system, the activity was an order of magnitude higher than that obtained at Al/Ti molar ratio of 750. The polymerization activities improved with elevating reaction temperature, and the catalytic activities continuously increased from 2.48×10^5 to 6.24×10^5 $g \cdot mol^{-1}(Ti) \cdot h^{-1}$ as the reaction temperature increased from 20 to 100 °C. Such phenomenon was also observed in our previous catalytic system of bis(imino-indolide)titanium dichloride.[11] Considering the reaction period of ethylene polymerization, the highest activity was obtained in a short period (at the beginning of the polymerization). For example, the data for the activities were observed from 37.2×10^5 to 4.22×10^5 $g \cdot mol^{-1}(Ti) \cdot h^{-1}$ within the period of 5 to 60 min. On the basis of data in Table 4 (entries 3 and 9-11), there was 1.55g polyethylene produced within 5 minutes at the beginning, however, only 0.11 g polyethylene formed in additional 10 minutes after the first 5 minutes. This could be cause of decomposition of the active sites because the complex was found to be unstable in its toluene solution.

for references, see page 26

Table 4. Ethylene Polymerization with **C1**/MAO[a]

Entry	Al/Ti	*T* (°C)	Time (min)	Polymer (g)	Activity (10^5 g·mol^{-1}(Ti)·h^{-1})
1	750	80	30	0.67	2.68
2	1500	80	30	1.21	4.84
3	3000	80	30	1.85	7.40
4	10000	80	30	5.80	23.2
5	1500	20	30	0.62	2.48
6	1500	40	30	0.75	3.00
7	1500	60	30	1.05	4.20
8	1500	100	30	1.56	6.24
9	3000	80	5	1.55	37.2
10	3000	80	15	1.66	13.3
11	3000	80	60	2.11	4.22

[a] Conditions: 5 μmol of catalysts; toluene (total volume 100 mL); 10 atm ethylene.

2.4.4 Catalytic Behavior of Complexes C2-C8

In the presence of MAO as cocatalyst, complexes **C2-C8** were investigated for their catalytic performances of ethylene polymerization with ethylene pressure both at 10 and 30 atm. The results were collected in Table 5.

Table 5. Ethylene Polymerization with **C2-C8**/MAO[a]

Entry	Complex	P(atm)	Polymer (g)	Activity (10^6 g·mol^{-1}(Ti)·h^{-1})	M_w[b] (10^4 g·mol^{-1})	M_w/M_n[b]
1	**C2**	10	3.15	5.04		
2	**C3**	10	3.24	5.18		
3	**C4**	10	3.43	5.49		
4	**C5**	10	2.94	4.70		
5	**C6**	10	3.02	4.83		
6	**C7**	10	2.65	4.24		
7	**C8**	10	2.53	4.05		
8	**C2**	30	5.24	8.38	19.3	6.8
9	**C3**	30	5.36	8.58	17.3	6.0
10	**C4**	30	6.08	9.72	15.7	9.1
11	**C5**	30	4.29	6.86	15.3	10
12	**C6**	30	4.47	7.15	28.0	16
13	**C7**	30	3.87	6.19	21.6	16
14	**C8**	30	3.76	6.02		

[a] Conditions: 2.5 μmol of catalysts; Al/Ti = 10000; 80 °C; 15 min; toluene (total volume 100 mL). [b] Determined by GPC.

Influence of the Ligand Environment on the Catalytic Behavior

The titanium complexes **C2-C8** were investigated as catalytic precursors for ethylene polymerization. A variety of amide groups in the 6-benzimidazolylpyridine-2-carboxylimidate ligands was investigated with regard to their steric and electronic effects on the catalytic activities and

for references, see page 26

polymer properties. Their differences originate from substituents on the phenyl ring attached to the nitrogen of the carboxylimidate group; according to the molecular structure of **C4**, their steric influences could be ignored due to far location of the substituents from the titanium center. Upon activation with MAO at 80 °C at 10 and 30 atm of ethylene pressure, all these compounds displayed high catalytic activities. The highest activity, 9.72×10^6 g·mol^{-1}(Ti)·h^{-1}, was obtained at 80 °C under 30 atm of ethylene using **C4**/MAO system. Their catalytic activities varied in the order of **C4** (with *i*-Pr substituents) > **C3** (with Et) > **C2** (with Me), meanwhile **C6** (with Cl) > **C5** (with F) and similar to alkyl-substituted **C7** and **C8**. In general, their catalytic activities remained comparable, because of similar coordination environment of their ligands. GPC analysis for the obtained polyethylenes showed their molecular weights to be in the range of $15.3 \times 10^4 - 28.0 \times 10^4$ g·mol^{-1}, higher than those obtained by similar coordination complexes of zirconium pyridine-2,6-bis(aryloxide) complexes.[12d] Similar to previous reports,[12c,d] the broad molecular weight distributions (6.0-16) of the polyethylenes indicated the possible multi-site nature of the catalytic species. Though the activities were indeed improved along with increasing ethylene pressure, the effects were not significant. To understand the influences of reaction conditions on catalytic behaviors, the catalytic system of **C4**/MAO was investigated in detail.

Effects of Al/Ti Molar Ratio, Reaction Temperature and Time on the Catalytic Behaviors of C4

As the catalytic system of **C4**/MAO showed better activities than others, the detailed investigation of reaction parameters on the catalytic activities was carried out with complex **C4** (Table 6). The amount of MAO was found to have drastic influence on ethylene polymerization activities. The activities increased from 2.4×10^5 g·mol^{-1}(Ti)·h^{-1} at Al/Ti molar ratio of 750 to 44.8×10^5 g·mol^{-1}(Ti)·h^{-1} with 15000 eq MAO. Functions of MAO in olefin polymerization included alkylation and abstraction of halogen or alkyl groups to generate the active species.[22] Generally, the catalytic activity increased at the beginning and then decreased along with increasing Al/Ti molar ratio. However, the activities of the current system increased continuously with no obvious decrease. This unique activity dependence on MAO might be considered for highly active system which consumed more cocatalyst of MAO.

The reaction temperature also affected the catalytic activity. According to the data in Table 6, the catalytic activity was very low below 40 °C, while its activities greatly increased at 60 °C and remained stable up to 80 °C. Compared to the maximum activity of traditional FI catalysts around 50 °C,[7] the thermal stability of the current catalytic system showed the potential to fit the industrial polymerization requirements. It was advantageous of a high catalytic activity at high polymerization temperature because the liquefiable polymerization at high temperature favored the viscosity of the reaction mixture with better mass transportation and temperature control.

It was interesting that the activity of **C4**/MAO system remained nearly constant over 60 min, while **C1**/MAO system was deactivated after 5 min. It could be related to the additional amide groups

for references, see page 26

having better electron-donating influence on the titanium and strengthening its metal-ligand bond. Moreover, the steric hindrance provided by the amide groups could stabilize the active site and suppress β-H elimination. With the view of maintaining catalytic properties of the complexes, the modification of the ligand structures was fulfilled.

GPC analysis revealed that the molecular weights of the obtained polyethylenes were both affected by the reaction temperature and Al/Ti malor ratio. It was noticed that Mw values were much higher for the polyethylene obtained at low temperature and low MAO concentration (up to 10^6 $g \cdot mol^{-1}$). Increasing temperature from 20 °C to 80 °C resulted in polyethylenes with significantly decreased molecular weights, from 123×10^4 to 9×10^4 $g \cdot mol^{-1}$, which were due to the more frequent chain transfers and terminations at elevated temperatures. When more MAO was employed, a sharp decrease in molecular weight and narrow molecular weight distributions of the resultant polyethylenes were observed. This trend is consistent with literature results,[12d] and indicated that the chain transfers to Al sites played significant roles in affecting the polymer molecular weights and their distributions. The absence of unsaturated end groups in the polymer chain indicated by IR analysis confirmed this hypothesis. Prolonged polymerization times led to a slight decrease in polyethylene molecular weights and broadened molecular weight distributions.

Table 6. Ethylene Polymerization with **C4**/MAO[a]

Entry	*T* (°C)	Al/Ti	Time (min)	Polymer (g)	Activity (10^5 $g \cdot mol^{-1}(Ti) \cdot h^{-1}$)	M_w[b] (10^4 $g \cdot mol^{-1}$)	M_w/M_n[b]
1	20	1500	30	0.21	0.84	123	8.5
2	40	1500	30	0.26	1.04	77.3	31
3	60	1500	30	0.67	2.68	25.1	12
4	80	1500	30	0.94	3.76	9.00	6.0
5	80	750	30	0.65	2.60	104	38
6	80	3000	30	1.58	6.32	52.3	12
7	80	10000	30	9.79	39.2	16.0	5.7
8	80	15000	30	11.2	44.8	16.8	3.8
9	80	3000	5	0.31	7.44	31.4	5.0
10	80	3000	15	0.82	6.56	28.2	12
11	80	3000	60	3.07	6.14	21.1	9.2

[a] Conditions: 5 μmol of catalysts; 10 atm ethylene; toluene (total volume 100 mL). [b] Determined by GPC.

for references, see page 26

2.5 Conclusions

Bis(2-(6-methylpyridin-2-yl)-benzimidazolyl)titanium dichloride (**C1**) and titanium bis(6-benzimidazolylpyridine-2-carboxylimidate) (**C2**–**C8**) were synthesized by treating the sodium salts of the ligand with titanium tetrachloride. All the complexes were characterized by ^{1}H NMR, ^{13}C NMR and elemental analyses, and the molecular structures of complex **C1** and **C4** were further confirmed by X-ray diffraction analysis. When activated with excess MAO, complexes **C1**–**C8** exhibited high catalytic activities for ethylene polymerization. These catalysts displayed good activity at elevated reaction temperature. The deactivation of complex **C1** was clearly observed after a short reaction period, however, catalytic systems of **C2**–**C8** retained good activity during one hour reaction. Their catalytic activities varied in the order of **C4** (with *i*-Pr substituent) > **C3** (with Et) > **C2** (with Me), meanwhile **C6** (with Cl) > **C5** (with F) and close similar of alkyl-substituted **C7** and **C8**. Increasing the amount of MAO and elevating reaction temperature resulted in much higher activity but lower molecular weights of the polyethylenes.

Acknowledgements

This work was supported by MOST No. 2006AA03Z553. We thank Mr. Saliu Alao Amolegbe (the CAS-TWAS Postgraduate Fellow from Nigeria) for the English corrections.

for references, see page 26

References and Notes

1. (a) Ittel, S. D.; Johnson, L. K.; Brookhart, M. *Chem. Rev.* **2000**, *100*, 1169-1203; (b) Mecking, S. *Angew. Chem. Int. Ed.* **2001**, *40*, 534-540; (c) Gibson, V. C.; Spitzmesser, S. K. *Chem. Rev.* **2003**, *103*, 283-315; (d) Speiser, F.; Braunstein, P.; Saussine, W. *Acc. Chem. Res.* **2005**, *38*, 784-793; (e) Sun, W.-H.; Zhang, D.; Zhang, S.; Jie, S.; Hou, J. *Kinet. Catal.* **2006**, *47*, 278-283; (f) Sui-Seng, C.; Castonguay, A.; Chen, Y.; Gareau, D.; Groux, L. F.; Zargarian, D. *Top. Catal.* **2006**, *37*, 81-90; (g) Stapleton, R. L.; Chai, J.; Taylor, N. J.; Collins, S. *Organometallics* **2006**, *25*, 2514-2524; (h) Gibson, V. C.; Redshaw, C.; Solan, G. A. *Chem. Rev.* **2007**, *107*, 1745-1776.
2. (a) Ziegler, K.; Holzkamp, E.; Breil, H.; Martin, H. *Angew. Chem.* **1955**, *67*, 541-547; (b) Ziegler, K.; Gellert, H. G. *Angew. Chem.* **1955**, *67*, 424-425; (c) Natta, G.; Pino, P.; Corradini, P.; Danusso, F.; Mantica, E.; Mazzanti, G.; Moraglio, G. *J. Am. Chem. Soc.* **1955**, *77*, 1708-1710; (d) Natta, G. *J. Polym. Sci.* **1955**, *16*, 143-154.
3. (a) Sinn, H.; Kaminsky, W.; Vollmer, H. J.; Woldt, R. *Angew. Chem. Int. Ed. Engl.* **1980**, *19*, 390-392; (b) Sinn, H.; Kaminsky, W. *Adv. Organomet. Chem.* **1980**, *18*, 99-149; (c) Kaminsky, W.; Külper, K.; Brintzinger, H. H.; Wild, F. *Angew. Chem. Int. Ed. Engl.* **1985**, *24*, 507-508; (d) Alt, H. G.; Köppl, A. *Chem. Rev.* **2000**, *100*, 1205-1221.
4. Weckhuysen, B. M.; Schoonheydt, R. A. *Catal. Today* **1999**, *51*, 215-221.
5. (a) Shapiro, P. J.; Bunel, E.; Schaefer, W. P.; Bercaw, J. E. *Organometallics* **1990**, *9*, 867-869; (b) Stevens, J. C.; Timmers, F. J.; Wilson, D. R.; Schmidt, G. F.; Nickias, P. N.; Rosen, R. K.; McKnight, G. W.; Lai, S. Eur. Pat. Appl. 0416815A2, **1991**; (c) Shapiro, P. J.; Cotter, W. D.; Schaefer, W. P.; Labinger, J. A.; Bercaw, J. E. *J. Am. Chem. Soc.* **1994**, *116*, 4623-4640; (d) Xu, S.; Jia, J.; Huang, J. *J. Polym. Sci., Part A: Polym. Chem.* **2007**, *45*, 4901-4913.
6. Nomura, K.; Liu, J.; Padmanabhan, S.; Kitiyanan, B. *J. Mol. Catal. A: Chem.* **2007**, *267*, 1-29.
7. (a) Matsui, S.; Tohi, Y.; Mitani, M.; Saito, J.; Makio, H.; Tanaka, H.; Nitabaru, M.; Nakano, T.; Fujita, T. *Chem. Lett.* **1999**, 1065-1066; (b) Tian, J.; Coates, G. W. *Angew. Chem. Int. Ed.* **2000**, *39*, 3626-3629; (c) Matsui, S.; Mitani, M.; Saito, J.; Tohi, Y.; Makio, H.; Matsukawa, N.; Takagi, Y.; Tsuru, K.; Nitabaru, M.; Nakano, T.; Tanaka, H.; Kashiwa, N.; Fujita, T. *J. Am. Chem. Soc.* **2001**, *123*, 6847-6856; (d) Makio, H.; Kashiwa, N.; Fujita, T. *Adv. Synth. Catal.* **2002**, *344*, 477-493; (e) Gott, A. L.; Clarke, A. J.; Clarkson, G. J.; Scott, P. *Organometallics* **2007**, *26*, 1729-1737.
8. (a) Yang, H.; Sun, W.-H.; Chang, F.; Li, Y. *Appl. Catal., A: Gen.* **2003**, *252*, 261-267; (b) Sun, W.-H.; Yang, H.; Li, Z.; Li, Y. *Organometallics* **2003**, *22*, 3678-3683; (c) Chang, F.; Zhang, D.; Xu, G.; Yang, H.; Li, J.; Song, H.; Sun, W.-H. *J. Organomet. Chem.* **2004**, *689*, 936-946.
9. (a) Yoshida, Y.; Matsui, S.; Takagi, Y.; Mitani, M.; Nakano, T.; Tanaka, H.; Kashiwa, N.; Fujita, T. *Organometallics* **2001**, *20*, 4793-4799; (b) Yoshida, Y.; Mohri, J.; Ishii, S.; Mitani, M.; Saito, J.; Matsui, S.; Makio, H.; Nakano, T.; Tanaka, H.; Onda, M.; Yamamoto, Y.; Mizuno, A.; Fujita, T. *J. Am. Chem. Soc.* **2004**, *126*, 12023-12032; (c) Tsurugi, H.; Matsuo, Y.; Yamagata, T.; Mashima, K. *Organometallics* **2004**, *23*, 2797-2805; (d) Yoshida, Y.; Matsui, S.; Fujita, T. *J. Organomet. Chem.* **2005**, *690*, 4382-4397; (e) Tsurugi, H.; Mashima, K. *Organometallics* **2006**, *25*, 5210-5212.
10. Li, J.; Gao, T.; Zhang, W.; Sun, W.-H. *Inorg. Chem. Commun.* **2003**, *6*, 1372-1374.
11. Zuo, W.; Sun, W.-H.; Zhang, S.; Hao, P.; Shiga, A. *J. Polym. Sci., Part A: Polym. Chem.* **2007**, *45*, 3415-3430.
12. (a) Mack, H.; Eisen, M. S. *J. Chem. Sci., Dalton Trans.* **1998**, 917-921; (b) Sudhakar, P.; Sundararajan, G. *J. Polym. Sci., Part A: Polym. Chem.* **2006**, *44*, 4006-4014; (c) Paolucci, G.; Zanella, A.; Sperni, L.; Bertolasi, V.; Mazzeo, M.; Pellecchia, C. *J. Mol. Catal. A: Chem.* **2006**, *258*, 275-283; (d) Chan, M. C. W.; Tam, K.-H.; Zhu, N.; Chiu, P.; Matsui, S. *Organometallics* **2006**, *25*, 785-792; (e) Keren, E.; Sundararajan, G. *J. Polym. Sci., Part A: Polym. Chem.* **2007**, *45*, 3599-3610; (f) Sudharkar, P. *J. Polym. Sci., Part A: Polym. Chem.* **2007**, *45*, 5470-5479.
13. (a) Braunstein, P.; Naud, F. *Angew. Chem. Int. Ed.* **2001**, *40*, 680-699; (b) Bassetti, M. *Eur. J. Inorg. Chem.* **2006**, 4473-4482.
14. (a) Britovsek, G. J. P.; Gibson, V. C.; Wass, D. F. *Angew. Chem. Int. Ed.* **1999**, *38*, 428-447; (b) Butenschon, H. *Chem. Rev.* **2000**, *100*, 1527-1564.
15. (a) Zhang, W.; Sun, W.-H.; Zhang, S.; Hou, J.; Wedeking, K.; Schultz, S.; Frohlich, R.; Song, H. *Organometallics* **2006**, *25*, 1961-1969; (b) Zhang, M.; Zhang, S.; Hao, P.; Jie, S.; Sui, W.-H.; Li, P.; Lu, X. *Eur. J. Inorg. Chem.* **2007**, 3816-3826; (c) Sun, W.-H.; Hao, P.; Zhang, S.; Shi, Q.; Zuo, W.; Tang, X.; Lu, X. *Organometallics* **2007**, *26*, 2720-2734; (d) Hao, P.; Zhang, S.; Sun, W.-H.; Shi, Q.; Adewuyi, S.; Lu, X.; Li, P. *Organometallics* **2007**, *26*, 2439-2446.
16. Zuo, W.; Zhang, S.; Liu, S.; Liu, X.; Sun, W.-H. *J. Polym. Sci., Part A: Polym. Chem.* **2008**, *46*, 3396-3410.
17. Basset, H. L.; Thomas, C. R. *J. Chem. Soc.* **1954**, 1188-1190.
18. Shen, M.; Hao, P.; Sun, W.-H. *J. Organomet. Chem.* **2008**, *693*, 1683-1695.
19. Sheldrick, G. M. SHELXL-97; University of Göttingen: Göttingen (Germany), **1997**.

for references, see page 26

20. Sun, W.-H.; Zhang, W.; Gao, T.; Tang, X.; Chen, L.; Li, Y.; Jin, X. *J. Organomet. Chem.* **2004**, *689*, 917-929.
21. (a) Giesbrecht, G. R.; Shafir, A.; Arnold, J. *Inorg. Chem.* **2001**, *40*, 6069-6072; (b) Thomson, R. K.; Zahariev, F. E.; Zhang, Z.; Patrick, B. O.; Wang, Y. A.; Schafer, L. L. *Inorg. Chem.* **2005**, *44*, 8680-8689.
22. Kaminsky, W. *Macromol. Chem. Phys.* **1996**, *197*, 3907-3945.

for references, see page 26

CHAPITRE III

N-(2-Benzimidazolylquinolin-8-yl)benzamidate Half-Titanocene Chlorides: Synthesis, Characterization and Their Catalytic Behavior towards Ethylene Polymerization

SHAOFENG LIU,[†] JIANJUN YI,[‡] WEIWEI ZUO,[†] KEFENG WANG,[†] DELIGEER WANG,[†,§] WEN-HUA SUN[*,†]

[†] *Key Laboratory of Engineering Plastics and Beijing National Laboratory for Molecular Sciences, Institute of Chemistry, Chinese Academy of Sciences, Beijing 100190, China;*

[‡] *Petrochemical Research Institute, PetroChina Limited, No. 20 Xueyuan Road, Beijing 100083, China.*

[§] *Department of Chemistry, Inner Mongolia Normal University, Hohhot 010022, China*

This Chapter has been published in *J. Polym. Sci., Part A: Polym. Chem.*, **2009**, *47*, 3154-3169.

Contributions from the various co-authors: Dr. JIANJUN YI assisted for the catalysis, Dr. WEIWEI ZUO for the synthesis, the catalysis and discussions, Dr. KEFENG WANG was involved in synthesis assistance, and professors DELIGEER WANG and WEN-HUA SUN are responsible for giving directions and providing discussions. I am most grateful to all of them.

Résumé du Chapitre III

Une série de complexes du titane du type Cp'TiLCl (**C1-C8**: Cp' = C_5H_5, MeC_5H_4, ou C_5Me_5; L = *N*-(benzimidazolyquinolin-8-yl)benzamidures)) a été préparée par réaction d'élimination de KCl à partir des précurseurs semi-titanocènes trichlorures et du sel de potassium de *N*-(2-benzimidazolyquinolin-8-yl)benzamidure correspondant. Ces complexes furent complètement caractérisés par analyses élémentaires et RMN et la structure moléculaire de **C2** et **C8** fut déterminée par diffraction des rayons X. La grande stabilité du complexe pentaméthylcyclopentadiénure **C8** fut mise en evidence par celle de sa solution laissée à l'air pendant une semaine. Le compose dinucléaire à pont oxo **C9** a été isolé à partir d'une solution à l'air du complexe cyclopentadienure correspondant **C3**. Les complexes **C1-C8** possèdent des activités catalytiques de bonnes à élevées pour la polymerization de l'éthylène et la copolymérisation éthylène / α-oléfine en présence de méthylaluminoxane (MAO) comme cocatalyseur. Dans le cas du système catalytique **C1**/MAO, la productivité en polymérisation augmente avec la température de réaction ou quand le rapport MAO /

Ti est accru. De manière générale, plus le système catalytique est actif, plus les poids moléculaires du polyéthylène diminuent.

3.1 Abstract of Chapter III

A series of *N*-(2-benzimidazolyquinolin-8-yl)benzamidate half-titanocene chlorides, Cp'TiLCl (**C1-C8**: Cp' = C_5H_5, MeC_5H_4, or C_5Me_5; L = *N*-(benzimidazolyquinolin-8-yl)benzamides)), was synthesized by the KCl elimination reaction of half-titanocene trichlorides with the corresponding potassium *N*-(2-benzimidazolyquinolin-8-yl)benzamide. These half-titanocene complexes were fully characterized by elemental and NMR analyses, and the molecular structures of complexes **C2** and **C8** were determined by the single-crystal X-ray diffraction. The high stability of the pentamethylcyclopentadienyl complex (**C8**) was evidenced by the stability of its solution in air for one week. The oxo-bridged dimeric complex (**C9**) was isolated from the solution of the corresponding cyclopentadienyl complex (**C3**) solution in air. Complexes **C1-C8** exhibited good to high catalytic activities towards ethylene polymerization and ethylene/α-olefin copolymerization in the presence of methylaluminoxane (MAO) cocatalyst. In the typical catalytic system of **C1**/MAO, the polymerization productivities were enhanced with either elevating reaction temperature or increasing the ratio of MAO to titanium precursor. In general, the higher the catalytic activity of the system, the lower molecular weight polyethylene was observed.

3.2 Introduction

Polyolefins have been used as the most popular synthetic polymers with annual market of billions' dollars; it has attracted great attention of scientists in both academic research and industrial units. Practical catalysts are dominated with Ziegler-Natta[1] and Phillips[2] catalysts along with the increasing share of constrained geometry catalysts (CGC)[3] derived from metallocene catalysts.[4] Driven towards polyolefins with unique and advanced properties through efficient incorporations of comonomer and/or finely controlling steric characteristics of branches, the phenomenal complex catalysts have been extensively investigated with both early- and late-transition metals.[5] Following metallocene catalysts initiated by Sinn and Kaminsky in the early 1980s,[4a,b] the emergence of CGC catalysts occurred by modification of metallocenes into bridged half-metallocene catalysts.[3] Recently, non-Cp complex catalysts such as bis(phenoxy-imino)titanium complexes, "FI Catalyst" independently developed by Fujita[6] and Coates,[7] and bis(pyrrolide-imino)titanium complexes "PI catalyst" by Mitsui Chemicals,[8] were also discovered as highly active catalysts. The "FI Catalyst" demonstrated high activities towards ethylene polymerization in a living manner, [6-7] while the "PI catalyst" showed good catalytic behavior towards copolymerization.[8]

The high stability of metallocene catalysts is conferred by the loading property on carriers as the core industrial practicing process with heterogeneous catalysts. However, the highly moisture-sensitive feature of group IVB metal complexes normally is a drawback for the supporting process of such complexes on inorganic carriers. Moreover, the bridged half-metallocene catalysts were quite limited due to the difficulty of synthesis and technical problem. The non-bridged half-metallocene is of great interest with the combining merits of metallocene and complex catalyst.[9] In this model, the ancillary ligands could be varied with mono-anionic donors resulting in the coordination version of either monodentate or bidentate species. Examples are aryloxy,[10] ketimide,[11] acetamidinato,[12] iminophenoxy,[13] pyridinylalkyloxy[14] and *N*-substituted (iminomethyl)pyrrolides.[15] In addition, half-metallocenes bearing dianionic ancillary ligands also demonstrated high activities in olefin polymerization,[16] however, such further exploration has been limited by the problem of finding suitable dianionic ligands.

In the course of our efforts to design late-transition metal complexes as catalysts in ethylene reactivity,[5d,5f] numerous types of heterocyclic compounds were prepared and used as practical catalysts.[17] More interestingly, a slight modification gave 6-(benzimidazol-2-yl)-*N*-organylpyridine-2-carboxamide derivatives, functionally acting as dianionic ligands in half-titanocene catalysts, which was active in ethylene polymerization.[18] As an extension, *N*-((benzimidazol-2-yl)quinolin-8-yl)benzamide derivatives, dianionic tridentate ligands, were reacted with half-titanocene trichlorides to form new half-titanocene complexes. In the presence of MAO, the *N*-((benzimidazol-2-yl)quinolin-8-yl)benzamidate half-titanocene chlorides obtained showed high catalytic activities toward ethylene polymerization and good catalytic behavior for copolymerizing ethylene with α-olefins. Herein we describe the synthesis and characterization of the titled titanium complexes as well as their catalytic

for references, see page 49

performances in ethylene polymerization and copolymerization.

3.3 Experimental Section

3.3.1 General Considerations

All manipulations of air and/or moisture-sensitive compounds were performed under a nitrogen atmosphere in a Vacuum Atmospheres glovebox or using standard Schlenk techniques. Methylaluminoxane (MAO, 1.46 M in toluene) was purchased from Albemarle, and potassium hydride (KH) from Beijing Chemical Regent Company and washed with hexane before use to remove the mineral oil. Tetrahydrofuran (THF), toluene, hexane and heptane were refluxed over sodium and benzophenone, distilled, and then stored under nitrogen atmosphere. Dichloromethane (CH_2Cl_2) was distilled over calcium hydride, and stored under nitrogen atmosphere. High purity ethylene was purchased from Beijing Yansan Petrochemical Co. and used as received. IR spectra were recorded on a Perkin Elmer FT-IR 2000 spectrometer using KBr disc in the range of 4000-400 cm^{-1}. Elemental analysis was performed on a Flash EA 1112 microanalyzer. ^1H NMR and ^{13}C NMR spectra were recorded on a Bruker DMX 300 MHz instrument at ambient temperature using TMS as an internal standard. DSC trace and melting points of polyethylenes were obtained from the second scanning run on a Perkin-Elmer DSC-7 at a heating rate of 10 °C /min.

3.3.2 Synthesis of *N*-(2-methylquinolin-8-yl)benzamide Derivatives

The compounds, *N*-(2-methylquinolin-8-yl)benzamide, 4-chloro-*N*-(2-methylquinolin-8-yl)benzamide and 4-bromo-*N*-(2-methylquinolin-8-yl)benzamide, were synthesized according to our previous method.[19]

4-Methoxy-N-(2-methylquinolin-8-yl)benzamide

According to our previous method,[19] 2-methylquinolin-8-amine (6.32 g, 40 mmol) was slowly added to xylene solution (100 mL) of 4-methoxybenzoic acid (6.08 g, 40 mmol). The mixture was stirred for 15 min and triphenyl phosphite (12.4 g, 40 mmol) was added slowly through a dropping funnel over the period of 15 min. It was then refluxed for 6 h and the solvent was removed under vacuum. The product, 4-methoxy-*N*-(2-methylquinolin-8-yl)benzamide, was purified by column chromatography (silica gel, petroleum ether / ethyl acetate = 10:1) and obtained in 92% yield (10.7 g). ^1H NMR ($CDCl_3$, 300 MHz): δ 10.77 (s, N-H, 1H), 8.90 (dd, J = 7.5 Hz, J = 7.2 Hz, 1H), 8.08 (d, J = 8.8 Hz, 2H), 8.06 (m, 1H), 7.51 (m, 2H), 7.36 (d, J = 8.5 Hz, 1H), 7.06 (d, J = 8.8 Hz, 2H), 3.92 (s, CH_3, 3H), 2.80 (s, CH_3, 3H). ^{13}C NMR ($CDCl_3$, 75 MHz): δ161.9, 159.5, 154.2, 133.4, 131.0, 126.5, 126.1, 124.4, 123.3, 119.4, 118.3, 113.3, 112.7, 111.0, 52.4, 22.4. FT-IR (KBr, cm^{-1}): 3340 (m), 3134 (m), 1680 (s), 1633 (m), 1600 (m), 1549 (s), 1512 (s), 1495 (s), 1435 (m), 1341 (w), 1315 (w), 1258 (m), 1228 (m), 1175 (m), 1027 (w), 833 (m), 760 (s), 678 (w), 590 (w). Mp: 130-131 ^oC. Anal. Calcd for $C_{18}H_{16}N_2O_2$: C, 73.95; H, 5.52; N, 9.58. Found: C, 73.85; H, 5.53; N, 9.47.

4-Methyl-N-(2-methylquinolin-8-yl)benzamide

for references, see page 49

Using the above procedure, 4-methylbenzoic acid was used instead of 4-methoxybenzoic acid. 4-Methyl-*N*-(2-methylquinolin-8-yl)benzamide was obtained as a white solid in 91% yield. ^{1}H NMR ($CDCl_3$, 300 MHz): δ 10.84 (s, N-H, 1H), 8.89 (dd, *J* = 7.0 Hz, *J* = 6.8 Hz, 1H), 8.06 (d, *J* = 8.4 Hz, 1H), 7.98 (d, *J* = 8.8 Hz, 2H), 7.54-7.47 (m, 2H), 7.37-7.33 (m, 1H), 7.22 (d, *J* = 8.4 Hz, 2H), 2.78(s, CH_3, 3H), 2.46 (s, CH_3, 3H). ^{13}C NMR ($CDCl_3$, 75 MHz): δ162.0, 159.7, 154.3, 134.3, 133.1, 126.8, 126.0, 124.5, 122.4, 119.7, 118.3, 114.2, 112.9, 111.2, 22.4, 20.1. FT-IR (KBr, cm^{-1}): 3345 (m), 3050 (w), 2913 (w), 1667 (s), 1601 (m), 1537 (s), 1510 (m), 1492 (s), 1433 (m), 1384 (m), 1338 (m), 1314 (m), 1263 (m), 1228 (m), 1190 (w), 1119 (w), 898 (w), 837 (m), 827 (m), 769 (m), 740 (m), 672 (m), 656 (m), 579 (w). Mp: 104-105 °C. Anal. Calcd for $C_{18}H_{16}N_2O$: C, 78.24; H, 5.84; N, 10.14. Found: C, 78.01; H, 5.86; N, 10.09.

4-Fluoro-N-(2-methylquinolin-8-yl)benzamide

Using the same procedure, 4-fluoro-*N*-(2-methylquinolin-8-yl)benzamide was obtained as a white solid in 82% yield. ^{1}H NMR ($CDCl_3$, 300 MHz): δ 10.76 (s, N-H, 1H), 8.87 (dd, *J* = 6.8 Hz, *J* = 6.2 Hz, 1H), 8.11-8.05 (m, 3H), 7.55-7.48 (m, 2H), 7.36 (d, *J* = 8.6 Hz, 1H), 7.22 (d, *J* = 8.9 Hz, 2H), 2.78 (s, CH_3, 3H). ^{13}C NMR ($CDCl_3$, 75 MHz): δ 161.1, 160.3, 154.3, 135.1, 133.5, 130.8, 128.5, 123.7, 123.4, 119.5, 118.6, 113.5, 113.0, 112.7, 22.5. FT-IR (KBr, cm^{-1}): 3333 (m), 3051 (w), 1669 (s), 1601 (m), 1539 (vs), 1488 (m), 1434 (m), 1386 (w), 1340 (m), 1318 (m), 1262 (m), 1228 (m), 1175 (w), 898 (w), 834 (m), 796 (m), 763 (m), 692 (m), 652 (w), 596 (m). Mp: 101-102 °C. Anal. Calcd for $C_{17}H_{13}FN_2O$: C, 72.85; H, 4.67; N, 9.99. Found: C, 72.81; H, 4.86; N, 10.09.

3.3.3 Synthesis and Characterization of *N*-((benzimidazol-2-yl)quinolin-8-yl)benzamide Derivatives (L1-L6)

N-(2-(1*H*-benzo[*d*]imidazol-2-yl)quinolin-8-yl)benzamide (**L3**), *N*-(2-(1*H*-benzo[*d*] imidazol-2-yl)quinolin-8-yl)-4-chlorobenzamide (**L5**) and *N*-(2-(1*H*-benzo[*d*]-imidazol-2-yl)quinolin-8-yl)-4-bromobenzamide (**L6**) were synthesized using our present method.[19]

N-(2-(1H-Benzo[d]imidazol-2-yl)quinolin-8-yl)-4-methoxybenzamide (L1)

A mixture of equivalent molar amounts of *o*-phenylenediamine (2.16 g, 20 mmol) and 4-methoxy-*N*-(2-methylquinolin-8-yl)benzamide (5.84 g, 20 mmol) with excess sulfur (3.20 g, 100 mmol) was heated to 170 °C and stirred for 12 h. After cooling to room temperature, 250 mL of THF was added, and the precipitated solid (including unreacted sulfur) was filtered off. The product, *N*-(2-(1*H*-benzo[*d*]imidazol-2-yl)quinolin-8-yl)-4-methoxybenzamide, was purified by column chromatography (silica gel, petroleum ether / ethyl acetate = 2:1) and obtained in 61% yield (4.80 g). ^{1}H NMR ($CDCl_3$, 300 MHz): δ 10.58 (s, N-H, 1H), 10.30 (s, N-H, 1H), 8.90 (d, *J* = 7.2 Hz, 1H), 8.59 (d, *J* = 8.5 Hz, 1H), 8.32 (d, *J* = 8.5 Hz, 1H), 8.03 (d, *J* = 8.6 Hz, 2H), 7.94-7.91 (m, 1H), 7.63-7.55 (m, 3H), 7.40-7.34 (m, 2H), 7.06 (d, *J* = 8.6 Hz, 2H), 3.93 (s, CH_3, 3H). ^{13}C NMR ($CDCl_3$, 75 MHz): δ 166.9, 162.6, 150.9, 146.4, 138.3, 137.4, 134.7, 129.5, 128.1, 127.7, 127.1, 121.9, 119.5, 117.8, 113.7, 55.1. FT-IR (KBr, cm^{-1}): 3228 (m), 3055 (w), 1658 (s), 1650 (s), 1599 (m), 1525 (s), 1480 (m), 1417 (m), 1380 (w), 1334

for references, see page 49

(m), 1318 (m), 1275 (m), 1241 (w), 847 (m), 760 (m), 735 (m), 698 (m), 594 (m). Mp: 273-274 °C. Anal. Calcd for $C_{24}H_{18}N_4O_2$: C, 73.08; H, 4.60; N, 14.20. Found: C, 73.21; H, 4.36; N, 14.19.

N-(2-(1H-Benzo[d]imidazol-2-yl)quinolin-8-yl)-4-methylbenzamide (L2)

Using the above procedure, the 4-methyl-*N*-(2-methylquinolin-8-yl)benzamide was used instead of 4-methoxy-*N*-(2-methylquinolin-8-yl)benzamide. *N*-(2-(1*H*-Benzo[*d*]imidazol-2-yl)quinolin-8-yl)-4-methylbenzamide was obtained as a white solid in 51% yield. ^{1}H NMR ($CDCl_3$, 300 MHz): δ 10.74 (s, N-H, 1H), 10.32 (s, N-H, 1H), 8.87 (d, *J* = 6.9 Hz, 1H), 8.54 (d, *J* = 8.5 Hz, 1H), 8.25 (d, *J* = 8.5 Hz, 1H), 7.95-7.91 (m, 3H), 7.61-7.58 (m, 1H), 7.54-7.51 (m, 2H), 7.39-7.36 (m, 2H), 7.30 (d, *J* = 7.9 Hz, 2H), 2.45 (s, CH_3, 3H). ^{13}C NMR ($CDCl_3$, 75 MHz): δ 167.5, 150.7, 146.2, 142.3, 138.6, 138.1, 137.3, 134.5, 132.0, 128.8, 127.4, 123.1, 121.9, 119.2, 117.8, 115.1, 20.5. FT-IR (KBr, cm^{-1}): 3220 (m), 3074 (w), 1665 (s), 1650 (m), 1592 (m), 1535 (s), 1481 (m), 1417 (m), 1380 (w), 1329 (m), 1319 (m), 1265 (m), 1250 (m), 876 (m), 762 (m), 736 (m), 690 (m), 595 (w). Mp: 279-280 °C. Anal. Calcd for $C_{24}H_{18}N_4O$: C, 76.17; H, 4.79; N, 14.81. Found: C, 76.08; H, 4.68; N, 14.66.

N-(2-(1H-Benzo[d]imidazol-2-yl)quinolin-8-yl)-4-fluorobenzamide (L4)

Using the same procedure, *N*-(2-(1*H*-benzo[*d*]imidazol-2-yl)quinolin-8-yl)-4- fluorobenzamide was obtained as a white solid in 36% yield. ^{1}H NMR ($CDCl_3$, 300 MHz): δ 10.75 (s, N-H, 1H), 10.25 (s, N-H, 1H), 8.83 (d, *J* = 6.9 Hz, 1H), 8.55 (d, *J* = 8.5 Hz, 1H), 8.25 (d, *J* = 8.5 Hz, 1H), 8.07-8.03 (m, 2H), 7.80-7.65 (m, 2H), 7.56-7.50 (m, 2H), 7.39-7.35 (m, 2H), 7.23 (d, *J* = 8.4 Hz, 1H), 7.19 (d, *J* = 8.4 Hz, 1H). ^{13}C NMR ($CDCl_3$, 75 MHz): δ165.5, 164.9, 163.0, 150.6, 145.5, 137.7, 137.2, 134.6, 130.9, 130.5, 130.4, 127.7, 127.3, 122.7, 121.7, 119.3, 117.3, 115.1, 114.9. FT-IR (KBr, cm^{-1}): 3231 (m), 3055 (w), 1669 (s), 1651 (s), 1596 (m), 1546 (s), 1481 (m), 1416 (m), 1382 (m), 1331 (w), 1319 (w), 1255 (m), 1219 (m), 905 (m), 787 (m), 724 (m), 691 (m), 596 (w). Mp: 271-272 °C. Anal. Calcd for $C_{23}H_{15}FN_4O$: C, 72.24; H, 3.95; N, 14.65. Found: C, 72.18; H, 3.98; N, 14.66.

3.3.4 Synthesis of Complexes (C1-C9)

η^5-Cyclopentadienyl[N-(2-(1H-benzo[d]imidazol-2-yl)quinolin-8-yl)-4-methoxybenzamide] chlorotitanium (C1)

To a stirred solution of *N*-(2-(1*H*-benzo[*d*]imidazol-2-yl)quinolin-8-yl)-4- methoxybenzamide (0.788 g, 2.00 mmol) in dried THF (30 mL) at -78 °C, KH (0.160 g, 4.00 mmol) was added. The mixture was allowed to warm to room temperature and stirred for additional 2 hrs. At -78 °C, 20 mL of a $CpTiCl_3$ (0.438 g, 2.00 mmol) solution in THF was added dropwise over a 30 min period. The resultant mixture was allowed to warm to room temperature and stirred for additional 12 h. The residue, obtained by removing the solvent under vacuum, was extracted with CH_2Cl_2 (3 × 20 mL) and the combined filtrates were concentrated in vacuum to reduce the volume to 20 mL. Heptane (45 mL) was layered and several days later, brown crystals were obtained (0.611 g, yield 57%). ^{1}H NMR ($CDCl_3$, 300 MHz): δ 8.44 (d, *J* = 8.4 Hz, 1H), 8.22 (d, *J* = 7.9 Hz, 1H), 7.81 (d, *J* = 8.0 Hz, 1H), 7.70 (d, *J* = 8.1 Hz, 1H), 7.64 (d, *J* = 8.3 Hz, 2H), 7.36 (dd, *J* = 7.2 Hz, *J* = 7.9 Hz, 1H), 7.28 (d, *J* = 7.5 Hz,

for references, see page 49

1H), 7.19-7.16 (m, 2H), 6.80 (d, *J* = 8.7 Hz, 2H), 6.72 (s, Cp, 5H), 6.42-6.37 (m, 1H), 3.80 (s, CH_3, 3H). ^{13}C NMR ($CDCl_3$, 75 MHz): δ 180.0, 162.8, 157.4, 156.8, 150.7, 148.6, 146.1, 142.6, 141.9, 132.1, 129.5, 128.3, 127.2, 125.4, 123.2, 122.0, 120.6, 117.6, 117.4, 116.7, 116.4, 114.1, 55.5. Anal. Calcd for $C_{29}H_{21}ClN_4O_2Ti$: C, 64.40; H, 3.91; N, 10.36. Found: C, 64.13; H, 3.88; N, 10.13.

η^5-Cyclopentadienyl[N-(2-(1H-benzo[d]imidazol-2-yl)quinolin-8-yl)-4-methylbenzamide] chlorotitanium (C2)

Using the same procedure for the synthesis of **C1**, **C2** was obtained as a dark red solid in 67% yield. ^{1}H NMR ($CDCl_3$, 300 MHz): δ 8.45 (d, *J* = 8.4 Hz, 1H), 8.23 (d, *J* = 8.3 Hz, 1H), 7.82 (d, *J* = 8.0 Hz, 1H), 7.73 (d, *J* = 8.1 Hz, 1H), 7.56 (d, *J* = 7.8 Hz, 2H), 7.36 (dd, *J* = 7.7 Hz, *J* = 7.3 Hz, 1H), 7.29 (d, *J* = 7.9 Hz, 1H), 7.20-7.15 (m, 2H), 7.12 (d, *J* = 7.9 Hz, 2H), 6.73 (s, Cp, 5H), 6.39-6.36 (m, 1H), 2.35 (s, CH_3, 3H). ^{13}C NMR ($CDCl_3$, 75 MHz): δ 180.1, 156.4, 150.9, 148.2, 145.8, 142.5, 142.3, 141.7, 132.5, 130.9, 129.8, 129.4, 128.1, 125.2, 123.4, 123.1, 122.0, 120.2, 119.7, 118.2, 117.4, 116.9, 21.6. Anal. Calcd for $C_{29}H_{21}ClN_4OTi$: C, 66.37; H, 4.03; N, 10.68. Found: C, 66.23; H, 4.08; N, 10.42.

η^5-Cyclopentadienyl[N-(2-(1H-benzo[d]imidazol-2-yl)quinolin-8-yl)benzamide] chlorotitanium (C3)

Using the same procedure for the synthesis of **C1**, **C3** was obtained as a dark red solid in 58% yield. ^{1}H NMR ($CDCl_3$, 300 MHz): δ 8.45 (d, *J* = 8.3 Hz, 1H), 8.24 (d, *J* = 8.1 Hz, 1H), 7.81 (d, *J* = 7.9 Hz, 1H), 7.72 (d, *J* = 8.1 Hz, 1H), 7.65 (d, *J* = 7.8 Hz, 2H), 7.43 (m, 1H), 7.30-7.27 (m, 4H), 7.18 (d, *J* = 7.9 Hz, 2H), 6.74 (s, Cp, 5H), 6.37-6.35 (m, 1H). ^{13}C NMR ($CDCl_3$, 75 MHz): δ 181.1, 159.6, 152.4, 148.9, 144.8, 143.5, 142.8, 141.7, 134.2, 131.1, 130.8, 129.4, 127.2, 125.9, 123.3, 122.6, 122.0, 121.2, 119.8, 118.7, 117.4, 116.3. Anal. Calcd for $C_{28}H_{19}ClN_4OTi$: C, 65.84; H, 3.75; N, 10.97. Found: C, 65.43; H, 4.01; N, 10.69.

η^5-Cyclopentadienyl[N-(2-(1H-benzo[d]imidazol-2-yl)quinolin-8-yl)-4-fluoro-benzamide] chlorotitanium (C4)

Using the same procedure for the synthesis of **C1**, **C4** was obtained as a dark red solid in 49%. ^{1}H NMR ($CDCl_3$, 300 MHz): δ 8.46 (d, *J* = 8.4 Hz, 1H), 8.24 (d, *J* = 8.4 Hz, 1H), 7.82 (d, *J* = 8.0 Hz, 1H), 7.71 (d, *J* = 8.2 Hz, 1H), 7.68 (d, *J* = 8.4 Hz, 1H), 7.65 (d, *J* = 8.3 Hz, 1H), 7.37 (dd, *J* = 7.2 Hz, *J* = 7.3 Hz, 1H), 7.30 (d, *J* = 7.4 Hz, 1H), 7.23 (d, *J* = 6.7 Hz, 1H), 7.20 (d, *J* = 7.3 Hz, 1H), 7.01 (d, *J* = 8.6 Hz, 1H), 6.97 (d, *J* = 7.4 Hz, 1H), 6.73 (s, Cp, 5H), 6.36 (d, *J* = 6.9 Hz, 1H). ^{13}C NMR ($CDCl_3$, 75 MHz): δ 178.9, 166.5, 163.1, 156.2, 151.0, 148.1, 147.8, 145.7, 142.6, 141.6, 132.1, 131.5, 129.2, 128.1, 125.3, 123.2, 122.1, 120.2, 117.5, 117.3, 117.1, 116.9, 115.9, 115.6. Anal. Calcd for $C_{28}H_{18}ClFN_4OTi$: C, 63.60; H, 3.43; N, 10.60. Found: C, 63.36; H, 3.31; N, 10.46.

η^5-Cyclopentadienyl[N-(2-(1H-benzo[d]imidazol-2-yl)quinolin-8-yl)-4-chloro-benzamide] chlorotitanium (C5)

Using the same procedure for the synthesis of **C1**, **C5** was obtained as a dark red solid in 51% yield. ^{1}H NMR ($CDCl_3$, 300 MHz): δ 8.46 (d, *J* = 8.4 Hz, 1H), 8.24 (d, *J* = 8.3 Hz, 1H), 7.82 (d, *J* = 8.0 Hz, 1H), 7.71 (d, *J* = 7.9 Hz, 1H), 7.60 (d, *J* = 8.0 Hz, 2H), 7.37 (dd, *J* = 7.3 Hz, *J* = 7.7 Hz, 1H), 7.30-7.28 (m, 3H), 7.21-7.17 (m, 2H), 6.74 (s, Cp, 5H), 6.37 (d, *J* = 7.0 Hz, 1H). ^{13}C NMR ($CDCl_3$, 75

for references, see page 49

MHz): δ 179.6, 160.2, 154.4, 145.3, 143.5, 143.1, 142.3, 141.2, 135.2, 132.9, 131.1, 128.4, 127.9, 125.7, 123.6, 123.1, 122.5, 121.2, 120.2, 119.1, 117.0, 116.2. Anal. Calcd for $C_{28}H_{18}Cl_2N_4OTi$: C, 61.68; H, 3.33; N, 10.28. Found: C, 61.43; H, 3.31; N, 10.06.

η^5-Cyclopentadienyl[N-(2-(1H-benzo[d]imidazol-2-yl)quinolin-8-yl)-4-bromo-benzamide] chlorotitanium (C6)

Using the same procedure for the synthesis of **C1**, **C6** was obtained as a dark red solid in 52% yield. ^{1}H NMR ($CDCl_3$, 300 MHz): δ 8.46 (d, *J* = 8.4 Hz, 1H), 8.25 (m, 1H), 7.82 (d, *J* = 8.0 Hz, 1H), 7.71 (d, *J* = 8.1 Hz, 1H), 7.51 (d, *J* = 8.2 Hz, 2H), 7.45 (d, *J* = 8.3 Hz, 2H), 7.38 (dd, *J* = 7.4 Hz, *J* = 7.6 Hz, 1H), 7.31-7.27 (m, 1H), 7.23-7.18 (m, 2H), 6.74 (s, Cp, 5H), 6.38 (d, *J* = 7.1 Hz, 1H). ^{13}C NMR ($CDCl_3$, 75 MHz): δ 179.0, 156.3, 150.8, 148.2, 147.7, 146.0, 142.8, 141.7, 134.7, 132.1, 131.4, 129.4, 128.3, 126.5, 125.5, 123.4, 122.3, 117.7, 117.4. Anal. Calcd for $C_{28}H_{18}BrClN_4OTi$: C, 57.03; H, 3.08; N, 9.50. Found: C, 57.14; H, 3.31; N, 9.96.

η^5-Methylcyclopentadienyl[N-(2-(1H-benzo[d]imidazol-2-yl)quinolin-8-yl)-4-methylbenzamide] chlorotitanium (C7)

Using the same procedure for the synthesis of **C1**, **C7** was obtained as a dark red solid in 62% yield. ^{1}H NMR ($CDCl_3$, 300 MHz): δ 8.44 (d, *J* = 8.2 Hz, 1H), 8.23 (d, *J* = 8.1 Hz, 1H), 7.81 (d, *J* = 8.1 Hz, 1H), 7.74 (d, *J* = 8.1 Hz, 1H), 7.58 (d, *J* = 7.7 Hz, 2H), 7.36 (dd, *J* = 7.4 Hz, *J* = 7.8 Hz, 1H), 7.30 (d, *J* = 8.0 Hz, 1H), 7.22-7.18 (m, 2H), 7.12 (d, *J* = 8.0 Hz, 2H), 6.39-6.36 (m, 1H), 6.05-5.97 (m, 4H), 2.35 (s, CH_3, 3H), 2.29 (s, CH_3, 3H). ^{13}C NMR ($CDCl_3$, 75 MHz): δ 180.5, 156.9, 151.7, 148.7, 146.9, 144.5, 143.4, 141.3, 132.8, 130.8, 129.8, 129.0, 128.1, 126.1, 124.3, 123.1, 122.3, 120.2, 119.6, 119.0, 117.4, 117.0, 20.9, 16.8. Anal. Calcd for $C_{30}H_{23}ClN_4OTi$: C, 66.87; H, 4.30; N, 10.40. Found: C, 66.73; H, 4.08; N, 10.23.

η^5--Pentamethylcyclopentadienyl[N-(2-(1H-benzo[d]imidazol-2-yl)quinolin-8-yl)-4-methylbenzamide] chlorotitanium (C8)

Using the same procedure for the synthesis of **C1**, **C8** was obtained as a dark red solid in 62% yield. ^{1}H NMR ($CDCl_3$, 300 MHz): δ 8.35 (d, *J* = 8.4 Hz, 1H), 8.22 (d, *J* = 8.44 Hz, 1H), 7.79 (d, *J* = 8.1 Hz, 1H), 7.74 (d, *J* = 8.1 Hz, 1H), 7.40 (d, *J* = 7.9 Hz, 2H), 7.26-7.24 (m, 1H), 7.20-7.16 (m, 1H), 7.14-7.12 (m, 2H), 6.99 (d, *J* = 7.9 Hz, 2H), 6.39-6.36 (m, 1H), 2.27 (s, CH_3, 3H), 1.93 (s, CH_3, 15H). ^{13}C NMR ($CDCl_3$, 75 MHz): δ 179.4, 157.2, 150.8, 149.7, 148.6, 145.2, 141.7, 141.5, 141.4, 136.5, 133.7, 129.9, 129.3, 129.2, 129.1, 128.5, 128.3, 124.3, 122.5, 120.1, 119.2, 118.9, 117.9, 116.7, 21.6, 12.8. Anal. Calcd for $C_{34}H_{31}ClN_4OTi$: C, 68.64; H, 5.25; N, 9.42. Found: C, 68.51; H, 5.02; N, 9.24.

Bis{η^5-cyclopentadienyl[N-(2-(1H-benzo[d]imidazol-2-yl)quinolin-8-yl)benzamide]titanium}(μ-oxo) (C9)

To a stirred solution of *N*-(2-(1*H*-benzo[*d*]imidazol-2-yl)quinolin-8-yl)benzamide (0.728 g, 2.00 mmol) in dried THF (30 mL) at -78 °C, KH (0.160 g, 4.00 mmol) suspending in 20 mL THF was added. The mixture was allowed to warm to room temperature and stirred for additional 2 h. The mixture was cooled to -78 °C and 20 mL of $CpTiCl_3$ (0.438, 2.00 mmol) solution in THF was added

for references, see page 49

dropwise over a 30 min period. The resultant mixture was allowed to warm to room temperature and stirred for additional 12 h. The residue, obtained by removing the solvent under vacuum, was extracted with CH_2Cl_2 (3 × 20 mL) and the combined filtrates were concentrated in vacuum to reduce the volume to 20 mL. Heptane (45 mL) was layered and the solution was opened to air. Bright red crystals were obtained one week later (0.629 g, yield 55%). ^{1}H NMR ($CDCl_3$, 300 MHz): δ 8.43 (d, J = 8.4 Hz, 2H), 8.25 (d, J = 8.1 Hz, 2H), 7.81 (d, J = 7.9 Hz, 2H), 7.70 (d, J = 8.1 Hz, 2H), 7.65 (d, J = 7.7 Hz, 4H), 7.42 (m, 2H), 7.29-7.27 (m, 8H), 7.18 (d, J = 7.7 Hz, 4H), 6.74 (s, Cp, 10H), 6.36-6.34 (m, 2H). ^{13}C NMR ($CDCl_3$, 75 MHz): δ 179.3, 156.9, 152.2, 148.1, 146.7, 143.6, 143.0, 141.6, 134.2, 131.2, 130.5, 129.1, 128.0, 126.1, 123.3, 122.9, 122.0, 121.1, 119.5, 118.3, 117.8, 116.9. Anal. Calcd for $C_{56}H_{38}N_8O_3Ti_2$: C, 69.58; H, 3.96; N, 11.59. Found: C, 69.48; H, 3.99; N, 11.22.

3.3.5 Procedures for Ethylene Polymerization and Copolymerization ethylene with α-olefin

A 250-mL autoclave stainless steel reactor equipped with a mechanical stirrer and a temperature controller was heated in vacuum for at least 2 hrs over 80 °C. It was allowed to cool to the required reaction temperature under ethylene atmosphere and then charged with toluene (with monomer), the desired amount of co-catalyst and a toluene solution of the catalytic precursor. The total volume was 100 mL. After reaching the reaction temperature, the reactor was sealed and pressurized to 10 atm of ethylene pressure. The ethylene pressure was kept constant during the reaction time by feeding the reactor with ethylene. After a period of desired reaction time, the polymerization reaction was quenched by addition of acidic ethanol. The precipitated polymer was washed with ethanol several times and dried in vacuum.

3.3.6 X-ray Structure Determinations

Crystals of **L5** suitable for single-crystal X-ray analysis were obtained by re-crystallization from its $CHCl_3/CH_3OH$ solution. Crystals of **C2** and **C8** suitable for single-crystal X-ray analysis were obtained by laying heptane on their CH_2Cl_2 solutions. Crystals of **C9** suitable for single-crystal X-ray analysis were obtained by slowly laying heptane on CH_2Cl_2 solutions of complex **C3** respectively, and then opening these solutions to air for one week. Single-crystal X-ray diffraction for **L5**, **C2**, **C8** and **C9** were performed on a Rigaku RAXIS Rapid IP diffractometer with graphite-monochromated Mo Kα radiation (λ = 0.71073 Å) at 173(2) K. Cell parameters were obtained by global refinement of the positions of all collected reflections. Intensities were corrected for Lorentz and polarization effects and empirical absorption. The structures were solved by direct methods and refined by full-matrix least-squares on $F2$. All non-hydrogen atoms were refined anisotropically. Structure solution and refinement were performed by using the SHELXL-97 package.[20] Crystal data collection and refinement details for all compounds are given in Table 1. CCDC-716519 (**L5**), 716520 (**C2**), 716521 (**C8**) and - 716521 (**C9**) contain the supplementary crystallographic data for this paper, which could be obtained free of charge from the Cambridge Crystallographic Data Centre via www.ccdc.cam.ac.uk/data_request/cif.

for references, see page 49

Table 1. Crystallographic Data and Refinement Details for **L5**, **C2**, **C8** and **C9**

	L5·$CHCl_3$	**C2**	**C8**·CH_2Cl_2	**C9**·$2CH_2Cl_2$
Formula	$C_{23}H_{15}ClN_4O$ ·$CHCl_3$	$C_{29}H_{21}ClN_4OTi$	$C_{34}H_{31}ClN_4OTi$ ·CH_2Cl_2	$C_{28}H_{19}N_4O_{1.5}Ti$ ·$2CH_2Cl_2$
formula wt	518.21	524.85	679.90	653.22
T (K)	173(2)	173(2)	173(2)	173(2)
wavelength (Å)	0.71073	0.71073	0.71073	0.71073
Cryst syst	Orthorhombic	Tetragonal	Triclinic	Rhombohedral
space group	*Pccn*	*I-4*	*P-1*	*R-3c*
a (Å)	20.930(4)	26.828(4)	7.4299(1)	20.488(3)
b (Å)	21.246(4)	26.828(4)	12.994(3)	20.488(3)
c (Å)	10.232(2)	7.5448(1)	16.170(3)	74.947(1)
α (deg)	90	90.00	89.02(3)	90.00
β (deg)	90	90.00	85.33(3)	90.00
γ (deg)	90	90.00	84.78(3)	120.0
V (Å^3)	4550.0(2)	5430.2(1)	1549.5(5)	27245(8)
Z	8	8	2	36
D_{calcd} (g cm^{-3})	1.513	1.284	1.457	1.433
μ (mm^{-1})	0.547	0.441	0.572	0.668
F (000)	2112	2160	704	11988
θ range (deg)	1.37-27.43	2.40-27.40	2.01-27.35	1.58-25.00
Limiting indices	-27<=h<=27 -27<=k<=27 -13<=l<=13	-34≤h≤34 -34≤k≤34 -9≤k≤9	-8≤h≤9 -16≤k≤16 -20≤k≤20	-20≤h≤20 -24≤k≤24 -88≤k≤88
no. of rflns collected	9810	6013	12608	10200
no.of unique rflns	5189	6012	6978	5347
completeness to θ (%)	100.0 (θ = 27.43°)	99.8 (θ = 27.40°)	99.5 (θ = 27.35°)	99.9 (θ = 25.00°)
abs cor	Empirical	Empirical	Empirical	Empirical
no. of params	298	325	397	366
goodness of fit on F^2	1.008	0.780	1.231	0.892
final R indices (I > 2σ(I))	R1 = 0.0509 wR2 = 0.0955	R1 = 0.0364 wR2 = 0.0844	R1 = 0.0809 wR2= 0.1550	R1 = 0.0753 wR2 = 0.1883
R indices (all data)	R1 = 0.1053 wR2 = 0.1101	R1 = 0.0478 wR2 = 0.0871	R1 = 0.1034 wR2= 0.1639	R1 = 0.1265 wR2 = 0.2051
Largest diff peak, hole (e Å^{-3})	0.573 and -0.488	0.244 and -0.324	1.103 and -0.761	0.898 and -0.861

3.4 Results and Discussion

3.4.1 Synthesis and Characterization of *N*-((benzimidazol-2-yl)quinolin-8-yl)benzamide Derivatives

The *N*-((benzimidazol-2-yl)quinolin-8-yl)benzamide derivatives act as dianionic tridentate ligands, and contain two types of functional groups i.e. carboxamide and benzimidazole. It is necessary to first create the carboxamide part, due to its stability during the formation of the benzimidazole moiety. In fact, the transformation of 2-methylquinolin-8-amine into 2-benzimidazole-quinoline will cause the amidocyanogen of amine group. There are several methods employed for the formation of the carboxamide.[19,21] The condensation reaction of 2-methylquinolin-8-amine and substituted benzoic acid in refluxing xylene directly formed a series of *N*-(2-methylquinolin-8-yl)benzamide derivatives (Scheme 1), but it is necessary to employ the triphenyl phosphite as dehydrating agent.[19,21a]

for references, see page 49

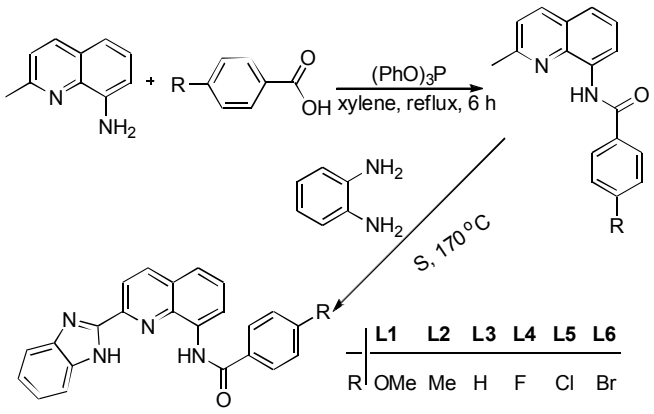

Scheme 1. Synthesis of ligands **L1-L6**.

Using literature procedures,[17,22] the reaction of solid *o*-phenylenediamine and *N*-(2-methylquinolin-8-yl)benzamide with sulfur oxidant provided the desired *N*-((benzimidazol-2-yl)quinolin-8-yl)benzamides in acceptable yields. All these organic compounds were routinely characterized and confirmed with elemental, IR spectroscopic, NMR analyses. For compound **L1**, in the IR spectra the strong and sharp peak of 1658 cm^{-1} can be ascribed to the stretching vibration of C=O, while δ 10.58 and 10.30 ppm in the low field of ^1H NMR spectrum could be ascribed to two N-H of benzimidazole and amide, respectively. Similar characteristics could be observed for other compounds **L2-L6**. In addition, the absolute structure of **L5** was further confirmed by X-ray analysis.

Crystals of **L5** suitable for single-crystal X-ray analysis were obtained by re-crystallization from its $CHCl_3/CH_3OH$ solution. The molecular structure was illustrated in Figure 1, and the selected bonds and angles were listed in Table 2. In the solid state of **L5**, one $CHCl_3$ molecule was incorporated. The bond lengths of C17-O1 (1.213(3) Å) and C17-N4 (1.375(3) Å) were in the typical value ranges of amide groups. The dihedral angle defined by the benzimidazole ring and the quinoline ring was 18.9°, while one of the phenyl ring on carbonyl with quinoline ring was 57.4°.

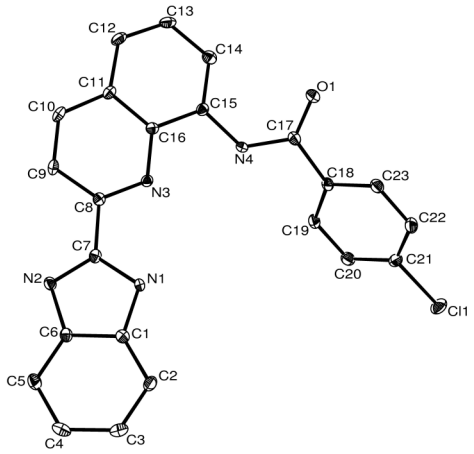

Figure 1. Molecular structure of **L5**. Thermal ellipsoids are shown at the 30% probability level. Hydrogen atoms and the chloroform molecule have been omitted for clarity.

for references, see page 49

Table 2. Selected Bonds (Å) and Angles (°) for **L5**

Bond Lengths			
N1-C7	1.356(3)	N3-C8	1.323(3)
N2-C7	1.322(3)	C15-C16	1.425(3)
N3-C16	1.365(3)	C17-N4	1.375(3)
N4-C15	1.414(3)	C17-O1	1.213(3)
Bond Angles			
C7-N1-C1	106.8(2)	C8-N1-C16	117.7(2)
C15-N1-C17	125.6(2)	N4-C17-O1	123.0(2)
N4-C17-C18	115.3(2)	C18-C17-O1	121.7(2)

3.4.2 Synthesis and Characterization of Half-titanocene Complexes

These *N*-((benzimidazol-2-yl)quinolin-8-yl)benzamides derivatives could coordinate as dianionic tridentate ligands. However, the direct reaction of these compounds with half-titanocene trichlorides did not form the desired complexes. It was necessary to deprotonate *N*-(benzimidazol-2-yl)quinolin-8-yl)benzamides derivatives by using potassium hydride to form dianionic potassium intermediate in tetrahydrofuran (THF) at -78 °C according to reported procedures.[18,23] Treating the obtained potassium salt with one equivalent of $Cp'TiCl_3$ in THF at -78 °C, followed by stirring at room temperature for 12 h, afforded dark red solutions. Dark red crystals for pure half-titanocene complexes with components of Cp'TiLCl (Cp' = C_5H_5, MeC_5H_4, or C_5Me_5; L = *N*-(benzimidazoly-quinolin-8-yl)benzamides; **C1-C8**) (Scheme 2) were obtained after recrystallization. Considering the synthetical process and the purification procedure, it is obvious that our catalysts have advantages compared to the bridged half-metallocene catalysts.[3] The elemental and NMR spectroscopic analyses confirmed their structures. For complex **C1**, the peaks at δ 10.58 ppm and 10.30 ppm of ^{1}H NMR which observed in compound **L1** disappeared, which confirmed the formation of Ti-N bonds in complexation. Similar characteristics were also observed for other complexes **C2-C8**. Several complexes were further characterized by X-ray analysis to confirm their real molecular structures.

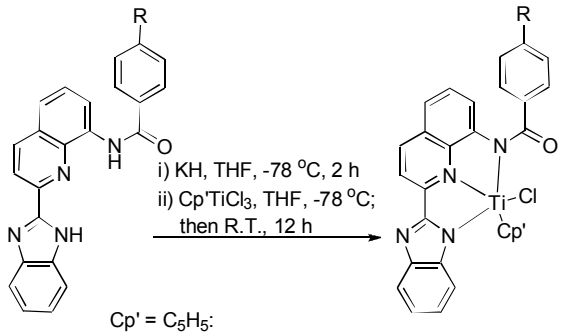

Cp' = C_5H_5:
C1, R = OMe; **C2**, R = Me; **C3**, R = H;
C4, R = F; **C5**, R = Cl; **C6**, R = Br;
Cp' = MeC_5H_5: **C7**, R = Me;
Cp' = C_5Me_5: **C8**, R = Me

Scheme 2. Synthesis of Complexes **C1-C8**

It was not surprising that the complexes with cyclopentadienyl (Cp) group were not stable enough

for references, see page 49

in solution.[18,24] When the CH_2Cl_2/heptane solution of **C3** was standing in air, its color was slowly changed from dark red to bright red; after one week in the air, bright-red crystals were obtained, which were analyzed and confirmed by single crystal X-ray diffraction to be the oxo-bridged bimetallic complex **C9** (Scheme 3). The newly formed oxo-bridged dimeric complex was very stable, consistent with our previous observation.[18] X-ray diffraction analysis reveals that, in addition to the formation of bridging Ti-O bonds, both of the two remaining amide oxygen atoms coordinate to the neighboring Ti atoms to form two six-coordinated Ti centers. Similar coordination between Ti and carbonyl oxygen atoms were once reported to form more stable complexes.[25]

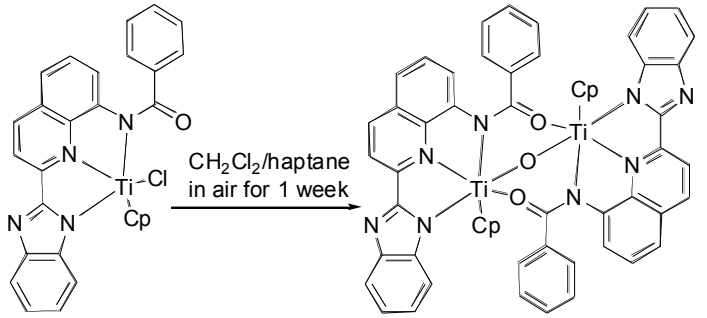

Scheme 3. Formation of Oxo-bridged Dimeric Complex **C9**

3.4.3 X-ray Crystallographic Analysis of Complexes C2, C8 and C9

Crystals of **C2** and **C8** suitable for single-crystal X-ray analysis were grown by slow diffusion of heptane into the CH_2Cl_2 solutions of **C2** and **C8**.Their molecular structures are illustrated in Figure 2 and 3, and the selected bonds and angles are shown in Table 3. In the solid state of **C8**, one CH_2Cl_2 molecule was incorporated without direct interaction with the metal center.

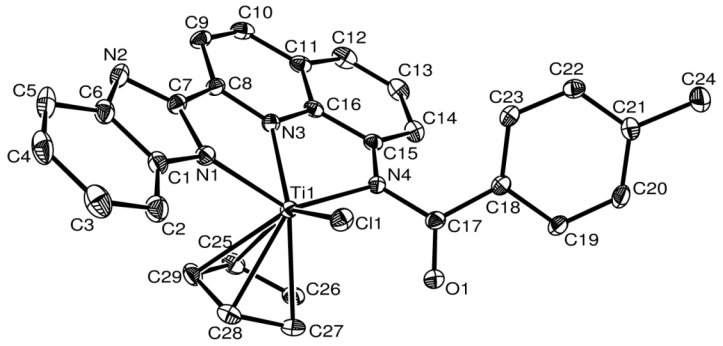

Figure 2. Molecular structure of complex **C2**. Thermal ellipsoids are shown at the 30% probability level. Hydrogen atoms have been omitted for clarity.

Figure 2 shows the molecular structure of **C2** with titanium coordinating to a chlorine atom, a Cp in η^5-binding fashion and a dianionic tridentate *N*-((benzimidazol-2-yl)quinolin-8-yl)-4-methylbenzamide ligand. It possesses a similar coordination feature with that in half-titanocene complex bearing dianionic 6-benzimidazolylpyridyl-2-carboximidate ligands.[18]

for references, see page 49

Table 3. Selected Bonds (Å) and Angles (°) for **C2** and **C8**

	C2	**C8**
	Bond Lengths	
Ti1-N1	2.111(1)	2.131(3)
Ti1-N3	2.145(1)	2.147(3)
Ti1-N4	2.101(2)	2.103(3)
Ti1-C25	2.356(3)	2.381(3)
Ti1-C26	2.346(3)	2.392(3)
Ti1-C27	2.351(3)	2.410(3)
Ti1-C28	2.381(3)	2.411(3)
Ti1-C29	2.391(3)	2.373(3)
Ti1-Cl1	2.268(8)	2.271(1)
	Bond Angles	
N1-Ti1-N3	72.08(7)	71.14(1)
N1-Ti1-N4	136.83(8)	133.33(1)
N3-Ti1-N4	71.82(8)	72.41(1)
Cl1-Ti1-N1	90.70(7)	91.51(9)
Cl1-Ti1-N3	129.65(6)	134.08(8)
Cl1-Ti1-N4	94.47(6)	93.43(9)

The chlorine atom (Cl1) stretches away from both the Cp ring and the ancillary ligand and the Ti1-Cl1 bond length is 2.268(8) Å, similar to the values found in related complexes.[18, 26] The distance between the centroid of the Cp ring and titanium is 2.0382 Å, consistent with values observed in similar complexes.[18,26] Notably, the Ti-C bond lengths (Ti1-C25; Ti1-C26; Ti1-C27; Ti1-C28; Ti1-C29) differ significantly, ranging from 2.346(3) to 2.391(3) Å (ΔTi-C = 0.045 Å), with one short, two medium, and two long bonds, indicating that the difference in Ti-C bond lengths reflected the different *trans* influence of the donor atoms in the basal plane. In contrast, there is only one single peak (6.73 ppm, s, 5H) for Cp in ^{1}H NMR and 122.0 ppm in ^{13}C NMR, suggesting no difference in its solution state. The *N*-(benzimidazolyl-quinolin-8-yl)-4-methylbenzamide ligand, in which one deprotonated benzimidazole-*N* atom, one quinoline-*N* atom and one deprotonated amide-*N* atom coordinated to the central metal, adopts a puckered chelating style with the dihedral angle defined by the two chelating rings (Ti1-N1-C7-C8-N3, Ti1-N3-Cl6-Cl5-N4) at 17.0°. The dihedral angle of the benzimidazole ring and the quinoline ring is 8.4°, which is much smaller than that of ligand **L5** due to chelation to metal center. The angles N1-Ti1-N3 and N3-Ti1-N4 are approximately same at 72.08(7)° and 71.82(8)° with a sum of 143.90(5)°, which is somewhat larger than the bite angle (N1-Ti1-N4 = 136.83(8)°). The three types of Ti-N bonds (Ti1-N1 = 2.112(1) Å, Ti1-N3 = 2.145(1) Å, Ti1-N4 = 2.101(2) Å) are in the common range for titanium complexes, but slightly different due to their different chemical environments. The distance between Ti1 and O1 is 3.222(2) Å, which is longer than the sum of titanium and oxygen radii, indicating no interaction between these two atoms. The *p*-methyl-substituted phenyl group was situated far away from the titanium center and the dihedral angle defined by Ti1-N1-C7-C8-N3-C16-C15-N4 ring and the phenyl group was 62.0°.

for references, see page 49

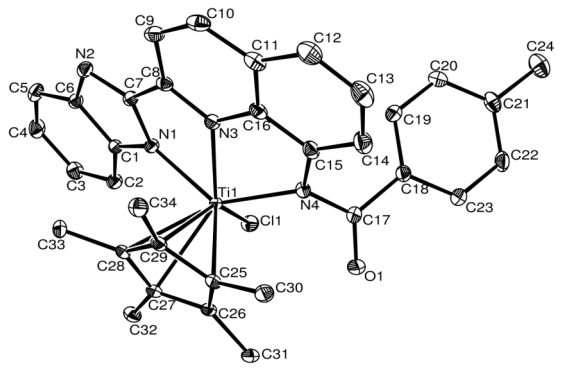

Figure 3. Molecular structure of complex **C8**. Thermal ellipsoids are shown at the 30% probability level. Hydrogen atoms and the dichloromethane molecule have been omitted for clarity.

Complex **C8** (Figure 3) possesses a similar coordination feature as that in **C2**, despite the substituents on the Cp ring. Notably, the distance between the centroid of the Cp^* ring and titanium was 2.066 Å, a little longer than that in **C2**, due to more hindrance around the metal center derived from Cp^* than Cp, leading to the angles N1-Ti1-Cl1 and N3-Ti1-Cl1 in **C8** somewhat larger than those in its analogue **C2** (91.51(9)° *v*s 90.70(7)°; 134.08(8)° *v*s 129.65(6)°). Such steric hindrance at the metal center made **C8** robust even in contact with air for long time regardless in solution or solid state, consistence with our previous results.[18] Actually, even complex **C2**, without substituents on its Cp moiet, can survive in the air for a long time. As far as the stability, the half-titanocene we present here are more similar as metallocene catalysts rather than complex catalysts. However, such steric hindrance of the Cp^* ring will reduce the space for olefin coordination and insertion, therefore, causing lower catalytic activities.

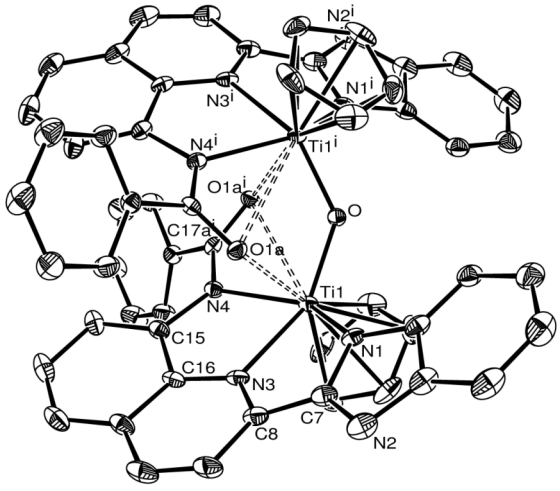

Figure 4. Molecular structure of complex **C9**. Thermal ellipsoids are shown at the 30% probability level. Hydrogen atoms and solvent molecules have been omitted for clarity.

for references, see page 49

Table 4. Selected Bonds (Å) and Angles (°) for **C9**

Bond Lengths			
Ti1-N1	2.108(5)	Ti1-N3	2.171(4)
Ti1-N4	2.164(4)	Ti1-O	1.814(2)
Ti1-O1A	2.444(4)	Ti1-C24	2.427(6)
Ti1-C25	2.427(6)	Ti1-C26	2.431(6)
Ti1-C27	2.394(6)	Ti1-C28	2.371(6)
C17-O1	1.237(6)	C17-N4	1.353(7)
Bond Angles			
N1-Ti1-N3	73.13(18)	N1-Ti1-N4	141.44(17)
N3-Ti1-N4	72.90(17)	N1-Ti1-O	99.17(15)
N3-Ti1-O	145.74(16)	N4-Ti1-O	98.64(18)
N1-Ti1-O1A	74.48(15)	N3-Ti1-O1A	68.43(14)
N4-Ti1-O1A	76.50(15)	O-Ti1-O1A	77.33(13)

Crystals of **C9** suitable for single-crystal X-ray analysis were obtained by layering heptane on CH_2Cl_2 solutions of complex **C3**, and then opening this solution to air for one week. The molecular structure was shown in Figure 4 and the selected bond lengths and angles were summarized in Table 4, respectively. The molecular structure of **C9** show a binuclear species bridged by an oxygen atom (O). Each titanium is bonded to one *N*-((benzimidazol-2-yl)quinolin-8-yl)-4-methylbenzamide ligand, one bridging oxygen atom and also one carbonyl oxygen atom from the neighboring ligand. Inspection of the carbonyl CO bond distances in **C9** indicates that coordination of oxygen to titanium results in a lengthening of the CO (C17-O1 = 1.237(6) Å) bond relative to the uncoordinated carbonyl oxygen in the mononuclear titanium complex **C2** (C17-O1 = 1.214(3) Å) and in the free ligand **L5** (C17-O1 = 1.213(3) Å). The effect of coordination of the carbonyl oxygen to the titanium is also evident from the changes in amide C-N bonds (C17-N4 = 1.404(5) Å in **C2** *v*s C17-N4 = 1.353(7) Å in **C9**). However, comparing with the data in Table 3, other structural parameters including bond lengths and bond angles are similar as those found in **C2**.

3.4.4 Ethylene Polymerization

The newly obtained complexes (**C1-C8**) were studied with methylaluminoxane (MAO) as cocatalyst for the polymerization of ethylene to examine their catalytic performance. Table 5 lists the results of ethylene polymerization with **C1-C8**/MAO systems at 10 atm of ethylene.

for references, see page 49

Table 5. Ethylene Polymerization with **C1-C8**/MAO[a]

Entry	Complex	Polymer (g)	Activity (10^6 g·mol^{-1}(Ti)·h^{-1})	M_w[b] (kg·mol^{-1})	M_w/M_n[b]
1	**C1**	1.53	12.2	65.4	2.30
2	**C2**	1.11	8.88	80.9	2.19
3	**C3**	1.01	8.08	109	3.03
4	**C4**	0.925	7.40	148	3.39
5	**C5**	0.718	5.74	134	2.95
6	**C6**	0.704	5.63	93.8	2.53
7	**C7**	1.05	8.40	85.5	2.68
8	**C8**	0.904	7.23	98.2	2.71

[a] Conditions: 0.5 μmol of catalysts; 10 atm ethylene; Al/Ti = 30000; 80 °C; 15 min; toluene (total volume 100 mL). [b] Determined by GPC.

Effect of the Ligand Environment on the Catalytic Behavior

The literature reported that half-titanocene systems showed the best activities around 10^5 g·mol^{-1}(Ti)·h^{-1}-10^6 g·mol^{-1}(Ti)·h^{-1} under mild conditions.[13,16e] Some of them, even under more drastic conditions (Al/Ti = 20000), exhibited no increase in catalytic activities. However, each of the catalyst systems examined here was found to be highly active, 5.63×10^6 g·mol^{-1}(Ti)·h^{-1}-12.2×10^6 g·mol^{-1}(Ti)·h^{-1}. Although our polymerization conditions are different from those of previous works, these activity values indicated that the newly developed catalysts are more active than the reported ones. The catalytic activities varied in the order of **C1** (with OMe substituent) > **C2** (with Me) > **C3** (with H) > **C4-C6** (with halides). These differences of activities among **C1-C6**/MAO systems are attributed to the electronic rather than the steric effect of the substituted group, because they are located far away from the central metal. These observations indicate that the electron donation from OMe and Me groups, increasing the electron density at the central metal, would stabilize the active center of olefin polymerization catalysts, which should be a cation including a methyl alkyl and a *cis*-located vacant coordination site for monomer binding, thus enhancing the activity.[27] In terms of the molecular weights of the obtained polyethylene, a reversed order was observed. The complexes containing electron-withdrawing groups (**C4-C6**) on the ancillary ligand generally yielded polyethylene with much higher molecular weights than those with electron-donating groups (**C1** and **C2**). Similar phenomenon was also observed in our previous catalytic systems.[8g,18] In addition, the M_w values were in the range of 65.4 to 148 kg·mol^{-1}, which were three times higher than those prepared by 6-benzimidazolylpyridyl-2-carboximidate half-titanocene complexes under similar polymerization conditions.[18] On the other hand, the substituents on the Cp' groups also affect catalytic activities and polymer properties. Complex **C2** containing Cp group without additional substituents exhibited higher activity than its analogues **C7** and **C8** (entry 2 *v*s 7 and 8, Table 5). The methyl substitutions on Cp groups appear to have mainly steric effects, which results in decreasing activity due to steric hindrance slowing down the insertion of monomer and the propagation rate. This is in agreement with the improved stability found in Cp* analogues, in which the metal center was efficiently protected from

for references, see page 49

the attack by the impurities. A similar trend was also observed in our previous 6-benzimidazolylpyridyl-2-carboximidate half-titanocene system.[18] As shown in Table 5, the introduction of methyl groups on Cp has led to increased polymer molecular weights (entry 2 *vs* 7 and 8, Table 5) and this can be explained by the steric effect of substituted Cp group, which has reduced the chain termination and transfer rate relative to the olefin insertion in the polymerization process.[28] Taken together, these findings demonstrate that very subtle changes in catalyst structure can lead to dramatic differences in catalytic properties. Complex **C9** has also been examined as catalytic precursor for ethylene polymerization, however, it was inactive under various reaction conditions. The cuase is the high stability of oxo-bridged titanium complexes, in which the Ti-O bonds are too stable to be activated by cocatalyst.

Effects of Al/Ti Molar Ratio and Reaction Temperature on the Catalytic Behaviors of C1

As the catalytic system of **C1**/MAO showed better activities than others, the detailed investigation of reaction parameters on the catalytic properties was carried out with complex **C1** (Table 6). Complex **C1** was able to show activity (~10^4 g·mol^{-1}(Ti)·h^{-1}) for ethylene polymerization since from Al/Ti ratio of 500 and it can make moderate performance (~10^5 g·mol^{-1}(Ti)·h^{-1}) when the ratio of Al/Ti was 1500. To study the effect of various MAO concentrations on the catalytic behavior of the **C1**/MAO system and to obtain even higher catalytic activities, the polymerizations were carried out at different Al/Ti ratios ranging from 10000 to 40000 (entries 1-6, Table 6). It is obvious that higher Al/Ti molar ratio is favorable for ethylene polymerization. The activities increased from 3.48 ×10^6 g·mol^{-1}(Ti)·h^{-1} at Al/Ti molar ratio of 10000 to 12.2 × 10^6 g·mol^{-1}(Ti)·h^{-1} with 30000 eq MAO, and a little decrease to 11.5 × 10^6 g·mol^{-1}(Ti)·h^{-1} with 40000 eq MAO. Such properties can be well clarified by the influence of Al concentration on the termination of polymer chains.[29] The GPC analysis revealed that the obtained polyethylene possesses M_w value in the range of 53.8 to 78.6 kg·mol^{-1} and molecular weight distribution ranging from 2.13 to 2.50. However, no obvious influence of Al/Ti molar ratio on M_w and M_w/M_n was observed.

Table 6. Ethylene Polymerization with **C1**/MAO[a]

Entry	Al/Ti	*T* (°C)	Polymer (g)	Activity (10^6 g·mol^{-1}(Ti)·h^{-1})	M_w[b] (kg·mol^{-1})	M_w/M_n[b]
1	10000	80	0.435	3.48	78.6	2.36
2	20000	80	0.677	5.42	70.9	2.45
3	25000	80	0.933	7.46	75.7	2.36
4	30000	80	1.53	12.2	65.4	2.30
5	35000	80	1.45	11.6	53.8	2.13
6	40000	80	1.44	11.5	68.6	2.50
7	30000	20	0.05	0.40	85.9	2.18
8	30000	40	0.288	2.30	78.9	3.37
9	30000	60	0.534	4.27	73.2	2.29

[a] Conditions: 0.5 μmol of catalysts; 10 atm ethylene; 15 min; toluene (total vol. 100 mL). [b] Determined by GPC.

for references, see page 49

According to the data in Table 6, the reaction temperature had a remarkable influence on the catalytic activity. The catalytic activity was very low at 20 °C, but it greatly increased at 40 °C and remained stable up to 80 °C. It was surprising that the activity at 80 °C (entry 4, Table 6) was 30 times higher than that at 20 °C (entry 7, Table 6). The repeated experiments displayed the same results. This observation was consistent with our previous reports,[8g,18] while it was in contrast to the traditional metallocene catalysts,[4] which usually exhibited lower activity at elevated temperatures due to decomposition of catalysts, and traditional FI catalysts, which showed better activity around 50 °C.[6-7] A similar trend was observed in mono-Cp aryloxide or arylsulfide titanium systems and it was said that the active species can be quite stable and persist over 60 min under 70 °C.[16e] However, the thermal stability of current catalytic system showed the potential to fit the industrial polymerization requirements, because the liquefiable polymerization at high temperature favored the viscosity of the reaction mixture with better mass transportation and temperature control.[8g,18] The resultant polyethylene showed reduced molecular weights with elevating temperatures, consistent with the titanium bis(6-benzimidazolylpyridyl-2-carboximidate) system[8g] and traditional metallocene catalysts.[4] Taking all the earlier results into account, it is clear that harsher conditions were propitious to ethylene polymerization, exhibiting higher activities without serious decrease in M_w.

3.4.5 Ethylene/1-hexene and Ethylene/1-octene Copolymerization

Linear low-density polyethylenes (LLDPE), which contain a low amount of short chain branches along the polymer backbone, are produced by the copolymerization of ethylene with 1-hexene or 1-octene.[4d,30] Introduction of short chain branches along the polyethylene backbone leads to lower regularity in the chain structure, and thus lower density, crystallinity and melting point, which make them have a great industrial interest and can be applied in packing, shrink flms and cable coatings. Complexes **C1-C8** had good performance on ethylene homopolymerization, which arose our inquisitive to investigate their catalytic properties for copolymerization of ethylene with 1-hexene and 1-octene. The results are summarized in Table 7.

Table 7. Copolymerization of ethylene with 1-hexene or 1-octene by **C1-C8**/MAO[a]

Entry	Complex	Polymer (g)	Activity[d]	Entry	Complex	Polymer (g)	Activity[d]
1[b]	**C1**	1.10	8.80	9[c]	**C1**	1.05	8.40
2[b]	**C2**	0.930	7.44	10[c]	**C2**	0.914	7.31
3[b]	**C3**	0.901	7.21	11[c]	**C3**	0.821	6.57
4[b]	**C4**	0.796	6.37	12[c]	**C4**	0.775	6.20
5[b]	**C5**	0.666	5.33	13[c]	**C5**	0.728	5.82
6[b]	**C6**	0.652	5.22	14[c]	**C6**	0.776	6.21
7[b]	**C7**	0.766	6.13	15[c]	**C7**	0.795	6.36
8[b]	**C8**	0.672	5.38	16[c]	**C8**	0.612	4.90

[a] Conditions: 0.5 μmol of catalysts; 10 atm ethylene; Al/Ti = 30000; 80 °C; 15 min; toluene (total volume 100 mL). [b] 1 mL 1-hexene was added. [c] 1 mL 1-octene was added. [d] 10^6 g·mol^{-1}(Ti)·h^{-1}.

for references, see page 49

All the catalysts showed high catalytic activities toward ethylene/1-hexene copolymerization and their catalytic activities varied with ligand environment in the same order as that in ethylene homopolymerization. DSC analysis of the resultant copolymers showed one sole melting point around 126 °C, which is lower than that of ethylene homopolymer (around 134 °C) produced under similar conditions. This indicated that the obtained polymeric sample was really poly (ethylene-1-hexene).[31] The ^{13}C NMR spectrum of ethylene/1-hexene copolymer produced by **C1**/MAO system (entry 1, Table 7) is shown in Figure 5, and it revealed about 2 mol% of 1-hexene being incorporated. The monomer sequence distributions determined by the ^{13}C NMR spectrum showed that the obtained poly (ethylene-1-hexene) contained isolated 1-hexene units, EHE, EHEE+EEHE, HEEE+EEEH etc.[32] GPC analysis revealed that the ethylene/1-hexene copolymers possessed much higher molecular weight (161 kg·mol^{-1}; entry 1, Table 7) than polyethylene that was produced under identical conditions (65.4 kg·mol^{-1}; entry 1, Table 5).

When compared to the structurally similar catalyst,[13a] although they were performed under different conditions, the current one possessed higher copolymerization activity and produced polymer of higher molecular weights. DSC and ^{13}C NMR analysis revealed that the title complexes possessed relatively lower 1-hexene incorporation ability. The steric hindrance from the bulky tridentate ligand could probably be the reason for such observation. It was reported that the bidentate cylopentadienyl phenoxy-imine titanium complexes showed 1-hexene incorporation upto 4.34 mol% and less bulky monodentate cyclopentadienyl ketimide titanium complexes exhibited a more than 20 mol% incorporation of 1-hexene.[13a,33]

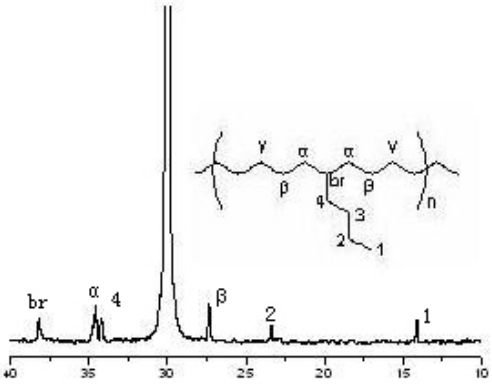

Figure 5. ^{13}C NMR spectrum of ethylene/1-hexene copolymer by **C1**/MAO system (entry 1, Table 7)

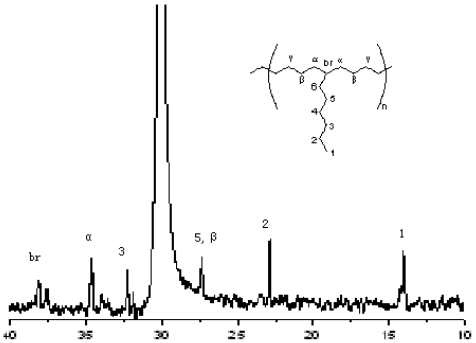

Figure 6. ^{13}C NMR spectrum of ethylene/1-octene copolymer by **C1**/MAO system (entry 9, Table 7)

for references, see page 49

Ethylene/1-octene copolymerizations were also studied under the same conditions and the results are illustrated in Table 7. When compared to ethylene/1-hexene copolymerization, slightly lower catalytic activities were observed (entry 9 *v*s entry 1, Table 7). Similarly to the ethylene/1-hexene copolymerization, DSC analysis of the resultant copolymers showed one sole melting point around 130 °C, which is lower than that of ethylene homopolymer (around 134 °C) but higher than that of ethylene/1-hexene copolymer (around 126 °C) produced under similar conditions. Figure 6 shows the ^{13}C NMR spectrum of ethylene/1-octene copolymer produced by **C1**/MAO system (entry 9, Table 7), and it indicated a 1.3 mol% incorporation of 1-octene. GPC analysis of the same sample (entry 9, Table 7) showed a molecular weight of 316 kg·mol^{-1} and PDI value of 2.36.

3.5 Conclusions

The *N*-(2-benzimidazolylquinolin-8-yl)benzamidate half-titanocene complexes were synthesized by treating the potassium salts of the ligands with Cp'$TiCl_3$ and well characterized by ^1H NMR, ^{13}C NMR and elemental analyses. Moreover, single-crystal X-ray analysis of **C2**, **C8** and **C9** were undertaken in order to provide precise structural details. The CpTiLCl analogue (**C3**) can be transformed to its dimeric derivative $(CpTiL)_2O$ (**C9**), due to the Ti-Cl bond hydrolysis, while the Cp*TiLCl analogue was found to be robust even in contact with air for a long time and this is attributed to the introduction of substituents on the cyclopentadienyl groups. When activated with excess amounts of MAO, complexes **C1-C8** exhibited remarkable catalytic activities for ethylene polymerization, especially at elevated reaction temperature. Their catalytic activities varied in the order of **C1** (with OMe substituent) > **C2** (with Me) > **C3** (with H) > **C4-C6** (with halide), and the M_w values of obtained polymers is in reversed order. Meanwhile, the substituents on the Cp' groups also had a large influence on catalytic properties, with complexes bearing methyl substituents affording decreased activities but higher polymer molecular weights. Polymerization temperature has a strong effect on the catalytic activity, with higher temperature improving the productivity efficiently. When activated by MAO, the newly synthesized complexes also showed high catalytic activities toward ethylene/1-hexene and ethylene/1-octene copolymerization. The resultant copolymers possessed much higher molecular weights than polyethylene produced under identical conditions.

Acknowledgement

This work was supported by NSFC No.20874105. We are grateful to Dr. Sheriff Adewuyi for his kind assistance in polishing the English usage.

for references, see page 49

References and Notes

1. (a) Ziegler, K.; Holzkamp, E.; Breil, H.; Martin, H. *Angew. Chem.* **1955**, *67*, 541-547; (b) Ziegler, K.; Gellert, H. G. *Angew. Chem.* **1955**, *67*, 424-425; (c) Natta, G.; Pino, P.; Corradini, P.; Danusso, F.; Mantica, E.; Mazzanti, G.; Moraglio, G. *J. Am. Chem. Soc.* **1955**, *77*, 1708-1710; (d) Natta, G. *J. Polym. Sci.* **1955**, *16*, 143-154.
2. (a) Hogan, J. P.; Banks, R. L. U.S. Patent 2,825,721, **1958**; (b) Groppo, E.; Lamberti, C.; Bordiga, S.; Spoto, G.; Zecchina, A. *Chem. Rev.* **2005**, *105*, 115-183.
3. (a) Shapiro, P. J.; Bunel, E.; Schaefer, W. P.; Bercaw, J. E. *Organometallics* **1990**, *9*, 867-869; (b) Stevens, J. C.; Timmers, F. J.; Wilson, D. R.; Schmidt, G. F.; Nickias, P. N.; Rosen, R. K.; McKnight, G. W.; Lai, S. Eur. Pat. Appl. 0416815A2, **1991**; (c) Shapiro, P. J.; Cotter, W. D.; Schaefer, W. P.; Labinger, J. A.; Bercaw, J. E. *J. Am. Chem. Soc.* **1994**, *116*, 4623-4640; (d) Braunschweig, H.; Breitling, F. M. *Coord. Chem. Rev.* **2006**, *250*, 2691-2720.
4. (a) Sinn, H.; Kaminsky, W.; Vollmer, H. J.; Woldt, R. *Angew. Chem. Int. Ed. Engl.* **1980**, *19*, 390-392; (b) Sinn, H.; Kaminsky, W. *Adv. Organomet. Chem.* **1980**, *18*, 99-149; (c) Brintzinger, H. H.; Fischer, D.; Mülhaupt, R.; Rieger, B.; Waymouth, R. M. *Angew. Chem. Int. Ed. Engl.* **1995**, *34*, 1143-1170; (d) McKnight, A. L.; Waymouth, R. M. *Chem. Rev.* **1998**, *98*, 2587-2598; (e) Alt, H. G.; Köppl, A. *Chem. Rev.* **2000**, *100*, 1205-1221.
5. (a) Boffa, L. S.; Novak, B. M. *Chem. Rev.* **2000**, *100*, 1479-1493; (b) Ittel, S. D.; Johnson, L. K.; Brookhart, M. *Chem. Rev.* **2000**, *100*, 1169-1203; (c) Gibson, V. C.; Spitzmesser, S. K. *Chem. Rev.* **2003**, *103*, 283-315; (d) Sun, W.-H.; Zhang, D.; Zhang, S.; Jie, S.; Hou, J. *Kinet. Catal.* **2006**, *47*, 278-283; (e) Matsugi, T.; Fujita, T. *Chem. Soc. Rev.* **2008**, *37*, 1264-1277; (f) Sun, W.-H.; Zhang, S.; Zuo, W. *C. R. Chim.* **2008**, *11*, 307-316.
6. (a) Matsui, S.; Tohi, Y.; Mitani, M.; Saito, J.; Makio, H.; Tanaka, H.; Nitabaru, M.; Nakano, T.; Fujita, T. *Chem. Lett.* **1999**, 1065-1066; (b) Matsui, S.; Mitani, M.; Saito, J.; Tohi, Y.; Makio, H.; Matsukawa, N.; Takagi, Y.; Tsuru, K.; Nitabaru, M.; Nakano, T.; Tanaka, H.; Kashiwa, N.; Fujita, T. *J. Am. Chem. Soc.* **2001**, *123*, 6847-6856; (c) Makio, H.; Kashiwa, N.; Fujita, T. *Adv. Synth. Catal.* **2002**, *344*, 477-493; (d) Sakuma, A.; Weiser, M.-S.; Fujita, T. *Polym. J.* **2007**, *39*, 193-207.
7. (a) Tian, J.; Coates, G. W. *Angew. Chem. Int. Ed.* **2000**, *39*, 3626-3629; (b) Tian, J.; Hustad, P. D.; Coates, G. W. *J. Am. Chem. Soc.* **2001**, *123*, 5134-5135; (c) Mason, A. F.; Coates, G. W. *J. Am. Chem. Soc.* **2004**, *126*, 16326-16327; (d) Edson, J. B.; Wang, Z.; Kramer, E. J.; Coates, G. W. *J. Am. Chem. Soc.* **2008**, *130*, 4968-4977.
8. (a) Yoshida, Y.; Matsui, S.; Takagi, Y.; Mitani, M.; Nakano, T.; Tanaka, H.; Kashiwa, N.; Fujita, T. *Organometallics* **2001**, *20*, 4793-4799; (b) Yoshida, Y.; Mohri, J.; Ishii, S.; Mitani, M.; Saito, J.; Matsui, S.; Makio, H.; Nakano, T.; Tanaka, H.; Onda, M.; Yamamoto, Y.; Mizuno, A.; Fujita, T. *J. Am. Chem. Soc.* **2004**, *126*, 12023-12032; (c) Tsurugi, H.; Matsuo, Y.; Yamagata, T.; Mashima, K. *Organometallics* **2004**, *23*, 2797-2805; (d) Yoshida, Y.; Matsui, S.; Fujita, T. *J. Organomet. Chem.* **2005**, *690*, 4382-4397; (e) Tsurugi, H.; Mashima, K. *Organometallics* **2006**, *25*, 5210-5212; (f) Zuo, W.; Sun, W.-H.; Zhang, S.; Hao, P.; Shiga, A. *J. Polym. Sci., Part A: Polym. Chem.* **2007**, *45*, 3415-3430; (g) Liu, S.; Zuo, W.; Zhang, S.; Hao, P.; Wang, D.; Sun, W.-H. *J. Polym. Sci., Part A: Polym. Chem.* **2008**, *46*, 3411-3423.
9. Nomura, K.; Liu, J.; Padmanabhan, S.; Kitiyanan, B. *J. Mol. Catal. A: Chem.* **2007**, *267*, 1-29.
10. (a) Nomura, K.; Naga, N.; Miki, M.; Yanagi, K. *Macromolecules* **1998**, *31*, 7588-7597; (b) Nomura, K.; Naga, N.; Miki, M.; Yanagi, K.; Imai, A. *Organometallics* **1998**, *17*, 2152-2154.
11. Zhang, S.; Piers, W. E.; Gao, X.; Parvez, M. *J. Am. Chem. Soc.* **2000**, *122*, 5499-5509.
12. (a) Richter, J.; Edelmann, F. T.; Noltemeyer, M.; Schmidt, H.-G.; Shmulinson, M.; Eisen, M. S. *J. Mol. Catal. A: Chem.* **1998**, *130*, 149-162; (b) Sita, L. R.; Babcock, J. R. *Organometallics* **1998**, *17*, 5228-5230; (c) Vollmerhaus, R.; Shao, P.; Taylor, N. J.; Collins, S. *Organometallics* **1999**, *18*, 2731-2733; (d) Jayaratne, K. C.; Sita, L. R. *J. Am. Chem. Soc.* **2000**, *122*, 958-959.
13. (a) Huang, J.; Lian, B.; Qian, Y.; Zhou, W.; Chen, W.; Zheng, G. *Macromolecules* **2002**, *35*, 4871-4874; (b) Bott, R. K. J.; Hughes, D. L.; Schormann, M.; Bochmann, M.; Lancaster, S. J. *J. Organomet. Chem.* **2003**, *665*, 135-149.
14. Doherty, S.; Errington, R. J.; Jarvis, A. P.; Collins, S.; Clegg, W.; Elsegood, M. R. J. *Organometallics* **1998**, *17*, 3408-3410.
15. (a) Yasumoto, T.; Yamagata, T.; Mashima, K. *Organometallics* **2005**, *24*, 3375-3377; (b) Yasumoto, T.; Yamagata, T.; Mashima, K. *Chem. Lett.* **2007**, *36*, 1030-1031; (c) Zuo, W.; Zhang, M.; Sun, W.-H. *J. Polym. Sci., Part A: Polym. Chem.* **2009**, *47*, 357-372.
16. (a) Sanz, M.; Cuenca, T.; Galakhov, M.; Grassi, A.; Bott, R. K. J.; Hughes, D. L.; Lancaster, S. J.; Bochmann, M. *Organometallics* **2004**, *23*, 5324-5331; (b) Tabernero, V.; Cuenca, T.; Herdtweck, E. *Eur. J. Inorg. Chem.* **2004**, 3154-3162; (c) Chen, J.; Zheng, Z.-J.; Pan, L.; Pan, D.; Li, Y.-S. *J. Polym. Sci., Part A: Polym. Chem.* **2005**, *43*, 1562-1568; (d) Chen, Q.; Huang, J.; Yu, J. *Inorg. Chem. Commun.* **2005**, *8*, 444-448; (e) Zhang, J.; Lin, Y.-J.; Jin, G.-X. *Organometallics* **2007**, *26*, 4042-4047.

for references, see page 49

17. (a) Zhang, W.; Sun, W.-H.; Zhang, S.; Hou, J.; Wedeking, K.; Schultz, S.; Frohlich, R.; Song, H. *Organometallics* **2006**, *25*, 1961-1969; (b) Hao, P.; Zhang, S.; Sun, W.-H.; Shi, Q.; Adewuyi, S.; Lu, X.; Li, P. *Organometallics* **2007**, *26*, 2439-2446; (c) Sun, W.-H.; Hao, P.; Zhang, S.; Shi, Q.; Zuo, W.; Tang, X.; Lu, X. *Organometallics* **2007**, *26*, 2720-2734; (d) Zhang, M.; Zhang, S.; Hao, P.; Jie, S.; Sui, W.-H.; Li, P.; Lu, X. *Eur. J. Inorg. Chem*. **2007**, 3816-3826; (e) Chen, Y.; Hao, P.; Zuo, W.; Gao, K.; Sun, W.-H. *J. Organomet. Chem*. **2008**, *693*, 1829-1840; (f) Zhang, M.; Gao, R.; Hao, X.; Sun, W.-H. *J. Organomet. Chem*. **2008**, *693*, 3867-3877.
18. Zuo, W.; Zhang, S.; Liu, S.; Liu, X.; Sun, W.-H. *J. Polym. Sci., Part A: Polym. Chem*. **2008**, *46*, 3396-3410.
19. Wang, K.; Shen, M.; Sun, W.-H. *Dalton Trans*. **2009**, 4085-4095.
20. Sheldrick, G. M. SHELXL-97; University of Göttingen: Göttingen (Germany), **1997**.
21. (a) Barnes, D. J.; Chapman, R. L.; Vagg, R. S.; Watton, E. C. *J. Chem. Eng. Data* **1978**, *23*, 349-350; (b) Chan, P.-M.; Yu, W.-Y.; Che, C.-M.; Cheung, K.-K. *J. Chem. Soc., Dalton Trans*. **1998**, 3183-3190; (c) Belda, O.; Kaiser, N.-F.; Bremberg, U.; Larhed, M.; Hallberg, A.; Moberg, C. *J. Org. Chem*. **2000**, *65*, 5868-5870; (d) Conlon, D. A.; Yasuda, N. *Adv. Synth. Catal.* **2001**, *343*, 137-138.
22. (a) Barni, E.; Savarino, P. *J. Heterocycl. Chem.* **1977**, *14*, 937-940; (b) Tsukamoto, G.; Yoshino, K.; Kohno, T.; Ohtaka, H.; Kagaya, H.; Ito, K. *J. Med. Chem*. **1980**, *23*, 734-738.
23. Sun, W.-H.; Zhang, W.; Gao, T.; Tang, X.; Chen, L.; Li, Y.; Jin, X. *J. Organomet. Chem*. **2004**, *689*, 917-929.
24. (a) Flores, J. C.; Chien, J. C. W.; Rausch, M. D. *Macromolecules* **1996**, *29*, 8030-8035; (b) Esteruelas, M. A.; López, A. M.; Mateo, A. C.; Oñate, E. *Organometallics* **2005**, *24*, 5084-5094; (c) Gurubasavaraj, P. M.; Roesky, H. W.; Sharma, P. M. V.; Oswald, R. B.; Dolle, V.; Herbst-Irmer, R.; Pal, A. *Organometallics* **2007**, *26*, 3346-3351.
25. Müller, J.; Kehr, G.; Fröhlich, R.; Erker, G. *Eur. J. Inorg. Chem*. **2005**, 2836-2841.
26. (a) Amor, F.; Fokken, S.; Kleinhenn, T.; Spaniol, T. P.; Okuda, J. *J. Organomet. Chem*. **2001**, *621*, 3-9; (b) González-Maupoey, M.; Cuenca, T.; Frutos, L. M.; Castaño, O.; Herdtweck, E. *Organometallics* **2003**, *22*, 2694-2704.
27. (a) Bochmann, M. *J. Chem. Soc., Dalton Trans*. **1996**, 255-270; (b) Chen, E. Y. X.; Marks, T. J. *Chem. Rev*. **2000**, *100*, 1391-1434.
28. Terao, H.; Ishii, S. I.; Saito, J.; Matsuura, S.; Mitani, M.; Nagai, N.; Tanaka, H.; Fujita, T. *Macromolecules* **2006**, *39*, 8584-8593.
29. Koltzenburg, S. *J. Mol. Catal. A: Chem.* **1997**, *116*, 355-363.
30. (a) Kaminsky, W. *Macromol. Chem. Phys*. **1996**, *197*, 3907-3945; (b) Galland, G. B.; Seferin, M.; Mauler, R. S.; Dos Santos, J. H. Z. *Polym. Int*. **1999**, *48*, 660-664.
31. Simanke, A. G.; Galland, G. B.; Freitas, L.; da Jornada, J. A. H.; Quijada, R.; Mauler, R. S. *Polymer* **1999**, *40*, 5489-5495.
32. (a) Randall, J. C. *J. Macromol. Sci., Rev. Macromol. Chem. Phys.* **1989**, *C29*, 201-317; (b) Seger, M. R.; Maciel, G. E. *Anal. Chem*. **2004**, *76*, 5734-5747.
33. Nomura, K.; Fujita, K.; Fujiki, M. *J. Mol. Catal. A: Chem*. **2004**, *220*, 133-144.

for references, see page 49

CHAPITRE IV

Syntheses, Characterization and the Ethylene (Co-) Polymerization Screening of 2-Benzimidazolyl-*N*-phenylquinoline-8-carboxamide Half-titanocene Chlorides

WEN-HUA SUN[*,†,‡] **SHAOFENG LIU**,[†] WENJUAN ZHANG,[†] YANNING ZENG,[†] DELIGEER WANG,[†,§] AND TONGLING LIANG[†]

[†] *Key laboratory of Engineering Plastics and Beijing Natural Laboratory for Molecular Science, Institute of Chemistry, Chinese Academy of Sciences, Beijing 100190, China*

[‡] *State Key Laboratory for Oxo Synthesis and Selective Oxidation, Lanzhou Institute of Chemical Physics, Chinese Academy of Sciences, Lanzhou 730000, China*

[§] *Department of Chemistry, Inner Mongolia Normal University, Hohhot 010022, China*

This Chapter has been published in *Organometallics*, **2010**, *29*, 732-741.

Contributions from the various co-authors: Professors Wen-Hua Sun and Deligeer Wang oriented and supervised the work, Dr. Wenjuan Zhang took part in discussions and helped in the preparation of the manuscript, Miss Yanning Zeng assisted for the synthesis and Dr. Tongling Liang for the resolution of the X-ray structure analyses.

Résumé du Chapitre IV

Une série de complexes cyclopentadiénure de titane dichlorure avec un ligand 2-benzimidazolyl-*N*-phenylquinoline-8-carboxamidure, CpTi**L**Cl (**C1**-**C6**: Cp = η^5-C_5H_5; **L** = dérivé de type 2-(*1H*-benzo[*d*]imidazol-2-yl)-*N*-(2,6-R^1-4-R^2-phenyl)quinoline-8-carboxamidure ; **C1**: R^1 = *i*-Pr, R^2 = H; **C2**: R^1 = Et, R^2 = H; **C3**: R^1 = Me, R^2 = H; **C4**: R^1 = Me, R^2 = Me; **C5**: R^1 = H, R^2 = H; **C6**: R^1 = F, R^2 = H), a été obtenue par réaction stoichiométrique entre le trichlorure de semi-titanocène et le 2-benzimidazolyl-*N*-phenylquinoline-8-carboxamidure de potassium correspondant. Tous les complexes ont été caractérisés par analyse élémentaire et RMN et dans les cas de **C1**, **C2** et **C6**, par diffraction des rayons X. En outre, le complexe dinucléaire à pont oxo **C7** fur isolé à partir d'une solution de **C6** à l'air. Les complexes **C1**-**C6**, après avoir été activés par du méthylaluminoxane (MAO), montrent une forte activité catalytique activities en polymerisation de l'éthylène et en copolymérisation de l'éthylène avec les α-oléfines. Avec le système **C1**/MAO, la productivité augmente avec l'augmentation de température ou avec un rapport MAO / Ti croissant mais les poids moléculaires des

polymères décroissent lorsque l'activité augmente. La copolymérisation de l'éthylène avec le 1-hexene ou le 1-octène conduit à des copolymères incorporant environ 2.0-5.0% mol de comonomère.

4.1 Abstract of Chapter IV

A series of 2-benzimidazolyl-*N*-phenylquinoline-8-carboxamide half-titanocene chlorides, CpTi**L**Cl (**C1**-**C6**: Cp = η^5-C_5H_5; **L** = 2-(*1H*-benzo[*d*]imidazol-2-yl)-*N*-(2,6-R^1-4-R^2-phenyl)quinoline-8-carboxamide derivatives; **C1**: R^1 = *i*-Pr, R^2 = H; **C2**: R^1 = Et, R^2 = H; **C3**: R^1 = Me, R^2 = H; **C4**: R^1 = Me, R^2 = Me; **C5**: R^1 = H, R^2 = H; **C6**: R^1 = F, R^2 = H), has been synthesized by the stoichiometric reaction of half-titanocene trichlorides with the corresponding potassium 2-benzimidazolyl-*N*-phenylquinoline-8-carboxamide. All complexes are fully characterized by elemental and NMR analyses, as well as the single-crystal X-ray diffraction for complexes **C1**, **C2** and **C6**. In addition, an oxo-bridged dinuclear complex **C7** is separated from the solution of **C6** in air. These complexes **C1**-**C6**, activated with methylaluminoxane (MAO), exhibit high catalytic activities towards both ethylene polymerization and copolymerization of ethylene with α-olefin. According to the catalytic system of **C1**/MAO, both elevating reaction temperature and increasing the ratio of MAO to titanium precursor enhance the productivities, however, the molecular weights of resultant polymers obtained decrease against their higher activities. Moreover, copolymerizations of ethylene with either 1-hexene or 1-octene effectively produce copolymers incorporated comonomers in 2.0-5.0% mol.

4.2 Introduction

Driven by industrial consideration for advanced polyolefins, significant developments have been focused on designing sophisticated procatalysts towards polyolefins with defined microstructures. A great deal of research has been conducted on highly active (co)polymerization of olefins by employing catalysts precursors of metallocenes[1] and half-metallocenes.[2] Regarding industrial applications, it is necessary to immobilize procatalysts on inorganic carriers in order to be suitable for processes of either gas phase or slurry reactors.[3] In addition to metallocenes,[1,4] the "constrained geometry" half-metallocene catalysts (namely CGC catalysts) have been successfully developed and commercialized,[2,5] however, their expediential ligands are limited. Recently, the bis(phenoxyimino) or ancillary phenoxylketimino titanium procatalysts have been developed for living polymerization,[6] meanwhile bis(iminopyrrolidato)titanium complexes have been explored for olefin copolymerization.[7] Due to highly electrophillic property of titanium, however, those common complexes are higher sensitive than metallocenes and half-metallocenes. Therefore, nonbridged half-metallocenes have been drawn much attention.

The non-bridged half-metallocene complexes, Cp'M(L)Xn (Cp' = cyclopentadienyl group; M = Ti, Zr, Hf; L = anionic ligand; X = halogen, alkyl), have performed with high efficiency in both catalytic activity and precise control of the copolymerization property.[8] To verify nonbridged half-titanocene catalysts, the ancillary ligands have been generally explored and acted as mono-anionic coordination ways of monodentate[9] or bidentate,[10] and dianionic tridentate coordination.[11] Beyond the better stabilities of dianionic tridentate half-titanocene catalysts, half-titanocene complexes bearing either *N*-

for references, see page 73

(2-benzimidazolylquinolin-8-yl)benzamidate[11f] or 6-benzimidazolylpyridyl-2-carboximidate[11e] have shown high activities in ethylene polymerization. The half-titanocene *N*-(2-benzimidazolylquinolin-8-yl)benzamidate catalysts (**A**, Chart 1) performed high activities for copolymerization of ethylene with α-olefins,[11f] but the half-titanocene 6-benzimidazolylpyridyl-2-carboximidate catalysts did not (**B**, Chart 1).[11e] The characteristic differences would be based on the frameworks of pyridine and quinoline, and the different coordinative atoms of oxygen or nitrogen from the carboximinate groups. Subsequently, the title half-titanocene complexes bearing 2-benzimidazolyl-*N*-phenylquinoline-8-carboxamide chlorides have been synthesized, and investigated for their catalytic behaviors. The title complexes, activated with methylaluminoxane (MAO), showed high activities in both ethylene polymerization and copolymerization of ethylene and 1-hexene or 1-octene. Herein we report the syntheses, characterization, and polymerization behavior of the title complexes in detail.

Chart 1 Development of Half-titanocene Catalysts

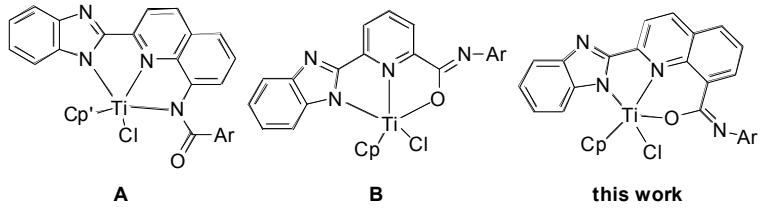

4.3 Results and Discussion

4.3.1 Synthesis and Characterization of 2-(Benzimidazol-2-yl)-*N*-phenylquinoline-8-carboxamide Derivatives and Their Half-titanocene Chlorides

There are several options of forming carboxamide groups.[12] Condensation reactions of 2-methylquinoline-8-carboxylic acid with substituted anilines in refluxing xylene, using trichlorophosphine as dehydrating agent,[12e,f] form a series of 2-methyl-*N*-phenylquinoline-8-carboxamide derivatives in high yields (Scheme 1). Then a further reaction of 2-methyl-*N*-phenylquinoline-8-carboxamides and *o*-phenylenediamine with excess sulfur as oxidant gives the corresponding derivatives of 2-(benzimidazol-2-yl)-*N*-phenylquinoline-8-carboxamides (**L1-L6**, Scheme 1) according to previous method.[13]

Scheme 1. Synthesis of Ligands **L1-L6**

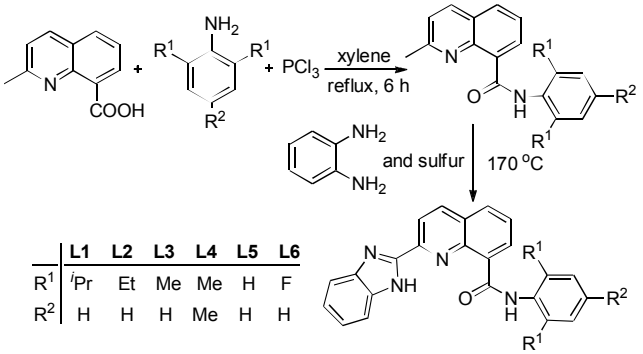

for references, see page 73

All the organic compounds are routinely characterized by elemental, IR spectroscopic and NMR analyses. For compound **L1** as an example, there is a strong and sharp peak at 1640 cm^{-1} in its IR spectrum ascribed to the stretching vibration of C=O, while the absorptions at δ 11.05 and 9.85 ppm in the its ^1H NMR spectrum could be ascribed to two NH groups of amide and benzimidazole, respectively. Similar characteristics have been observed for compounds **L2**-**L6**.

These 2-(benzimidazol-2-yl)-*N*-phenylquinoline-8-carboxamide derivatives could potentially act as the dianionic tridentate ligands. The reaction of these compounds with half-titanocene trichloride, however, does not produce the desired complexes. It is necessary for these compounds to be treated with two equivalents of KH in tetrahydrofuran (THF) for forming the potassium dianionic intermediates. The stoichiometric reaction of the potassium dianionic intermediates with $CpTiCl_3$ affords the complexes CpTi**L**Cl (**C1**-**C6**, Cp = C_5H_5; **L** = 2-(benzimidazol-2-yl)-*N*-phenylquinoline-8-carboxamide) (Scheme 2) in high yields. All complexes are fully characterized by elemental and NMR spectroscopic analyses. Comparing the NMR spectra, the peaks of **L1** at δ 11.05 ppm and 9.85 ppm (ascribed to the *NH* signals of amide and benzimidazole) disappear in that of complex **C1**, indicating the successful deprotonation and formation of Ti-N bonds. Similar changes are also observed in the NMR spectra of complexes **C2**-**C6** and their corresponding ligands. In addition, there are two sets of resonances of $CH(CH_3)_2$ (3.51 ppm and 2.83 ppm) for **C1**, which is different from only one (3.41 ppm) for **L1**. It is assumed that the aryl-N bond in complex **C1** cannot freely rotate in solution because of the steric hindrance of the *ortho*-isopropyl groups of the N-aryl rings. A similar characteristic is also observed for complex **C2** with four sets of signals for -CH_2CH_3 and two sets of signals for -CH_2CH_3 (1.57 ppm and 1.07 ppm) due to the *ortho*-ethyl groups of the *N*-aryl rings. Other complexes (**C3**-**C6**) show no asymmetrical signal for the *ortho*-methyl groups of the N-aryl rings, therefore, the free rotation of aryl-N bonding of complexes **C3**-**C6** is considered in solution.

All complexes are highly sensitive to air and moisture. The CH_2Cl_2/*n*-heptane solution of **C6** exposed to the air affords the oxo-bridged bimetallic complex **C7**, which is more stable. Its analogical complexes are also obtained in our previous works.[11e,f,14]

Scheme 2. Synthesis of Complexes **C1**-**C6**

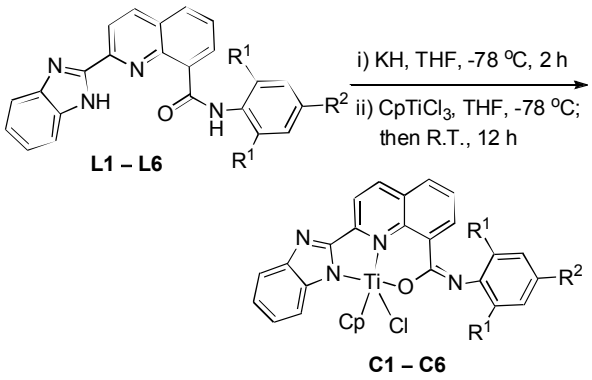

for references, see page 73

Crystals of **C1**, **C2** and **C6** suitable for the single-crystal X-ray diffraction analysis have been obtained by slow diffusion of *n*-heptane into their CH_2Cl_2 solutions. Their molecular structures are illustrated in Figures 1-3, respectively. Selected bond lengths and angles are given in Table 1.

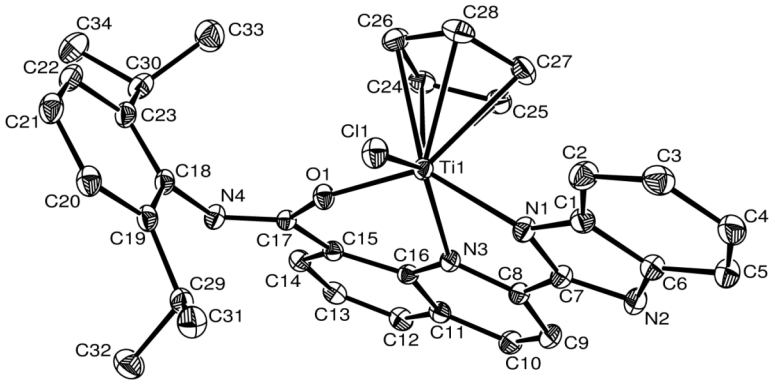

Figure 1. Molecular structure of complex **C1**. Thermal ellipsoids are shown at the 30% probability level. Hydrogen atoms have been omitted for clarity.

Table 1. Selected Bond Lengths (Å) and Angles (°) for **C1**, **C2** and **C6**

	C1	**C2**	**C6**
	Bond Lengths (Å)		
Ti1-N1	2.082(2)	2.088(3)	2.084(2)
Ti1-N3	2.233(2)	2.257(3)	2.246(2)
Ti1-O1	1.854(2)	1.883(2)	1.898(2)
Ti1-C24	2.349(3)	2.368(3)	2.371(2)
Ti1-C25	2.365(3)	2.370(3)	2.355(3)
Ti1-C26	2.365(3)	2.353(3)	2.351(2)
Ti1-C27	2.395(3)	2.347(3)	2.374(2)
Ti1-C28	2.382(3)	2.359(3)	2.382(3)
Ti1-Cl1	2.313(9)	2.292(1)	2.287(9)
C17-O1	1.326(3)	1.330(4)	1.320(3)
C17-N4	1.273(3)	1.273(4)	1.283(3)
	Bond Angles(°)		
N1-Ti1-N3	74.19(8)	74.08(1)	74.46(8)
N1-Ti1-O1	136.19(9)	137.34(1)	138.29(8)
N3-Ti1-O1	78.92(8)	77.53(1)	77.93(8)
Cl1-Ti1-N1	88.82(7)	86.97(8)	88.33(6)
Cl1-Ti1-N3	140.37(6)	134.87(7)	137.20(6)
Cl1-Ti1-O1	90.47(7)	91.15(7)	91.25(6)

The molecular structure of **C1** in Figure 1 clearly shows the η^5-binding fashion of cyclopentadienyl group as a cap coordinating a titanium atom, in addition, the titanium atom is in a square-pyramidal environment with the basal positions being occupied by a chloride and three atoms (O^N^N) of the tridentate dianionic 2-(benzimidazol-2-yl)-*N*-phenylquinoline-8-carboxamide. This coordination geometry is also observed with other half-titanocene complexes bearing dianionic ligands such as 6-benzimidazolyl-pyridyl-2-carboximidates (**A**, Chart 1)[11f] and *N*-benzimidazolylquinolin-8-benzamides

for references, see page 73

(**B**, Chart 1).[11e] Consistent with values observed in the analogue complexes,[11] the Ti-Cl bond length (Ti1-Cl1) is 2.313(9) Å, meanwhile the distance between the centroid of the cyclopentadienyl group and titanium is 2.047 Å. The bond lengths between titanium and the carbons of cyclopentadienyl group range from 2.349(3) to 2.395(3) Å (Ti1-C24; Ti1-C25; Ti1-C26; Ti1-C27; Ti1-C28), indicating the slight difference (*Δ*Ti-C = 0.046 Å) caused by the different *trans*-bonding atoms in the basal plane. According to its spectra, there is one singlet ascribed to the Cp ring in the ^{1}H NMR (6.23 ppm, s, 5H) and ^{13}C NMR (121.1 ppm), suggesting its conjugated characteristics in the solution state. The 2-(benzoimidazol-2-yl)-*N*-(2,6-diisopropylphenyl)quinoline-8-carboxamide ligand adopts a puckered chelating style with the dihedral angle 21.1° defined by the two chelating rings (Ti1-N1-C7-C8-N3, Ti1-N3-Cl6-Cl5-C17-O1), which is larger than that of analogue complex in model **A** (17.0°). Meanwhile the dihedral angle between the benzimidazole and quinoline rings is 5.0°, which is smaller than that of corresponding analogue of model **A** (8.4°).[11f] The two Ti-N bond lengths (Ti1-N1 = 2.082(2) Å, Ti1-N3 = 2.233(2) Å) are in the usual range for titanium complexes, but slightly different due to their different chemical environments. The Ti1-O1 bond length is 1.854(2) Å, which is similar to the Ti-O bond in (η^5-C_5H_5)Ti{2,2'-S(OC_6H_2-4-Me-6-^{t}Bu)$_2$}Cl and (η^5-C_5H_5)Ti(η^2-MBMP)Cl,[15] but shorter than the Ti-O bond of 6-benzimidazolylpyridyl-2-carboximidate half-titanocene (1.967(3) Å).[11f] The C17-O1 bond length (1.326(3) Å) is longer than C=O bond (1.19-1.23 Å) but shorter than C-O single bond (1.42-1.46 Å), meanwhile C17-N4 bond (1.273(3) Å) is shorter than typically C-N single bond. These characteristics indicate the conjugated feature within the carboximidate group.

The complexes **C2** (Figure 2) and **C6** (Figure 3) possess similar coordination features to **C1**, despite the different substituents on the phenyl groups. Similarly, elongated C17-O1 (1.330(4) Å in **C2**, 1.320(3) Å in **C6**) and shorter C17-N4 (1.273(4) Å in **C2**, 1.283(3) in **C6**) bond lengths are observed, indicating partial delocalization within the carboximidate group. The dihedral angles between the quinoline and the 2,6-substituted phenyl rings are notably different as the 57° in **C1**, 74.6° in **C2** and 80.6° in **C6**, respectively. Bulky hindrance of the *ortho*-substituents of the imino-aryl rings affects the rotation of N-aryl bond and then causes the difference in coordination. This is consistent with the results indicated by their NMR spectra, two sets of signals of *CH*(CH_3)$_2$ (3.51 ppm and 2.83 ppm) for **C1** while four sets of signals for -*CH*$_2$$CH_3$ and two sets of signals for -CH_2*CH*$_3$ (1.57 ppm and 1.07 ppm) for **C2**. The structural differences also affect their catalytic behaviors during olefin polymerization, which will be discussed in the respective section.

for references, see page 73

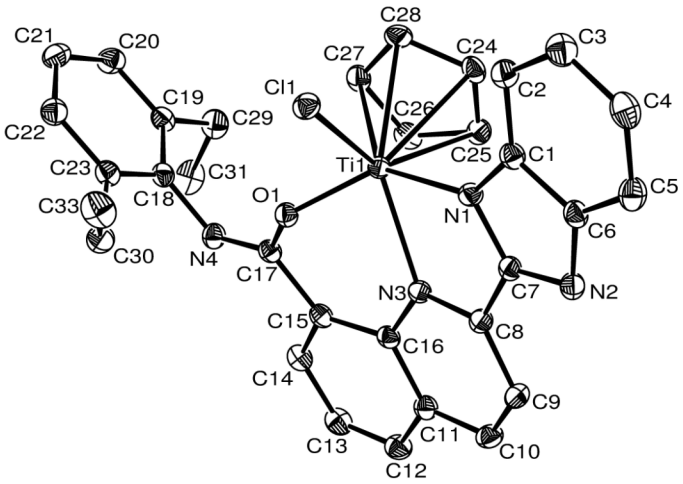

Figure 2. Molecular structure of complex **C2**. Thermal ellipsoids are shown at the 30% probability level. Hydrogen atoms have been omitted for clarity.

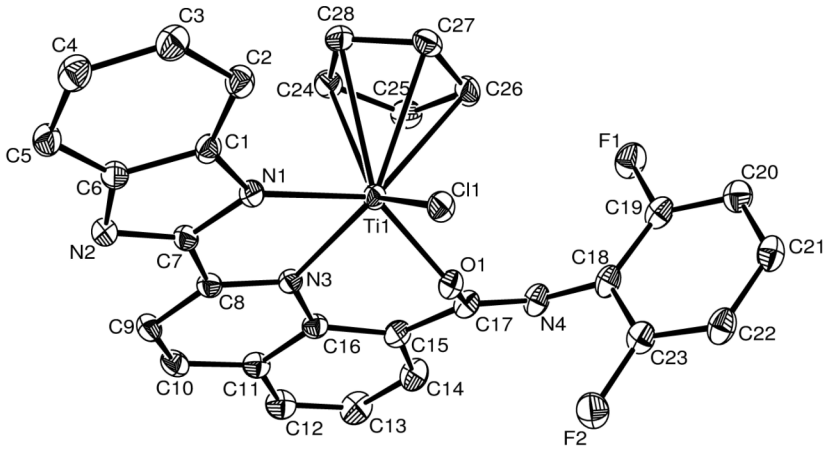

Figure 3. Molecular structure of complex **C6**. Thermal ellipsoids are shown at the 30% probability level. Hydrogen atoms have been omitted for clarity.

Crystals of **C7** suitable for single-crystal X-ray analysis are obtained by layering *n*-heptane on a CH_2Cl_2 solution of complex **C6**, and the mixture was left in air for one week. The molecular structure is shown in Figure 4 and selected bond lengths and angles are summarized in Table 2, respectively. The molecular structure of **C7** shows a binuclear species bridged by an oxygen atom (O), which is similar to our previously reported.[11b,c] The bond lengths Ti1-O3 (1.823(1) Å) and Ti2-O3 (1.7982(1) Å) are common in titanium complexes and the angle Ti1-O3-Ti2 is 177.2°. Each titanium center is bonded to one 2-benzimidazolyl-*N*-phenylquinoline-8-carboxamide ligand, one bridging oxygen atom and one η^5-binding Cp ring. In each unit, the coordination geometry around the titanium center can also be described as square-pyramidal. Compared with the data in Table 1, the structural parameters including bond lengths and angles are similar to those of **C6**.

for references, see page 73

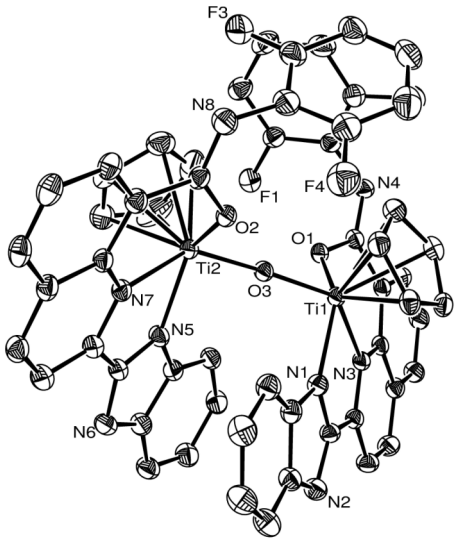

Figure 4. Molecular structure of complex **C7**. Thermal ellipsoids are shown at the 30% probability level. Hydrogen atoms have been omitted for clarity.

Table 2. Selected Bond Lengths (Å) and Angles (°) for **C7**

Bond Lengths			
Ti1-N1	2.096(3)	Ti1-N3	2.270(2)
Ti1-O1	1.935(2)	Ti1O3	1.823(1)
Ti1-C24	2.362(4)	Ti1-C25	2.392(3)
Ti1-C26	2.401(3)	Ti1-C27	2.362(3)
Ti1-C28	2.334(3)	C17-O1	1.320(3)
C1-N4	1.275(4)	Ti2-O2	1.922(2)
Ti2-O3	1.7982(1)		
Bond Angles			
N1-Ti1-N3	73.71(9)	N1-Ti1-O1	137.12(1)
N3-Ti1-O1	77.13(9)	N1-Ti1-O3	88.04(9)
N3-Ti1-O3	134.76(9)	O1-Ti1-O3	90.79(9)
N5-Ti2-N7	73.36(9)	N5-Ti2-O2	136.96(1)
N7-Ti2-O2	78.29(9)	N5-Ti2-O3	85.46(9)
N7-Ti2-O3	134.21(9)	O2-Ti2-O3	91.96(9)
Ti1-O3-Ti2	177.21(1)		

4.3.2 Catalytic Behavior toward Ethylene Polymerization

According to our experience and results obtained with model catalysts **A** and **B** (Chart 1),[11e,f] the title complexes (**C1-C6**) were investigated for ethylene polymerization in the presence of methylaluminoxane (MAO) as a cocatalyst. The detailed investigation of complex **C1** is carried out for the optimum reaction condition of the Al/Ti molar ratio, temperature and time.

Effects of Al/Ti Molar Ratio, Temperature and Time on the Catalytic Behavior In view of the better performance observed by complexes containing *ortho*-isopropyl groups of the imino-aryl rings in the model catalysts **A** and **B** (Chart 1),[11e,f] the catalytic system of **C1**/MAO were investigated in detail by changing the reaction parameters, and the results are summarized in Table 3. A higher Al/Ti molar ratio leads to higher activity for ethylene polymerization (entries 1-5, Table 3). The activities

for references, see page 73

increase from 2.29 × 10^6 g·mol^{-1}(Ti)·h^{-1} with the Al/Ti molar ratio of 10000 to 5.86 × 10^6 g·mol^{-1}(Ti)·h^{-1} with the Al/Ti molar ratio of 30000. However, slightly lower activity of 5.75 × 10^6 g·mol^{-1}(Ti)·h^{-1} is obtained with a Al/Ti molar ratio of 35000. Such phenomenon is common and well clarified by the influence of Al concentration on the termination of polymer chains.[16] When the ratio of Al/Ti increases, the polyethylene obtained exhibits lower M_w values (entries 1-5, Table 3) because of increasing chain transfer with higher MAO concentration.[16-17]

Table 3. Ethylene Polymerization with **C1**/MAO[a]

Entry	Al/Ti	T (°C)	Polymer (g)	Activity (10^6g·mol^{-1}(Ti)·h^{-1})	T_m[b] (°C)	M_w[c] (kg·mol^{-1})	M_w/M_n[c]
1	10000	80	0.191	2.29	133.6	1052	4.9
2	20000	80	0.271	3.25	133.5	739	3.0
3	25000	80	0.411	4.93	134.8	563	2.4
4	30000	80	0.488	5.86	134.0	461	2.3
5	35000	80	0.479	5.75	133.0	329	3.9
6	30000	20	0.198	2.38	132.2	1613	2.4
7	30000	60	0.436	5.23	133.0	595	3.7
8	30000	70	0.446	5.35	133.5	522	3.6
9	30000	100	0.470	5.64	132.5	415	3.5
10[d]	30000	80	0.270	6.48	134.2	233	3.4
11[e]	30000	80	1.26	5.04	134.0	588	3.0

[a] Conditions: 0.5 μmol **C1**; 10 atm ethylene; 10 min; toluene (total volume 100 mL). [b] Determined by DSC. [c] Determined by GPC. [d] time: 5 min, [e] time: 30 min.

The influence of the reaction temperature was also studied. The catalytic activity is lower at 20 °C (entry 6, Table 3), but increased with the reaction temperature elevated up to 80 °C (entries 7, 8 and 4, Table 3), and slightly decreased at 100 °C (entry 9, Table 3). The observation is consistent with results obtained by the model catalyst **A** (Chart 1),[11f] suggesting that ligands with the quinoline backbone play an important role in stabilizing the active species at high temperature. This behavior is in the contrast to the traditional metallocene catalysts possessing lower activity at elevated temperatures,[1,4] and classical FI catalysts showing the highest activity around 50 °C.[6] The better thermal stability of these current catalytic systems is potentially of benefit to fit the industrial polymerization, because the liquefiable polymerization at high temperature favors the viscosity of the reaction mixture with better mass transportation and temperature control.[11e,f] Though the molecular weights of polyethylenes obtained decrease with elevating reaction temperatures (entries 4, 6-9, Table 3) due to a faster chain transfer and termination at higher temperature, their molecular weights are high enough and comparable with useful polyethylene.

Regarding the lifetime of **C1**/MAO system, the ethylene polymerization is conducted over different time period namely 5, 10 and 30 minutes (entries 10, 4 and 11, Table 3). Their productivities are almost linear along with reaction time (Figure 5), and the molecular weights of obtained polyethylenes increase, which suggests that the active species are well maintained with slowly deactivated over the prolonged reaction time.

for references, see page 73

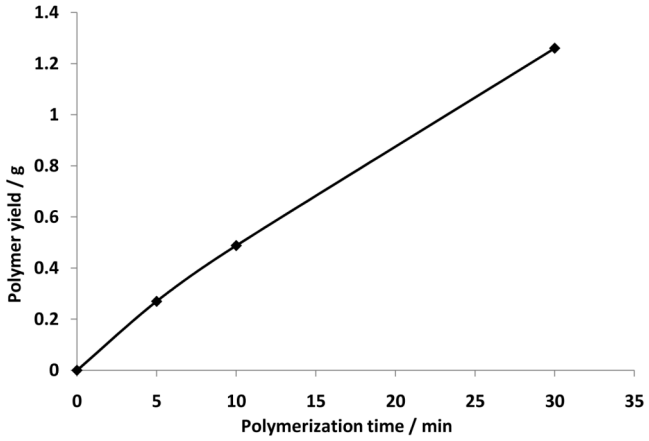

Figure 5. Relationship of the polymer amounts and reaction time (Entries 4, 10 and 11, Table 3).

Effect of the Ligand Environment on the Catalytic Behavior Based on the results observed with the **C1**/MAO system, the title complexes were investigated with the Al/Ti molar ratio of 30000 at 80 °C under 10 atm ethylene. All of them show high activities towards ethylene polymerization (Table 4). Compared with the model catalysts **A** and **B** (chart 1),[11e,f] the title catalysts show much better stability at 80 °C, however, slightly lower activities are observed compared to maximum activities obtained at different conditions. There are observable effects of the ligands' environment, and the activities of complexes decrease in the order as: **C1** (R^1= ^{i}Pr) > **C2** (Et) > **C3** (Me) > **C5** (H) > **C6** (F). The activity of the **C4**/MAO is higher than that by the **C3**/MAO system, but lower than that of the **C1**/MAO. Indicated by the NMR and structural differences of the complexes, steric hindrance caused by *ortho*-substituents of the imino-aryl rings protect active species and result in high activity.[17] On the other hand, the additional methyl group of **C4** increases the electron density of central deficient titanium. The complex **C4** has a better solubility in solution, and its active species are better stabilized resulting in a higher activity.[17-18]

Table 4. Ethylene Polymerization Results with **C1**-**C6**/MAO[a]

Entry	Complex	Polymer (g)	Activity (10^6 g·mol^{-1}(Ti)·h^{-1})	T_m [b] (°C)	M_w [c] (kg·mol^{-1})	M_w/M_n [c]
1	**C1**	0.488	5.86	134.0	461	2.3
2	**C2**	0.460	5.52	132.8	432	4.7
3	**C3**	0.446	5.35	132.8	347	4.6
4	**C4**	0.484	5.81	132.6	382	3.7
5	**C5**	0.356	4.27	131.6	190	3.5
6	**C6**	0.326	3.91	134.3	235	2.5

[a] Conditions: 0.5 μmol of catalysts; 10 atm ethylene; Al/Ti = 30000; 80 °C; 10 min; toluene (total volume 100 mL). [b] Determined by DSC. [c] Determined by GPC.

The properties of the polyethylene obtained, the melting points and molecular weights (Table 4), are characteristic of linear and high-density polyethylene (HDPE) with the T_m values in the ranges of 131-135 °C and their M_w values in the ranges of 190 to 461 kg·mol^{-1}, which are much higher than those of

for references, see page 73

polymers obtained by the model catalysts **A** and **B** (chart 1)[11e,f] and related catalytic systems.[10f,g] Moreover, the M_w values of polyethylenes obtained by model catalyst **A**[11f] are three times higher than those of polyethylenes obtained by model catalyst **B**.[11e] Such phenomena emphasize the important roles of different frameworks of ligands, which cause the different catalytic behavior of their complexes. The title procatalysts and model catalyst **A**[11f] employ the rigid quinoline instead of the centric pyridine ring of model catalyst **B**,[11e] enlarging the coordination ring. Therefore, the ligands of the title procatalysts and model catalyst **A**[11f] occupy more space around the active titanium center. It is supposed that the chain transfer process of the half-titanocene catalyst requires more space in the coordination sphere of the titanium than the olefin insertion state does.[19] So the title catalysts produce polyethylenes with high molecular weights than catalyst **A**, which are also higher than catalyst **B**. Due to bulky substituents, the catalysts (**C1** and **C2**) produce polyethylenes with higher molecular weight than catalyst **C5** containing ligands with less steric influence. The active species of olefin polymerization are generally recognized as cationic ones, which are formed by alkylation and abstraction of halogen or ligands using alkylaluminum or alkylaluminoxane agents.[17-18] Regarding the current half-titanocene catalysts, there is only one Ti-Cl bond for alkylation to form the titanium alkyl complex. The introduction of MAO alkylated the Ti-Cl bond and open an additional site ligated by ligand in order to coordinate with the approaching monomer. According our previous report, the cleavage of Ti-O bond possibly occurs during polymerization.[11e]

4.3.3 Copolymerization of Ethylene/1-Hexene and Ethylene/1-Octene

The copolymerization of ethylene with 1-hexene and 1-octene by complexes **C1-C6** are also investigated. All catalysts exhibit high activities toward copolymerization of ethylene with 1-hexene or 1-octene, and their results are tabulated in Table 5.

Table 5. Copolymerization of Ethylene with 1-Hexene or 1-Octene by **C1-C6**/MAO[a]

Entry	Complex	Polymer (g)	Activity (10^6 g·mol^{-1}(Ti)·h^{-1})	T_m[b] (°C)	M_w[c] (kg·mol^{-1})	M_w/M_n[c]
1[d]	**C1**	0.388	4.66	116.8	198	4.3
2[d]	**C2**	0.358	4.30	117.4	175	4.9
3[d]	**C3**	0.341	4.09	117.0	142	2.6
4[d]	**C4**	0.332	3.98	117.9	154	2.9
5[d]	**C5**	0.277	3.32	117.1	90.0	3.4
6[d]	**C6**	0.208	2.50	116.6	125	2.4
7[e]	**C1**	0.283	3.40	121.5	125	3.1
8[e]	**C2**	0.278	3.34	121.1	90.1	2.4
9[e]	**C3**	0.260	3.12	121.3	66.4	2.9
10[e]	**C4**	0.263	3.16	121.4	61.6	5.3
11[e]	**C5**	0.198	2.38	120.6	51.5	2.8
12[e]	**C6**	0.163	1.96	120.9	55.7	3.2

[a] Conditions: 0.5 μmol of catalysts; 10 atm ethylene; Al/Ti = 30000; 80 °C; 10 min; toluene (total volume 100 mL). [b] Determined by DSC. [c] Determined by GPC. [d] 5 mL 1-hexene was added. [e] 5 mL 1-octene was added.

for references, see page 73

The copolymers of ethylene/1-hexene by **C1**-**C6** have the similar T_m values. Upon variation of the environment of metal center with different ligands, their catalysts perform the catalytic activities with the same order as the ethylene polymerization: **C1** (*i*-Pr) > **C2** (Et) > **C3** (Me) > **C5** (H) > **C6** (F), suggesting that bulkier and electron-donating groups are favorable for copolymerization. The title catalysts show a little lower activity than model catalyst **A** (chart 1), however, the T_m values (about 117 °C) of the resultant copolymers by current catalysts are much lower than these (about 127 °C) of copolymers by catalyst **A** (chart 1). These are consistent with the observation of the higher incorporation of 1-hexene by the current catalytic system. The copolymer (entry 1, Table 5), confirmed by ^{13}C NMR in Figure 6, show the character of linear low density polyethylene[20] and contain 4.3 mol% of 1-hexene incorporation. In fact, the copolymers by catalyst **A** (chart 1) only contain about 2 mol% of 1-hexene incorporation,[11f] therefore the current systems provide polymers with higher incorporation of 1-hexene.[21] The resultant copolymers possess lower molecular weights (90-198 kg·mol^{-1}) than the polyethylenes obtained in Table 4, but still higher than those obtained by $Cp^*Ti(O\text{-}2,6\text{-}^iPr_2C_6H_3)Cl_2$.[9a]

The copolymerization of ethylene/1-octene is similar in behavior to that of ethylene/1-hexene (Table 5), but slightly lower activities are observed (entry n *vs* entry n+6, n = 1-6, Table 5). The DSC analysis of the resultant copolymers by **C1**-**C6** shows one sole melting point around 121 °C, which is lower than that of polyethylene obtained and higher than that of copolymer of ethylene/1-hexene. The incorporation of 1-octene into the copolymer obtained is also higher than that (1.3 mol%) of copolymer by catalyst **A** (Chart 1), which is confirmed by the ^{13}C NMR spectrum in Figure 7 (entry 7, Table 5) indicating a 2.4 mol% incorporation of 1-octene. The molecular weights of poly(ethylene-1-octene) (51-125 kg·mol^{-1}) are slightly lower than those of poly(ethylene-1-hexene) obtained.

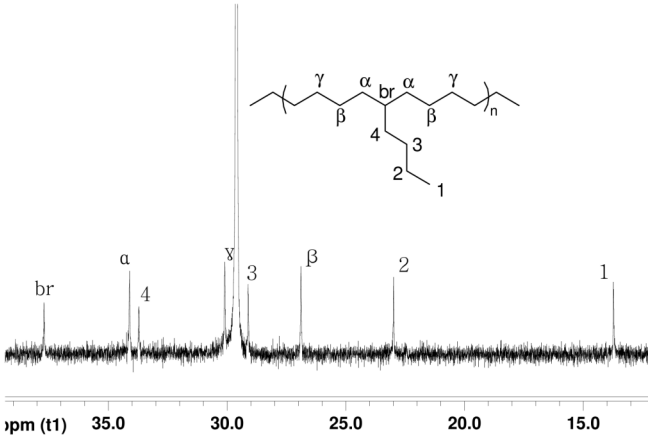

Figure 6. ^{13}C NMR spectrum of ethylene/1-hexene copolymer by **C1**/MAO system (entry 1, Table 5)

for references, see page 73

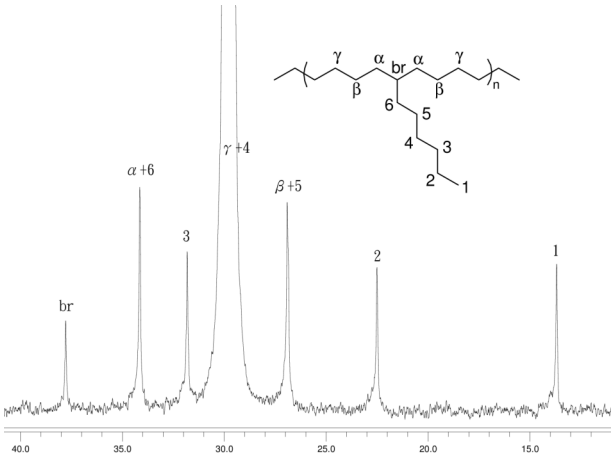

Figure 7. ^{13}C NMR spectrum of ethylene/1-octene copolymer by **C1**/MAO system (entry 7, Table 5)

The title catalysts and model catalyst **A** (chart 1)[11f] show good incorporation behavior of α-olefins, and the title catalysts are superior. The backbones of the ligands frameworks play the important roles of their incorporation behavior and better thermal stability. Compared with negative copolymerization performed by the centric pyridine ring of model catalyst **B**,[11c] the quinoline derivative ligands of the title complexes and model catalyst **A**[11f] perhaps are more interesting for further investigating.

4.4 Conclusions

The title half-titanocene complexes bearing 2-benzimidazolyl-*N*-phenylquinoline-8-carboxamide (**C1**-**C6**) have been synthesized and characterized by ^{1}H NMR, ^{13}C NMR and elemental analyses. The molecular structures of **C1**, **C2** and **C6** are confirmed by X-ray diffraction studies. The complexes **C1**-**C6**, activated with excess MAO, exhibit high catalytic activities towards ethylene polymerization, especially at elevated reaction temperature. The bulky substituents of the imino-aryl rings are favorable for both the catalytic activity and molecular weight (M_w) of the resultant polymer by the procatalyst. The title catalysts showed good copolymerization behavior of ethylene with 1-hexene or 1-octene, which is better than the model catalyst **A**.[11f] In view of the lack of copolymerization by model catalyst **B**,[11e] the rigid quinoline ring within the title and model catalyst **A**[11f] plays an important role due to the different coordination. Beyond the improved incorporation and enhanced activity, the title catalysts have the advantage of maintaining high activities at elevated reaction temperature (80 °C).

4.5 Experimental Section

4.5.1 General Considerations

All manipulations of air and/or moisture-sensitive compounds were performed under a nitrogen atmosphere or using standard Schlenk techniques. Methylaluminoxane (MAO, 1.46 M in toluene) was purchased from Albemarle, and potassium hydride (KH) from Beijing Chemical Regent Company was washed with *n*-hexane before use to remove mineral oil contained. Tetrahydrofuran (THF), toluene, n-

for references, see page 73

hexane and n-heptane were refluxed over sodium and benzophenone, distilled, and then stored under nitrogen atmosphere. Dichloromethane (CH_2Cl_2) was distilled over calcium hydride, and stored under nitrogen atmosphere. High pure ethylene was purchased from Beijing Yansan Petrochemical Co. and used as received. IR spectra were recorded on a Perkin Elmer FT-IR 2000 spectrometer using KBr disc in the range of 4000-400 cm^{-1}. Elemental analysis was performed on a Flash EA 1112 microanalyzer. ^1H NMR and ^{13}C NMR spectra were recorded on a Bruker DMX 400 MHz instrument at ambient temperature using TMS as an internal standard. DSC traces and melting points of polyethylenes were obtained from the second scanning run on a Perkin-Elmer DSC-7 at a heating rate of 10 °C /min. ^1H NMR and ^{13}C NMR spectra of the polymers were recorded on a Bruker DMX-300 MHz instrument at 110 °C in deuterated 1,2-dichlorobenzene with TMS as an internal standard. Molecular weights and polydispersity indices (PDI) of (co-)polyethylenes were determined using a PL-GPC220 instrument at 135 °C in 1,2,4-trichlorobenzene with polystyrene as the standard.

4.5.2 Synthesis and Characterization of 2-(Benzimidazol-2-yl)-*N*-phenylquinoline-8-carboxamide Derivatives (L1-L6)

2-(*1H*-Benzo[d]imidazol-2-yl)-*N*-(2,6-diisopropylphenyl)quinoline-8-carboxamide (L1). Firstly, 2,6-diisopropylbenzenamine (3.54 g, 20 mmol) was slowly added to a xylene solution (100 mL) of 2-methylquinoline-8-carboxylic acid (3.74 g, 20 mmol) at room temperature. The mixture was stirred for 15 min and heated up to 80 °C. Trichlorophosphine (0.913 g, 6.7 mmol) was added slowly through a dropping funnel over the period of 15 min. It was then refluxed for 6 h and the solvent was removed by vacuum evaporation. 2-methyl-*N*-(2,6-diisopropylphenyl)quinoline-8-carboxamide was purified by column chromatography (silica gel, petroleum ether/ethyl acetate = 5:1) and obtained in 75% yield (5.21 g, 15.0 mmol). ^1H NMR ($CDCl_3$, 400 MHz): δ 12.90 (s, N-H, 1H), 8.93 (d, J = 7.3 Hz, 1H, quin), 8.22 (d, J = 8.4 Hz, 1H, quin), 7.98 (d, J = 8.0 Hz, 1H, quin), 7.66 (t, J = 7.7 Hz, 1H, quin), 7.40 (d, J = 8.4 Hz, 1H, quin), 7.34 (t, J = 7.6 Hz, 1H, aryl), 7.27 (d, J = 7.6 Hz, 2H, aryl), 3.30 (sept, J = 6.8 Hz, 2H, C*H*(CH_3)$_2$), 2.75 (s, 3H, CH_3), 1.25 (m, 12H, CH(C*H*$_3$)$_2$). ^{13}C NMR ($CDCl_3$, 100 MHz): δ 165.3, 158.8, 146.1, 145.5, 138.1, 134.5, 133.0, 132.0, 128.3, 127.8, 127.0, 126.0, 123.5, 122.0, 29.2, 25.6, 23.1. FT-IR (KBr, cm^{-1}): 3068 (w), 2962 (m), 2867 (w), 1647 (s), 1616 (m), 1593 (m), 1568 (m), 1524 (s), 1498 (m), 1455 (m), 1364 (m), 1325 (m), 1265 (m), 1207 (m), 1046 (m), 1008 (m), 878 (m), 836 (s), 790 (s), 743 (s), 664 (m). Mp: 207 °C. Anal. calcd (%) for $C_{23}H_{26}N_2O$: C, 79.73; H, 7.56; N, 8.09. Found: C, 79.85; H, 7.53; N, 8.07.

The mixture of equivalent molar amounts of *o*-phenylenediamine (1.08 g, 10 mmol) and 2-methyl-*N*-(2,6-diisopropylphenyl)quinoline-8-carboxamide (3.46 g, 10 mmol) with excess sulfur (1.60 g, 50 mmol) was heated to 170 °C and stirred for 12 h. On cooling to room temperature, 250 mL of THF was added, and the precipitated solid (including unreacted sulfur) was filtered off. The final product, 2-(*1H*-benzo[d]imidazol-2-yl)-*N*-(2,6-diisopropylphenyl)quinoline-8-carboxamide (**L1**), was purified by column chromatography (silica gel, petroleum ether/ethyl acetate = 2:1) and obtained in 58% yield

for references, see page 73

(2.60 g, 5.80 mmol). ^{1}H NMR ($CDCl_3$, 400 MHz): δ 11.05 (s, N-H, 1H, amide), 9.85 (s, N-H, 1H, imidazole), 8.83 (d, *J* = 7.2 Hz, 1H, quin), 8.67 (d, *J* = 8.5 Hz, 1H, quin), 8.48 (d, *J* = 8.5 Hz, 1H, quin), 8.08 (d, *J* = 8.0 Hz, 1H, quin), 7.87 (d, *J* = 5.4 Hz, 1H, aryl), 7.76 (t, *J* = 7.6 Hz, 1H, quin), 7.44-7.37 (m, 2H, aryl), 7.33-7.31 (m, 4H, aryl), 3.41 (sept, *J* = 6.7 Hz, 2H, C*H*$(CH_3)_2$), 1.28 (d, *J* = 6.7 Hz, 12H, CH(C*H*$_3)_2$). ^{13}C NMR ($CDCl_3$, 100 MHz): δ 165.8, 149.9, 148.6, 146.4, 145.1, 144.5, 139.1, 134.8, 134.1, 132.2, 132.0, 130.5, 129.1, 128.6, 127.5, 125.1, 123.9, 123.5, 120.8, 120.0, 111.5, 29.4, 24.0. FT-IR (KBr, cm-1): 3220 (m), 2961 (s), 1640 (s), 1599 (m), 1565 (m), 1513 (m), 1416 (m), 1363 (w), 1313 (m), 1274 (m), 1213 (w), 853 (m), 740 (m), 651 (m). Mp: 238-239 °C. Anal. calcd (%) for $C_{29}H_{28}N_4O$: C, 77.65; H, 6.29; N, 12.49. Found: C, 77.61; H, 6.36; N, 12.49.

2-(*1H*-Benzo[d]imidazol-2-yl)-*N*-(2,6-diethylphenyl)quinoline-8-carboxamide (L2). Using the above procedure, 2,6-diethylbenzenamine was used instead of 2,6-diisopropylbenzenamine to prepare 2-methyl-*N*-(2,6-diethylphenyl)quinoline-8-carboxamide in 79% yield. Then 2-methyl-*N*-(2,6-diethylphenyl)quinoline-8-carboxamide react with *o*-phenylenediamine to give the 2-(*1H*-benzo[d]imidazol-2-yl)-*N*-(2,6-diethylphenyl)quinoline-8-carboxamide (**L2**) in 53% yield. 2-Methyl-*N*-(2,6-diethylphenyl)quinoline-8-carboxamide: ^{1}H NMR ($CDCl_3$, 400 MHz): δ 12.96 (s, N-H, 1H, amide), 8.92 (d, *J* = 7.3 Hz, 1H, quin), 8.20 (d, *J* = 8.4 Hz, 1H, quin), 7.96 (d, *J* = 8.0 Hz, 1H, quin), 7.65 (t, *J* = 7.7 Hz, 1H, quin), 7.39 (d, *J* = 8.4 Hz, 1H, quin), 7.26 (t, *J* = 7.3 Hz, 1H, aryl), 7.20 (d, *J* = 7.0 Hz, 2H, aryl), 2.76 (s, 3H, CH_3), 2.75 (q, *J* = 7.5 Hz, 4H, C*H*$_2$CH$_3$), 1.23 (t, *J* = 7.5 Hz, 6H, CH_2C*H*$_3$). ^{13}C NMR ($CDCl_3$, 100 MHz): δ 164.9, 158.9, 145.5, 141.5, 138.2, 134.5, 134.4, 132.2, 128.2, 127.4, 126.4, 125.9, 123.8, 122.1, 25.6, 25.5, 14.9. FT-IR (KBr, cm^{-1}): 3069 (w), 2962 (m), 2866 (m), 1665 (s), 1595 (m), 1565 (m), 1523 (s), 1459 (m), 1368 (m), 1320 9m), 1268 (m), 1208 (m), 1144 (m), 1010 (w), 857 (w), 737 (m), 683 (m). Mp: 188-189 °C. Anal. calcd (%) for $C_{21}H_{22}N_2O$: C, 79.21; H, 6.96; N, 8.80. Found: C, 79.11; H, 6.86; N, 9.09. 2-(*1H*-Benzo[d]imidazol-2-yl)-*N*-(2,6-diethylphenyl)quinoline-8-carboxamide (**L2**): ^{1}H NMR ($CDCl_3$, 400 MHz): δ 11.34 (s, N-H, 1H, amide), 10.11 (s, N-H, 1H, imidazole), 8.77 (d, *J* = 7.2 Hz, 1H, quin), 8.64 (d, *J* = 8.6 Hz, 1H, quin), 8.46 (d, *J* = 8.6 Hz, 1H, quin), 8.07 (t, *J* = 8.0 Hz, 1H, quin), 7.86 (d, *J* = 7.2 Hz, 1H, quin), 7.73 (t, *J* = 7.6 Hz, 1H, aryl), 7.38-7.27 (m, 4H, aryl), 7.18 (d, *J* = 7.5 Hz, 2H, aryl), 2.76 (q, *J* = 7.5 Hz, 4H), 1.17 (t, *J* = 7.5 Hz, 6H). ^{13}C NMR ($CDCl_3$, 100 MHz): δ 165.1, 149.9, 148.7, 145.1, 144.3, 141.3, 139.0, 135.0, 134.3, 133.6, 132.3, 129.8, 129.0, 127.9, 127.4, 126.2, 124.8, 123.3, 120.6, 120.2, 111.6, 25.1, 14.4. FT-IR (KBr, cm^{-1}): 3187 (m), 2965 (m), 1643 (s), 1602 (m), 1565 (m), 1522 (m), 1417 (m), 1372 (w), 1315 (m), 1212 (w), 915 (w), 853 (m), 744 (s), 655(m). Mp: 220-221 °C. Anal. calcd (%) for $C_{27}H_{24}N_4O$: C, 77.12; H, 5.75; N, 13.32. Found: C, 77.08; H, 5.68; N, 13.36.

2-(*1H*-Benzo[d]imidazol-2-yl)-*N*-(2,6-dimethylphenyl)quinoline-8-carboxamide (L3). Using the above procedure, 2,6-dimethylbenzenamine was used instead of 2, 6-diisopropylbenzenamine to prepare 2-methyl-*N*-(2,6-dimethylphenyl)quinoline-8-carboxamide in 74% yield. Then 2-methyl-*N*-(2,6-dimethylphenyl)quinoline-8-carboxamide react with *o*-phenylenediamine to prepare the 2-(*1H*-benzo[d]imidazol-2-yl)-*N*-(2,6-dimethylphenyl)quinoline-8-carboxamide (**L3**) in 50% yield. 2-

for references, see page 73

Methyl-*N*-(2,6-dimethylphenyl)quinoline-8-carboxamide: ^{1}H NMR ($CDCl_3$, 400 MHz): δ 13.08 (s, N-H, 1H, amide), 8.92 (d, *J* = 7.3 Hz, 1H, quin), 8.21 (d, *J* = 8.4 Hz, 1H, quin), 7.97 (d, *J* = 8.0 Hz, 1H, quin), 7.66 (t, *J* = 7.7 Hz, 1H, quin), 7.40 (d, *J* = 8.4 Hz, 1H, quin), 7.19-7.13 (m, 3H, aryl), 2.79 (s, 3H, CH_3), 2.40 (s, 6H, CH_3). ^{13}C NMR ($CDCl_3$, 100 MHz): δ 164.1, 158.8, 145.4, 138.1, 135.7, 135.2, 134.3, 132.0, 128.2, 127.0, 126.6, 125.9, 123.5, 122.0, 25.6, 19.2. FT-IR (KBr, cm^{-1}): 3089 (m), 2915 (m), 1666 (s), 1617 (m), 1595 (m), 1566 (m), 1536 (s), 1431 (m), 1374 (m), 1326 (m), 1268 (m), 1137 (m), 1036 (m), 850 (m), 805 (m), 776 (m), 689 (m), 658 (m). Mp: 124-125 °C. Anal. calcd (%) for $C_{19}H_{18}N_2O$: C, 78.59; H, 6.25; N, 9.65. Found: C, 78.61; H, 6.26; N, 9.79. 2-(*1H*-Benzo[d]imidazol-2-yl)-*N*-(2,6-dimethylphenyl)quinoline-8-carboxamide (**L3**): ^{1}H NMR ($CDCl_3$, 400 MHz): δ 11.56 (s, N-H, 1H, amide), 10.28 (s, N-H, 1H, imidazole), 8.74 (m, 1H, quin), 8.62 (d, *J* = 8.6 Hz, 1H, quin), 8.46 (d, *J* = 8.6 Hz, 1H, quin), 8.06 (t, *J* = 8.0 Hz, 1H, quin), 7.86 (d, *J* = 7.1 Hz, 1H, quin), 7.71 (t, *J* = 7.6 Hz, 1H, aryl), 7.38-7.26 (m, 3H, aryl), 7.14-7.06 (m, 3H, aryl), 2.33 (s, 6H, CH_3). ^{13}C NMR ($CDCl_3$, 100 MHz): δ 164.5, 150.1, 149.1, 146.4, 145.1, 144.2, 138.5, 135.2, 135.0, 134.8, 132.2, 129.0, 128.8, 127.8, 127.2, 126.9, 124.4, 122.9, 120.5, 120.3, 111.7, 18.7. FT-IR (KBr, cm^{-1}): 3184 (m), 2916 (w), 1643 (s), 1601 (m), 1565 (m), 1523 (m), 1473 (w), 1416 (m), 1372 (w), 1314 (m), 1272 (m), 1215 (m), 1115 (w), 899 (w), 852 (m), 768 (m), 742 (m), 655 (m). Mp: 181-182 °C. Anal. calcd (%) for $C_{25}H_{20}N_4O$: C, 76.51; H, 5.14; N, 14.28. Found: C, 76.60; H, 4.98; N, 14.13.

2-(*1H*-Benzo[d]imidazol-2-yl)-*N*-(2,4,6-trimethylphenyl)quinoline-8-carboxamide (L4). Similarly, 2,4,6-trimethylbenzenamine was used instead of 2, 6-diisopropylbenzenamine to prepare 2-methyl-*N*-(2,4,6-trimethylphenyl)quinoline-8-carboxamide in 82% yield. Then 2-methyl-*N*-(2,4,6-trimethylphenyl)quinoline-8-carboxamide react with *o*-phenylenediamine to produce the 2-(*1H*-benzo[d]imidazol-2-yl)-*N*-(2,4,6-trimethylphenyl)quinoline-8-carboxamide (**L4**) in 60% yield. 2-Methyl-*N*-(2,4,6-trimethylphenyl)quinoline-8-carboxamide: ^{1}H NMR ($CDCl_3$, 400 MHz): δ 12.95 (s, N-H, 1H, amide), 8.91 (d, *J* = 7.4 Hz, 1H, quin), 8.20 (d, *J* = 8.4 Hz, 1H, quin), 7.96 (d, *J* = 8.0 Hz, 1H, quin), 7.65 (t, *J* = 7.6 Hz, 1H, quin), 7.39 (d, *J* = 8.4 Hz, 1H, quin), 6.99 (s, 2H, aryl), 2.78 (s, 3H, CH_3), 2.35 (s, 6H, CH_3), 2.33 (s, 3H, CH_3). ^{13}C NMR ($CDCl_3$, 100 MHz): δ 164.1, 158.6, 145.2, 137.9, 136.0, 134.8, 134.1, 133.0, 131.8, 128.8, 128.4, 126.8, 125.7, 121.9, 25.4, 21.0, 19.0. FT-IR (KBr, cm^{-1}): 3085 (m), 2916 (m), 1665 (s), 1607 (m), 1589 (m), 1566 (m), 1546 (s), 1432 (m), 1375 (m), 1316 (m), 1137 (m), 1038 (m), 851 (m), 776 (m), 690 (m), 655 (m). Mp: 140-141 °C. Anal. calcd (%) for $C_{20}H_{20}N_2O$: C, 78.92; H, 6.62; N, 9.20. Found: C, 78.88; H, 6.86; N, 9.10.

2-(*1H*-Benzo[*d*]imidazol-2-yl)-*N*-(2,4,6-trimethylphenyl)quinoline-8-carboxamide (**L4**): ^{1}H NMR ($CDCl_3$, 400 MHz): δ 13.65 (s, N-H, 1H, amide), 11.64 (s, N-H, 1H, imidazole), 8.77 (d, *J* = 8.6 Hz, 1H, quin), 8.62 (d, *J* = 7.3 Hz, 1H, quin), 8.53 (d, *J* = 8.6 Hz, 1H, quin), 8.30 (d, *J* = 8.1 Hz, 1H, quin), 7.84 (t, *J* = 7.7 Hz, 1H, quin), 7.69 (m, 2H, aryl), 7.31-7.30 (m, 2H, aryl), 6.97 (s, 2H, aryl), 2.28 (s, 9H, CH_3). ^{13}C NMR ($CDCl_3$, 100 MHz): δ 164.0, 150.8, 149.4, 145.0, 139.6, 138.2, 135.6, 135.3, 134.4, 132.6, 131.2, 129.0, 128.8, 127.6, 120.7, 21.1, 19.1. FT-IR (KBr, cm^{-1}): 3060 (m), 2916 (m), 1639 (s), 1600 (m), 1565 (m), 1529 (m), 1500 (m), 1417 (m), 1315 (m), 1273 (m), 1210 (w), 1143 (w),

for references, see page 73

1115 (m), 905 (w), 856 (m), 745 (s), 655 (m). Mp: 234-235 °C. Anal. calcd (%) for $C_{26}H_{22}N_4O$: C, 76.83; H, 5.46; N, 13.78. Found: C, 76.88; H, 5.60; N, 13.69.

2-(*1H*-Benzo[d]imidazol-2-yl)-*N*-phenylquinoline-8-carboxamide (L5). Similarly, aniline was used instead of 2,6-diisopropylbenzenamine to prepare 2-methyl-*N*-phenylquinoline-8-carboxamide in 71% yield. Then 2-methyl-*N*-phenylquinoline-8-carboxamide was reacted with *o*-phenylenediamine to prepare the 2-(*1H*-benzo[*d*]imidazol-2-yl)-*N*-phenylquinoline-8-carboxamide (**L5**) in 60% yield. 2-Methyl-*N*-phenylquinoline-8-carboxamide: ^{1}H NMR ($CDCl_3$, 400 MHz): δ 14.05 (s, N-H, 1H, amide), 8.92 (d, *J* = 7.4 Hz, 1H, quin), 8.20 (d, *J* = 8.4 Hz, 1H, quin), 7.95 (d, *J* = 8.0 Hz, 1H, quin), 7.89 (m, 2H, aryl and quin), 7.66 (t, *J* = 7.6 Hz, 1H, quin), 7.42 (m, 3H, aryl), 7.15 (t, *J* = 8.0 Hz, 1H, aryl), 2.90 (s, 3H, CH_3). ^{13}C NMR ($CDCl_3$, 100 MHz): δ 164.5, 158.4, 144.2, 139.5, 138.0, 133.9, 132.1, 129.1, 127.7, 126.8,125.8, 123.8, 121.9, 120.2, 25.4. FT-IR (KBr, cm^{-1}): 3064 (w), 2921 (m), 1670 (s), 1619 (m), 1594 (m), 1558 (s), 1499 (m), 1489 (m), 1444 (m), 1374 (m), 1330 (m), 1308 (m), 1267 (m), 1237 (w), 1137 (m), 1030 (w), 910 (m), 874 (m), 779 (m), 751 (s), 688 (m), 664 (m). Mp: 109-110 °C. Anal. calcd (%) for $C_{17}H_{14}N_2O$: C, 77.84; H, 5.38; N, 10.68. Found: C, 77.82; H, 5.60; N, 10.69. 2-(*1H*-Benzo[d]imidazol-2-yl)-*N*-phenylquinoline-8-carboxamide (**L5**): ^{1}H NMR ($CDCl_3$, 400 MHz): δ 13.62 (s, N-H, 1H, amide), 13.44 (s, N-H, 1H, imidazole), 8.80 (d, *J* = 8.5 Hz, 1H, quin), 8.72 (d, *J* = 7.3 Hz, 1H, quin), 8.49 (d, *J* = 8.5 Hz, 1H, quin), 8.31-8.29 (m, 3H, ph and quin), 7.85 (t, *J* = 7.6 Hz, 1H, quin), 7.82-7.70 (m, 2H, aryl), 7.46 (t, *J* = 7.4 Hz, 2H, aryl), 7.36-7.34 (m, 2H, aryl), 7.15 (t, *J* = 7.2 Hz, 1H, aryl). ^{13}C NMR ($CDCl_3$, 100 MHz): δ 163.5, 161.1, 158.3, 153.0, 150.3, 148.2, 144.7, 139.9, 138.1, 134.2, 132.9, 129.7, 129.2, 128.6, 127.7, 124.0, 120.0, 111.5. FT-IR (KBr, cm^{-1}): 3088 (m), 2910 (m), 1654 (s), 1618 (m), 1568 (m), 1531 (m), 1501 (m), 1418 (m), 1310 (m), 1270 (m), 1215 (w), 1145 (w), 1112 (m), 895 (w), 856 (m), 747 (s), 651 (m). Mp: 166 °C. Anal. calcd (%) for $C_{23}H_{16}N_4O$: C, 75.81; H, 4.43; N, 15.38. Found: C, 75.85; H, 4.48; N, 15.66.

2-(*1H*-Bbenzo[d]imidazol-2-yl)-*N*-(2,6-difluorophenyl)quinoline-8-carboxamide (L6). Similarly, 2,6-difluorobenzenamine was used instead of 2,6-diisopropylbenzenamine to prepare 2-methyl-*N*-diflurophenylquinoline-8-carboxamide in 72% yield. And 2-methyl-*N*-difluorophenylquinoline-8-carboxamide react with *o*-phenylenediamine to give the 2-(*1H*-benzo[d]imidazol-2-yl)-*N*-phenylquinoline-8-carboxamide (**L6**) in 46% yield. 2-Methyl-*N*-difluorophenylquinoline-8-carboxamide: ^{1}H NMR ($CDCl_3$, 400 MHz): δ 13.63 (s, N-H, 1H, amide), 8.87 (d, *J* = 7.3 Hz, 1H, quin), 8.17 (d, *J* = 8.4 Hz, 1H, quin), 7.95 (d, *J* = 8.0 Hz, 1H, quin), 7.63 (t, *J* = 7.6 Hz, 1H, quin), 7.37 (d, *J* = 8.4 Hz, 1H, quin), 7.20 (m, 1H, aryl), 7.03 (d, *J* = 8.0 Hz, 1H, aryl), 7.01 (d, *J* = 8.0 Hz, 1H, aryl), 2.80 (s, 3H, CH_3). ^{13}C NMR ($CDCl_3$, 100 MHz): δ 164.3, 159.1, 158.9, 156.6, 144.9, 138.0, 134.3, 132.5, 127.4, 126.8, 126.5, 125.8, 122.1, 111.9, 25.4. FT-IR (KBr, cm^{-1}): 3080 (w), 2915 (m), 1671 (s), 1617 (m), 1599 (m), 1568 (m), 1516 (s), 1435 (m), 1375 (m), 1321 (m), 1268 (m), 1138 (m), 1037 (m), 851 (m), 808 (m), 776 (m), 687 (m), 651 (m). Mp: 131-132 °C. Anal. calcd (%) for $C_{17}H_{12}F_2N_2O$: C, 68.45; H, 4.05; N, 9.39. Found: C, 68.29; H, 4.06; N, 9.69.

for references, see page 73

2-(*1H*-Benzo[d]imidazol-2-yl)-*N*-(2,6-difluorophenyl)quinoline-8-carboxamide (**L6**): ^{1}H NMR ($CDCl_3$, 400 MHz): δ 12.25 (s, N-H, 1H, amide), 10.50 (s, N-H, 1H, imidazole), 8.90 (d, *J* = 7.3 Hz, 1H, quin), 8.68 (d, *J* = 8.6 Hz, 1H, quin), 8.50 (d, *J* = 8.6 Hz, 1H, quin), 8.10 (d, *J* = 8.1 Hz, 1H, quin), 7.92 (d, *J* = 7.7 Hz, 1H, aryl), 7.78 (dd, J_1 = 7.6 Hz, J_2 = 7.6 Hz, 1H, quin), 7.60 (d, *J* = 7.7 Hz, 1H, aryl), 7.41 (dd, J_1 = 7.1 Hz, J_2 = 8.6 Hz, 1H, aryl), 7.36 (dd, J_1 = 8.3 Hz, J_2 = 7.3 Hz, 1H, aryl), 7.31-7.24 (m, 1H, aryl), 7.17 (d, *J* = 8.9 Hz, 2H, aryl). ^{13}C NMR ($CDCl_3$, 100 MHz): δ 165.0, 155.5, 150.0, 148.3, 144.7, 139.2, 138.3, 134.5, 132.8, 128.9, 128.8, 127.3, 127.2, 119.9, 111.7. FT-IR (KBr, cm^{-1}): 3238 (m), 3049 (w), 2954 (w), 1665 (s), 1602 (m), 1566 (m), 1534 (w), 1499 (w), 1473 (m), 1415 (m), 1318 (m), 1248 (m), 1109 (w), 1038 (w), 1009 (s), 853 (m), 820 (w), 744 (m), 703 (w), 655 (m). Mp: 202-203 °C. Anal. calcd (%) for $C_{23}H_{14}F_2N_4O$: C, 69.00; H, 3.52; N, 13.99. Found: C, 69.11; H, 3.58; N, 13.90.

4.5.3 Synthesis of Complexes (C1-C7)

(η^5-Cyclopentadienyl)[2-(benzimidazol-2-yl)-*N*-(2,6-diisopropylphenyl)quinoline-8-carboximidate] chlorotitanium (C1). To a THF solution (30 mL) of 2-(*1H*-benzo[d]imidazol-2-yl)-*N*-(2,6-diisopropylphenyl)quinoline-8-carboxamide (0.449 g, 1.00 mmol), KH (0.080 g, 2.00 mmol) was added at -78 °C. The mixture was allowed to warm to room temperature and stirred for additional 2 h. At -78 °C, 20 mL THF solution of a $CpTiCl_3$ (0.219 g, 1.00 mmol) was added dropwise over a 30 min period. The resultant mixture was allowed to warm to room temperature and stirred for 12 h. The residue, obtained by removing the solvent under vacuum, was extracted with CH_2Cl_2 (3 × 20 mL) and the combined filtrates were concentrated in vacuum to reduce the volume to 20 mL. *n*-Heptane (45 mL) was layered and several days later, dark red crystals were obtained (0.396 g, 0.665 mmol, yield 67%). ^{1}H NMR ($CDCl_3$, 400 MHz): δ 9.21 (d, *J* = 7.4 Hz, 1H, quin), 8.55 (s, 2H, quin), 8.10 (d, *J* = 7.9 Hz, 1H, quin), 7.96 (d, *J* = 8.0 Hz, 1H, quin), 7.82 (d, *J* = 7.2 Hz, 1H, aryl), 7.80 (d, *J* = 7.5 Hz, 1H, aryl), 7.33 (d, *J* = 7.4 Hz, 1H, aryl), 7.29-7.26 (m, 1H, aryl), 7.19-7.12 (m, 3H, aryl), 6.23 (s, 5H, Cp), 3.51 (m, 1H, C*H*$(CH_3)_2$), 2.83 (m, 1H, C*H*$(CH_3)_2$), 1.42 (m, 6H, CH(C*H*$_3)_2$), 1.23 (m, 3H, CH(C*H*$_3)_2$), 0.99 (m, 3H, CH(C*H*$_3)_2$). ^{13}C NMR ($CDCl_3$, 100 MHz): δ 154.3, 143.0, 142.8, 137.8, 137.3, 136.0, 132.3, 129.9, 129.2, 128.4, 128.3, 127.7, 125.4, 125.2, 123.7, 123.2, 122.5, 121.1, 120.0, 119.5, 118.9, 118.7, 32.0, 29.8, 23.1, 22.8, 21.5, 14.3. Anal. calcd (%) for $C_{34}H_{31}ClN_4OTi$: C, 68.64; H, 5.25; N, 9.42. Found: C, 68.63; H, 5.28; N, 9.43.

η^5-Cyclopentadienyl[2-(benzimidazol-2-yl)-*N*-(2,6-diethylphenyl)quinoline-8-carboximidate] chlorotitanium (C2). Using the same procedure for the synthesis of **C1**, **C2** was obtained as a dark red solid in 61% yield. ^{1}H NMR ($CDCl_3$, 400 MHz): δ 9.36 (d, *J* = 6.0 Hz, 1H, quin), 8.43 (d, *J* = 6.9 Hz, 1H, quin), 8.14 (d, *J* = 7.5 Hz, 1H, quin), 8.08 (d, *J* = 6.0 Hz, 1H, quin), 7.81 (m, 1H, aryl), 7.38-7.36 (m, 3H, aryl), 6.96 (t, *J* = 7.0 Hz, 1H, quin), 6.89 (d, *J* = 7.2 Hz, 1H, aryl), 6.71 (m, 1H, aryl), 6.04 (m, 1H, aryl), 5.86 (s, 5H, Cp), 3.27-3.17 (m, 1H, C*H*$(CH_3)_2$), 2.96-2.90 (m,1H, C*H*$(CH_3)_2$), 2.68-2.60 (m,1H, C*H*$(CH_3)_2$), 2.49-2.45 (m, 1H, C*H*$(CH_3)_2$), 1.57 (t, *J* = 7.3 Hz, 3H, CH(C*H*$_3)_2$), 1.07 (t, *J* = 7.2 Hz, 3H, CH(C*H*$_3)_2$). ^{13}C NMR ($CDCl_3$, 100 MHz): δ 165.0, 150.8, 149.4, 144.4, 141.6, 139.5,

for references, see page 73

135.7, 135.4, 132.6, 132.0, 131.7, 129.4, 128.7, 127.5, 127.2, 126.1, 125.8, 124.3, 122.8, 120.7, 120.1, 112.7, 24.9, 14.6. Anal. calcd (%) for $C_{32}H_{27}ClN_4OTi$: C, 67.80; H, 4.80; N, 9.88. Found: C, 67.73; H, 4.80; N, 9.82.

η^5-Cyclopentadienyl[2-(benzimidazol-2-yl)-*N*-(2,6-dimethylphenyl)quinoline-8-carboximidate] chlorotitanium (C3). Using the same procedure for the synthesis of **C1**, **C3** was obtained as a dark red solid in 58% yield. ^{1}H NMR ($CDCl_3$, 400 MHz): δ 9.22 (d, *J* = 6.9 Hz, 1H, quin), 8.54 (s, 2H, quin), 8.09 (d, *J* = 7.4 Hz, 1H, quin), 7.95 (d, *J* = 7.7 Hz, 1H, aryl), 7.82-7.80 (m, 1H, aryl), 7.34 (t, *J* = 7.1 Hz, 1H, quin), 7.30-7.26 (m, 1H, aryl), 7.14 (d, *J* = 7.3 Hz, 2H, aryl), 7.04 (d, *J* = 7.0 Hz, 2H, aryl), 6.22 (s, -5H, Cp), 2.39 (s, 6H, CH_3). ^{13}C NMR ($CDCl_3$, 100 MHz): δ 155.4, 146.7, 145.0, 144.8, 143.2, 142.7, 138.0, 137.2, 135.5, 132.5, 129.9, 129.2, 128.4, 128.0, 127.6, 125.5, 125.2, 123.7, 121.2, 119.9, 118.9, 118.6, 19.0. Anal. calcd (%) for $C_{30}H_{23}ClN_4OTi$: C, 66.87; H, 4.30; N, 10.40. Found: C, 66.73; H, 4.21; N, 10.50.

η^5-Cyclopentadienyl[2-(benzimidazol-2-yl)-*N*-(2,4,6-trimethylphenyl)quinoline-8-carboximidate] chlorotitanium (C4). Using the same procedure for the synthesis of **C1**, **C4** was obtained as a dark red solid in 69%. ^{1}H NMR ($CDCl_3$, 400 MHz): δ 9.20 (d, *J* = 7.3 Hz, 1H, quin), 8.53 (s, 2H, quin), 8.06 (d, *J* = 7.8 Hz, 1H, quin), 7.95 (d, *J* = 7.9 Hz, 1H, aryl), 7.82-7.76 (m, 2H, aryl), 7.34 (t, *J* = 7.4 Hz, 1H, quin), 7.30-7.26 (m, 1H, aryl), 6.95 (s, 2H, aryl), 6.22 (s, 5H, Cp), 2.36 (s, 3H, CH_3), 2.29 (s, 6H, CH_3). ^{13}C NMR ($CDCl_3$, 100 MHz): δ 155.3, 145.2, 143.0, 142.7, 142.1, 135.6, 132.7, 132.2, 129.8, 129.5, 129.1, 128.5, 128.3, 128.1, 127.4, 125.3, 125.1, 123.4, 121.1, 119.9, 118.7, 118.4, 21.0, 18.9. Anal. calcd (%) for $C_{31}H_{25}ClN_4OTi$: C, 67.34; H, 4.56; N, 10.13. Found: C, 67.36; H, 4.39; N, 10.16.

η^5-Cyclopentadienyl[2-(benzimidazol-2-yl)-*N*-phenylquinoline-8-carboximidate] chlorotitanium (C5). Using the same procedure for the synthesis of **C1**, **C5** was obtained as a dark red solid in 50% yield. ^{1}H NMR ($CDCl_3$, 400 MHz): δ 9.16 (d, *J* = 6.8 Hz, 1H, quin), 8.54 (s, 2H, quin), 8.07 (d, *J* = 7.6 Hz, 1H, quin), 8.02 (d, *J* = 8.1 Hz, 1H, aryl), 7.84 (d, *J* = 8.1 Hz, 1H, aryl), 7.78 (t, *J* = 7.5 Hz, 1H, quin), 7.65 (d, *J* = 7.7 Hz, 2H, aryl), 7.47 (t, *J* = 7.5 Hz, 2H, aryl), 7.38 (t, *J* = 7.4 Hz, 1H, aryl), 7.31-7.29 (m, 1H, aryl), 7.17 (d, *J* = 7.0 Hz, 1H, aryl), 6.27 (s, 5H, Cp). ^{13}C NMR ($CDCl_3$, 100 MHz): δ 157.1, 150.5, 149.0, 145.6, 144.5, 141.4, 139.2, 136.1, 134.9, 133.4, 132.1, 129.9, 128.9, 128.1, 127.3, 126.1, 124.5, 121.0, 120.3, 119.8, 117.6, 111.5. Anal. calcd (%) for $C_{28}H_{19}ClN_4OTi$: C, 65.84; H, 3.75; N, 10.97. Found: C, 65.84; H, 3.71; N, 10.96.

η^5-Cyclopentadienyl[2-(benzimidazol-2-yl)-*N*-(2,6-difluorophenyl)quinoline-8-carboximidate] chlorotitanium (C6). Using the same procedure for the synthesis of **C1**, **C6** was obtained as a dark red solid in 62% yield. ^{1}H NMR ($CDCl_3$, 400 MHz): δ 9.16 (d, *J* = 7.4 Hz, 1H, quin), 8.54 (s, 2H, quin), 8.10 (d, *J* = 7.8 Hz, 1H, quin), 7.93 (d, *J* = 8.0 Hz, 1H, aryl), 7.81 (d, *J* = 7.8 Hz, 1H, aryl), 7.77 (t, *J* = 7.7 Hz, 1H, quin), 7.35 (t, *J* = 7.5 Hz, 1H, aryl), 7.29 (t, *J* = 7.6 Hz, 1H, aryl), 7.13-7.09 (m, 1H, aryl), 7.04 (d, *J* = 7.6 Hz, 1H, aryl), 7.02 (d, *J* = 7.6 Hz, 1H, aryl), 6.32 (s, 5H, Cp). ^{13}C NMR ($CDCl_3$, 100 MHz): δ 159.5, 157.0, 150.2, 149.5, 144.8, 144.5, 139.6, 135.8, 134.8, 133.4, 132.4, 129.2, 128.9,

for references, see page 73

128.4, 127.5, 127.2, 124.2, 120.7, 120.2, 119.6, 117.2, 111.8. Anal. calcd (%) for $C_{28}H_{17}ClF_2N_4OTi$: C, 61.51; H, 3.13; N, 10.25. Found: C, 61.50; H, 3.11; N, 9.98.

Bis{η^5-cyclopentadienyl[2-(benzimidazol-2-yl)-*N*-(2,6-difluorophenyl)quinoline-8-carboximidate]titanium}(μ-oxo) (C7). According to our previous report,[11b,c] dimeric complex **C7** was prepared by slowly diffusion *n*-heptane into a dichloromethane solution of **C6** in the air. Red crystals were obtained one week later in 45% yield. ^{1}H NMR ($CDCl_3$, 400 MHz): δ 9.33 (d, J = 7.1 Hz, 2H, quin), 8.42 (d, J = 8.0 Hz, 2H, quin), 8.11 (d, J = 7.9 Hz, 4H, quin), 7.81 (dd, J_1 = 7.6 Hz, J_2 = 8.0 Hz, 2H, quin), 7.38 (d, J = 8.0 Hz, 2H, aryl), 7.31 (d, J = 7.3 Hz, 2H, aryl), 7.17-7.16 (m, 2H, aryl), 7.12-7.10 (m, 4H, aryl), 6.68 (m, 2H, aryl), 6.09 (s, 10H, Cp), 5.88 (m, 2H, aryl). ^{13}C NMR ($CDCl_3$, 100 MHz): δ 162.8, 157.4, 157.3, 155.1, 154.1, 146.1, 143.9, 141.7, 136.7, 132.9, 129.1, 128.3, 128.1, 127.1, 122.7, 122.4, 119.5, 118.9, 115.7, 112.1, 111.7. Anal. calcd (%) for $C_{56}H_{34}F_4N_8O_3Ti_2$: C, 64.76; H, 3.30; N, 10.79. Found: C, 64.70; H, 3.39; N, 10.82.

4.5.4 Procedures for Ethylene Polymerization and Copolymerization of Ethylene with α-Olefin

A 250-mL autoclave stainless steel reactor equipped with a mechanical stirrer and a temperature controller was heated in vacuum for at least 2 h above 80 °C. It was allowed to cool to the required reaction temperature under ethylene atmosphere and then charged with toluene (with monomer), the desired amount of co-catalyst and a toluene solution of the catalytic precursor. The total volume is 100 mL. After reaching the reaction temperature, the reactor is sealed and pressurized to 10 atm of ethylene pressure. The ethylene pressure is kept constant during the reaction time by feeding the reactor with ethylene. After a period of desired reaction time, the polymerization reaction is quenched by addition of acidic ethanol. The precipitated polymer is washed with ethanol several times and dried at 60 °C under vacuum overnight.

4.5.5 X-ray Structure Determinations

Crystals of **C1**, **C2** and **C6** suitable for single-crystal X-ray analysis are obtained by layering heptane on their CH_2Cl_2 solutions. Crystals of **C7** suitable for single-crystal X-ray analysis are obtained by slowly laying heptane on CH_2Cl_2 solution of complex **C6** respectively, and then opening this solution to air for one week. Single-crystal X-ray diffraction for **C1**, **C2**, **C6** and **C7** are performed on a Rigaku RAXIS Rapid IP diffractometer with graphite-monochromated Mo Kα radiation (λ = 0.71073 Å) at 173(2) K. Cell parameters are obtained by global refinement of the positions of all collected reflections. Intensities are corrected for Lorentz and polarization effects and numerical absorption. The structures are solved by direct methods and refined by full-matrix least-squares on F^2. All non-hydrogen atoms are refined anisotropically. Structure solution and refinement are performed by using the SHELXL-97 package.[22] Crystal data collection and refinement details for all compounds are available in the Supporting Information.

for references, see page 73

Acknowledgment

This work is supported by NSFC Nos. 20874105 and 20904059. We are grateful to Prof. Manfred Bochmann for his kindness in proofreading the manuscript.

Supporting Information Available

The GPC diagrams of corresponding polyolefins, crystal data and processing parameters for complexes **C1**, **C2**, **C6** and **C7** and their CIF file giving X-ray crystal structural data. This material is available free of charge via the Internet at http://pubs.acs.org.

for references, see page 73

References

1. (a) Brintzinger, H. H.; Fischer, D.; Mülhaupt, R.; Rieger, B.; Waymouth, R. M. *Angew. Chem. Int. Ed. Engl.* **1995**, *34*, 1143-1170; (b) Kaminsky, W. *Macromol. Chem. Phys.* **1996**, *197*, 3907-3945.
2. (a) McKnight, A. L.; Waymouth, R. M. *Chem. Rev.* **1998**, *98*, 2587-2598; (b) Braunschweig, H.; Breitling, F. M. *Coord. Chem. Rev.* **2006**, *250*, 2691-2720.
3. Kaminsky, W.; Winkelbach, H. *Top. Catal.* **1999**, *7*, 61-67.
4. (a) Sinn, H.; Kaminsky, W.; Vollmer, H. J.; Woldt, R. *Angew. Chem. Int. Ed. Engl.* **1980**, *19*, 390-392; (b) Alt, H. G.; Köppl, A. *Chem. Rev.* **2000**, *100*, 1205-1221.
5. (a) Shapiro, P. J.; Bunel, E.; Schaefer, W. P.; Bercaw, J. E. *Organometallics* **1990**, *9*, 867-869; (b) Stevens, J. C.; Timmers, F. J.; Wilson, D. R.; Schmidt, G. F.; Nickias, P. N.; Rosen, R. K.; McKnight, G. W.; Lai, S. Eur. Pat. Appl. 0416815A2, **1991**; (c) Shapiro, P. J.; Cotter, W. D.; Schaefer, W. P.; Labinger, J. A.; Bercaw, J. E. *J. Am. Chem. Soc.* **1994**, *116*, 4623-4640.
6. (a) Matsui, S.; Tohi, Y.; Mitani, M.; Saito, J.; Makio, H.; Tanaka, H.; Nitabaru, M.; Nakano, T.; Fujita, T. *Chem. Lett.* **1999**, 1065-1066; (b) Tian, J.; Coates, G. W. *Angew. Chem. Int. Ed.* **2000**, *39*, 3626-3629; (c) Matsui, S.; Mitani, M.; Saito, J.; Tohi, Y.; Makio, H.; Matsukawa, N.; Takagi, Y.; Tsuru, K.; Nitabaru, M.; Nakano, T.; Tanaka, H.; Kashiwa, N.; Fujita, T. *J. Am. Chem. Soc.* **2001**, *123*, 6847-6856; (d) Tian, J.; Hustad, P. D.; Coates, G. W. *J. Am. Chem. Soc.* **2001**, *123*, 5134-5135; (e) Makio, H.; Kashiwa, N.; Fujita, T. *Adv. Synth. Catal.* **2002**, *344*, 477-493; (f) Sakuma, A.; Weiser, M.-S.; Fujita, T. *Polym. J.* **2007**, *39*, 193-207; (g) Edson, J. B.; Wang, Z.; Kramer, E. J.; Coates, G. W. *J. Am. Chem. Soc.* **2008**, *130*, 4968-4977; (h) Matsugi, T.; Fujita, T. *Chem. Soc. Rev.* **2008**, *37*, 1264-1277.
7. (a) Yoshida, Y.; Matsui, S.; Takagi, Y.; Mitani, M.; Nakano, T.; Tanaka, H.; Kashiwa, N.; Fujita, T. *Organometallics* **2001**, *20*, 4793-4799; (b) Yoshida, Y.; Mohri, J.; Ishii, S.; Mitani, M.; Saito, J.; Matsui, S.; Makio, H.; Nakano, T.; Tanaka, H.; Onda, M.; Yamamoto, Y.; Mizuno, A.; Fujita, T. *J. Am. Chem. Soc.* **2004**, *126*, 12023-12032; (c) Zuo, W.; Sun, W.-H.; Zhang, S.; Hao, P.; Shiga, A. *J. Polym. Sci., Part A: Polym. Chem.* **2007**, *45*, 3415-3430.
8. (a) Nomura, K.; Liu, J.; Padmanabhan, S.; Kitiyanan, B. *J. Mol. Catal. A: Chem.* **2007**, *267*, 1-29; (b) Nomura, K. *Dalton Trans.* **2009**, 8811-8823.
9. (a) Nomura, K.; Naga, N.; Miki, M.; Yanagi, K. *Macromolecules* **1998**, *31*, 7588-7597; (b) Nomura, K.; Naga, N.; Miki, M.; Yanagi, K.; Imai, A. *Organometallics* **1998**, *17*, 2152-2154; (c) Zhang, S.; Piers, W. E.; Gao, X.; Parvez, M. *J. Am. Chem. Soc.* **2000**, *122*, 5499-5509; (d) Nomura, K.; Fujita, K.; Fujiki, M. *J. Mol. Catal. A: Chem.* **2004**, *220*, 133-144; (e) Mahanthappa, M. K.; Cole, A. P.; Waymouth, R. M. *Organometallics* **2004**, *23*, 836-845; (f) Esteruelas, M. A.; López, A. M.; Mateo, A. C.; Oñate, E. *Organometallics* **2006**, *25*, 1448-1460; (g) Shah, S. A. A.; Dorn, H.; Voigt, A.; Roesky, H. W.; Parisini, E.; Schmidt, H.-G.; Noltemeyer, M. *Organometallics* **1996**, *15*, 3176-3181; (h) Tamm, M.; Randoll, S.; Herdtweck, E.; Kleigrewe, N.; Kehr, G.; Erker, G.; Rieger, B. *Dalton Trans.* **2008**, 459.
10. (a) Doherty, S.; Errington, R. J.; Jarvis, A. P.; Collins, S.; Clegg, W.; Elsegood, M. R. J. *Organometallics* **1998**, *17*, 3408-3410; (b) Richter, J.; Edelmann, F. T.; Noltemeyer, M.; Schmidt, H.-G.; Shmulinson, M.; Eisen, M. S. *J. Mol. Catal. A: Chem.* **1998**, *130*, 149-162; (c) Sita, L. R.; Babcock, J. R. *Organometallics* **1998**, *17*, 5228-5230; (d) Vollmerhaus, R.; Shao, P.; Taylor, N. J.; Collins, S. *Organometallics* **1999**, *18*, 2731-2733; (e) Jayaratne, K. C.; Sita, L. R. *J. Am. Chem. Soc.* **2000**, *122*, 958-959; (f) Huang, J.; Lian, B.; Qian, Y.; Zhou, W.; Chen, W.; Zheng, G. *Macromolecules* **2002**, *35*, 4871-4874; (g) Bott, R. K. J.; Hughes, D. L.; Schormann, M.; Bochmann, M.; Lancaster, S. J. *J. Organomet. Chem.* **2003**, *665*, 135-149; (h) Yasumoto, T.; Yamagata, T.; Mashima, K. *Organometallics* **2005**, *24*, 3375-3377; (i) Zuo, W.; Zhang, M.; Sun, W.-H. *J. Polym. Sci., Part A: Polym. Chem.* **2009**, *47*, 357-372; (j) Keaton, R. J.; Jayaratne, K. C.; Henningsen, D. A.; Koterwas, L. A.; Sita, L. R. *J. Am. Chem. Soc.* **2001**, *123*, 6197-6198; (k) Zhang, H.; Katao, S.; Nomura, K.; Huang, J. *Organometallics* **2007**, *26*, 5967-5977.
11. (a) Chen, Q.; Huang, J.; Yu, J. *Inorg. Chem. Commun.* **2005**, *8*, 444-448; (b) Chan, M. C. W.; Tam, K.-H.; Zhu, N.; Chiu, P.; Matsui, S. *Organometallics* **2006**, *25*, 785-792; (c) Zhang, J.; Lin, Y.-J.; Jin, G.-X. *Organometallics* **2007**, *26*, 4042-4047; (d) Liu, S.; Zuo, W.; Zhang, S.; Hao, P.; Wang, D.; Sun, W.-H. *J. Polym. Sci., Part A: Polym. Chem.* **2008**, *46*, 3411-3423; (e) Zuo, W.; Zhang, S.; Liu, S.; Liu, X.; Sun, W.-H. *J. Polym. Sci., Part A: Polym. Chem.* **2008**, *46*, 3396-3410; (f) Liu, S.; Yi, J.; Zuo, W.; Wang, K.; Wang, D.; Sun, W.-H. *J. Polym. Sci., Part A: Polym. Chem.* **2009**, *47*, 3154-3169.
12. (a) Barnes, D. J.; Chapman, R. L.; Vagg, R. S.; Watton, E. C. *J. Chem. Eng. Data* **1978**, *23*, 349-350; (b) Chan, P.-M.; Yu, W.-Y.; Che, C.-M.; Cheung, K.-K. *J. Chem. Soc., Dalton Trans.* **1998**, 3183-3190; (c) Belda, O.; Kaiser, N.-F.; Bremberg, U.; Larhed, M.; Hallberg, A.; Moberg, C. *J. Org. Chem.* **2000**, *65*, 5868-5870; (d) Conlon, D. A.; Yasuda, N. *Adv. Synth. Catal.* **2001**, *343*, 137-138; (e) Senier, A.; Shepheard, F. G. *J. Chem. Soc., Trans.* **1909**, *95*, 441-445; (f) Grimmel, H. W.; Guenther, A.; Morgan, J. F. *J. Am. Chem. Soc.* **1946**, *68*, 539-542.
13. (a) Barni, E.; Savarino, P. *J. Heterocycl. Chem.* **1977**, *14*, 937-940; (b) Tsukamoto, G.; Yoshino, K.; Kohno, T.; Ohtaka, H.; Kagaya, H.; Ito, K. *J. Med. Chem.* **1980**, *23*, 734-738; (c) Sun, W.-H.; Hao, P.; Zhang, S.; Shi, Q.; Zuo, W.; Tang, X.; Lu, X. *Organometallics* **2007**, *26*, 2720-2734.

for references, see page 73

14. (a) Flores, J. C.; Chien, J. C. W.; Rausch, M. D. *Macromolecules* **1996**, *29*, 8030-8035; (b) Esteruelas, M. A.; López, A. M.; Mateo, A. C.; Oñate, E. *Organometallics* **2005**, *24*, 5084-5094; (c) Müller, J.; Kehr, G.; Fröhlich, R.; Erker, G. *Eur. J. Inorg. Chem*. **2005**, 2836-2841; (d) Gurubasavaraj, P. M.; Roesky, H. W.; Sharma, P. M. V.; Oswald, R. B.; Dolle, V.; Herbst-Irmer, R.; Pal, A. *Organometallics* **2007**, *26*, 3346-3351.
15. (a) Amor, F.; Fokken, S.; Kleinhenn, T.; Spaniol, T. P.; Okuda, J. *J. Organomet. Chem.* **2001**, *621*, 3-9; (b) González-Maupoey, M.; Cuenca, T.; Frutos, L. M.; Castaño, O.; Herdtweck, E. *Organometallics* **2003**, *22*, 2694-2704.
16. Koltzenburg, S. *J. Mol. Catal. A: Chem.* **1997**, *116*, 355-363.
17. Chen, E. Y. X.; Marks, T. J. *Chem. Rev.* **2000**, *100*, 1391-1434.
18. Bochmann, M. *J. Chem. Soc., Dalton Trans*. **1996**, 255-270.
19. (a) Woo, T. K.; Margl, P. M.; Lohrenz, J. C. W.; Blöchl, P. E.; Ziegler, T. *J. Am. Chem. Soc*. **1996**, *118*, 13021-13030; (b) Woo, T. K.; Margl, P. M.; Ziegler, T.; Blöchl, P. E. *Organometallics* **1997**, *16*, 3454-3468; (c) Sinnema, P.-J.; Hessen, B.; Teuben, J. H. *Macromol. Rapid Commun.* **2000**, *21*, 562-566.
20. Simanke, A. G.; Galland, G. B.; Freitas, L.; da Jornada, J. A. H.; Quijada, R.; Mauler, R. S. *Polymer* **1999**, *40*, 5489-5495.
21. (a) Seger, M. R.; Maciel, G. E. *Anal. Chem.* **2004**, *76*, 5734-5747; (b) Galland, G. B.; Quijada, R.; Mauler, R. S.; de Menezes, S. C. *Macromol. Rapid Commun*. **1996**, *17*, 607-613.
22. Sheldrick, G. M. SHELXL-97; University of Göttingen: Göttingen (Germany), **1997**.

for references, see page 73

CHAPITRE V

Syntheses, Characterization and Ethylene (Co-) Polymerization Screening of Amidate Half-titanocene Dichlorides

SHAOFENG LIU,[†] WEN-HUA SUN,*[,†,‡] YANNING ZENG,[†] DELIGEER WANG,[†,§] WENJUAN ZHANG,[†] AND YAN LI[†]

[†] *Key laboratory of Engineering Plastics and Beijing Natural Laboratory for Molecular Science, Institute of Chemistry, Chinese Academy of Sciences, Beijing 100190, China*
[‡] *State Key Laboratory for Oxo Synthesis and Selective Oxidation, Lanzhou Institute of Chemical Physics, Chinese Academy of Sciences, Lanzhou 730000, China*
[§] *Department of Chemistry, Inner Mongolia Normal University, Hohhot 010022, China*

This Chapter has been published in *Organometallics*, **2010**, *29*, 2459-2464

Contributions from the various co-authors: Professors Wen-Hua Sun and Deligeer Wang supervised the work and provided direction and discussions, Miss Yanning Zeng assisted for the synthesis, Dr. Wenjuan Zhang for discussions and composition and Ms. Yan Li for X-ray structure analyses.

Résumé du Chapitre V

Une série d'amidates du chlorure de semi-titanocène, Cp′Ti**L**Cl_2 [Cp′ = Cp (pour η^5-C_5H_5) ou Cp^* (pour η^5-C_5Me_5), **L** = *N*-(2-méthylquinolin-8-yl)-*p*-R-benzamidure, **C1**: Cp′ = Cp, R = OMe; **C2**: Cp′ = Cp, R = Me; **C3**: Cp′ = Cp, R = H; **C4**: Cp′ = Cp, R = F; **C5**: Cp′ = Cp, R = Cl; **C6**: Cp′ = Cp^*, R = OMe; **C7**: Cp′ = Cp^*, R = Me], a été synthétisée par réaction stoichiométrique entre Cp′$TiCl_3$ et les amidates correspondants. Tous les complexes furent caractérisés par analyse élémentaire et RMN. Les structures moléculaires des complexes **C2** et **C4** furent confirmées par diffraction des rayons X. Les fragments amidate sont coordinés au titane par l'azote et l'oxygène de l'imine/alcoxyde. Par comparaison avec les systèmes catalytiques Cp$TiCl_3$/MAO ou Cp^*TiCl_3/MAO, **C1-C7**/MAO présentent une activité catalytique bien plus élévée pour la polymérisation de l'éthylène. Les pré-catalyseurs C**6** et **C7** porteurs d'un anneau Cp^* ont une activité supérieure à leurs analogues **C1-C5** contenant le ligand Cp, tandis que les groupes électrodonneurs des ligands amidates influencent positivement les résultats catalytiques, conduisant à une activité accrue. Une augmentation du rapport MAO / Ti ou une diminution de la température de réaction augmente la productivité mais les poids moléculaires des polymères formés diminuent lorsque l'activité catalytique augmente. De plus, le système **C6**/MAO se montre très actif en copolymérisation de l'éthylène avec le 1-hexène ou le 1-octène.

5.1 Abstract of Chapter V

A series of amidate half-titanocene dichlorides, Cp′Ti**L**Cl_2 [Cp′ = Cp (as η^5-C_5H_5) or Cp^* (as η^5-C_5Me_5), **L** = *N*-(2-methylquinolin-8-yl)-*p*-R-benzamides. **C1**: Cp′ = Cp, R = OMe; **C2**: Cp′ = Cp, R = Me; **C3**: Cp′ = Cp, R = H; **C4**: Cp′ = Cp, R = F; **C5**: Cp′ = Cp, R = Cl; **C6**: Cp′ = Cp^*, R = OMe; **C7**: Cp′ = Cp^*, R = Me], have been synthesized by the stoichiometric reaction of Cp′$TiCl_3$ with the corresponding potassium amidates. All complexes were fully characterized by elemental and NMR analyses. The molecular structures of complexes **C2** and **C4** are confirmed by single-crystal X-ray diffraction, and the amidate moieties coordinate to the titanium center by N and O atoms of the imine/alkoxide. In comparison with the catalytic behavior by $CpTiCl_3$/MAO or Cp^*TiCl_3/MAO systems, the systems of **C1-C7**/MAO show much higher activities towards ethylene polymerization. The precatalysts (C**6** and **C7**) bearing Cp^* ligand exhibit higher activities than their analogues (**C1-C5**) containing Cp ligand, while the amidate ligands containing electron-donating groups positively affect the catalytic behavior of their titanium precatalysts, leading to better activity. Both increasing the ratio of MAO to titanium and reducing reaction temperature enhance the productivities, however, the molecular weights of the resulting polymers decrease with increasing activities. Moreover, the **C6**/MAO system performs with high activity in the copolymerization of ethylene and 1-hexene or 1-octene.

5.2 Introduction

Polyolefins remain the most produced type of synthetic polymers, the synthesis of which employs commercial catalysts of Ziegler-Natta,[1] Phillip[2] and metallocenes.[3] In particular, the constrained-geometry compounds (CGC) of half-metallocenes, representative as single-site catalysts, are favorable to produce polyolefins with controlled molecular weight, specific tacticity, and narrow molecular weight distribution, as well as the better comonomer incorporation.[4] Since the 1990s, inspired by the fast developments in coordination and organometallic chemistry, more and more transition metal procatalysts have been designed and investigated for olefin polymerization.[5] Examples of chelating ligands are amidinate,[6] amide[7] and alkoxy[8] etc, in which two significant procatalysts named as FI[9] and PI[10] catalysts have drawn much attention due to their high activities and their unique abilities to control polymer microstructures. The catalytic behavior of these complexes and also the properties of the resultant polyolefin could be finely tuned by modifying the substituents of the procatalyst ligand.[11] Attempts to combine the merits of the individual systems have led to the successful development of a series of non-bridged half-metallocene procatalyst as Cp′M(L)Xn (M = Ti, Zr, Hf; L = anionic ligand; X = halogen or alkyl),[12] which exhibited promising catalytic behavior and overcame the synthetic problems associated with metallocene[3] and/or CGC procatalysts.[4] Therefore, the half-titanocene Cp′M(L)Xn procatalysts containing a dianionic[13] or monoanionic[14] amidate ligands have been investigated in our group.

for references, see page 86

Considering the ease of syntheses and variations of catalytic behavior of amidate metal complexes,[15] the title complexes were synthesized and characterized. Unexpectedly, *N*-(2-methylquinolin-8-yl)-*p*-R-benzamidates coordinate as imine/alkoxide in μ_2-OCN mode of the amidate moiety, however, the quinolinyl group does not coordinate to the titanium atom. All title precatalysts (**C1**-**C7**) show high activities towards ethylene polymerization, and the representative precatalyst (**C6**) exhibits high activity in the copolymerization of ethylene with 1-hexene or 1-octene. Herein the syntheses and characterizations of the title complexes are detailed along with their catalytic behavior in olefin polymerization.

5.3 Results and Discussion

5.3.1 Synthesis and Characterization of Half-titanocene Complexes

All *N*-(2-methylquinolin-8-yl)benzamide derivatives were prepared according to previous reported method.[13b,16] These compounds could be deprotonated by reacting with potassium hydride in tetrahydrofuran (THF) at room temperature, and the resulting potassium compounds further reacted with one equivalent of Cp′$TiCl_3$ (Cp′ = Cp or Cp^*) in THF to afford red solutions. Brown crystals of analytically pure amidate half-titanocene complexes, Cp′Ti**L**Cl_2 (**C1**-**C7**: Cp′ = Cp or Cp^*; **L** = *N*-(2-methylquinolin-8-yl)-*p*-R-benzamides) (Scheme 1), were isolated in good yields (77.2-89.0%). The molecular structures are consistent with the ^{1}H and ^{13}C NMR spectra (see experimental section). Regarding the proton resonances of their ^{1}H NMR spectra, the protons of the amidate ligand appear between 10.5 to 10.9 ppm, but disappear in the title complexes due to the formation of Ti-N bonds. In all complexes, the ^{1}H NMR resonances are high-field shifted because of the decrease in electron-density in the aromatic rings upon coordinating with titanium.

Scheme 1. Synthesis of Complexes **C1**-**C7**

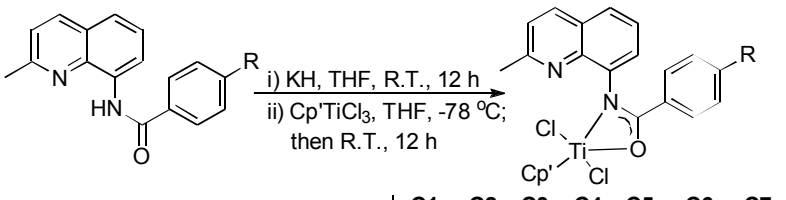

	C1	C2	C3	C4	C5	C6	C7
R	OMe	Me	H	F	Cl	OMe	Me
Cp'	Cp	Cp	Cp	Cp	Cp	Cp*	Cp*

Crystals of **C2** and **C4** suitable for single-crystal X-ray analysis were grown by slow diffusion of heptane into toluene solutions of **C2** and **C4**. Their molecular structures are illustrated in Figure 1 (**C2**) and the supporting information (**C4**), respectively, with selected bonds and angles shown in Table 1.

for references, see page 86

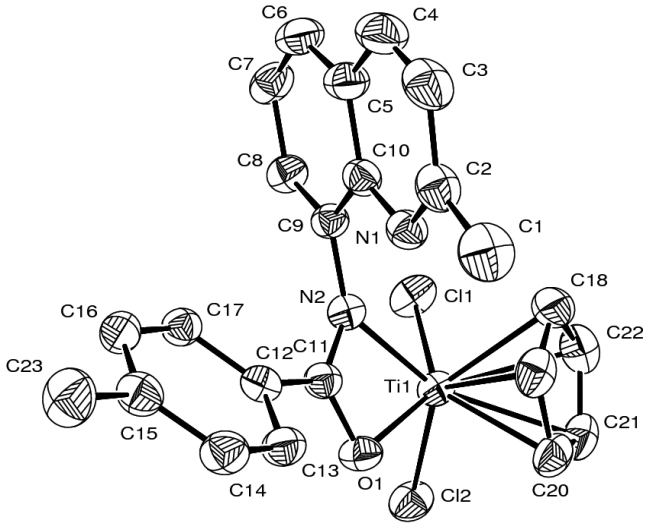

Figure 1. ORTEP view of the molecular structure of **C2** (ellipsoids enclose 50% electronic density; H atoms are omitted for clarity).

Table 1. Selected Bonds (Å) and Angles (°) for **C2** and **C4**

	C2	**C4**
Bond Lengths		
Ti1-O1	2.0697(2)	2.070(2)
Ti1-C11	2.512(3)	2.515(3)
Ti1-N2	2.117(2)	2.123(2)
Ti1-C18	2.332(3)	2.340(3)
Ti1-C19	2.341(3)	2.346(3)
Ti1-C20	2.348(3)	2.346(3)
Ti1-C21	2.352(3)	2.355(3)
Ti1-C22	2.341(3)	2.357(3)
Ti1-Cl1	2.2944(1)	2.2883(1)
Ti1-Cl2	2.2906(9)	2.2888(1)
C11-N2	1.309(3)	1.301(3)
C11-O1	1.296(3)	1.299(3)
Bond Angles		
N2-Ti1-Cl1	86.16(7)	130.15(7)
N2-Ti1-Cl2	129.76(7)	86.08(7)
N2-Ti1-O1	62.26(8)	62.10(8)
Cl1-Ti1-O1	136.97(6)	86.05(7)
Cl2-Ti1-O1	86.63(6)	135.99(6)
Cl1-Ti1-Cl2	93.42(4)	93.82(5)
N2-C11-O1	112.4(2)	112.6(2)

Considering the centroid of Cp as a single coordination site, the molecular structure of complex **C2** (Figure 1) consists of a distorted square-pyramid configuration, in which the Cp group lies in the apical site and the amidate moiety acts as a bidentate ligand together with the two chlorides in the bottom plane. The sum of the metallocyclic bond angles is 359.6°, indicating the coplanarity of titanium with all atoms of the bidentate amidate group in the η^2 fashion. The bonding motif of the amidate ligand is a nonsymmetric one bonded via the imine/alkoxide mode, which is in contrast to the

for references, see page 86

coordination manner of amidate found in tridentate titanium complexes.[13,17] The C-O bond (C11-O1 = 1.296(3) Å) is somewhat shorter than normal, which together with the C-N bond length (C11-N2 = 1.309(3) Å), suggests a delocalized bonding motif within the amidate backbone; the negative charge is more localized on the nitrogen. The Ti-N bond (Ti1-N2 = 2.117(2) Å) and Ti-O bond (Ti1-O1 = 2.0697(2) Å) are similar to previous amidate-based titanium complexes.[15a,b,15d] The Cp ring is planar (maximum deviation from the plane of 0.003 Å for C20) with a typical Ti-Cp_{cent} distance of 2.017 Å. The dihedral angle of the planes defined by the Cp ring and the chelating ring is 23.7°, while the dihedral angles between the chelating ring and the phenyl group or quinoline ring are 35.9 or 61.1°, respectively. Two chlorine atoms are located *cis* to each other, meanwhile the Ti-Cl bonds are almost identical (Ti1-Cl1 = 2.2944(1) Å and Ti1-Cl2 = 2.2906(9) Å) with an angle of 93.4°.

The molecular structures of complexes **C2** and **C4** (see Supporting Information) are quite similar without distinct differences in structural feature.

5.3.2 Catalytic Behavior toward Ethylene Polymerization

Influences of Al/Ti Molar Ratio, Reaction Temperature and Time on the Catalytic Behavior of C6. Pre-catalyst **C6** has been used under various reaction parameters for the optimum conditions in ethylene polymerization. Good catalytic performances are observed in the presence of MAO or MMAO as cocatalyst, in which employing MAO gives better result than that with MMAO. For example, for the molar ratio of Al/Ti = 1500 : 1 under 10 atm ethylene pressure, the catalytic activity is 1560 kg mol^{-1}(Ti) h^{-1} using MMAO, while the system with MAO gives an activity of 2170 kg mol^{-1}(Ti) h^{-1} (entry 3, Table 2). Therefore the detail investigations employing MAO have been carried out through varying the ratios of Al/Ti, reaction temperature and time, and their results are tabulated in Table 2.

Table 2. Ethylene Polymerization with **C6**/MAO[a]

Entry	Al/Ti	*t* (min)	*T* (°C)	PE (g)	Activity (kg·mol^{-1}(Ti)·h^{-1})	T_m[b] (°C)	M_w[c] (kg·mol^{-1})	M_w/M_n[c]
1	500	10	30	0.713	856	128.1	54.7	17
2	1000	10	30	1.33	1600	127.7	42.2	15
3	1500	10	30	1.81	2170	125.3	30.5	13
4	2000	10	30	1.53	1840	126.8	25.3	12
5	1500	10	40	1.55	1860	125.6	5.81	1.7
6	1500	10	50	1.44	1730	125.3	5.55	1.8
7	1500	10	60	0.754	905	125.0	4.80	1.6
8	1500	5	30	1.17	2810	125.2	22.3	7.1
9	1500	30	30	2.63	1050	125.8	40.8	17

[a] Conditions: 5 μmol Ti; 10 atm ethylene; toluene (total volume 100 mL). [b] Determined by DSC. [c] Determined by GPC.

According to observations at different Al/Ti ratios ranging from 500 to 2000 (entries 1-4, Table 2), the maximum activity is shown at an Al/Ti molar ratio of 1500 (entry 3, Table 2). Such phenomenon can be well explained by the influence of the Al concentration on the termination of polymer

for references, see page 86

chains.[5f,18] In addition, the obtained polyethylene exhibits lower M_w values when the ratio of Al : Ti is increased, because of the chain transfer increasing with high Al concentration.[18-19]

Regarding the thermal stability of complex **C6**, its activities significantly decreased with increasing the reaction temperature from 30 to 60 °C (entries 3, 5-7, Table 2). In contrast to the current system, half-titanocene chlorides bearing tridentate *N*-(2-benzimidazolylquinolin-8-yl)benzamidates exhibit higher activities at higher temperature and possess good thermal stability.[13b] The multidentate coordination of ligands increases the thermal stability of half-titanocene complexes and their active species. The observation that the activity decreased at high temperature was also found in the type of Cp_2TiCl_2 system due to the bimolecular disproportionation termination.[20] In terms of the molecular weights of the resulting polyethylenes (PEs), remarkable differences have been found between reactions at 30 °C and above 40 °C. At 30 °C, **C6**/MAO system affords PEs with bimodal molecular weight distribution, while PEs with single-modal distribution are obtained in the case with temperature at 40 °C or above (Fig. 2). The influence of reaction temperature or activator on molecular weight distribution is also observed in α-diimine nickel or bis(imine)pyridine iron complexes.[21] It is assumed that the active species above 40 °C are uniform, however, those active sites could not be prolonged in ethylene insertions for high molecular weight PEs. Due to highly exothermal reaction of polymerization, we meet trouble to control reaction temperature lower than 30 °C. The catalytic system produces highly active species for ethylene polymerization at 30 °C, while active species would be changed with polymerization affecting reaction temperature.

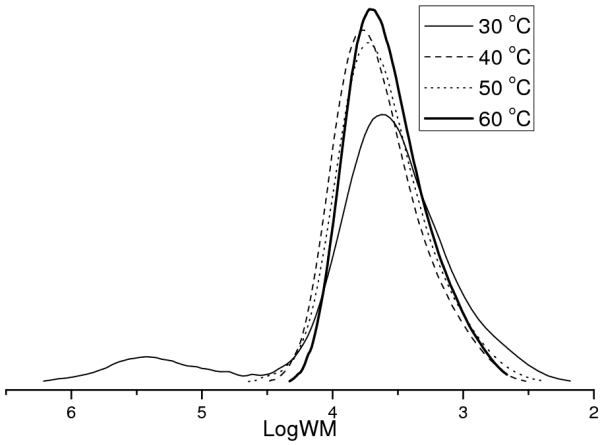

Figure 2. GPC profiles of PEs obtained from entries 3,5-7 in Table 2.

Regarding the lifetime of **C6**/MAO system (entries 3, 8 and 9, Table 2), the activities decrease with the length of the reaction at 5, 10 or 30 minutes.

Ligand Environmental Effect on the Catalytic Behavior of Procatalysts (C1-C7). Using the above optimum conditions (10 atm ethylene, 30 °C and Al/Ti 1500), the precatalysts (**C1-C7**) have been examined to better understand the substituent effects of the ligands. For comparison, the polymerization using $CpTiCl_3$ was also conducted. Their results are collected in Table 3. In general,

for references, see page 86

all procatalysts show high activities in the range of 978 to 2170 kg·mol^{-1}(Ti)·h^{-1} (entries 1-7, Table 3), while $CpTiCl_3$ gave an activity of 282 kg·mol^{-1}(Ti)·h^{-1}.

Table 3. Ethylene Polymerization with **C1-C7**/MAO[a]

Entry	Pre-cat.	PE (g)	Activity (kg·mol^{-1}(Ti)·h^{-1})	T_m[b] (°C)	M_w[c] (kg·mol^{-1})	M_w/M_n[c]
1	**C1**	1.28	1540	127.7	231	4.3
2	**C2**	1.11	1330	129.3	188	5.5
3	**C3**	0.966	1160	130.8	336	8.6
4	**C4**	0.815	978	131.8	437	4.1
5	**C5**	0.840	1080	132.1	180	5.6
6	**C6**	1.81	2170	125.3	30.5	13
7	**C7**	1.72	2060	126.7	20.1	5.8
8	$CpTiCl_3$	0.235	282	129.0	99.2	3.0

[a] Conditions: 5 μmol Ti; 10 atm ethylene; Al/Ti = 1500; 30 °C; 10 min; total volume, 100 mL. [b] Determined by DSC. [c] Determined by GPC.

Their catalytic activities vary in the order: **C6** (R = OMe and Cp′ = Cp*) > **C7** (Me and Cp*) > **C1** (OMe and Cp) > **C2** (Me and Cp) > **C3** (H and Cp) > **C5** (Cl and Cp) > **C4** (F and Cp). In terms of sterics, the bulky Cp* enhances the activity of its precatalyst (**C6** *vs* **C1**, and **C7** *vs* **C2**) because the active species are better protected in the polymerization process.[18] On the other hand, the electronic donating substituents of the amidates and Cp* could increase the electron density of titanium and stabilize the active species, which is favorable for the alkyl-Ti bond and a *cis*-located vacant coordination site for ethylene, therefore it results in a better activity.[18,22] In addition, the molecular weights of resulting PEs are also catalyst-dependent, the M_w values of PEs by precatalysts **C1-C5** (180-437 kg·mol^{-1}) are far higher than that produced by $CpTiCl_3$ (99.2 kg·mol^{-1}). Concerning the same ancillary ligands, the precatalysts bearing Cp* produced lower molecular weights of PEs than those ligated by Cp (**C6** *vs* **C1**, and **C7** *vs* **C2**). The less resistance around the active species would be favorable for producing polyolefin with higher molecular weights. It is supposed that in the titanium cyclopentadienylamide catalytic systems, chain increase processes occupy more space in the coordination sphere of titanium than chain transfer. Therefore bulky ligands occupying more space around titanium disfavor chain propagation, but increase the chain transfer and result PEs with lower molecular weights.

5.3.3 Copolymerization of Ethylene/1-Hexene and Ethylene/1-Octene

In addition to ethylene polymerization for PEs, the copolymerization of ethylene with 1-hexene or 1-octene was also investigated, using the representative example of procatalyst **C6**. The detailed copolymerization of ethylene/1-hexene or octene by **C6**/MAO has been successfully carried out, and their results are illustrated in Table 4.

for references, see page 86

Table 4. Copolymerization of ethylene with 1-hexene or 1-octene with **C6**/MAO[a]

Entry	1-Hexene (mol L^{-1})	1-Octene (mol L^{-1})	Polymer (g)	Activity ($kg \cdot mol^{-1}(Ti) \cdot h^{-1}$)	T_m[b] (°C)	M_w[c] ($kg \cdot mol^{-1}$)	M_w/M_n[c]
1	0.1	0	1.98	2380	112.9	223	7.7
2	0.2	0	1.86	2230	108.4	195	3.3
3	0.5	0	1.78	2140	104.0	473	4.6
4	1.0	0	1.22	1460	94.4	299	2.6
5	0	0.1	1.71	2050	109.8	257	3.5
6	0	0.2	1.44	1730	105.3	268	2.8
7	0	0.5	1.23	1480	104.7	239	1.8
8	0	1.0	1.07	1280	93.5	230	3.4
9[d]	0.5	0	0.158	31.6	110.9	54.5	1.6

[a] Conditions: 5 μmol of catalysts; 10 atm ethylene; 10 min; Al/Ti = 1500; 30 °C; toluene (total volume 100 mL). [b] Determined by DSC. [c] Determined by GPC. [d] 1 atm ethylene; 60 min; toluene (total volume 50 mL).

In comparison with its ethylene polymerization activity (2170 $kg \cdot mol^{-1}(Ti) \cdot h^{-1}$, entry 6, Table 3), the positive effect of comonomer is observed with low concentration of 1-hexene (entries 1 and 2, Table 4), however, the activities decrease with further increase of the concentration of 1-hexene (entries 3 and 4, Table 4). This is similar to observations for the imino-indolate half-titanocenes.[14] DSC analysis shows melting points of obtained polymers in the range 103 to 94 °C, and the ^{13}C NMR spectrum (Fig. 3) of the resulting poly(ethylene-co-1-hexene) (entry 3, Table 4) reveals a typical spectrum of linear low density polyethylene (LLDPE) with a 14.7 mol% of 1-hexene incorporation. Comparing the properties of the copolymers obtained by our previous half-titanocene procatalysts,[13b] though reaction parameters are not same, reaction conditions for each catalytic system were optimized, our current system produced copolymers with higher 1-hexene incorporation. Less crowding around titanium in the systems employed herein is a possible reason for this. The 1-hexene incorporation ability herein is also higher than those by other reported.[23] At a fixed 1-hexene concentration, increasing ethylene pressure leads to higher productivity and molecular weight (entries 1 *vs* 9, Table 4).

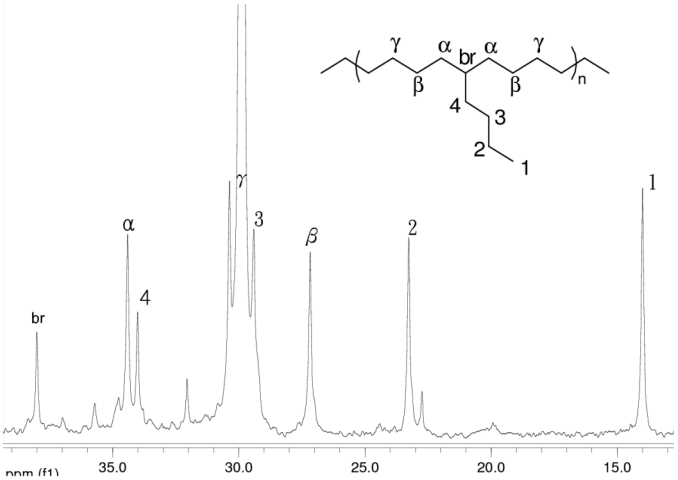

Figure 3. ^{13}C NMR spectrum of ethylene/1-hexene copolymer by **C6**/MAO system (entry 3, Table 4)

for references, see page 86

Similarly, the ethylene/1-octene copolymerization was also studied, and the results are summarized in Table 4. Comparison of the ethylene/1-hexene copolymerization with the ethylene/1-octene copolymerization reveals a slightly lower activities (entry n *vs* n + 4, n = 1-4, Table 4). DSC analysis of the resultant copolymers shows melting points from 93 to 110 °C. Figure 4 shows the ^{13}C NMR spectrum of ethylene/1-octene copolymer produced by **C6**/MAO system (entry 7, Table 4), and it indicates a 16.3 mol% incorporation of 1-octene.

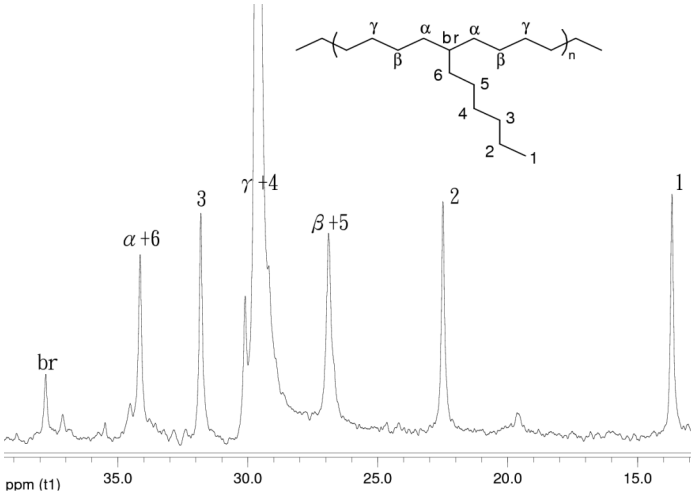

Figure 4. ^{13}C NMR spectrum of ethylene/1-octene copolymer by **C6**/MAO system (entry 7, Table 4)

5.4 Conclusions

The amidate half-titanocene dichlorides, Cp′Ti(**L**)Cl_2 (Cp′ = Cp or Cp*; L = amidate ligand, **C1**-**C7**), have been synthesized and fully characterized, including single-crystal X-ray diffraction for **C2** and **C4**. All procatalysts show high activity towards ethylene polymerization in the presence of MAO. The procatalysts bearing substituted cyclopentadienyl groups give higher activity, whilst the use of more electron donating groups of arylamidates enhances the catalytic activities of the corresponding precatalysts. It is likely there is a single active species above 40 °C, which produces PEs with narrow molecular weights. Regarding results by procatalyst **C6**, the copolymerization of ethylene with 1-hexene or 1-octene produced copolymers incorporating branching of about 15 mol%.

5.5 Experimental Section

5.5.1 General Considerations

All manipulations of air and/or moisture-sensitive compounds were performed under a nitrogen atmosphere in a glovebox or using standard Schlenk techniques. *N*-(2-methylquinolin-8-yl)benzamide derivatives were prepared as already reported.[13b,16] Methylaluminoxane (MAO, 1.46 M in toluene) was purchased from Albemarle. Potassium hydride (KH) was bought from Beijing Chemical Regent Company and washed with hexane before usage to remove mineral oil contained. Tetrahydrofuran (THF), toluene, hexane and heptane were refluxed over sodium and benzophenone, distilled, and then

for references, see page 86

stored under nitrogen atmosphere. Dichloromethane (CH_2Cl_2) was distilled over calcium hydride, and stored under nitrogen atmosphere. High purety ethylene was purchased from Beijing Yansan Petrochemical Co. and used as received. IR spectra were recorded on a Perkin Elmer FT-IR 2000 spectrometer using KBr disc in the range of 4000-400 cm^{-1}. Elemental analysis was performed on a Flash EA 1112 microanalyzer. ^1H NMR and ^{13}C NMR spectra were recorded on a Bruker DMX 400 MHz instrument at ambient temperature using TMS as an internal standard. DSC trace and melting points of polyethylenes were obtained from the second scanning run on a Perkin-Elmer DSC-7 at a heating rate of 10 °C /min. ^1H NMR and ^{13}C NMR spectra of the polymers were recorded on a Bruker DMX-300 MHz instrument at 110 °C in deuterated 1,2-dichlorobenzene with TMS as an internal standard. Molecular weights and polydispersity indices (PDI) of (co-)polyethylene were determined using a PL-GPC220 instrument at 135 °C in 1,2,4-trichlorobenzene with polystyrene as the standard.

5.5.2 Synthesis of complexes (C1-C7)

η^5-Cyclopentadienyl[*N*-(2-methylquinolin-8-yl)-*p*-methoxybenzamide]titanium dichlorides (C1). To a stirred solution of 4-methoxy-*N*-(2-methylquinolin-8-yl)benzamide (0.585 g, 2.00 mmol) in dried THF (30 mL) at room temperature, KH (0.080 g, 2.00 mmol) was added. The mixture was allowed to stir for 12 h and a yellow suspension was obtained. At -78 °C, 20 mL of a $CpTiCl_3$ (0.438 g, 2.00 mmol) solution in THF was added dropwise over a 30 min period. The resultant mixture was allowed to warm to room temperature and stirred for additional 12 h. The residue, obtained by removing the solvent under vacuum, was extracted with toluene (3 × 20 mL). The combined filtrates were concentrated in vacuum to reduce the volume to 5 mL, and then filtered to give a red solid (0.781 g, 1.64 mmol, yield 82%). ^1H NMR ($CDCl_3$, 400 MHz): δ 8.02 (d, J = 8.4 Hz, 1H, quin), 7.65 (d, J = 7.7 Hz, 2H, quin), 7.47 (dd, J_1 = 7.7 Hz, J_2 = 7.8 Hz, 1H, quin), 7.29 (d, J = 8.4 Hz, 2H, aryl), 7.22 (d, J = 8.4 Hz, 1H, quin), 7.04 (s, 5H, Cp), 6.57 (d, J = 8.3 Hz, 2H, aryl), 3.69 (s, 3H, OCH_3), 2.59 (s, 3H, CH_3). ^{13}C NMR ($CDCl_3$, 100 MHz): δ 173.8, 162.8, 158.3, 142.6, 141.9, 136.4, 131.0, 127.6, 126.3, 126.0, 125.9, 123.5, 122.2, 121.5, 113.5, 55.4, 25.4. Anal. Calcd for $C_{23}H_{20}Cl_2N_2O_2Ti$: C, 58.13; H, 4.24; N, 5.90. Found: C, 58.03; H, 4.28; N, 5.53.

η^5-Cyclopentadienyl[*N*-(2-methylquinolin-8-yl)-*p*-methylbenzamide]titanium dichlorides (C2). Using the same procedure as for the synthesis of **C1**, **C2** was obtained as a red solid in 81% yield (0.739 g, 1.61 mmol). ^1H NMR ($CDCl_3$, 400 MHz): δ 8.01 (d, J = 8.3 Hz, 1H, quin), 7.64 (d, J = 7.8 Hz, 2H, quin), 7.46 (m, 1H, quin), 7.27-7.16 (m, 3H, quin and aryl), 7.05 (s, 5H, Cp), 6.89 (d, J = 8.0 Hz, 2H, aryl), 2.58 (s, 3H, CH_3), 2.21 (s, 3H, CH_3). ^{13}C NMR ($CDCl_3$, 100 MHz): δ 174.4, 158.3, 143.0, 142.4, 141.8, 136.4, 129.5, 128.8, 128.1, 127.5, 126.5, 125.9, 123.5, 122.1, 121.5, 25.3, 21.6. Anal. Calcd for $C_{23}H_{20}Cl_2N_2OTi$: C, 60.16; H, 4.39; N, 6.10. Found: C, 60.13; H, 4.66; N, 5.92.

η^5-Cyclopentadienyl[*N*-(2-methylquinolin-8-yl)benzamide]titanium dichlorides (C3). Using the same procedure for the synthesis of **C1**, **C3** was obtained as a red solid in 77% yield (0.687 g, 1.54 mmol). ^1H NMR ($CDCl_3$, 400 MHz): δ 8.00 (d, J = 8.4 Hz, 1H, quin), 7.68 (d, J = 7.4 Hz, 1H, quin),

for references, see page 86

7.63 (d, *J* = 7.9 Hz, 1H, quin), 7.46 (m, 1H, quin), 7.33 (d, *J* = 7.6 Hz, 2H, aryl), 7.28-7.23 (m, 1H, quin), 7.19-7.16 (m, 1H, aryl), 7.08 (d, *J* = 7.7 Hz, 2H, aryl), 7.04 (s, 5H, Cp). ^{13}C NMR ($CDCl_3$, 100 MHz): δ 174.7, 158.3, 142.1, 141.6, 136.4, 132.1, 130.0, 128.9, 128.3, 127.9, 127.5, 127.3, 126.2, 125.9, 125.3, 123.5, 122.1. Anal. Calcd for $C_{22}H_{18}Cl_2N_2OTi$: C, 59.36; H, 4.08; N, 6.29. Found: C, 59.10; H, 4.26; N, 6.29.

η^5-Cyclopentadienyl[*N*-(2-methylquinolin-8-yl)-*p*-fluorobenzamide]titanium dichlorides (C4). Using the same procedure as for the synthesis of **C1**, **C4** was obtained as a red solid in 84% yield (0.778 g, 1.68 mmol). ^{1}H NMR ($CDCl_3$, 400 MHz): δ 8.11-8.07 (m, 1H, quin), 8.02 (d, *J* = 8.4 Hz, 1H, quin), 7.70 (d, *J* = 7.4 Hz, 1H, quin), 7.66 (d, *J* = 8.1 Hz, 1H, quin), 7.52-7.47 (m, 1H, quin), 7.37-7.33 (m, 1H, aryl), 7.25-7.23 (m, 1H, aryl) 7.03 (s, 5H, Cp), 6.77 (d, *J* = 8.2 Hz, 2H, aryl), 2.57 (s, 3H, CH_3). ^{13}C NMR ($CDCl_3$, 100 MHz): δ 173.6, 158.4, 141.9, 141.4, 136.5, 131.1, 131.0, 129.1, 128.3, 127.6, 126.2, 126.1, 126.0, 125.4, 123.6, 122.3, 122.2, 25.3. Anal. Calcd for $C_{22}H_{17}Cl_2FN_2OTi$: C, 57.05; H, 3.70; N, 6.05. Found: C, 57.03; H, 3.96; N, 5.99.

η^5-Cyclopentadienyl[*N*-(2-methylquinolin-8-yl)-*p*-chlorobenzamide] titanium dichlorides (C5). Using the same procedure as for the synthesis of **C1**, **C5** was obtained as a red solid in 80% yield (0.763 g, 1.59 mmol). ^{1}H NMR ($CDCl_3$, 400 MHz): δ 8.02 (d, *J* = 8.0 Hz, 2H, quin), 7.70 (d, *J* = 7.3 Hz, 1H, quin), 7.65 (d, *J* = 8.0 Hz, 1H, quin), 7.54-7.47 (m, 1H, quin), 7.28-7.26 (m, 2H, aryl), 7.06 (d, *J* = 7.9 Hz, 2H, aryl), 7.03 (s, 5H, Cp), 2.57 (s, 3H, CH_3). ^{13}C NMR ($CDCl_3$, 100 MHz): δ 173.8, 164.2, 158.4, 157.4, 141.8, 136.5, 129.9, 129.1, 129.0, 128.7, 128.3, 128.2, 123.6, 122.6, 122.2, 25.3. Anal. Calcd for $C_{22}H_{18}Cl_3N_2OTi$: C, 55.09; H, 3.57; N, 5.84. Found: C, 54.93; H, 3.76; N, 5.88.

η^5-Pentamethylcyclopentadienyl[*N*-(2-methylquinolin-8-yl)-*p*-methoxybenzamide] titanium dichlorides (C6). Using the same procedure as for the synthesis of **C1**, **C6** was obtained as a red solid in 89% yield (0.970 g, 1.78 mmol). ^{1}H NMR ($CDCl_3$, 400 MHz): δ 7.93 (d, *J* = 8.4 Hz, 1H, quin), 7.87 (d, *J* = 7.4 Hz, 1H, quin), 7.56 (d, *J* = 8.0 Hz, 1H, quin), 7.45 (dd, J_1 = 8.4 Hz, J_2 = 8.4 Hz, quin), 7.30 (d, *J* = 8.5 Hz, 2H, aryl), 7.09 (d, *J* = 8.4 Hz, 1H, quin), 6.53 (d, *J* = 8.5 Hz, 2H), 3.67 (s, 3H, CH_3), 2.49 (s, 3H, CH_3), 2.34(s, 15H, CH_3). ^{13}C NMR ($CDCl_3$, 100 MHz): δ 174.8, 162.4, 157.1, 141.9, 136.5, 136.0, 134.1, 130.5, 129.1, 126.1, 122.4, 116.3, 114.0, 112.9, 55.5, 25.4, 13.8. Anal. Calcd for $C_{28}H_{30}Cl_2N_2O_2Ti$: C, 61.67; H, 5.55; N, 5.14. Found: C, 61.55; H, 5.76; N, 5.18.

η^5-Pentamethylcyclopentadienyl[*N*-(2-methylquinolin-8-yl)-*p*-methylbenzamide] titanium dichlorides (C7). Using the same procedure as for the synthesis of **C1**, **C7** was obtained as a red solid in 85% yield (0.901 g, 1.70 mmol). ^{1}H NMR ($CDCl_3$, 400 MHz): δ 7.95 (d, *J* = 8.3 Hz, 1H, quin), 7.82 (d, *J* = 7.3 Hz, 1H, quin), 7.50 (d, *J* = 8.0 Hz, 1H, quin), 7.42 (dd, J_1 = 8.3 Hz, J_2 = 8.3 Hz, 1H, quin), 7.35 (d, *J* = 8.5 Hz, 2H, aryl), 7.09 (d, *J* = 8.3 Hz, 1H, quin), 6.76 (d, *J* = 8.5 Hz, 2H, aryl), 2.47 (s, 3H, CH_3), 2.35(s, 15H, CH_3), 2.21 (s, 3H, CH_3). ^{13}C NMR ($CDCl_3$, 100 MHz): δ 174.2, 161.4, 155.1, 141.0, 137.5, 136.0, 134.7, 132.5, 129.8, 128.1, 123.4, 116.5, 114.1, 112.9, 25.4, 21.6, 13.8. Anal. Calcd for $C_{28}H_{30}Cl_2N_2OTi$: C, 63.53; H, 5.71; N, 5.29. Found: C, 63.46; H, 5.75; N, 5.25.

for references, see page 86

5.5.3 Procedures for Ethylene Polymerization and Copolymerization of Ethylene with α-Olefin

A 250-mL autoclave stainless steel reactor equipped with a mechanical stirrer and a temperature controller is heated in vacuum for at least 2 h at 80 °C. It is allowed to cool to the required reaction temperature under ethylene atmosphere and then charged with toluene (with co-monomer), the desired amount of co-catalyst (MAO) and a toluene solution of the catalytic precursor. The total volume is 100 mL. After reaching the reaction temperature, the reactor is sealed and pressurized to 10 atm of ethylene pressure. The ethylene pressure is kept constant during the reaction time by feeding the reactor with ethylene. After a period of desired reaction time, the polymerization reaction is quenched by addition of a solution of ethanol containing HCl. The precipitated polymer is washed with ethanol several times and dried in vacuum.

5.5.4 X-ray Structure Determination

Crystals of **C2** and **C4** suitable for single-crystal X-ray analysis were obtained by layering heptane on their toluene solutions. Single-crystal X-ray diffraction for **C2** and **C4** are performed on a Rigaku RAXIS Rapid IP diffractometer with graphite-monochromated Mo Kα radiation (λ = 0.71073 Å) at 173(2) K. Cell parameters are obtained by global refinement of the positions of all collected reflections. Intensities are corrected for Lorentz and polarization effects and empirical absorption. The structures are solved by direct methods and refined by full-matrix least-squares on F^2. All non-hydrogen atoms are refined anisotropically. Structure solution and refinement are performed by using the SHELXL-97 package.[24] Crystal data collection and refinement details for all compounds are available in the Supporting Information.

Supporting Information Available

The GPC diagrams of corresponding polyolefins, ORTEP view of the molecular structure of **C4**, crystal data and processing parameters for complexes **C2** and **C4** and their CIF file giving X-ray crystal structural data. These materials are available free of charge via the Internet at http://pubs.acs.org.

Acknowledgment

This work is supported by NSFC Nos. 20874105 and 20904059.

for references, see page 86

References

1. (a) Natta, G. *J. Polym. Sci.* **1955**, *16*, 143-154; (b) Natta, G.; Pino, P.; Corradini, P.; Danusso, F.; Mantica, E.; Mazzanti, G.; Moraglio, G. *J. Am. Chem. Soc.* **1955**, *77*, 1708-1710; (c) Ziegler, K.; Gellert, H. G. *Angew. Chem.* **1955**, *67*, 424-425; (d) Ziegler, K.; Holzkamp, E.; Breil, H.; Martin, H. *Angew. Chem.* **1955**, *67*, 541-547.
2. Weckhuysen, B. M.; Schoonheydt, R. A. *Catal. Today* **1999**, *51*, 215-221.
3. (a) Sinn, H.; Kaminsky, W.; Vollmer, H. J.; Woldt, R. *Angew. Chem. Int. Ed. Engl.* **1980**, *19*, 390-392; (b) Alt, H. G.; Köppl, A. *Chem. Rev.* **2000**, *100*, 1205-1221.
4. (a) Shapiro, P. J.; Bunel, E.; Schaefer, W. P.; Bercaw, J. E. *Organometallics* **1990**, *9*, 867-869; (b) Shapiro, P. J.; Cotter, W. D.; Schaefer, W. P.; Labinger, J. A.; Bercaw, J. E. *J. Am. Chem. Soc.* **1994**, *116*, 4623-4640; (c) McKnight, A. L.; Waymouth, R. M. *Chem. Rev.* **1998**, *98*, 2587-2598.
5. (a) Brintzinger, H. H.; Fischer, D.; Mülhaupt, R.; Rieger, B.; Waymouth, R. M. *Angew. Chem. Int. Ed. Engl.* **1995**, *34*, 1143-1170; (b) Britovsek, G. J. P.; Gibson, V. C.; Wass, D. F. *Angew. Chem. Int. Ed.* **1999**, *38*, 428-447; (c) Ittel, S. D.; Johnson, L. K.; Brookhart, M. *Chem. Rev.* **2000**, *100*, 1169-1203; (d) Gibson, V. C.; Spitzmesser, S. K. *Chem. Rev.* **2003**, *103*, 283-315; (e) Braunschweig, H.; Breitling, F. M. *Coord. Chem. Rev.* **2006**, *250*, 2691-2720; (f) Gibson, V. C.; Redshaw, C.; Solan, G. A. *Chem. Rev.* **2007**, *107*, 1745-1776; (g) Sun, W.-H.; Zhang, S.; Zuo, W. *C. R. Chim.* **2008**, *11*, 307-316.
6. (a) Flores, J. C.; Chien, J. C. W.; Rausch, M. D. *Organometallics* **1995**, *14*, 2106-2108; (b) Herskovicskorine, D.; Eisen, M. S. *J. Organomet. Chem.* **1995**, *503*, 307-314; (c) Volkis, V.; Shmulinson, M.; Averbuj, C.; Lisovskii, A.; Edelmann, F. T.; Eisen, M. S. *Organometallics* **1998**, *17*, 3155-3157.
7. (a) Clark, H. C. S.; Cloke, G. N.; Hitchcock, P. B.; Love, J. B.; Wainwright, A. P. *J. Organomet. Chem.* **1995**, *501*, 333-340; (b) Scollard, J. D.; McConville, D. H. *J. Am. Chem. Soc.* **1996**, *118*, 10008-10009; (c) Scollard, J. D.; McConville, D. H.; Payne, N. C.; Vittal, J. J. *Macromolecules* **1996**, *29*, 5241-5243; (d) Horton, A. D.; de With, J.; van der Linden, A. J.; van de Weg, H. *Organometallics* **1996**, *15*, 2672-2674; (e) Warren, T. H.; Schrock, R. R.; Davis, W. M. *Organometallics* **1998**, *17*, 308-321; (f) Baumann, R.; Davis, W. M.; Schrock, R. R. *J. Am. Chem. Soc.* **1997**, *119*, 3830-3831; (g) Gibson, V. C.; Kimberley, B. S.; White, A. J. P.; Williams, D. J.; Howard, P. *Chem. Commun.* **1998**, 313-314.
8. (a) Vanderlinden, A.; Schaverien, C. J.; Meijboom, N.; Ganter, C.; Orpen, A. G. *J. Am. Chem. Soc.* **1995**, *117*, 3008; (b) Fokken, S.; Spaniol, T. P.; Kang, H. C.; Massa, W.; Okuda, J. *Organometallics* **1996**, *15*, 5069-5072.
9. (a) Matsui, S.; Tohi, Y.; Mitani, M.; Saito, J.; Makio, H.; Tanaka, H.; Nitabaru, M.; Nakano, T.; Fujita, T. *Chem. Lett.* **1999**, 1065-1066; (b) Tian, J.; Coates, G. W. *Angew. Chem. Int. Ed.* **2000**, *39*, 3626-3629; (c) Matsui, S.; Mitani, M.; Saito, J.; Tohi, Y.; Makio, H.; Matsukawa, N.; Takagi, Y.; Tsuru, K.; Nitabaru, M.; Nakano, T.; Tanaka, H.; Kashiwa, N.; Fujita, T. *J. Am. Chem. Soc.* **2001**, *123*, 6847-6856; (d) Makio, H.; Kashiwa, N.; Fujita, T. *Adv. Synth. Catal.* **2002**, *344*, 477-493; (e) Sakuma, A.; Weiser, M.-S.; Fujita, T. *Polym. J.* **2007**, *39*, 193-207; (f) Edson, J. B.; Wang, Z.; Kramer, E. J.; Coates, G. W. *J. Am. Chem. Soc.* **2008**, *130*, 4968-4977.
10. Yoshida, Y.; Matsui, S.; Takagi, Y.; Mitani, M.; Nakano, T.; Tanaka, H.; Kashiwa, N.; Fujita, T. *Organometallics* **2001**, *20*, 4793-4799.
11. Matsugi, T.; Fujita, T. *Chem. Soc. Rev.* **2008**, *37*, 1264-1277.
12. Nomura, K.; Liu, J.; Padmanabhan, S.; Kitiyanan, B. *J. Mol. Catal. A: Chem.* **2007**, *267*, 1-29.
13. (a) Zuo, W.; Zhang, S.; Liu, S.; Liu, X.; Sun, W.-H. *J. Polym. Sci., Part A: Polym. Chem.* **2008**, *46*, 3396-3410; (b) Liu, S.; Yi, J.; Zuo, W.; Wang, K.; Wang, D.; Sun, W.-H. *J. Polym. Sci., Part A: Polym. Chem.* **2009**, *47*, 3154-3169; (c) Sun, W.-H.; Liu, S.; Zhang, W.; Zeng, Y.; Wang, D.; Liang, T. *Organometallics* **2010**, *29*, 732-741.
14. Zuo, W.; Zhang, M.; Sun, W.-H. *J. Polym. Sci., Part A: Polym. Chem.* **2009**, *47*, 357-372.
15. (a) Thomson, R. K.; Zahariev, F. E.; Zhang, Z.; Patrick, B. O.; Wang, Y. A.; Schafer, L. L. *Inorg. Chem.* **2005**, *44*, 8680-8689; (b) Li, C.; Thomson, R. K.; Gillon, B.; Patrick, B. O.; Schafer, L. L. *Chem. Commun.* **2003**, 2462-2463; (c) Zhang, Z.; Schafer, L. L. *Org. Lett.* **2003**, *5*, 4733-4736; (d) Zhang, Z.; Leitch, D. C.; Lu, M.; Patrick, B. O.; Schafer, L. L. *Chem. Eur. J.* **2007**, *13*, 2012-2022.
16. Wang, K.; Shen, M.; Sun, W.-H. *Dalton Trans.* **2009**, 4085-4095.
17. Liu, S.; Zuo, W.; Zhang, S.; Hao, P.; Wang, D.; Sun, W.-H. *J. Polym. Sci., Part A: Polym. Chem.* **2008**, *46*, 3411-3423.
18. Chen, E. Y. X.; Marks, T. J. *Chem. Rev.* **2000**, *100*, 1391-1434.
19. Koltzenburg, S. *J. Mol. Catal. A: Chem.* **1997**, *116*, 355-363.
20. (a) Chien, J. C. W. *J. Am. Chem. Soc.* **1959**, *81*, 86-92; (b) Mallin, D. T.; Rausch, M. D. *J. Organomet. Chem.* **1990**, *381*, 35-44; (c) Vanka, K.; Xu, Z.; Ziegler, T. *Organometallics* **2005**, *24*, 419-430.
21. (a) Zou, H.; Hu, S.; Huang, H.; Zhu, F.; Wu, Q. *Eur. Polym. J.* **2007**, *43*, 3882-3891; (b) Wang, Q.; L., L.; Fan, Z. *Eur. Polym. J.* **2004**, *40*, 1881-1886.
22. Bochmann, M. *J. Chem. Soc., Dalton Trans.* **1996**, 255-270.

for references, see page 86

23. (a) Huang, J.; Lian, B.; Qian, Y.; Zhou, W.; Chen, W.; Zheng, G. *Macromolecules* **2002**, *35*, 4871-4874; (b) Nomura, K.; Fujita, K.; Fujiki, M. *J. Mol. Catal. A: Chem.* **2004**, *220*, 133-144.
24. Sheldrick, G. M. SHELXL-97; University of Göttingen: Göttingen (Germany), **1997**.

for references, see page 86

CHAPITRE VI

Palladium and Iridium Complexes with a *N,P,N*-bis(pyridine)phenylphosphine Ligand

SHAOFENG LIU,[a,b] RICCARDO PELOSO,[a,c] and PIERRE BRAUNSTEIN*[a]

[a] *Laboratoire de Chimie de Coordination, Institut de Chimie (UMR 7177 CNRS), Université de Strasbourg, 4 rue Blaise Pascal, F-67070 Strasbourg Cedex, France.*

[b] *Key Laboratory of Engineering Plastics and Beijing National Laboratory for Molecular Sciences, Institute of Chemistry, Chinese Academy of Sciences, Beijing 100190, China.*

[c] *current address: Instituto de Investigaciones Químicas - Departamento de Química Inorgánica, Universidad de Sevilla - Consejo Superior de Investigaciones Científicas, Avda. Américo Vespucio 49, Isla de la Cartuja, 41092 Sevilla, Spain.*

This Chapter has been published in *Dalton Trans.*, **2010**, *39*, 2563-2572.

Contributions from the various co-authors: Dr. Riccardo Peloso provided assistance for the syntheses, discussions and preparation of the manuscript, Professor Pierre Braunstein supervised the work and provided guidance.

Résumé du Chapitre VI

Des complexes du Pd(II) contenant le ligand neutre *N,P,N*-ligand bis(2-picolyl)phenylphosphine ($N_{py}PN_{py}$) ont été préparés et caractérisés par spectroscopies IR et RMN et diffraction des rayons X. Le complexe neutre $[PdCl_2(N_{py}PN_{py}\text{-}N,P)]$ (**1**) a été obtenu sélectivement et avec un bon rendement par réaction de $[PdCl_2(NCPh)_2]$ avec le ligand dans le dichlorométhane. Les complexes cationiques $[PdCl(N_{py}PN_{py}\text{-}N,P,N)]PF_6$ (**2**) et $[Pd(N_{py}PN_{py}\text{-}N,P,N)(NCMe)](PF_6)_2$ (**5**) furent obtenus à partir des mêmes réactifs après addition, respectivement, de un ou deux équivalents de $TlPF_6$. Nous avons mis en évidence qu'un échange dynamique des cycles pyridiniques de **1** se produit à l'échelle de temps de la RMN et des mécanismes possibles sont discutés. Comme sous-produit de la synthèse de **2**, le complexe dinucléaire $[Pd_2Cl_2(\mu\text{-}N_{py}PN_{py})_2](PF_6)_2$ (**3**) a été isolé de manière inattendue avec un rendement de 10%. La détermination de sa structure moléculaire à l'état solide a révélé la présence de deux ligands $N_{py}PN_{py}$ pontants. Le complexe cationique $[Pd_2Cl_2(\mu\text{-}N_{py}PN_{py})_2]^{2+}$ fut ensuite obtenu de manière sélective par réaction de *cis*-$[Pd(N_{py}PN_{py}\text{-}N,P)_2](BF_4)_2$ (**4**) avec $[PdCl_2(cod)]$. Les études RMN ^1H et $^{31}P\{^1H\}$ NMR ont montré que **3** se convertit lentement en **2** dans le DMSO. Les complexes de l'Iridium(I) $[IrCl(cod)(N_{py}PN_{py})]$ (**6**) et $[Ir(cod)(N_{py}PN_{py}\text{-}N,P,N)]BAr^F$ (**7**) ont également été préparés et ce dernier possède une géométrie de coordination bipyramide trigonale avec le ligand

for references, see page 108

$N_{py}PN_{py}$ lié au métal dans un mode de coordination faciale. Le complexe **7** représente un exemple rare de complexe de l'Ir(I) comportant un ligand *N,P,N*-chelatant.

6.1 Abstract of Chapter VI

A variety of Pd(II) complexes containing the neutral *N,P,N*-ligand bis(2-picolyl)phenylphosphine ($N_{py}PN_{py}$) have been synthesised and characterized by IR and NMR spectroscopy and X-ray diffraction. The neutral complex [$PdCl_2(N_{py}PN_{py}$-*N,P*)] (**1**) has been selectively obtained in high yield by reaction of [$PdCl_2(NCPh)_2$] with the ligand in dichloromethane. The cationic complexes [$PdCl(N_{py}PN_{py}$-*N,P,N*)]PF_6 (**2**) and [$Pd(N_{py}PN_{py}$-*N,P,N*)(NCMe)]$(PF_6)_2$ (**5**) have been prepared from the same reagents by addition to the reaction mixture of one or two equivalents of $TlPF_6$, respectively. It was found that dynamic exchange of the pyridine rings of **1** occurs on the NMR time-scale and possible mechanisms are discussed. As a by-product of the synthesis of **2,** the unexpected dinuclear complex [$Pd_2Cl_2(\mu$-$N_{py}PN_{py})_2](PF_6)_2$ (**3**) has been isolated in a 10% yield. Its molecular structure in the solid state has revealed the presence of two $N_{py}PN_{py}$ bridging ligands. The cationic complex [$Pd_2Cl_2(\mu$-$N_{py}PN_{py})_2]^{2+}$ was then selectively obtained by reaction of *cis*-[$Pd(N_{py}PN_{py}$-*N,P*)$_2](BF_4)_2$ (**4**) with [$PdCl_2$(cod)]. ^{1}H- and $^{31}P\{^1H\}$ NMR studies have demonstrated that **3** converts slowly into **2** in DMSO solution. The Ir(I) complexes [IrCl(cod)($N_{py}PN_{py}$)] (**6**) and [Ir(cod)($N_{py}PN_{py}$-*N,P,N*)]BAr^F (**7**) have also been prepared, the latter exhibiting a trigonal bipyramidal geometry with the ligand in a facial coordination mode. Compound **7** represents a rare example of Ir(I) complex bearing a *N,P,N*-chelating ligand.

6.2 Introduction

The synthesis and coordination chemistry of heterotopic ligands bearing phosphorus and nitrogen donor atoms represent increasingly active fields of research owing to the properties that such ligands confer to their metal complexes in stoichiometric or catalytic reactions.[1] The significantly different electronic and hard-soft properties of the donor functions largely influence their metal coordination behaviour and account for the observation of monodentate *P*- or *N*-coordination and static or dynamic (hemilabile) *P,N*-chelation.[1b]

In the course of our studies on *P,N*-ligands in which the P donor function is of the phosphine, phosphonite or phosphinite-type and the N donor belongs to a pyridine or an oxazoline heterocycle, we observed that some of their mononuclear complexes of Ru(II),[1f,2] Ni(II),[1g,3] Co(II)[4] and Pd(II)[2d,5] or Fe-Cu[6] and Fe-Co[7] bimetallic complexes led to active precatalysts for a number of reactions.

for references, see page 108

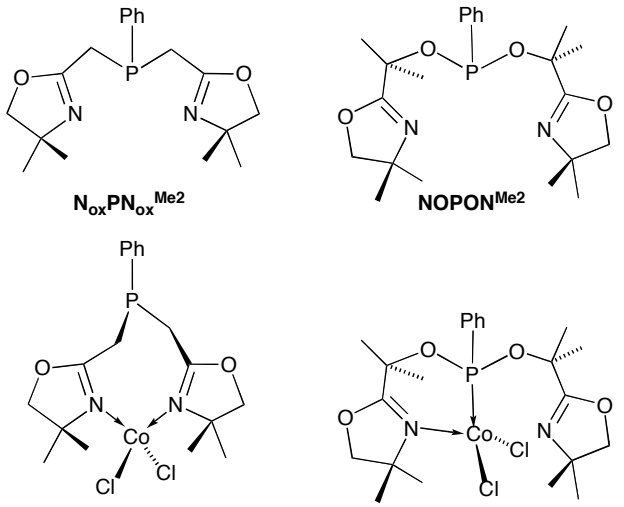

Scheme 1. The ligands $N_{ox}PN_{ox}^{Me2}$ and $NOPON^{Me2}$ and contrasting bonding modes of the heterofunctional ligands in complexes $[CoCl_2(NOPON^{Me2}\text{-}P,N)]$ and $[CoCl_2(N_{ox}PN_{ox}^{Me2}\text{-}N,N)]$

As an extension to *N,P,N*-tridentate ligands containing oxazoline heterocycles, we compared the bonding behaviour of the bis(oxazoline)phenylphosphine (abbreviated below for clarity as $N_{ox}PN_{ox}^{Me2}$) and bis(oxazoline)phenylphosphonite ligands (abbreviated $NOPON^{Me2}$) (Scheme 1), which unexpectedly revealed that the former can behave as a *N,N*-chelate towards Co(II) and Fe(II),[3b,8] in contrast to the situation in $[CoCl_2(NOPON^{Me2}\text{-}P,N)]$[8] (Scheme 1).

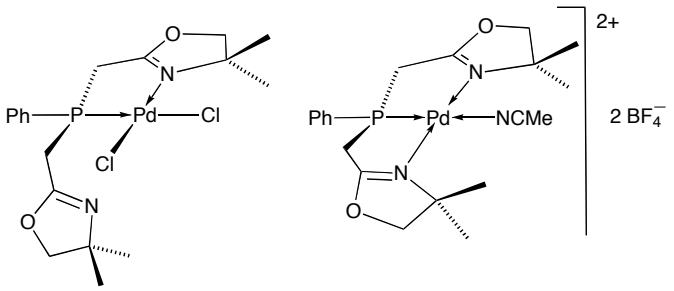

Scheme 2. The complexes $[PdCl_2(NPN^{Me2}\text{-}P,N)]$ and $[Pd(NPN^{Me2}\text{-}N,P,N)(NCMe)](BF_4)_2$

As far as bis(oxazoline)phosphine ligands are concerned, only *P,N*- or *N,P,N*-coordination modes have been observed in Pd(II) complexes (Scheme 2).[3b,8] We wished to extend these studies to *N,P,N*-ligands where N represents a pyridine donor ($N_{py}PN_{py}$) and compare its coordination properties with those of $N_{ox}PN_{ox}^{Me2}$, in particular towards Pd(II) complexes.

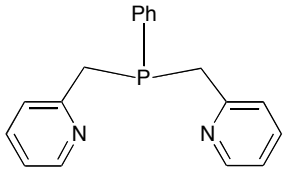

Scheme 3. The $N_{py}PN_{py}$ ligand

For this purpose, the ligand selected was bis(2-picolyl)phenylphosphine ($N_{py}PN_{py}$, Scheme 3), a flexible, symmetric and neutral *N,P,N*-ligand containing two pyridine arms and a phosphine-type P

for references, see page 108

donor.[9] We have also performed preliminary studies on the coordination chemistry of this ligand with Ir(I) systems, in order to investigate its behaviour with a d^8 metal which often gives rise to penta-coordinated complexes. Moreover, *N,N,N*-,[10] *P,C,P*-,[11] and, very recently, *P,N,P*-Ir(I)[12] chelated complexes have proved to be effective in a number of challenging catalytic reactions and in C-H bonds activation. In this context, the preparation of new *N,P,N*-chelated Ir complexes represents a desirable development of this chemistry.[13] Herein, we report the synthesis and the characterization of Pd(II) and Ir(I) complexes bearing the neutral bis(2-picolyl)phenylphosphine ($N_{py}PN_{py}$) ligand.

6.3 Results and Discussion

The reaction between $[PdCl_2(NCPh)_2]$ and an equimolar amount of $N_{py}PN_{py}$ in CH_2Cl_2 resulted in the formation of a yellow precipitate, which was characterized by multinuclear NMR and IR spectroscopy, elemental analysis and X-ray diffraction and identified as the mononuclear complex $[PdCl_2(N_{py}PN_{py}$-*N,P*)] (**1**). The compound is poorly soluble in most organic solvents and only DMF and DMSO allowed us to prepare concentrated solutions of **1**. The $^{31}P\{^1H\}$ NMR spectrum of **1** in DMSO shows a sharp singlet at 49.7 ppm, thus confirming the coordination of the ligand through the phosphorous atom, whose resonance is downfield shifted by about 60 ppm with respect to the free ligand. At this point, we cannot say whether this resonance corresponds to the neutral complex or, in view of the high donor number (DN = 29.8) of DMSO,[14] to the cation of $[PdCl(N_{py}PN_{py}$-*N,P*)(DMSO)]Cl which would form upon dissolution of the neutral complex in DMSO. The ^1H NMR spectrum of **1** at room temperature exhibits broad signals due to the picolyl moieties of the ligand, whereas the phenyl protons give rise to sharp signals. In particular, the presence of eight broad resonances in the pyridine region indicates the non-equivalence of the two pyridine rings, which are likely to be involved in a dynamic slow exchange of the nitrogen donors N^1 and N^2 on the NMR time scale (Scheme 4). We shall come back to this point later in the discussion.

for references, see page 108

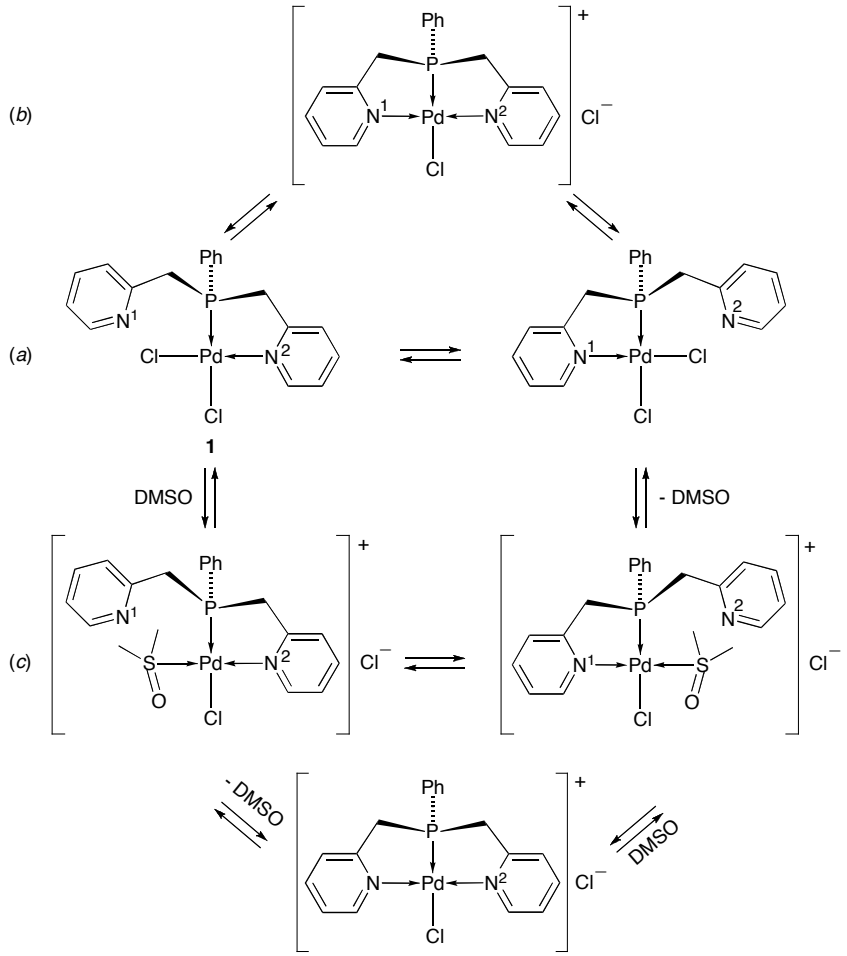

Scheme 4 Possible mechanisms for the dynamic exchange of the pyridine rings at the Pd centre in **1**

Although it was not possible to assign all the signals in the pyridine region, by comparison with the values found for [PdCl($N_{py}PN_{py}$-*N,P,N*)]PF_6 (**2**, *vide infra*), we suggest that the H ortho to the coordinated nitrogen in **1** resonates at 9.32 ppm and that of the non-coordinated pyridine moiety at 8.39 ppm. In order to better understand this dynamic behaviour, we performed variable temperature ^{1}H NMR experiments from 25 to 80 °C. The gradual broadening of the eight pyridine resonances resulted in the coalescence of the signals at 65 °C, which gave rise to four broad peaks at 8.89, 7.86, 7.62, 7.34 ppm. By means of a line shape analysis, the rates of exchange were estimated at different temperatures and this allowed us to calculate the following activation parameters by an Eyring plot: $\Delta H^{\#}$ = (50 ± 3) kJ·mol^{-1}, $\Delta S^{\#}$ = (-43 ± 8) J·mol^{-1}·K^{-1}. As far as the $^{13}C\{^1H\}$ NMR spectrum of **1** is concerned, it is worth observing that the signals of the coordinated picolyl moiety (py^2, py^6, py^4 and CH_2) are downfield shifted with respect to those of the non-coordinated one. This is likely to result from a decrease of the electron-density at the pyridine ring upon coordination. The far IR spectrum of the compound displays two strong absorption at 337 and 301 cm^{-1}, which are ascribed to the Pd-Cl stretching vibrations of the *cis*-$PdCl_2$ moiety.[15]

for references, see page 108

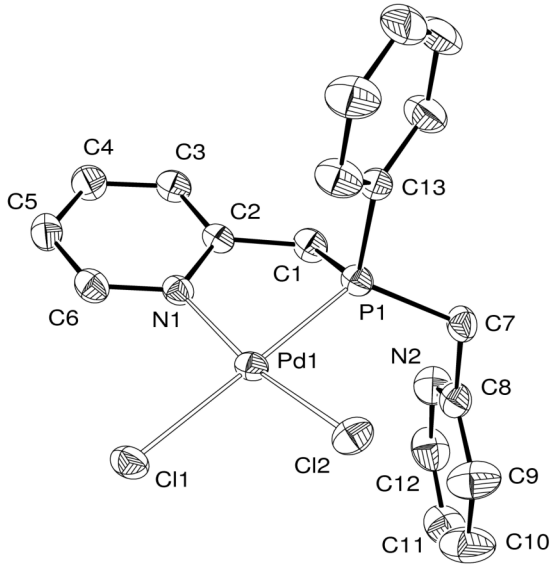

Fig. 1 ORTEP of complex **1** with ellipsoids drawn at the 50% probability level. Selected bond distances (Å) and angles (deg): Pd1-Cl1 2.3825(9), Pd1-Cl2 2.2945(9), Pd1-P1 2.200(1), Pd1-N1 2.075(3), N1-Pd1-P1 83.29(8), N1-Pd1-Cl1 94.97(8), Cl1-Pd1-Cl2 92.80(4), Cl2-Pd1-P1 89.02(4).

The molecular structure of **1** (Fig. 1) in the solid state confirmed that the $N_{py}PN_{py}$ ligand behaves as a bidentate *N,P*-chelate, one of the pyridine rings remaining non-coordinated, as also observed in the related $N_{ox}PN_{ox}$ Pd(II) complex.[8] Similarly, it has been previously observed that a hemilabile bis(oxazoline)phenylphosphonite acts as *N,P*-bidentate ligand in the complex [Pd(η^1-C_3H_5)Cl(NOPON^{Me2})].[16] The phosphorous atom becomes a stereogenic centre upon coordination and both enantiomers are present in the unit cell. The palladium atom lies in a distorted square-planar coordination environment, as shown by the bond angles about the metal, which range from 83.29(8) (N1-Pd1-P1) to 94.97(8)° (N1-Pd1-Cl1). The Pd-Cl bond distances of 2.2945(9) Å and 2.3825(9) Å, for the positions *trans* to nitrogen and *trans* to phosphorous, respectively, reflect the higher *trans* influence of the latter donor.[17] The molecular structure of the analogous complex [$PdBr_2$($N_{py}PN_{py}$-*N,P*)] ($^{31}P\{^1H\}$ NMR: δ 49.4 ppm) was determined for comparison and is very similar to that of **1**.

Abstraction of a chloride anion from **1** was expected to induce a tridentate chelating behaviour of the $N_{py}PN_{py}$ ligand. The reaction was performed directly by reacting in THF the palladium complex [$PdCl_2(NCPh)_2$] with the ligand in the presence of one equivalent of $TlPF_6$, which was added after several hours. The reaction proceeded heterogeneously because of the formation first of the insoluble complex **1** and gave rise to a mixture of two complexes, which were separated by crystallization. The main-product was the expected complex [PdCl($N_{py}PN_{py}$-*N,P,N*)]PF_6 (**2**), whereas the by-product was shown by X-ray diffraction to be the unexpected cationic dinuclear complex [Pd_2Cl_2(μ-$N_{py}PN_{py}$)$_2$]$(PF_6)_2$ (**3**). The NMR spectra of the two compounds in DMSO-d_6 at room temperature are different. In particular, the ^{1}H NMR spectrum of the dinuclear complex exhibits a doublet at 9.27 ppm due to two equivalent py^6 protons, whereas the py^6 protons of the mononuclear complex **2** resonate at 9.06 ppm. This allowed us to estimate the molar ratio between the mononuclear and the dinuclear complexes in the crude, which was found to be about 7/1. Although compound **3** is indefinitely stable

for references, see page 108

in the solid state, we observed that it converts slowly into compound **2** in DMSO solution, the conversion being complete after 4 days at room temperature or 10 h at 80 °C. We wondered whether the formation of the dinuclear complex was due to the heterogeneous conditions of the synthesis and, consequently, we repeated the reaction under homogeneous conditions by changing the nature of the solvent (DMSO instead of THF). As expected, the addition of one equivalent of $TlPF_6$ to a DMSO-d_6 solution of **1**, which forms in the first step of the synthesis of **2** and **3**, afforded selectively the mononuclear, cationic complex **2**. The $^{31}P\{^1H\}$ NMR spectrum of pure **2** in DMSO-d_6 exhibits two broad signals at 83.7 and 56.4 ppm, which are attributed to two different cationic complexes present in solution, namely $[PdCl(N_{py}PN_{py}\text{-}N,P,N)]^+$ and a complex resulting from coordination of a DMSO molecule and displacement of a pyridine group, $[PdCl(N_{py}PN_{py}\text{-}N,P)(DMSO)]^+$ (Scheme 5). The intensities of the two broad resonances provide an estimate of the molar ratio between the two species in equilibrium, which is about 3:1 ($[PdCl(N_{py}PN_{py}\text{-}N,P,N)]^+$ / $[PdCl(N_{py}PN_{py}\text{-}N,P)(DMSO)]^+$).

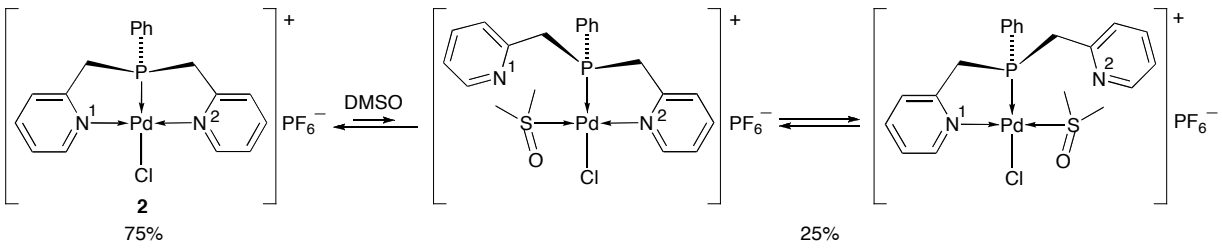

Scheme 5 Dynamic behaviour of **2** in DMSO solution

The two broad $^{31}P\{^1H\}$ NMR resonances (56.4 and 83.7 ppm) are found in the same region as those exhibited by **1** and the dicationic complex $[Pd(NCMe)(N_{py}PN_{py}\text{-}N,P,N)](PF_6)_2$ (**5**, *vide infra*), which occur respectively at 49.7 and 86.6 ppm in DMSO-d_6. So, it seems likely that the peak at 56.4 ppm is due to a complex where $N_{py}PN_{py}$ acts as a bidentate *N,P*-donor ligand, similarly to **1**, while the peak at 83.7 ppm is due to a complex where it behaves as a tridentate *N,P,N*-donor ligand, similarly to $[Pd(NCMe)(N_{py}PN_{py}\text{-}N,P,N)](PF_6)_2$. This hypothesis is also consistent with the fact that the ^1H NMR spectrum of **2** in DMSO-d_6 shows broad signals in both the pyridine and methylene regions. This is probably caused by the exchange equilibrium of the two pyridine moieties around the palladium atom in the $[PdCl(N_{py}PN_{py}\text{-}N,P)(DMSO)]^+$ species, as assumed for compound **1** (see below). In the $^{13}C\{^1H\}$ NMR spectrum of **2**, two sets of signals are observed, as expected: broad resonances corresponding to the DMSO substituted species and sharp resonances due to the $[PdCl(N_{py}PN_{py}\text{-}N,P,N)]^+$ cation. The far IR spectrum of **2** exhibits an absorption at 343 cm^{-1}, which is likely to be due to the Pd-Cl stretching vibration, and a strong band at 556 cm^{-1} tentatively assigned to the Pd-N stretching vibration.[18]

for references, see page 108

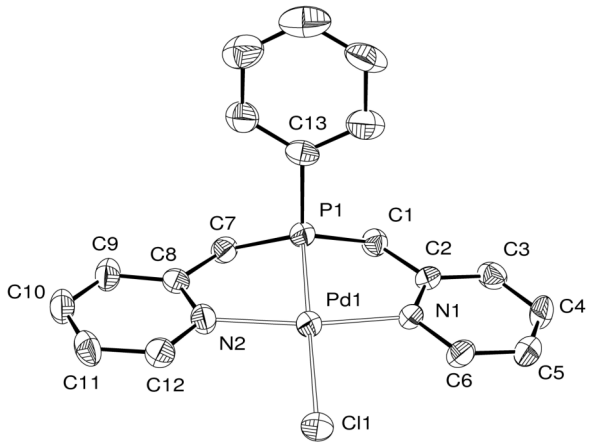

Fig. 2 ORTEP of the cationic complex in **2**·CH_2Cl_2 with ellipsoids drawn at the 50% probability level. Selected bond distances (Å) and Angles (deg): Pd1-Cl1 2.388(2), Pd1-P1 2.171(2), Pd1-N1 2.057(4), Pd1-N2 2.056(4), N1-Pd1-P1 83.35(13), N2-Pd1-P1 83.71(14), N1-Pd1-Cl1 96.80(13), N2-Pd1-Cl1 96.42(14), Cl1-Pd1-P1 177.50(5).

The molecular structure of the cationic complex $[PdCl(N_{py}PN_{py}$ -*N,P,N*$)]^+$ in **2**·CH_2Cl_2 is shown in Fig. 2. Its coordination geometry approximates square-planar, with the N-Pd-P angles being of 83.3(1)° and 83.7(1)°. There is no symmetry element in the molecule. In spite of the positive charge of the complex, the Pd-Cl bond distance of 2.388(2) Å does not differ significantly from that observed in **1** (*trans* to P). The Pd-P (2.171(2) Å) and Pd-N (2.057(4) and 2.056(4) Å) bond distances are slightly shorter than in complex **1**.

Let us now come back to the dynamic exchange involving complex **1**. It could formally occur by three different mechanisms: an associative displacement of N2 for N1, without chloride dissociation (Scheme 4a), chloride displacement by N1 to give a cationic complex with a tridentate N,P,N ligand $[PdCl(N_{py}PN_{py}$-*N,P,N*$)]Cl$ closely related to **2** (see below) and chloride recoordination and displacement of N2 (Scheme 4b), or dissociation of **1** in DMSO, nitrogen/DMSO exchange followed by chloride recoordination (Scheme 4c). In order to check their feasibility, we mixed equimolar amounts of **1** and **2** in a NMR tube and observed at room temperature a $^{31}P\{^1H\}$ resonance at 83.7 and a more intense and broad one at 50.3 ppm. The former corresponds to $[PdCl(N_{py}PN_{py}$-*N,P,N*$)]^+$ and the latter to the overlap between those assigned to **1** (49.7 ppm) and to $[PdCl(N_{py}PN_{py}$-*N,P*$)(DMSO)]^+$ (56.4 ppm). When the temperature was raised to 80 °C, the resonance at 83.7 ppm disappeared and the other was found at 49.1 ppm. These experiments suggest that **1** and **2** give rise to a common cationic species in solution and that the latter exchanges with **2** at higher temperature. This is consistent with a mechanism such as that shown in Scheme 4c. We verified independently that the cation in **2**, $[PdCl(N_{py}PN_{py}$-*N,P,N*$)]^+$, reacts with excess $(NMe_4)Cl$ in DMSO to give a single species, according to $^{31}P\{^1H\}$ spectroscopy, characterized by a singlet at 49.7 ppm, which is exactly the value found for **1**. Whether this is the dichloro complex or its solvento derivative (see above), this experiment demonstrates that a pyridine donor of the tridentate form of the $N_{py}PN_{py}$ ligand can be readily displaced by chloride to give a complex with a $N_{py}PN_{py}$-*N,P* chelate. This is again consistent with a

for references, see page 108

mechanism of the type shown in Scheme 4c. When complex **2** was treated in DMSO with only half an equivalent of $(NMe_4)Cl$, a sharp resonance was still present at 83.8 ppm, corresponding to the complex with the tridentate $N_{py}PN_{py}$ ligand, and a broad resonance was observed at 52.3 ppm which could correspond to the complexes **1** and $[PdCl(N_{py}PN_{py}$-*N,P*$)(DMSO)]Cl$ in slow exchange on the NMR time-scale.

The $^{31}P\{^1H\}$ NMR spectrum of **3** in DMSO-d_6 shows a broad resonance at 47.5 ppm, whereas the ^1H NMR spectrum displays sharp signals in the aromatic region and broad signals due to the methylene protons. Consistent with the molecular structure of **3** in the solid state, the two pyridine moieties of the each ligand are not equivalent. Particularly remarkable is the difference between the resonances of the protons *ortho* to the nitrogen, which is more than 1 ppm. As expected for the *trans* arrangement of the $PdCl_2$ moiety, the far IR spectrum of **3** contains only one absorption at 346 cm^{-1} for the Pd-Cl stretching vibration.[15a]

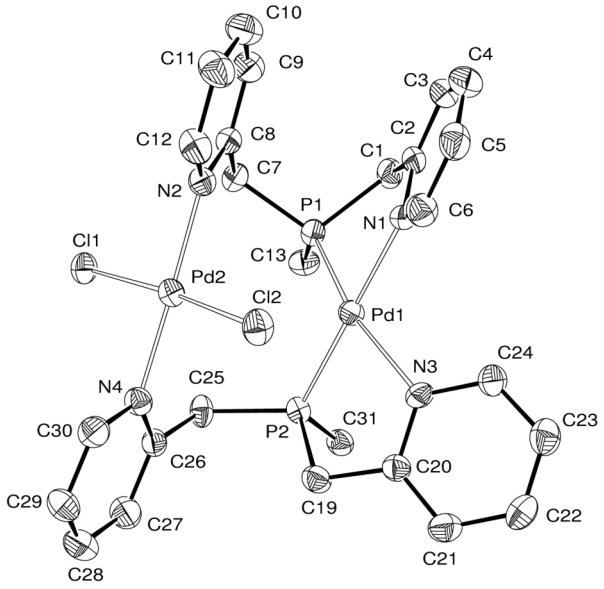

Fig. 3 ORTEP of the dinuclear cationic complex in **3**·2(CH_2Cl_2) with ellipsoids drawn at the 50% probability level. Only the *ipso* carbons of the P-phenyl groups are shown for clarity. Selected bond distances (Å) and angles (deg): Pd1-P1 2.224(1), Pd1-P2 2.242(1), Pd1-N1 2.116(3), Pd1-N3 2.123(3), Pd2-Cl1 2.315(1), Pd2-Cl2 2.301(1), Pd2-N2 2.047(3), Pd2-N4 2.020(3), N1-Pd1-P1 81.85(9), N3-Pd1-P2 82.08(9), N4-Pd2-N2 177.0(1), Cl2-Pd2-Cl1 174.95(4).

The solid-state structure of **3** deserves a more detailed description. It is shown in Figure 3. The cationic complex (Fig. 3) consists of two square-planar palladium units linked by two bridging $N_{py}PN_{py}$ ligands, which *P,N*-chelate one palladium centre (Pd1) and act as N donor ligands towards the other one (Pd2). The coordination environment of Pd2 is completed by two chlorides in *trans* position to each other. Thus, this dinuclear dicationic complex features an unusual charge differenciation between the two metal centres, Pd(1) formally carrying the doubly positive charge and the Pd(2) moiety being neutral.

The coordination geometry around Pd1 shows a pronounced distortion from planarity, the P1-Pd2-N3 angle being 161.4(1)°, significantly smaller than the related P2-Pd1-N1 of 179.0(1)°. The angle

for references, see page 108

between the two mean coordination planes, defined by the atoms Pd1,P1,P2,N1,N3 and Pd2,Cl1,Cl2,N4,N2 is 13.09(4)°. The phosphorous atoms become stereogenic centres upon coordination and exhibit opposite configurations, the resulting isomer being the *meso* diastereoisomer. The Pd2-Cl bond distances are in the usual range and the Pd1-N bond distances are affected by the *trans* influence of the phosphine and are significantly longer than the Pd2-N bond distances.[17] A similar coordination behaviour of the $N_{py}PN_{py}$ ligand has been recently observed in the Ag(I) complex $[Ag(N_{py}PN_{py})]_2(BF_4)_2$[9a] in which the two metal centres are additionally linked by an Ag-Ag bond.

The unexpected structure of **3** prompted us to develop a more straightforward and selective synthesis of this compound. Looking at the different coordination environments of the two palladium centres in **3**, it seemed convenient to first prepare a dicationic complex bearing two $N_{py}PN_{py}$ ligands, and then react this complex with a Pd(II) precursor containing the $PdCl_2$ fragment. The reaction between $[Pd(NCMe)_4](BF_4)_2$ and $N_{py}PN_{py}$ in a 1:2 molar ratio in dichloromethane afforded a pale yellow solid, which was identified by spectroscopy and X-ray diffraction as the mononuclear complex *cis*-$[Pd(N_{py}PN_{py}\text{-}N,P)_2](BF_4)_2$ (**4**).

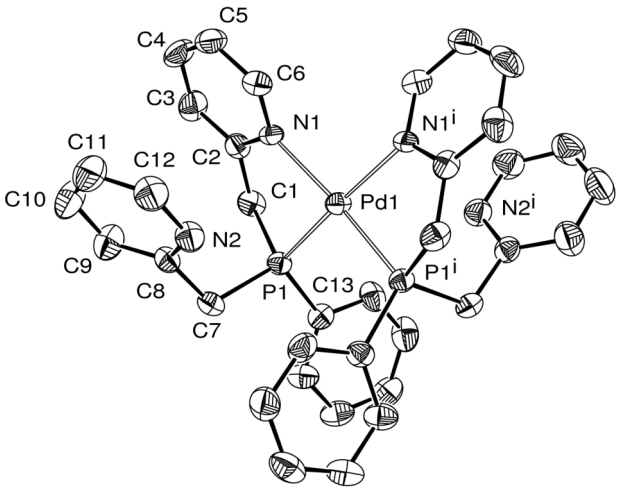

Fig. 4 ORTEP of the cationic complex in **4**·2(CH_2Cl_2) with ellipsoids drawn at the 50% probability level. Selected bond distances (Å) and angles (deg): Pd1-N1 2.108(3), Pd1-P1 2.229(1), N1-Pd1-$N1^i$ 98.4(2), N1-Pd1-P1 82.21(9), P1-Pd1-$P1^i$ 98.65(6). Symmetry operation generating equivalent atoms (^{i}): -x, y, -z.

In the molecular structure of **4**·2(CH_2Cl_2) (Figure 4), a C_2 symmetry axis passes through the metal atom and the middle points of the P...P and N...N segments. The phosphorous atoms thus display the same configuration and the complex is consequently chiral. Both enantiomers are present in the unit cell. As expected, the Pd-P and Pd-N bond distances in **4** (2.229(1) and 2.108(3) Å, respectively) are very similar to those observed in complex **3**. Compound **4** was reacted in DMSO-d_6 with an equimolar amount of $[PdCl_2(cod)]$. The ^{1}H- and $^{31}P\{^1H\}$ NMR spectra of the resulting solution revealed the selective formation of the dinuclear cationic complex $[Pd_2Cl_2(\mu\text{-}N_{py}PN_{py})_2]^{2+}$ of **3** (Scheme 6).

for references, see page 108

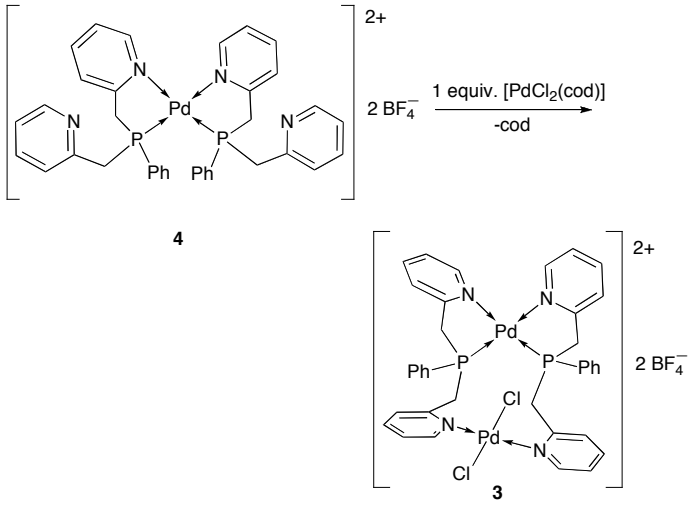

Scheme 6 Selective formation of **3** from **4** and $[PdCl_2(cod)]$

Furthermore, the synthesis of a dicationic Pd(II) complex containing the $N_{py}PN_{py}$ ligand was realized by extracting both chloride anions from the coordination sphere of the metal. Thus, the one-pot 1:1 reaction between $[PdCl_2(NCPh)_2]$ and the $N_{py}PN_{py}$ in the presence of two equivalents of $TlPF_6$ in MeCN afforded selectively a pale yellow compound in high yield, which was identified as the expected complex $[Pd(N_{py}PN_{py}\text{-}N,P,N)(NCMe)](PF_6)_2$ (**5**).

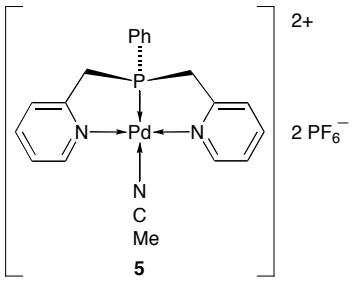

As far as the NMR spectra of **5** in DMSO are concerned, the main difference to be noted with respect to compounds **1-3** is the absence of broad signals. Moreover, the picolyl moieties are equivalent as proved by the ^1H and $^{13}C\{^1H\}$ NMR spectra. These observations are consistent with a tridentate coordination behaviour of the ligand, where the pyridine moieties are strongly bound to the metal and not displaced by the DMSO, at variance with the situation suggested for compound **2**. Nevertheless, the displacement of the acetonitrile by a dimethylsulphoxide molecule was established by the presence of the signals of free acetonitrile in both ^1H- and $^{13}C\{^1H\}$ NMR spectra. The $^{31}P\{^1H\}$ NMR spectrum of **5** displays a sharp singlet at 86.6 ppm. The difference between this value and that observed for **2** is only 3.3 ppm and suggests that the phosphorous nuclei in the two complexes lie in a very similar electronic environment. The increase of the formal charge of the cationic complex from +1 (for **2**) to +2 (for **5**) does not affect significantly the chemical shift of the phosphorous atom but causes, as expected, a slight downfield shift. As anticipated, the ^1H NMR of **5** in DMSO-d_6 displays only sharp signals. The ABX spin system for the CH_2P protons was expected to give rise to two doublet of doublets ($^2J_{HH,}$ and two $^2J_{PH}$). In fact, two triplets are observed in the methylene region, thus

for references, see page 108

suggesting that the $^2J_{PH}$ are very similar to the $^2J_{HH}$. The ABX spin system could be converted into an AB spin system by recording the $^1H\{^{31}P\}$ NMR spectrum of **5**, which showed two doublets at 5.21 and 4.29 ppm with $^2J_{HH}$ = 17.7 Hz. In the far IR spectrum of **5**, the Pd-N stretching vibration causes a strong absorption at 554 cm^{-1}.[18] A view of the molecular structure of the cationic complex in **5**·MeCN is depicted in Fig. 5. Bond distances and angles in the Pd($N_{py}PN_{py}$) fragment are in most cases identical to those observed in **2**·CH_2Cl_2, the main difference being a shorter Pd-P distance in **5**. This is probably due to the decrease in the overall charge of cation from +1 (in **2**) to +2 (in **5**).

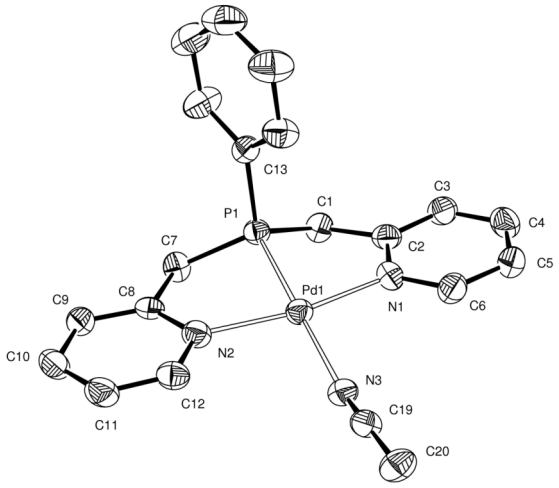

Fig. 5 ORTEP of the cationic complex in **5**·MeCN with ellipsoids drawn at the 50% probability level. Selected bond distances (Å) and angles (deg): Pd1-P1 2.163(1), Pd1-N1 2.063(4), Pd1-N2 2.051(4), Pd1-N3 2.125(4), N1-Pd1-P1 83.4(1), N2-Pd1-P1 82.6(1), N1-Pd1-N3 97.0(2), N2-Pd1-N3 97.1(2), N3-Pd1-P1 178.1(1).

It appeared interesting to extend our study of the $N_{py}PN_{py}$ ligand to another d^8 transition metal system. Since it was previously reported that $N_{py}PN_{py}$ acts as a facial tridentate ligand in octahedral Fe(II)[3b] and Cr(III)[19] complexes, we wondered which type of coordination geometry would have been obtained for a metal cation that can have either square planar or trigonal bipyramidal coordination environment. Ir(I) was expected to be a good candidate for this purpose. Moreover, although the chemistry of iridium complexes containing tridentate ligands such as *P,C,P*-pincer[11] or tris(pyrazolyl)borate ligands[10] has been extensively studied, to the best of our knowledge, only two structurally characterized iridium compounds bearing a chelated *N,P,N*-ligand have been reported to date.[13,20]

The 1:2 reaction between the iridium(I) precursor $[Ir(\mu\text{-}Cl)(cod)]_2$ and $N_{py}PN_{py}$ afforded an air-sensitive orange compound in high yield. Although the attempts to get crystals suitable for X-ray diffraction failed, the formation of a new complex of formula [IrCl(cod)($N_{py}PN_{py}$)] (**6**) was inferred from spectroscopic and elemental analysis data. The coordination of the $N_{py}PN_{py}$ ligand through its phosphorous atom was demonstrated by the $^{31}P\{^1H\}$ NMR spectrum in $CDCl_3$, which consists in a sharp singlet at 24.7 ppm, 30 ppm downfield shifted with respect to the free ligand. Differently from what observed for compounds **1**-**3**, all the signals in the ^1H NMR spectrum of **6** are sharp. Moreover,

for references, see page 108

four sharp signals in the pyridine region and only one ABX spin system in the CH_2 region were detected. These observations are consistent with a tridentate behaviour of the $N_{py}PN_{py}$ ligand, whose picolyl moieties would be symmetrically coordinated to the metal centre. As shown in Scheme 7 and Figure 6, the two *P*,*N*-chelating arms are not equivalent and the fact that only one ABX spin system due to the CH_2P protons is observed (two doublets of doublets at 5.01 and 3.77 ppm with $^2J_{HH}$ = 17.6 Hz and $^3J_{PH}$ = 13.5 and 9.7 Hz) could be due to rapid exchange or to an equilibrium between a trigonal bipyramidal and a square-base pyramidal coordination geometry that would render the two P,N arms equivalent. Three resonances between 3.50 and 1.80 ppm are due to the coordinated cod ligand. In particular, the protons of the methylene groups of the cyclooctadiene become non-equivalent upon coordination and give rise to two multiplets. The $^{13}C\{^1H\}$ NMR spectrum **6** displays two doublets at 63.0 ($^2J_{PH}$ = 8.7 Hz) and 33.0 ($^3J_{PH}$ = 1.8 Hz) ppm, attributed to the CH and the CH_2 carbons of the cod, respectively. IR spectroscopy was very useful to better understand the molecular structure of **6**. In particular, the far IR spectrum of the compound did not show any strong absorption around 300 cm^{-1} and this led us to rule out the presence of Ir-Cl bonds.[21] In agreement with the spectroscopic data and the elemental analysis, we propose that **6** is a penta-coordinated cationic complex. As far as the coordination environment of the metal is concerned, two different geometries have been reported for Ir(I) complexes containing cyclooctadiene and phosphine ligands, namely trigonal bipyramidal and square pyramidal.[22] In most of them, the metal centre lies in a distorted trigonal bipyramidal environment, the double bonds of the cod ligand occupying an equatorial and an apical position, as shown in Scheme 7.

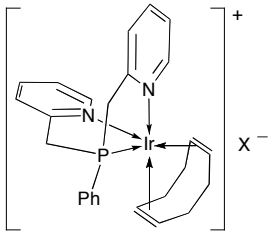

6 X = Cl
7 X = BAr^F

Scheme 7. Structures of **6** and **7** based on the X-ray diffraction structure of **7**

It was hoped that the substitution of the chloride anion with a (tetra)arylborate would promote the crystallization of the complex and increase its solubility in solvents of low polarity. Therefore, we reacted $[Ir(\mu\text{-}Cl)(cod)]_2$ with the $N_{py}PN_{py}$ ligand and added two equivalents of $NaBAr^F$ to the reaction mixture. The yellow crystalline product, which was isolated in high yield after removing the NaCl formed, was fully characterized by IR and NMR spectroscopic methods, elemental analysis, and X-ray diffraction, and identified as the cationic complex $[Ir(cod)(N_{py}PN_{py}\text{-}N,P,N)]BAr^F$ (**7**). Its $^{31}P\{^1H\}$ NMR spectrum in $CDCl_3$ displays a sharp singlet at 24.2 ppm, with a difference of only 0.5 ppm with respect to that of **6**. This suggests a very similar chemical environment around the phosphorous donor

for references, see page 108

atom. With the exception of the signals due to the counteranion, the $^{13}C\{^1H\}$ NMR spectra of **6** and **7** are also very similar in terms of chemical shifts and coupling constants. The main difference between the ^1H NMR spectra of **6** and **7** concerns the ABX spin system due to the CH_2P protons. As previously mentioned, the two diastereotopic protons of **6** give rise to two doublets of doublets at 5.01 and 3.77 ppm. In the case of **7**, instead, they give rise to a multiplet between 3.90-3.80 ppm. By means of spectral simulation we could estimate the parameters of this ABX spin system as δ_A = 3.86 ppm, δ_B = 3.84 ppm, $^2J_{AB}$ = 18.4 Hz, $^2J_{AX}$ = 2.6 Hz and $^2J_{BX}$ = 19.6 Hz. A view of the molecular structure of the cation $[Ir(cod)(N_{py}PN_{py})]^+$ of **7** in the solid state is shown in Figure 6.

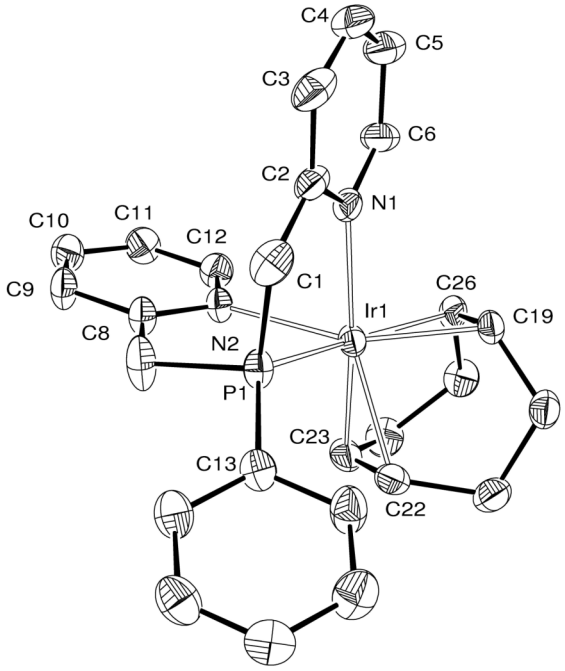

Fig. 6 ORTEP of the cationic complex in **7** with ellipsoids drawn at the 30% probability level. Selected bond distances (Å) and angles (deg): Ir1-N1 2.150(5), Ir1-N2 2.274(5), Ir1-P1 2.277(2), Ir1-C22/23 2.032(4), Ir1-C19/26 1.992(4), C22-C23 1.398(10), C19-C26 1.443(9), N1-Ir1-N2 83.9(2), N1-Ir1-P1 81.0(2), N2-Ir1-P1 79.0(1), C22/23-Ir1-C16/C26 85.5(3).

The coordination geometry around the metal is best described as trigonal bipyramidal. Two equatorial (P, N) and one apical (N) positions are occupied by the donor atoms of the $N_{py}PN_{py}$ ligand, which acts as a facial, tridentate *N,P,N*-donor. Similarly, in the octahedral Cr^{III} complex $[CrCl_3(N_{py}PN_{py}$-*N,P,N*)] the ligand exhibits a facial coordination mode with the phosphorous atom in an apical position.[19] The two C=C double bonds of the cyclooctadiene complete the coordination sphere of the metal. The apical Ir-N bond (2.150(5) Å) is shorter than the equatorial one (2.274(5) Å).

6.4 Conclusions

New coordination complexes of Pd(II) and Ir(I) bearing the neutral ligand $N_{py}PN_{py}$ have been prepared in high yields from $[PdCl_2(NCPh)_2]$ or $[Ir(\mu\text{-}Cl)(cod)]_2$ and the ligand. The solid-state structures of the compounds (**1-5** and **7**) point out the versatility of the $N_{py}PN_{py}$ molecule, which can

for references, see page 108

act as *N,P*-chelating ligand (in **1** and **4**), *N,P,N-mer*-chelating ligand (in **2** and **5**), (*N,P*)-*N* bridging ligand (in **3**), *N,P,N-fac*-chelating ligand (in **7**). On the basis of NMR experiments in DMSO-d_6, the hemilability of $N_{py}PN_{py}$ in **1** has been demonstrated, the two pyridine moieties being involved in a dynamic exchange in the coordination sphere of the metal. Dynamic processes in DMSO solution have also been observed for complex **2** and an equilibrium between the species $[PdCl(N_{py}PN_{py}\text{-}N,P,N)]^+$ and $[PdCl(N_{py}PN_{py}\text{-}N,P)(DMSO)]^+$ has been inferred. The unexpected dinuclear compound **3** has been isolated as a by-product of the synthesis of its isomer **2**. We have also demonstrated that, in spite of the stability of **3** in the solid state, it can be converted into **2** in DMSO solution. A rational, stepwise-preparation of **3** has been described, which involves the preparation of the dicationic complex *cis*-$[Pd(N_{py}PN_{py}\text{-}N,P)_2]$ $(BF_4)_2$ (**4**) and its reaction with $[PdCl_2(cod)]$. The Ir(I) cationic complex $[Ir(cod)(N_{py}PN_{py}\text{-}N,P,N)]BAr^F$ (**7**) is, to the best of our knowledge, only the third Ir(I) complex containing a *N,P,N*-chelating ligand to be structurally characterized.[20,23]

6.5 Experimental Section

6.5.1 General Considerations

All operations were carried out using standard Schlenk techniques under inert atmosphere. Solvents were dried, degassed, and freshly distilled prior to use. Et_2O and THF were dried over sodium/benzophenone. Pentane was dried over sodium. CH_2Cl_2 and acetonitrile was distilled from CaH_2. DMF, DMSO-d_6 and $CDCl_3$ were dried over 4 Å molecular sieves, degassed by freeze-pump-thaw cycles and stored under argon. Unless otherwise stated, NMR spectra were recorded at room temperature on a Bruker AVANCE 300 spectrometer (^{1}H, 300 MHz; ^{13}C, 75.47 MHz; ^{19}F, 282.4 MHz; ^{31}P, 121.5 MHz) or on a Bruker AVANCE 400 spectrometer (^{1}H, 400 MHz; ^{13}C, 100.60 MHz, ^{31}P, 162.0 MHz,) and referenced using the residual proton solvent (^{1}H) or solvent (^{13}C) resonance. Assignments are based on DEPT135, COSY, HMQC and HMBC experiments. IR spectra were recorded in the region 4000-100 cm^{-1} on a Nicolet 6700 FT-IR spectrometer equipped with a Smart Orbit ATR accessory (Ge or diamond crystals). Elemental analyses were performed by the "Service de microanalyses", Université de Strasbourg. Yields of the complexes are based on the metal. $[Ir(\mu\text{-}Cl)(cod)]_2$ and $TlPF_6$ were purchased from UMICORE and Alfa Aesar and used as received. Bis(2-picolyl)phenylphosphine ($N_{py}PN_{py}$),[3b] $[PdCl_2(NCPh)_2]$,[24] $Na[B(3,5\text{-}(CF_3)_2C_6H_3)_4]$,[25] $[Pd(NCMe)_4](BF_4)_2$,[26] and $[PdCl_2(cod)]$[27] were prepared according to literature methods. Other chemicals were commercially available and used as received.

6.5.2 Synthesis of $[PdCl_2(N_{py}PN_{py})]$ (1)

Solid $[PdCl_2(NCPh)_2]$ (0.722 g, 1.88 mmol) was added to a solution of $N_{py}PN_{py}$ (0.550 g, 1.88 mmol) in dichloromethane (20 mL) to give a yellow suspension, which was stirred overnight. The solvent was removed under vacuum affording a yellow powder which was washed with diethyl ether (2 × 20 mL) and dried *in vacuo* overnight (Yield: 0.697 g, 1.32 mmol, 79%). Selected IR absorptions (pure,

for references, see page 108

diamond orbit): 1604m, 1587m, 1468ms, 1436s, 1107m, 844s, 803s, 785s, 744s, 684s, 337m, 301m cm^{-1}. $^{1}H\{^{31}P\}$ NMR (400.13 MHz, DMSO-d_6): δ 9.31 (br, 1H, py^6), 8.38 (br, 1H, py^6), 8.04 (br, 1H, py^4), 7.87 (d, 2H, $^{3}J_{HH}$ = 7.5 Hz, *o*-aryl), 7.81 (br, 1H, py^3), 7.71 (br, 1H, py^4), 7.58 (t, 1H, $^{3}J_{HH}$ = 7.4 Hz, *p*-aryl), 7.51-7.35 (m, 4H, *m*-aryl, py^5 and py^3), 7.24 (br, 1H, py^5), 4.70 and 4.25 (AB spin system, 2H, $^{2}J_{HH}$ = 16.4 Hz, CH_2), 4.25 and 4.08 (AB spin system, 2H, $^{2}J_{HH}$ = 14.4 Hz, CH_2) ppm. $^{13}C\{^{1}H\}$ NMR (75.5 MHz, DMSO-d_6): δ 162.5 (s, coordinated py^2), 153.4 (s, uncoordinated py^2), 152.2 (s, coordinated py^6), 149.6 (s, uncoordinated py^6), 140.8 (s, coordinated py^4), 137.5 (s, uncoordinated py^4), 132.6 (s, *p*-aryl), 132.2 (d, $^{2}J_{PC}$ = 10.0 Hz, *o*-aryl), 129.5 (d, $^{3}J_{PC}$ = 11.2 Hz, *m*-aryl), 127.7 (d, $^{1}J_{PC}$ = 52.2 Hz, *ipso*-aryl), 125.7 (s, py), 124.8 (s, py), 124.1 (s, py), 122.9 (s, py), coordinated CH_2 partially masked by the solvent resonance, 34.8 (d, $^{1}J_{PC}$ = 31.3 Hz, uncoordinated CH_2) ppm. $^{31}P\{^{1}H\}$ NMR (121.5 MHz, DMSO-d_6): δ 49.7 (s) ppm. Anal. Calcd for $C_{18}H_{17}Cl_2N_2PPd$: C, 46.03; H, 3.65; N, 5.96. Found: C, 45.53; H, 3.83; N, 5.86. Crystals suitable for X-ray diffraction were grown by slow cooling of a concentrated solution of the pure compound in DMF.

6.5.3 Synthesis of $[PdCl(N_{py}PN_{py})]PF_6$ (2) and $[Pd_2Cl_2(\mu\text{-}N_{py}PN_{py})_2](PF_6)_2$ (3)

Solid $[PdCl_2(NCPh)_2]$ (0.690 g, 1.80 mmol) was added to a solution of $N_{py}PN_{py}$ (0.525 g, 1.80 mmol) in THF (20 mL) to give a yellow suspension, which was stirred overnight. $TlPF_6$ (0.629 g, 1.80 mmol) was added and the mixture was stirred for 12 h. The solvent was removed by evaporation under reduced pressure and the solid residue was extracted in DMF and the solution was filtered to remove TlCl. Et_2O was added and a yellow solid separated out which was shown by ^{1}H NMR to contain two products (see text). After filtration and washing of the yellow solid with CH_2Cl_2 (3 × 10 mL), the combined filtrates were concentrated to 10 mL under reduced pressure to give yellow crystals of $[Pd_2Cl_2(\mu\text{-}N_{py}PN_{py})_2](PF_6)_2$, suitable for X-ray diffraction (0.100 g, 0.086 mmol, 10% yield based on Pd). The insoluble pale yellow residue was identified as $[PdCl(N_{py}PN_{py})]PF_6$ (0.762 g, 1.32 mmol, 73%). Selected IR absorptions (pure, diamond orbit) for $[PdCl(N_{py}PN_{py})]PF_6$: 1666w, 1606w, 1474w, 1439w, 1110w, 835vs, 768m, 688m, 556s, 343m cm^{-1}. The following NMR data correspond to those of the complex $[PdCl(NPN)]^+$, which are sharp signals. ^{1}H NMR (300.13 MHz, DMSO-d_6): δ 9.06 (d, 2H, $^{3}J_{HH}$ = 4.9 Hz, py^6), 8.25-8.20 (m, 2H, py^4), 7.99-7.90 (m, 4H, py^3 and *o*-aryl), 7.68-7.51 (m, 5H, py^5, *p*- and *m*-aryl), 5.30-5.19 (m, 2H, $^{2}J_{HH} \approx {}^{2}J_{PH} \approx$ 17.3 Hz, C*H*H), 4.39-4.23 (m, 2H, $^{2}J_{HH} \approx {}^{2}J_{PH} \approx$ 17.3 Hz, CH*H*) ppm. $^{13}C\{^{1}H\}$ NMR (75.5 MHz, DMSO-d_6): δ 164.9 (s, py^2), 153.6 (s, py^6), 142.0 (s, py^4), 133.9-124.9 (m, $py^{3,5}$ and aryl), 38.5 (d, $^{1}J_{PC}$ = 36.7 Hz, CH_2) ppm. $^{31}P\{^{1}H\}$ NMR (121.5 MHz, DMSO-d_6): δ 83.7 (br, $N_{py}PN_{py}$), -143.0 (sept, $^{1}J_{PF}$ = 712 Hz, PF_6^-) ppm. Anal. Calcd for $C_{18}H_{17}ClF_6N_2P_2Pd$: C, 37.33; H, 2.96; N, 4.84. Found: C, 37.55; H, 3.06; N, 4.82. Crystals suitable for X-ray diffraction were grown by cooling at room temperature a hot solution of the pure compound in dichloromethane.

$[Pd_2Cl_2(\mu\text{-}N_{py}PN_{py})_2](PF_6)_2$ (**3**). Selected IR absorptions (pure, diamond orbit): 1606w, 1572w, 1476w, 1437w, 1102m, 836vs, 759m, 746m, 694m, 555s, 346m cm^{-1}. ^{1}H NMR (300.13 MHz, DMSO-

for references, see page 108

d_6): δ 9.27 (d, 2H, $^3J_{HH}$ = 5.4 Hz, py^6), 8.20-8.17 (m, 2H, py), 8.10-8.05 (m, 2H, py^4), 7.98-7.93 (m, 2H, py), 7.78-7.67 (m, 8H, py and *o*-aryl), 7.60-7.51 (m, 6H, py and *p*-aryl), 7.40-7.34 (m, 4H, *m*-aryl), 5.66 (br, 2H, CH_2), 4.77-4.30 (m, 4H, CH_2), 3.94 (br, 2H, CH_2) ppm. $^{31}P\{^1H\}$ NMR (121.5 MHz, DMSO-d_6): δ 47.5 (br, $N_{py}PN_{py}$), -143.0 (sept, $^1J_{PF}$ = 712 Hz, PF_6^-) ppm. We could not record the $^{13}C\{^1H\}$ NMR spectrum of the pure compound because it isomerises slowly to the monomer in DMSO solution. Anal. Calcd for $C_{18}H_{17}ClF_6N_2P_2Pd$: C, 37.33; H, 2.96; N, 4.84. Found: C, 36.61; H, 3.17; N, 4.72.

6.5.4 Synthesis of $[Pd(N_{py}PN_{py})_2](BF_4)_2$ (4)

Solid $[Pd(NCCH_3)_4](BF_4)_2$ (0.222 g, 0.50 mmol) was added to a solution of $N_{py}PN_{py}$ (0.292 g, 1.00 mmol) in dichloromethane (20 mL). The resulting yellow suspension was stirred overnight at room temperature. The solvent was concentrated to 5 mL under reduced pressure affording a pale yellow powder, which was washed with diethyl ether (2 × 20 mL) and dried *in vacuo* overnight (Yield: 0.337 g, 0.39 mmol, 78%). Selected IR absorptions (pure, diamond orbit): 1605w, 1588w, 1571w, 1473m, 1437m, 1397w, 1315m, 1162m, 1028vs, 888s, 833m, 752s, 692s cm^{-1}. ^1H NMR (300.13 MHz, DMSO-d_6): δ 8.25 (d, 4H, $^3J_{HH}$ = 5.2 Hz, py^6), 7.82 (t, 4H, $^3J_{HH}$ = 7.7 Hz, py^4), 7.74-7.67 (m, 6H, *p*- and *o*-aryl), 7.54-7.47 (m, 8H, py^3 and *m*-aryl), 7.32 (t, 4H, py^5), 4.33-4.16 (m, 8H, CH_2) ppm. $^{13}C\{^1H\}$ NMR (75.5 MHz, DMSO-d_6): δ 155.7 (s, py^2), 150.6 (s, py^6), 139.7 (s, py^4), 133.7 (s, *p*-aryl), 132.4 (d, J_{PC} = 11.1 Hz, aryl), 129.7 (d, J_{PC} = 11.8 Hz, aryl), 125.2 (d, $^1J_{PC}$ = 56.3 Hz, *ipso*-aryl), 125.2 (d, $^3J_{PC}$ = 11.1, py^3), 124.1 (s, py^5), 36.7 (d, $^1J_{PC}$ = 30.2 Hz, CH_2) ppm. $^{31}P\{^1H\}$ NMR (121.5 MHz, DMSO-d_6): δ 47.0 (s) ppm. Anal. Calcd for $C_{36}H_{34}B_2F_8N_4P_2Pd$ C, 50.01; H, 3.96 N, 6.48. Found: C, 49.97; H, 3.86; N, 6.49. Crystals suitable for X-ray diffraction were grown by layering Et_2O on a concentrated dichloromethane solution of the pure compound.

6.5.5 Synthesis of $[Pd(N_{py}PN_{py})(MeCN)](PF_6)_2$ (5)

Solid $[PdCl_2(NCPh)_2]$ (0.384 g, 1.00 mmol) was added to a solution of $N_{py}PN_{py}$ (0.290 g, 1.00 mmol) in acetonitrile (20 mL). The yellow suspension was stirred overnight, $TlPF_6$ (0.698 g, 2.00 mmol) was then added and the mixture was further stirred for 12 h. After filtration and washing of the solid residue with acetonitrile (3 × 10 mL), the combined filtrates were concentrated to 5 mL, and Et_2O (20 mL) was added affording the precipitation of pure $[Pd(N_{py}PN_{py})(NCMe)](PF_6)_2$ as a pale yellow solid (Yield: 0.584 g, 0.80 mmol, 80%). Selected IR absorptions (pure, diamond orbit): 1609w, 1476w, 1437w, 1111m, 832vs, 776m, 742m, 689m, 554s cm^{-1}. $^1H\{^{31}P\}$ NMR (400.13 MHz, DMSO-d_6): δ 8.51 (d, 2H, $^3J_{HH}$ = 5.4 Hz, py^6), 8.26 (td, 2H, $^3J_{HH}$ = 7.9 Hz, $^4J_{HH}$ = 1.5 Hz, py^4), 8.00 (d, $^3J_{HH}$ = 7.9 Hz, 2H, py^3), 7.70-7.67 (m, 3H, py^5 and *p*-aryl), 7.64-7.62 (m, 2H, *o*-aryl), 7.55-7.51 (m, 2H, *m*-aryl), 5.21 and 4.29 (AB spin system, $^2J_{HH}$ = 17.7 Hz, 4H, CH_2), 2.07 (s, 3H, free CH_3CN) ppm. $^{13}C\{^1H\}$ NMR (75.5 MHz, DMSO-d_6): δ 164.0 (s, py^2), 151.6 (s, py^6), 142.4 (s, py^4), 134.1 (d, $^4J_{PC}$ = 2.6 Hz, *p*-aryl), 131.7 (d, $^2J_{PC}$ = 11.2 Hz, *o*-aryl), 130.4 (d, $^3J_{PC}$ = 12.7 Hz, *m*-aryl), 126.3 (d, $^3J_{PC}$ = 15.3 Hz, py^3),

for references, see page 108

125.7 (s, py^5), 124.4 (d, $^1J_{PC}$ = 58.6 Hz, *ipso*-aryl), 118.5 (s, free CH_3CN), CH_2 partially masked by the solvent resonance, 1.5 (s, free CH_3CN). $^{31}P\{^1H\}$ NMR (121.5 MHz, DMSO-d_6): δ 86.6 (s, $N_{py}PN_{py}$), —143.0 (sept, $^1J_{PF}$ = 712 Hz, PF_6^-) ppm. Anal. Calcd for $C_{20}H_{20}F_{12}N_3P_3Pd\cdot CH_3CN$: C, 34.28; H, 3.01; N, 7.27. Found: C, 33.61; H, 3.17; N, 6.98. Crystals suitable for X-ray diffraction were grown by layering Et_2O on a concentrated acetonitrile solution of the pure compound.

6.5.6 Synthesis of [IrCl(cod)($N_{py}PN_{py}$)] (6)

Solid [Ir(μ-Cl)(cod)]$_2$ (0.260 g, 0.387 mmol) was added to a solution of the $N_{py}PN_{py}$ ligand (0.220 g, 0.787 mmol) in CH_2Cl_2 (10 mL). The orange solution stirred for 1 h. The solvent was evaporated under reduced pressure to give an orange solid, which was washed with pentane (2 × 5 mL) and dried *under vacuum* (Yield: 0.430 g, 0.684 mmol, 88%). Selected IR absorptions (pure, diamond orbit): 1597m, 1472ms, 1435ms, 1106ms, 1011m, 744s, 695s cm^{-1}. ^{1}H NMR (300.13 MHz, $CDCl_3$): δ 8.76 (dd, 2H, $^3J_{HH}$ = 5.6 Hz, $^4J_{HH}$ = 1.0 Hz, py^6), 7.92-7.85 (m, 2H, *o*-aryl), 7.79 (d, 2H, $^3J_{HH}$ = 7.9 Hz, py^3), 7.70-7-62 (m, 2H, py^4), 7.59-7.47 (m, 3H, *m*-, *p*-aryl), 7.14-7.06 (m, 2H, py^5), 5.01 and 3.77 (ABX spin system, 4H, $^2J_{HH}$ = 17.6 Hz, $^2J_{PH}$ = 13.5 Hz and 9.7 Hz, PCH_2), 3.40 (s, 4H, CH cod), 2.40-2.20 (m, 4H, CH_2 cod), 1.95-1.75 (m, 4H, CH_2 cod) ppm. $^{13}C\{^1H\}$ NMR (75.5 MHz, $CDCl_3$): δ 161.9 (d, $^2J_{PC}$ = 6.2 Hz, py^6), 150.7 (d, $^3J_{PC}$ = 3.5 Hz, py^2), 138.3 (s, py^4), 131.9 (d, $^2J_{PC}$ = 11.2 Hz, *o*-aryl), 131.3 (d, $^4J_{PC}$ = 2.3 Hz, *p*-aryl), 129.4 (d, $^3J_{PC}$ = 10.6 Hz, *m*-aryl), 126.6 (d, $^1J_{PC}$ = 49.7 Hz, *ipso*-aryl), 125.4 (d, $^3J_{PC}$ = 9.7 Hz, py^3), 123.9 (s, py^5), 63.0 (d, $^2J_{PC}$ = 8.7 Hz, CH cod), 41.8 (d, $^2J_{PC}$ = 28.7 Hz, CH_2P), 33.0 (d, $^3J_{PC}$ = 1.8 Hz, CH_2 cod) ppm. $^{31}P\{^1H\}$ NMR (121.5 MHz, $CDCl_3$): δ 24.7 (s) ppm. Anal. Calcd for $C_{26}H_{29}ClIrN_2P$: C, 49.71; H, 4.65; N, 4.46. Found: C, 49.76; H, 4.93; N, 4.12.

6.5.7 Synthesis of [Ir(cod)($N_{py}PN_{py}$)]BAr^F (7)

Solid [Ir(μ-Cl)(cod)]$_2$ (0.160 g, 0.238 mmol) was added to a solution of the $N_{py}PN_{py}$ ligand (0.142 g, 0.486 mmol) in CH_2Cl_2 (10 mL). The orange solution was stirred for 1 h and then $NaBAr^F$ was added. The resulting yellow mixture was stirred overnight and filtered to remove NaCl. The solvent was removed under reduced pressure and the resulting yellow powder was washed with pentane (2 × 5 mL) and dried *under vacuum* (Yield: 0.440 g, 0.302 mmol, 63%). Crystals suitable for X-ray diffraction were grown by layering Et_2O and pentane on a concentrated solution of the compound in CH_2Cl_2. Selected IR absorptions (pure, diamond orbit): 1608 (w), 1571(mw), 1354(m), 1277(vs), 1159(s), 1120(vs) cm^{-1}. ^{1}H NMR (300.13 MHz, $CDCl_3$): 8.86 (d, 2H, $^3J_{HH}$ = 4.8 Hz, py^6), 7.80-7.66 (m, 10H, *o*-aryl, *o*-BAr^F), 7.64-7.58 (m, 3H, *p*-, *m*-aryl), 7.57-7.44 (m, 6H, py^4, *p*-BAr^F), 7.34 (d, 2H, $^3J_{HH}$ = 7.8 Hz, py^3), 7.08 (t, 2H, $^3J_{HH}$ = 6.2 Hz, py^5), 3.90-3.80 (m, ABX spin system, 4H, values from spectral simulation: $^2J_{HH}$ = 18.4 Hz, $^2J_{PH}$ = 19.6 Hz and 2.6 Hz, PCH_2), 3.46 (s, 4H, CH cod), 2.40-2.25 (m, 4H, CH_2 cod), 1.98-1.88 (m, 4H, CH_2 cod) ppm. $^{13}C\{^1H\}$ NMR (75.5 MHz, $CDCl_3$): δ 161.7 (q, $^1J_{BC}$ = 49.8 Hz, *ipso*-aryl BAr^F), 160.2 (d, $^2J_{PC}$ = 7.3 Hz, py^2), 151.6 (d, $^3J_{PC}$ = 4.1 Hz, py^6), 138.7 (s, py^4), 134.8 (s, *o*-aryl BAr^F), 132.2 (d, $^4J_{PC}$ = 2.6 Hz, *p*-aryl), 131.0 (d, $^2J_{PC}$ = 11.3 Hz, *o*-aryl), 129.9 (d, $^3J_{PC}$

for references, see page 108

= 10.7 Hz, *m*-aryl), 128.9 (qq, $^2J_{CF}$ = 31.5 Hz, $^3J_{BC}$ = 2.8 Hz, *C*CF_3), 124.7 (s, py[5]), *ipso*-aryl masked, 124.5 (q, $^1J_{CF}$ = 272.5 Hz, CF_3), 124.0 (d, $^3J_{PC}$ = 9.5 Hz, py[3]), 117.5 (sept, $^3J_{CF}$ = 3.8 Hz, *p*-aryl BAr^F), 64.3 (d, $^2J_{PC}$ = 8.7 Hz, CH cod), 42.8 (d, $^2J_{PC}$ = 27.4 Hz, CH_2P), 32.9 (d, $^2J_{PC}$ = 1.8 Hz, CH_2 cod) ppm. $^{31}P\{^1H\}$ NMR (121.5 MHz, $CDCl_3$): δ 24.2 (s) ppm. ^{19}F NMR (282.4 MHz, $CDCl_3$): –62.8 ppm. Anal. Calcd for $C_{58}H_{41}BF_{24}IrN_2P$: C, 47.85; H, 2.84; N, 1.92. Found: C, 47.89; H, 2.86; N, 1.82.

6.5.8 Determination of the Crystal Structures

Diffraction data were collected at 173(2)K, on a Kappa CCD diffractometer using graphite-monochromated Mo-Kα radiation (λ = 0.71073 Å).[28] The structures were solved by direct methods using the SHELX 97 software,[28] and the refinement was by full-matrix least squares on F^2. A MULTISCAN absorption correction was applied on **7**.[29] All non-hydrogen atoms were refined anisotropically. The hydrogen atoms were introduced into the geometrically calculated positions (SHELXS-97 procedures) and refined *riding* on the corresponding parent atoms. In **7**, six CF_3 groups of the anion were found disordered. These groups were refined as disordered in two positions having the carbon atom in common, and with constrained anisotropic parameters.

Acknowledgements

We thank the Centre National de la Recherche Scientifique (CNRS), the Ministère de l'Enseignement Supérieur et de la Recherche (Paris) and the Université de Strasbourg for support, the French Embassy in Beijing for a doctoral grant to S. L. and Professor Wen-Hua Sun (Institute of Chemistry, Chinese Academy of Sciences, Beijing) for support. We are grateful to Drs Lydia Brelot (X-ray structure analyses) and Roberto Pattacini (X-ray structure analyses and discussions), Dr Weiwei Zuo for experimental assistance, and Dr Joaquín López-Serrano for helpful discussions on NMR analyses.

for references, see page 108

Notes and References

1. (a) Helmchen, G.; Pfaltz, A. *Acc. Chem. Res.* **2000**, *33*, 336-345; (b) Braunstein, P.; Naud, F. *Angew. Chem., Int. Ed.* **2001**, *40*, 680-699; (c) Rechavi, D.; Lemaire, M. *Chem. Rev.* **2002**, *102*, 3467-3493; (d) McManus, H. A.; Guiry, P. J. *Chem. Rev.* **2004**, *104*, 4151-4202; (e) Desimoni, G.; Faita, G.; Jøensen, K. A. *Chem. Rev.* **2006**, *106*, 3561-3651; (f) Braunstein, P.; Graiff, C.; Naud, F.; Pfaltz, A.; Tiripicchio, A. *Inorg. Chem.* **2000**, *39*, 4468-4475; (g) Speiser, F.; Braunstein, P.; Saussine, L. *Acc. Chem. Res.* **2005**, *38*, 784-793; (h) Hou, J.; Sun, W.-H.; Zhang, S.; Ma, H.; Deng, Y.; Lu, X. *Organometallics* **2006**, *25*, 236; (i) Braunstein, P. *Chem. Rev.* **2005**, *106*, 134-159; (j) Maggini, S. *Coord. Chem. Rev.* **2009**, *253*, 1793-1832; (k) Espinet, P.; Soulantica, K. *Coord. Chem. Rev.* **1999**, *193-195*, 499-556.
2. (a) Braunstein, P.; Fryzuk, M. D.; Naud, F.; Rettig, S. J. *J. Chem. Soc., Dalton Trans.* **1999**, 589-594; (b) Braunstein, P.; Naud, F.; Pfaltz, A.; Rettig, S. J. *Organometallics* **2000**, *19*, 2676-2683; (c) Braunstein, P.; Naud, F.; Graiff, C.; Tiripicchio, A. *Chem. Commun.* **2000**, 897-898; (d) Braunstein, P.; Naud, F.; Rettig, S. J. *New J. Chem.* **2001**, *25*, 32-39.
3. (a) Kermagoret, A.; Braunstein, P. *Organometallics* **2008**, *27*, 88-99; (b) Kermagoret, A.; Tomicki, F.; Braunstein, P. *Dalton Trans.* **2008**, 2945-2955.
4. Jie, S.; Agostinho, M.; Kermagoret, A.; Cazin, C. S. J.; Braunstein, P. *Dalton Trans.* **2007**, 4472-4482.
5. (a) Braunstein, P.; Fryzuk, M. D.; Le Dall, M.; Naud, F.; Rettig, S.; Speiser, F. *Dalton Trans.* **2000**, 1067-1074; (b) Agostinho, M.; Braunstein, P.; Welter, R. *Dalton Trans.* **2007**, 759-770.
6. Braunstein, P.; Clerc, G.; Morise, X. *New J. Chem.* **2003**, *27*, 68-72.
7. Braunstein, P.; Clerc, G.; Morise, X.; Welter, R.; Mantovani, G. *Dalton Trans.* **2003**, 1601-1605.
8. Kermagoret, A.; Braunstein, P. *Dalton Trans.* **2008**, 585-587.
9. (a) Hung-Low, F.; Renz, A.; Klausmeyer, K. K. *Eur. J. Inorg. Chem.* **2009**, 2994-3002; (b) Lindner, E.; Rauleder, H.; Hiller, W. *Z. Naturforsch., B: Anorg. Chem., Org. Chem.* **1983**, *38B*, 417-425.
10. Slugovc, C.; Padilla-Martinez, I.; Sirol, S.; Carmona, E. *Coord. Chem. Rev.* **2001**, *213*, 129-157.
11. Goldman, A. S.; Roy, A. H.; Huang, Z.; Ahuja, R.; Schinski, W.; Brookhart, M. *Science* **2006**, *312*, 257-261.
12. Whited, M. T.; Zhu, Y.; Timpa, S. D.; Chen, C.-H.; Foxman, B. M.; Ozerov, O. V.; Grubbs, R. H. *Organometallics* **2009**, *28*, 4560-4570.
13. Peloso, R.; Pattacini, R.; Cazin, C. S. J.; Braunstein, P. *Inorg. Chem.* **2009**, *48*, 11415-11424.
14. Linert, W.; Fukuda, Y.; Camart, A. *Coord. Chem. Rev.* **2001**, *218*, 113-152.
15. (a) Pfeffer, M.; Braunstein, P.; Dehand, J. *Spectrochim. Acta* **1974**, *30A*, 341-355; (b) Kong, P.-C.; Rochon, F. D. *Can. J. Chem.* **1981**, *59*, 3293-3296.
16. Braunstein, P.; Naud, F.; Dedieu, A.; Rohmer, M.-M.; DeCian, A.; Rettig, S. J. *Organometallics* **2001**, *20*, 2966-2981.
17. Appelton, T. G.; Clark, H. C.; Manzer, L. E. *Coord. Chem. Rev.* **1973**, *10*, 335-442.
18. Morita, H.; Shimomura, S.; Kawaguchi, S. *Bull. Chem. Soc. Jpn.* **1979**, *52*, 1838-1843.
19. Klausmeyer, K. K.; Hung, F. *Acta Crystallogr., Sect. E: Struct.* **2006**, *E62*, m2415-m2416.
20. Camerano, J. A.; Casado, M. A.; Ciriano, M. A.; Tejel, C.; Oro, L. A. *Chem. Eur. J.* **2008**, *14*, 1897-1905.
21. Schramm, K. D.; Tulip, T. H.; Ibers, J. A. *Inorg. Chem.* **1980**, *19*, 3183-3185.
22. (a) Churchill, M. R.; Bezman, S. A. *Inorg. Chem.* **1972**, *11*, 2243-2247; (b) Churchill, M. R.; Bezman, S. A. *Inorg. Chem.* **1973**, *12*, 260-265; (c) Frazier, J. F.; Merola, J. S. *Polyhedron* **1992**, *11*, 2917-2927.
23. Xiao, L.; Gao, R.; Zhang, M.; Li, Y.; Cao, X.; Sun, W.-H. *Organometallics* **2009**, *28*, 2225-2233.
24. Anderson, G. K.; Lin, M. *Inorg. Synth.* **1990**, *28*, 60-63.
25. Yakelis, N. A.; Bergman, R. G. *Organometallics* **2005**, *24*, 3579-3581.
26. Wayland, B. B.; Schramm, R. F. *Inorg. Chem.* **1969**, *8*, 971-976.
27. Hartley, F. R. The chemistry of Platinum and Palladium; Elsevier: Amsterdam, **1973**.
28. Bruker-Nonius *Kappa CCD Reference Manual, Nonius BV, The Netherlands, 1998; Sheldrick, G. M. SHELXL-97, Program for the refinement of crystal structures, University of Göttingen, Germany, 1997.*
29. Spek, L. *J. Appl. Crystallogr., 2003, 36, 7; B. Blessing, Acta Crystallogr., Sect. A: Found. Crystallogr.,* 1995*, A51,* 33-38.

for references, see page 108

CHAPITRE VII

Electrophilic Activation and the Formation of An Unusual Tl^{+}/Cr^{3+} Tetranuclear Ion-complex Adduct

SHAOFENG LIU,[a,b] RICCARDO PELOSO,[a,c] ROBERTO PATTACINI[a] and PIERRE BRAUNSTEIN*[a]

[a] *Laboratoire de Chimie de Coordination, Institut de Chimie (UMR 7177 CNRS), Université de Strasbourg, 4 rue Blaise Pascal, F-67081 Strasbourg Cedex, France.*
[b] *Key Laboratory of Engineering Plastics and Beijing National Laboratory for Molecular Sciences, Institute of Chemistry, Chinese Academy of Sciences, Beijing 100190, China.*
[c] *Current address: Instituto de Investigaciones Químicas - Departamento de Química Inorgánica, Universidad de Sevilla - Consejo Superior de Investigaciones Científicas, Avda. Américo Vespucio 49, Isla de la Cartuja, 41092 Sevilla, Spain.*

This Chapter has been published in *Dalton Trans.*, **2010**, *39*, 7881-7883

Contributions from the various co-authors: We are grateful to Dr. Riccardo Peloso for discussions and assistance, Dr. Roberto Pattacini for X-ray structure analyses and discussions, Professor Pierre Braunstein for discussions and supervision.

Résumé du Chapitre VII

La réaction de $TlPF_6$ avec le complexe du Cr(III) *fac*-[$CrCl_3$(NPN)] (NPN = bis(2-picolyl)phényl phosphine) ne conduit pas à la précipitation attendue de TlCl mais à l'addition du cation Tl^+ au fragment $CrCl_3$. Ceci conduit à un adduit pseudo-dimère qui possède à l'état solide une structure tétranucléaire centrosymétique inhabituelle.

7.1 Abstract of Chapter VII

Reaction of $TlPF_6$ with the Cr(III) complex *fac*-[$CrCl_3$(NPN)] (NPN = bis(2-picolyl)phenyl phosphine) did not lead to precipitation of TlCl but rather to addition of the Tl^+ cation to the $CrCl_3$ moiety, which resulted in a pseudo-dimeric adduct which has an unusual tetranuclear centrosymmetric structure in the solid-state.

7.2 Introduction

The strong propensity of $TlPF_6$ to react with halide-containing coordination and organometallic complexes with formation of cationic complexes and poorly soluble TlX salts[1] is often exploited to enhance the electrophilic properties of the metal centre and hence its reactivity.[2] Moreover, compared with analogous reagents such as $AgPF_6$,[3] $TlPF_6$ does not readily undergo redox reactions and is therefore particularly convenient in inorganic and organometallic synthesis. However, coordination of a Tl^+ cation to a metal-bound halide has been reported in some cases.[4] We recently found that the reaction of the Pt(II) complex [Pt(CH_2Ph)Cl(PCH_2-ox)] (PCH_2-ox = κ^2-*P,N*-(oxazolinylmethyl)diphenylphosphine) with $TlPF_6$ selectively afforded an unexpected bimetallic complex containing a new benzyl-stabilized Tl-Pt bond while retaining the Pt-Cl bond.[5] In view of the considerable interest for the study of Cr-based homogeneous catalysts for ethylene oligomerization and polymerization,[6] triggered by the pioneering discoveries at Union Carbide[6a] and Phillips Petroleum,[6b] we decided to prepare Cr(III) complexes with hybrid ligands and during attempts to form a cationic complex by chloride abstraction, we unexpectedly obtained a novel Cr(III)/Tl(I) ion-complex adduct exhibiting unusual interactions involving the Tl^+ cation of possible relevance to catalysts activation steps.

7.3 Results and Discussion

The 1:1 reaction between [$CrCl_3(THF)_3$] and bis(2-picolyl)phenylphosphine (NPN)[7] afforded an air-stable, blue complex in high yield. It was characterized by IR spectroscopy, elemental analysis and X-ray diffraction and identified as the mononuclear complex *fac*-[$CrCl_3$(NPN)] (**1**). Its crystal structure has been determined (see ESI)† for comparison with that of the acetonitrile adduct [$CrCl_3$(NPN)]·MeCN.[8] Abstraction of a chloride anion from **1** in the absence of a coordinating solvent was expected to induce the formation of a cationic, Cl-bridged dinuclear complex of the type generated in catalytic ethylene oligomerization from similar Cr(III) complexes and $AlEt_2Cl$.[9] A mononuclear cationic Cr(III) complex would most likely result from reaction with $TlPF_6$ in the presence of a donor solvent.[10] We thus reacted complex **1** with one equivalent of $TlPF_6$ in dichloromethane and observed a colour change from blue to purple. After filtration, a purple solid was isolated which showed in the FTIR spectrum a very strong absorption at 880 cm^{-1} due to the P-F stretching vibration of the PF_6^- anion.

for references, see page 114

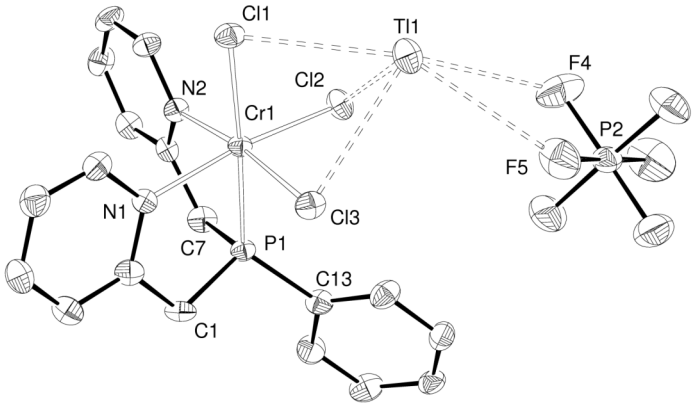

Fig. 1 ORTEP of complex **2** (asymmetric unit) with ellipsoids drawn at the 50% probability level. Selected bond distances (Å) and angles (deg): Cr1-N1 2.122(5), Cr1-N2 2.124(5), Cr1-P1 2.3512(16), Cr1-Cl1 2.3628(16), Cr1-Cl2 2.3106(17), Cr1-Cl3 2.3280(16), Tl1-Cl1 3.1816(15), Tl1-Cl2 3.1519(15), Tl1-Cl3 3.1381(15), Tl1-F4 3.258(6), Tl1-F5 3.223(5), Cr1-Cl1-Tl1 84.20(5), Cr1-Cl2-Tl1 85.72(5), Cr1-Cl3-Tl1 85.76(5).

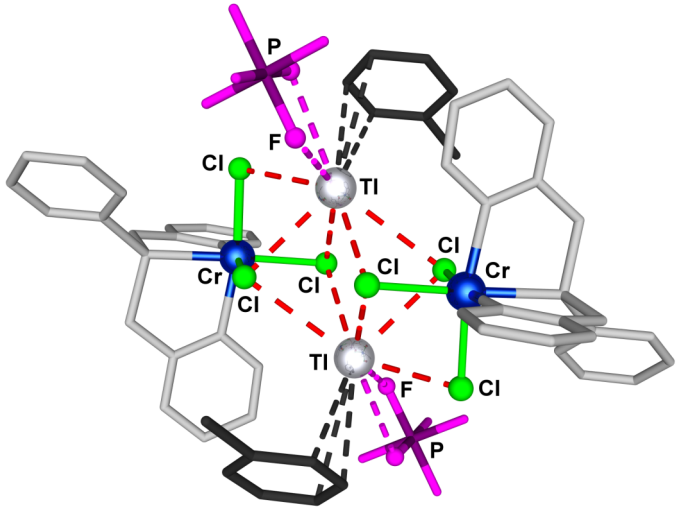

Fig. 2 View of the crystal structure of **2**, showing the centrosymmetric pseudo-dimer [**1**·(TPF_6)]$_2$. Intermolecular Ph-P fragments interacting with the pseudo-dimer are depicted in black. (symmetry operation generating equivalent atoms: -x, -y, -z).

Single crystals of this purple compound, **2**, were grown by layering Et_2O on a concentrated acetone solution of the complex and were analysed by X-ray diffraction. It is a bimetallic adduct which exhibits the unexpected structure depicted in Fig. 1. The crystal formula is $[CrCl_3(NPN)TlPF_6]$, corresponding to a 1:1 stoichiometry between **1** and $TlPF_6$. In the solid-state, **2** is best described as a centrosymmetric tetranuclear compound containing two Tl^+ cations, two PF_6^- anions, and two neutral *fac*-$[CrCl_3(NPN)]$ complexes (Fig. 2).

Each Tl cation shows contacts with: a) three chlorides from one molecule of **1** [Tl···Cl distances: 3.1816(15), 3.1519(15) and 3.1381(15) Å]; b) two chlorides from the centro symmetrically generated **1** [3.303(14) and 3.407(15) Å]; and c) with two fluorine from the PF_6 anion [3.258(6) and 3.223(5) Å]. In addition, the pseudo-dimer interacts with adjacent molecules of **1**, through long intermolecular Tl···C contacts [shortest: 3.459(7) Å].

This pseudo-dimer **2** can be thus described, in the solid state, as a tetranuclear, bimetallic Cr_2Tl_2

for references, see page 114

ion-complex, containing a $Cr_2Tl_2Cl_6$ core, showing four pseudo μ_3-Cl and two pseudo μ-Cl ligands. The $Cr_2Tl_2Cl_6$ core shares similarities with that of $[(Cp^{Ph}CrCl_3)_2Tl_2]$ (Cp^{Ph} = pentaphenyl-cyclopentadienyl), prepared by addition of TlCl to $[(Cp^{Ph}Cr(\mu\text{-}Cl)Cl]_2$.[4b] The $[(Cp^{Ph}CrCl_3)_2Tl_2]$ structure showed Tl···Cl separations similar to those in **2** and it was further stabilized by Tl···$ClCH_2Cl$ (from dichloromethane) and Tl···C (from one of the phenyl groups) contacts, in parallel to the Tl···F_2PF_4 and Tl···C ones observed in **2**.

Three of the Tl···Cl distances shown in Fig.1 compare well with the interionic distance found in the NaCl form of TlCl (3.15 Å), while the remaining two are similar to that in its CsCl form (3.32 Å).[4a] The Tl···F separations are slightly longer than those observed in $TlPF_6$ [3.18(4) Å].[11] The Tl···C contacts are slightly shorter than the sum of the van der Waals radii of Tl^+ and an aromatic ring (3.73 Å).[4d,12] The Tl···Cr separation of 3.7665(8) Å is too long for a direct metal-metal interaction.

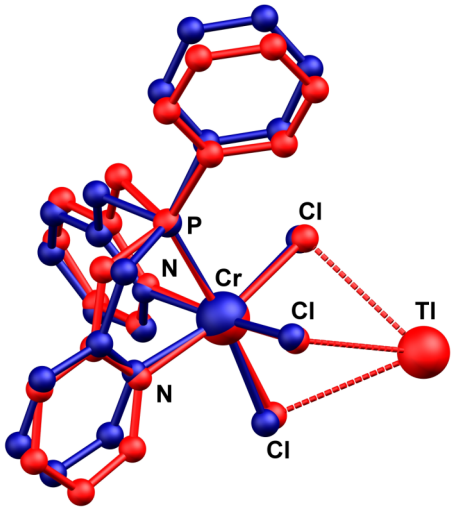

Fig. 3 Comparison between the structures in the crystals of **1** (blue) in **2** (red) illustrating the slight closing of the $CrCl_3$ cone angle in the *fac*-$[CrCl_3(NPN)]$ moiety of the latter. The P and Cr atom pairs are coincident. For **2**, the thallium cation is also shown.

Although the structure of the *fac*-$[CrCl_3(NPN)]$ unit in **2** is similar to that of pure **1**, interesting differences are observed (Fig. 3). Along with slight changes in the NPN ligand arrangement, the three chloride atoms in **2** are slightly deviated toward the Tl^+ cation, consistently with an attractive interaction (see ESI for a detailed comparison).

To the best of our knowledge, the bimetallic complex **2** is the first reported adduct of $TlPF_6$ to a chromium complex. It is stable in dichloromethane, but slowly converts into unidentified products in acetone or acetonitrile with precipitation of TlCl. Similarly, $[(P(CH_2C_2PPh_2)_3RuH(\mu\text{-}Cl)Tl]_2^{2+}$ and $[([9]aneS_3)(PPh_3)Ru(\mu\text{-}Cl)_2Tl]_2^{2+}$ were found to decompose in O-coordinating solvents.[4j,k]

After activation with MAO, **1** was active for ethylene oligomerization (2900 $g\cdot g(Cr)^{-1}\cdot h^{-1}$), producing a mixture of butenes (12%; of which 99% α-butene), hexenes (22%; 88% α-hexene), octenes (17%; 87% α-octene), decenes (9%; 72% α-decene) and higher α-olefins. Similar

for references, see page 114

activities and product distribution were observed for the **2**/MAO system, suggesting that under these catalytic conditions, the Cr(III)/Tl(I) pseudodimer **2** may be not persistent.

7.4 Conclusions

Our results emphasize the care to be exerted when using common halide abstractors to generate *in situ* reactive species since they may not always fulfil their anticipated function. The fact that Tl^+ cation forms bimetallic compounds instead of removing a halide anion with precipitation of TlX may be explained by the formation of multiple stabilizing interactions between the Tl^+ cation and its direct environment. This applies to both stoichiometric and catalytic applications. Interestingly, a Cr-Cl-Al linkage was recently evidenced in an adduct of $AlMe_3$ to a $[Cr(NNN)MeCl_2]$ complex and was suggested to represent an early stage of the catalyst activation.[6v]

Acknowledgement

We thank the Centre National de la Recherche Scientifique (CNRS), the Ministère de l'Enseignement Supérieur et de la Recherche (Paris) and the Université de Strasbourg for support, the French Embassy in Beijing for a doctoral grant to S. L. and Prof. Wen-Hua Sun (Institute of Chemistry, Chinese Academy of Sciences, Beijing) for support. We are grateful to Mr. Marc Mermillon-Fournier for technical assistance.

Notes and References

† Electronic Supplementary Information (ESI) available: ORTEP plots, experimental details. CCDC 771851 and 771852. For ESI and crystallographic data in CIF or other electronic format, see DOI: 10.1039/b000000x/

‡ Synthesis of *fac*-$[CrCl_3(NPN)]$ (**1**). Solid $[CrCl_3(THF)_3]$ (0.438 g, 1.17 mmol) was added to a solution of NPN (0.342 g, 1.17 mmol) in dichloromethane (20 mL) to give a blue suspension, which was stirred overnight. The solvent was removed under vacuum affording a blue powder which was washed with diethyl ether (2 × 20 mL) and dried *in vacuo* overnight (Yield: 0.508 g, 1.12 mmol, 96%). Selected IR absorptions (pure, diamond ATR): 1606s, 1563w, 1485s, 1436s, 1380w, 1314w, 1264w, 1163w, 1110m, 1061w, 1020m, 864s, 808w, 767m, 743m, 689m cm^{-1}.[8]

Synthesis of *fac*-$[CrCl_3(NPN)TlPF_6]$ (**2**). Solid $TlPF_6$ (0.116 g, 0.333 mmol) was added to a blue suspension of *fac*-$[CrCl_3(NPN)]$ (0.150 g, 0.333 mmol) in dichloromethane (10 mL). A purple suspension slowly formed, which was stirred overnight. The volume of the solution was reduced to 5 mL by evaporation under reduced pressure. After filtration, a purple solid was obtained (0.260 g, 0.325 mmol, 98%). Selected IR absorptions (pure, diamond ATR): 1611m, 1570w, 1487m, 1438m, 1373w, 1317w, 1171w, 1111w, 1066w, 1026m, 881vs, 789w, 752m, 692w cm^{-1}. Anal. Calcd for $C_{18}H_{17}Cl_3CrF_6N_2P_2Tl$: C, 27.02; H, 2.14; N, 3.50. Found: C, 27.22; H, 2.57; N, 3.44.

§ Crystal data for **1**: $C_{18}H_{17}Cl_3CrN_2P$, M = 450.66, monoclinic, a = 14.2128(5) Å, b = 13.4012(5) Å, c =

for references, see page 114

21.8650(7) Å, β = 113.705(2)°, V = 3813.2(2) Å^3, T = 173(2) K, space group $P2_1/c$, Z = 8, μ = 1.108 mm^{-1}, 15041 reflections measured, 8300 independent reflections (R_{int} = 0.0608). The final R_1 values were 0.0483 ($I > 2\sigma(I)$). The final $wR(F^2)$ values were 0.1057 ($I > 2\sigma(I)$). The final R_1 values were 0.1178 (all data). The final $wR(F^2)$ values were 0.1233 (all data). The goodness of fit on F^2 was 0.954.

Crystal data for **2**: $C_{18}H_{17}Cl_3CrN_2P{\cdot}F_6P{\cdot}Tl$, M = 800.00, triclinic, a = 8.9323(4) Å, b = 12.0205(5) Å, c = 12.8804(4) Å, α = 72.356(2)°, β = 71.627(2)°, γ = 69.739(2)°, V = 1201.70(8) Å^3, T = 173(2) K, space group P-1, Z = 2, μ = 7.672 mm^{-1}, 9090 reflections measured, 5504 independent reflections (R_{int} = 0.0279). The final R_1 values were 0.0372 ($I > 2\sigma(I)$). The final $wR(F^2)$ values were 0.1115 ($I > 2\sigma(I)$). The final R_1 values were 0.0469 (all data). The final $wR(F^2)$ values were 0.1247 (all data). The goodness of fit on F^2 was 1.088.

¥ A 175-mL stainless steel dry autoclave, equipped with a glass container (125 mL) to protect the inner walls from corrosion, was charged with the desired amount of precatalyst (**1** or **2**; $4{\cdot}10^{-5}$ mol in 12 mL of PhCl), then cocatalyst (MAO; $12{\cdot}10^{-3}$ mol, in 8 mL of toluene; 300:1 Al/Cr), under stirring. The reactor was then pressurized with 10 bar of ethylene (the pressure was maintained during the experiments via a continuous feed of ethylene from a reserve bottle placed on a balance to allow continuous monitoring of the ethylene uptake) and heated to reach 80 °C. After 90 min, the reactor was cooled down with an acetone-dry ice bath and when the inner temperature reached ca. 0 °C, the cooling bath was removed allowing the temperature to slowly rise to 18 °C. The pressure was released and the gaseous phase was transferred into a 10 L polyethylene tank filled with water. An aliquot of this gaseous phase was transferred into a Schlenk flask, previously evacuated, for GC analysis (Thermoquest GC8000 Top Series gas chromatograph using a HP Pona column, 50 m, 0.2 mm diameter, 0.5 µm film thickness). The products in the glass container were hydrolyzed in situ by the addition of ethanol (10 mL), the container was weighted, its content was transferred into a Schlenk flask, and separated from the metal complexes and wax by trap-to-trap evaporation (20 °C, 0.8 mBar) into a second Schlenk flask previously immersed in liquid nitrogen in order to avoid any loss of product. An aliquot of the liquid fraction was used for GC analysis. The wax was quenched with 5% hydrochloric acid in ethanol, washed with ethanol and dried under vacuum at 60 °C to constant weight.

1. Sasaki, Y.; Takizawa, M.; Umemoto, K.; Matsuura, N. *Bull. Soc. Chim. Japan* **1981**, *54*, 65-68.
2. (a) Kuang, S.-M.; Fanwick, P. E.; Walton, R. A. *Inorg. Chem.* **2002**, *41*, 147-151; (b) Antiñolo, A.; Carrillo, F.; Chaudret, B.; Fajardo, M.; García-Yuste, S.; Lahoz, F. J.; Lanfranchi, M.; López, J. A.; Otero, A.; Pellinghelli, M. A. *Organometallics* **1995**, *14*, 1297-1301; (c) Filippou, A. C.; Grünleitner, W. *J. Organomet. Chem.* **1989**, *378*, 387-399; (d) Bruce, M. R. M.; Tyler, D. R. *Organometallics* **1985**, *4*, 528-533.
3. Barron, P. F.; Dyason, J. C.; Healy, P. C.; Engelhardt, L. M.; Skelton, B. W.; White, A. H. *J. Chem. Soc., Dalton Trans.* **1986**, 1965-1970.
4. (a) Paredes, P.; Díez, J.; Gamasa, M. P. *Organometallics* **2008**, *27*, 2597-2607; (b) Davis, K. B.; Harris, T. D.; Castellani, M. P.; Golen, J. A.; Rheingold, A. L. *Organometallics* **2007**, *26*, 4843-4845; (c) Szymczak, N. K.; Han, F.; Tyler, D. R. *Dalton Trans.* **2004**, 3941-3942; (d) Kunrath, F. A.; Casagrande, O. L.; Toupet, L.; Carpentier, J. F. *Eur. J. Inorg. Chem.* **2004**, 4803-4806; (e) Drouin, S. D.; Foucault, H. M.; Yap, G. P. A.; Fogg, D. E. *Organometallics* **2004**, *23*, 2583-2590; (f) Devic, T.; Batail, P.; Fourmigué, M.; Avarvari, N. *Inorg. Chem.* **2004**, *43*, 3136-3141; (g) Becker, C.; Kieltsch, I.; Broggini, D.; Mezzetti, A. *Inorg. Chem.* **2003**, *42*, 8417-8429; (h) Barthazy, P.; Togni, A.; Mezzetti, A. *Organometallics* **2001**, *20*, 3472-3477; (i) Kahwa, I. A.; Miller, D.; Mitchel, M.; Fronczek, F. R.; Goodrich, R. G.; Williams, D. J.; O'Mahoney, C. A.; Slawin, A. M. Z.; Ley, S. V.; Groombridge, C. J. *Inorg. Chem.* **1992**, *31*, 3963-3970; (j) Blake, A. J.; Christie, R. M.; Roberts, Y. V.; Sullivan, M. J.; Schröder, M.; Yellowlees, L. J. *J. Chem. Soc., Chem. Commun.* **1992**, 848-850; (k) Bianchini, C.; Masi, D.; Linn, K.; Mealli, C.; Peruzzini, M.; Zanobini, F. *Inorg. Chem.* **1992**, *31*, 4036-4037; (l) Ezomo, O. J.; Mingos, D. M. P.; Williams, I. D. *J. Chem. Soc., Chem. Commun.* **1987**, 924-925.

for references, see page 114

5. Oberbeckmann-Winter, N.; Braunstein, P.; Welter, R. *Organometallics* **2004**, *23*, 6311-6318.
6. (a) Manyik, R. M.; Walker, W. E.; Wilson, T. P. US3300458 (to Union Carbide Corporation), **1967**; (b) Reagan, W. K. EP0417477 (to Phillips Petroleum Company), **1991**; (c) Bazan, G. C.; Rogers, J. S.; Fang, C. C. *Organometallics* **2001**, *20*, 2059-2064; (d) Gibson, V. C.; Newton, C.; Redshaw, C.; Solan, G. A.; White, A. J. P.; Williams, D. J. *J. Chem. Soc., Dalton Trans.* **2002**, 4017-4023; (e) McGuinness, D. S.; Wasserscheid, P.; Keim, W.; Morgan, D.; Dixon, J. T.; Bollmann, A.; Maumela, H.; Hess, F.; Englert, U. *J. Am. Chem. Soc.* **2003**, *125*, 5272-5273; (f) McGuinness, D. S.; Wasserscheid, P.; Keim, W.; Hu, C. H.; Englert, U.; Dixon, J. T.; Grove, C. *Chem. Commun.* **2003**, 334-335; (g) Morgan, D. H.; Schwikkard, S. L.; Dixon, J. T.; Nair, J. J.; Hunter, R. *Adv. Synth. Catal.* **2003**, *345*, 939-942; (h) Bollmann, A.; Blann, K.; Dixon, J. T.; Hess, F. M.; Killian, E.; Maumela, H.; McGuinness, D. S.; Morgan, D. H.; Neveling, A.; Otto, S.; Overett, M.; Slawin, A. M. Z.; Wasserscheid, P.; Kuhlmann, S. *J. Am. Chem. Soc.* **2004**, *126*, 14712-14713; (i) Dixon, J. T.; Green, M. J.; Hess, F. M.; Morgan, D. H. *J. Organomet. Chem.* **2004**, *689*, 3641-3668; (j) Agapie, T.; Schofer, S. J.; Labinger, J. A.; Bercaw, J. E. *J. Am. Chem. Soc.* **2004**, *126*, 1304-1305; (k) Overett, M. J.; Blann, K.; Bollmann, A.; Dixon, J. T.; Haasbroek, D.; Killian, E.; Maumela, H.; McGuinness, D. S.; Morgan, D. H. *J. Am. Chem. Soc.* **2005**, *127*, 10723-10730; (l) Agapie, T.; Day, M. W.; Henling, L. M.; Labinger, J. A.; Bercaw, J. E. *Organometallics* **2006**, *25*, 2733-2742; (m) Schofer, S. J.; Day, M. W.; Henling, L. M.; Labinger, J. A.; Bercaw, J. E. *Organometallics* **2006**, *25*, 2743-2749; (n) Jabri, A.; Temple, C.; Crewdson, P.; Gambarotta, S.; Korobkov, I.; Duchateau, R. *J. Am. Chem. Soc.* **2006**, *128*, 9238-9247; (o) Wass, D. F. *Dalton Trans.* **2007**, 816-819; (p) McGuinness, D. S.; Overett, M.; Tooze, R. P.; Blann, K.; Dixon, J. T.; Slawin, A. M. Z. *Organometallics* **2007**, *26*, 1108-1111; (q) Zhang, J.; Braunstein, P.; Hor, T. S. A. *Organometallics* **2008**, *27*, 4277-4279; (r) Jabri, A.; Mason, C. B.; Sim, Y.; Gambarotta, S.; Burchell, T. J.; Duchateau, R. *Angew. Chem. Int. Ed.* **2008**, *47*, 9717-9721; (s) Jie, S.; Pattacini, R.; Rogez, G.; Loose, C.; Kortus, J.; Braunstein, P. *Dalton Trans.* **2009**, 97-105; (t) Klemps, C.; Payet, E.; Magna, L.; Saussine, L.; Le Goff, X. F.; Le Floch, P. *Chem. Eur. J.* **2009**, *15*, 8259-8268; (u) Vidyaratne, I.; Nikiforov, G. B.; Gorelsky, S. I.; Gambarotta, S.; Duchateau, R.; Korobkov, I. *Angew. Chem. Int. Ed.* **2009**, *48*, 6552-6556; (v) Zhang, J.; Li, A.; Hor, T. S. A. *Organometallics* **2009**, *28*, 2935-2937; (w) Rozenel, S. S.; Chomitz, W. A.; Arnold, J. *Organometallics* **2009**, *28*, 6243-6253; (x) Gao, R.; Liang, T.; Wang, F.-S.; Sun, W.-H. *J. Organomet. Chem.* **2009**, *694*, 3701-3707; (y) McGuinness, D. S. *Organometallics* **2009**, *28*, 244-248.
7. Liu, S.; Peloso, R.; Braunstein, P. *Dalton Trans.* **2010**, *39*, 2563-2572.
8. Klausmeyer, K. K.; Hung, F. *Acta Crystallogr. Sect. E: Struct. Rep. Online* **2006**, *E62*, M2415-M2416.
9. Temple, C.; Jabri, A.; Crewdson, P.; Gambarotta, S.; Korobkov, I.; Duchateau, R. *Angew. Chem. Int. Ed.* **2006**, *45*, 7050-7053.
10. Thomas, B. J.; Theopold, K. H. *J. Am. Chem. Soc.* **1988**, *110*, 5902-5903.
11. Goreshnik, E.; Mazej, Z. *Solid State Sciences* **2008**, *10*, 303-306.
12. (a) Pauling, L. C. The Nature of the Chemical Bond; Cornell University Press: Ithaca, NY, **1960**; (b) Bondi, A. *J. Phys. Chem.* **1964**, *68*, 441-451.

for references, see page 114

CHAPITRE VIII

Reactions between An Ethylene Oligomerization Cr(III) Pre-catalyst and Al-based Activators: Alkyl and Cationic Complexes with A Tridentate *N,P,N* Ligand

SHAOFENG LIU,[a,b] ROBERTO PATTACINI,[a] PIERRE BRAUNSTEIN*[a]

[a] *Laboratoire de Chimie de Coordination, Institut de Chimie (UMR 7177 CNRS), Université de Strasbourg, 4 rue Blaise Pascal, CS 90032, F-67081 Strasbourg Cedex, France.*

[b] *Key Laboratory of Engineering Plastics and Beijing National Laboratory for Molecular Sciences, Institute of Chemistry, Chinese Academy of Sciences, Beijing 100190, China.*

This Chapter has been accepted for publication in *Organometallics* (**DOI:** 10.1021/om200243a)

Contributions from the various co-authors: Dr. Roberto Pattacini performed the X-ray structure analyses and contributed to the discussions and Professor Pierre Braunstein provided supervision and discussions and contributed to the preparartion of the manuscript. I am most grateful to them.

Résumé du Chapitre VIII

La réaction du complexe de Cr(III) *fac*-[Cr(NPN)Cl_3] (**1**) (NPN = bis(2-picolyl)phénylphosphine) avec du MAO (méthylalumoxane) conduit à une méthylation partielle pour donner le complexe *fac*-[Cr(NPN)$Cl_{2.23}Me_{0.77}$] (**2**) alors que la réaction avec $AlMe_3$ dans le toluène donne lieu à la formation d'un complexe dicationique dinucléaire à double ponts chlorure [{*fac*-Cr(NPN)Me(μ-Cl)}$_2$][$AlMe_xCl_{4-x}$]$_2$ (**3**·[$AlMe_xCl_{4-x}$]$_2$). Le complexe *fac*-[Cr(NPN)Cl_2Et] (**4**) a été isolé en bons rendements à partir de la réaction de **1** avec $AlEt_3$; il contient un exemple rare de fonction Cr(III)-Et. Par réaction de **1** with $EtAlCl_2$, nous avons obtenu et caractérisé le complexe dinucléaire du Cr(III) [{*fac*-Cr(NPN)}$_2$(μ-Cl)$_3$][$AlCl_4$]$_3$ (**5**·[$AlCl_4$]$_3$) qui contient trois ponts chlorures. Une fois activé par le MAO et mis dans des conditions comparables, les complexes **1-5** montrent des propriétés catalytiques semblables mais dans le cas du système **4**/MAO, l'oligomère principal est le 1-décène. Les complexes alkyles neutres **2** et **4** et les complexes cationiques **3** et **5** n'ont pas montré d'activité catalytique pour l'oligomérisation de l'éthylène en absence de MAO. Les structures cristallines des complexes **2**, **3**·[$AlMe_xCl_{4-x}$]$_2$, **4** et **5**·[$AlCl_4$]$_3$ ont été déterminées par diffraction des rayons X.

8.1 Abstract of Chapter VIII

To gain a deeper knowledge of the nature of the species formed *in situ* by reaction of a catalyst precursor complex and typical cocatalysts used for ethylene oligomerization or polymerization, the Cr(III) complex *fac*-[Cr(NPN)Cl_3] (**1**) (NPN = bis(2-picolyl)phenylphosphine) was reacted with MAO and partial methylation to give the mononuclear complex *fac*-[Cr(NPN)$Cl_{2.23}Me_{0.77}$] (**2**) was observed, whereas reaction with $AlMe_3$ in toluene led to partial halide abstraction and produced the dinuclear, chloride-bridged dicationic complex [{*fac*-Cr(NPN)Me(μ-Cl)}$_2$][$AlMe_xCl_{4-x}$]$_2$ (**3**·[$AlMe_xCl_{4-x}$]$_2$), in which the metal centers are bridged by two chloride ligands. The complex *fac*-[Cr(NPN)Cl_2Et] (**4**) was isolated in high yield from the reaction of **1** with $AlEt_3$ and contains a rare example of Cr(III)-Et function. Upon treatment of **1** with $EtAlCl_2$, the dinuclear Cr(III) complex [{*fac*-Cr(NPN)}$_2$(μ-Cl)$_3$][$AlCl_4$]$_3$ (**5**·[$AlCl_4$]$_3$) was obtained which contains three bridging chlorides. Thus, under the conditions investigated, MAO and $AlEt_3$ behaved as alkylation agents, whereas $AlMe_3$ and $EtAlCl_2$ reacted as cationization agents. Once activated with MAO and under comparable conditions, **1-5** exhibited similar catalytic properties, with activities between 2700-2800 g C_2H_4/(g Cr·h), but the major oligomer produced using the **4**/MAO system was 1-decene. The neutral alkyl complexes **2** and **4** and the cationic complexes **3** and **5** did not exhibit catalytic activity for ethylene oligomerization in the absence of MAO. The structures of the complexes **2**, **3**·[$AlMe_xCl_{4-x}$]$_2$, **4** and **5**·[$AlCl_4$]$_3$ have been determined by single crystal X-ray diffraction.

8.2 Introduction

The chromium-based Phillips[1-2] and Union Carbide[3-4] heterogeneous catalysts (Cr/SiO_2) are widely applied in the large-scale industrial production of olefins and responsible for the production of more than one-third of the polyethylene sold worldwide.[5] In contrast to Ziegler-Natta catalysts,[6-7] Phillips-type catalysts can be used to produce a wide range of polyethylenes without the need for an activator.[8] However, the ill-defined nature of these paramagnetic chromium catalysts has resulted in intensive debate about the nature of the active species and the reaction mechanisms and has prompted considerable efforts to develop better defined homogenous Cr-based catalysts.[9-14] For this purpose, several Cr-based catalytic systems have been recently developed which involve multidentate ligands containing NN,[15-24] NNN,[24-48] PPP,[49-52] PP,[53-73] PNP,[74-77] SNS,[75-82] SPS,[76] PSP,[76] NSN,[34,42,83-84] NO,[21,85-89] NNO,[24,31,34,83,85,89-91] CNC,[92-95] CC,[96] CN,[93] CS,[93] NPN,[24,97-98] PNS,[75] PPO,[65,99] or N_2P_2[100-101] donor sets, with the expectation that they could allow a better control of the metal coordination sphere than monodentate ligands and that the resulting steric and electronic modifications would lead to an improvement of the performances of their complexes. In addition to their relevance to ethylene polymerization catalysis, chromium complexes have gained increasing significance as oligomerization catalysts,[8,11] in particular, with a focus on the selective trimerization[11-12,25-26,36-37,55,61,64,76,80-81,83,102-106] or

for references, see page 132

tetramerization[23,53,59,62-63,69-71,107-109] of ethylene since 1-hexene and 1-octene are used i.a. as comonomers in the production of linear low-density polyethylene (LLDPE). Rather than a conventional Cossee-Arlman linear chain growth mechanism,[110-111] the highly selective trimerization or tetramerization of ethylene is believed to involve a series of metallacycles, as first proposed by Manyik *et al.* in 1977 and then expanded by Briggs.[102,112] Chromacyclopentane and chromacycloheptane complexes have been characterized and the latter shown to readily liberate 1-hexene.[103,113] Conclusive experimental support for the metallacyclic mechanism was provided when deuterated ethylene was used for labeling studies. No H/D scrambling occurred, in contrast to conventional oligomerization involving an insertion/β-elimination mechanism.[65,93,99,108,114] However, Müller and Rosenthal have suggested an alternative mechanism for ethylene tetramerization which involves dinuclear metallacycles.[115] Olefin oligomerization via metallacycles has been recently reviewed.[113] Despite these intensive studies, considerable debate remains on the initiation step of the catalytic cycle, the chromium oxidation state in the active species, the chain growth, transfer and termination mechanisms, as well as their relationship with the catalytic activity and selectivity. It is therefore not surprising that much effort has been devoted to attempts at isolating active intermediates of the catalytic cycle. For this purpose, the chemistry of chromium complexes with aluminium-based activators (e.g. methylalumoxane (MAO), AlR_3, Et_2AlCl, $EtAlCl_2$ and $AlMe_2Cl$) has been investigated and numerous chromium alkyl and bimetallic Cr-Al complexes have been reported.[15,35,37,79,82,104-105,116]

In our ongoing research on the coordination chemistry and catalytic behavior of metal complexes bearing heterotopic ligands, we have used bis(2-picolyl)phenylphosphine (NPN),[117] a flexible, symmetric and neutral *N*,*P*,*N*-ligand containing two pyridine arms connected by a CH_2 spacer to a phosphine-type P donor, and observed that some of its complexes exhibit catalytic activity for ethylene oligomerization.[117] This ligand has also been used to form W(0),[118] Mo(0),[118] Cr(0),[118] Ag(I),[119] Cu(I),[119] Li(I),[120] Sn(II),[120] Ir(I),[121] Pd(II)[121] complexes and the Cr(III) complex *fac*-$[Cr(NPN)Cl_3]$[122] which represents a rare example of Cr-NPN system active for ethylene oligomerization in the presence of MAO as cocatalyst.[97] Reaction of this complex with 1 equiv. of $TlPF_6$ unexpectedly afforded the novel Cr(III)/Tl(I) complex ion **A** in which the unusual interactions involving the Tl^+ cation are of possible relevance to catalyst activation steps.[122]

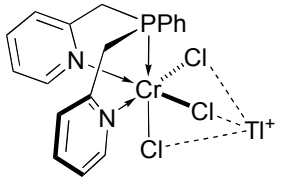

A

This result indicates that the NPN ligand system has an unanticipated ability to stabilize a Cr(III) complex in the presence of an electrophile, which was also observed for a SNS system (SNS = $RSCH_2CH_2N(H)CH_2CH_2SR$) in the presence of aluminum activators.[79] To gain a better insight into the catalytic properties and coordination chemistry of such Cr(III) complexes, we embarked on a project

for references, see page 132

aimed at isolating compounds formed by reactions between *fac*-[Cr(NPN)Cl_3] and Al-based activators and study their performances as ethylene oligomerization catalysts or pre-catalysts.

8.3 Results and Discussion

8.3.1 Reactions of complex 1 with various cocatalysts.

The complex *fac*-[Cr(NPN)Cl_3] (**1**) was prepared in high yield as reported in the literature.[97] Treatment of **1** with 10 equiv. of commercial MAO at room temperature in toluene afforded air-sensitive green crystals in 56% yield (Scheme 1).

Scheme 1. Reactions of **1** with MAO, $AlMe_3$, $AlEt_3$ or $EtAlCl_2$

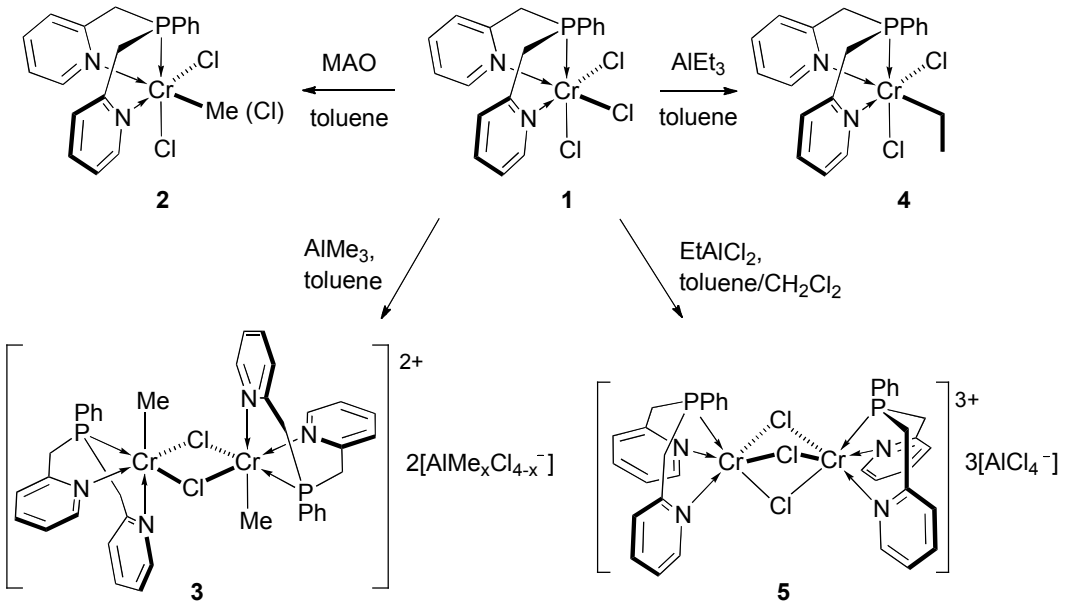

Their crystallographic analysis (Figure 1) indicated a structure and average formulation corresponding to *fac*-[Cr(NPN)$Cl_{2.23}Me_{0.77}$] (**2**). The metal center in **2** is coordinated by the tridentate NPN ligand, through the P and N atoms, in a *fac* arrangement. Two chlorides are bound in *trans* position with respect to P1 and N1, while a disorder involves the coordination site *trans* to N2.[37] This site is occupied by both a terminal chloride and a methyl group with occupancy factors of 0.23 and 0.77, respectively (see Experimental section). A detailed discussion on bond lengths is therefore not appropriate, since this disorder also affects the distances in *trans* position to the carbon atom (N2), and to a lesser extent, in *cis* positions. The strong absorptions at 333 and 314 cm^{-1} in the far-IR spectrum are tentatively assigned to ν(Cr-Cl) vibrations.

for references, see page 132

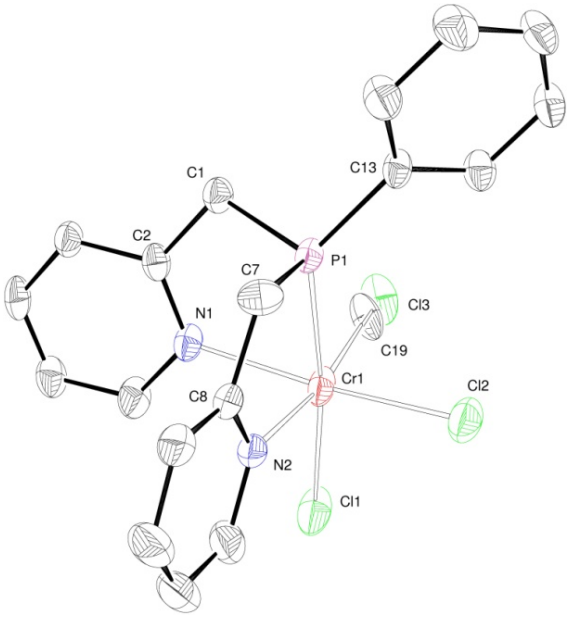

Figure 1. ORTEP of the molecular structure of **2**. Ellipsoids at 30% probability level. The coordination site trans to N2 is occupied by both Cl3 and C19 in a disordered fashion (see text). Hydrogen atoms omitted for clarity. Selected distances (Å) and angles (deg): Cr1-P1 2.3582(14), Cr1-N1 2.166(4), Cr1-N2 2.237(5), Cr1-Cl1 2.3474(16), Cr1-Cl2 2.3070(16), Cr1-Cl3 2.291(15), Cr1-C19 1.988(13); N1-Cr1-P1 78.94(11), N2-Cr1-P1 79.30(11), N1-Cr1-N2 83.07(15), Cl1-Cr1-P1 172.69(6), N1-Cr1-Cl2 169.52(12), N2-Cr1-C19 170.4(10).

The reaction of **1** with 10 equiv. of $AlMe_3$ in toluene, followed by recrystallization from toluene/CH_2Cl_2/pentane solution at room temperature, yielded greenish-brown crystals of a dinuclear, chloride-bridged dicationic complex [{*fac*-Cr(NPN)Me(μ-Cl)}$_2$][$AlMe_xCl_{4-x}$]$_2$ (**3**·[$AlMe_xCl_{4-x}$]$_2$ with x >1, see below) in 54% yield. In the centrosymmetric structure of **3** (Figure 2), the metal centers are bridged by two chlorides and each Cr(III) is coordinated by the NPN ligand in a tridentate, facial mode. The slightly distorted octahedral coordination of the metal is completed by a methyl group. The P and one of the N donors are each in *trans* position with respect to a bridging chloride, whereas the methyl ligand occupies a position trans to the second N atom. The higher *trans* influence exerted by the P donor compared to pyridine results only in a slight elongation of the Cr1-Cl1^{i} distance (2.3937(12) Å) compared to the Cr1-Cl1 bond length of 2.3780(12) Å. The Cr-Cr distance of 3.4629(9) Å indicates the absence of direct metal-metal interaction, as expected for these two Cr(III) centers. The axial angle N2-Cr1-C19 of 166.89(16)° is significantly distorted from the ideal 180°, probably due to the steric influence of the neighbouring pyridine (see C19^{i} methyl and N2 pyridine, Figure 2, and centrosymmetry-related groups).

for references, see page 132

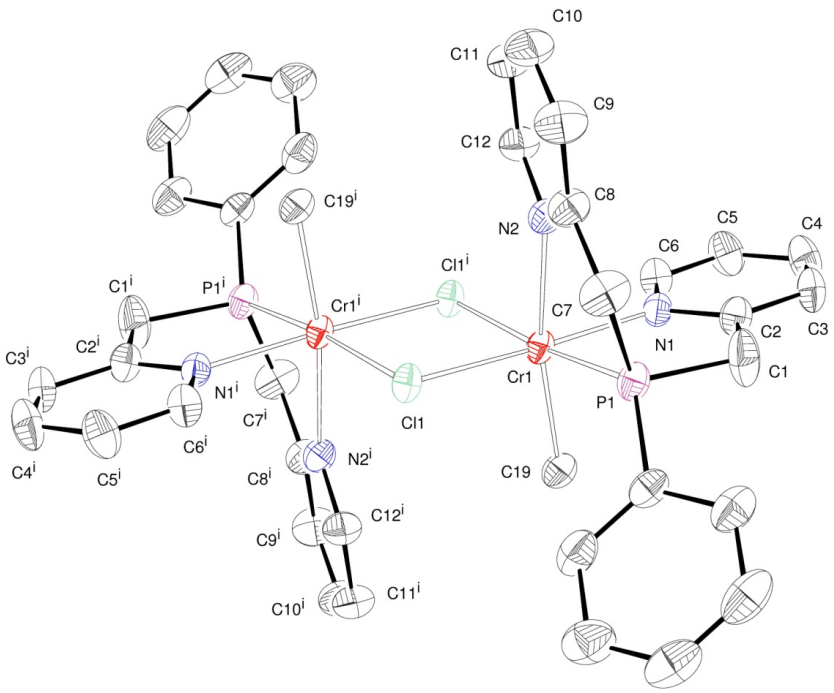

Figure 2. ORTEP of the molecular structure of **3** in **3**·$[AlMe_xCl_{4-x}]_2$. Ellipsoids at 40% probability level. Hydrogen atoms and $[AlMe_xCl_{4-x}]^-$ (x >1) anions omitted for clarity. Selected distances (Å) and angles (deg): Cr1-P1 2.3472(13), Cr1-C19 2.071(4), Cr1-N1 2.096(3), Cr1-N2 2.235(3), Cr1-Cl1 2.3780(12), Cr1-$Cl1^i$ 2.3937(12); N1-Cr1-P1 83.38(10), N2-Cr1-P1 77.49(10), N1-Cr1-N2 86.09(12), $Cl1^i$-Cr1-P1 173.29(4), $N1^i$-Cr1-$Cl1^i$ 173.88(10), N2-Cr1-C19 166.89(16), Cl1-Cr1-$Cl1^i$ 86.94(4), Cr1-Cl1-$Cr1^i$ 93.06(4).

A disorder involves the anion: two of the tetrahedral sites of the aluminate are occupied both by a chloride and a methyl, with unequal occupancy factors. This anion is thus likely to be a mixture of $[AlMe_xCl_{4-x}]^-$ (x > 1) species. The refinement of the occupancy factors suggests an approximate $[AlMe_2Cl_2]^-$ average composition. When dinuclear **3** was crystallized from THF, the mononuclear complex **6** was obtained as a result of the cleavage of the chloride bridges of **3** and transfer of an anionic ligand from aluminum to chromium. It was isolated in the crystalline form as **6**·THF but the quality of the crystals limited that of the structural data which do not allow a detailed discussion, although they confirm the connectivities within this molecule (See Supporting Information for **6**·THF). This complex is isostructural with **2** and the disorder found in **6**·THF is very similar to that in **2**, the coordination site *trans* to N2 being also occupied by a terminal chloride and a methyl group, but their mutual occupancy factors are 0.5/0.5.

Scheme 2. Structure of **6** in **6**·THF from X-ray diffraction data (see text)

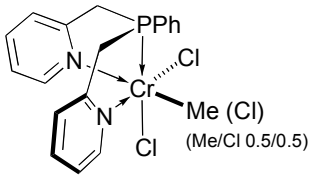

6

for references, see page 132

Commercial MAO generally contains residual $AlMe_3$. However, reactions of **1** with MAO or with pure $AlMe_3$ gave different products in our study. When the commercial MAO was pre-treated by removing $AlMe_3$ *in vacuo* at 60 °C for 6 h, the reaction between MAO and compound **1** was obviously slower, as indicated by the observation of the blue starting material **1** even after overnight reaction at room temperature, but at 60 °C in toluene, it gave the same result as the reaction of **1** with untreated MAO in 12 h.

When **1** was reacted with 10 equiv. of $AlEt_3$, the ethylchromium complex *fac*-[Cr(NPN)Cl_2Et] (**4**) was formed and isolated as green crystals, in higher yield (84%) than **2**. This complex provides a rather rare example of Cr(III)-Et function,[15,79,116,123-125] β-H elimination being a typical decomposition pathway.[33,104-105] The molecular structure (Figure 3) of **4** is similar to that of **2**, with an ethyl group (C19, C20) replacing the disordered C19/Cl3 ligand. The Cr1-N2 distance is significantly longer than Cr1-N1, owing to the *trans* influence exerted by the alkyl ligand. Slight changes in the conformation of the NPN tridentate ligand are observed between **2** and **4**. The P1, C7, C8, N2 chelation ring adopts in **4** an envelope conformation, whereas in **2** these atoms are almost coplanar. This brings the pyridyl ring containing N2 in a non coplanar position with respect to the P1, N2, Cl1, C19 plane [angle between the mean planes: 23.74(7)°], differently from **2**, in which this pyridyl ring is almost coplanar with the aforementioned plane [4.2(1)°]. A similar change is observed for the P1, C1, C2, N1 chelate [envelope in **2**, planar in **4**]. These slight conformation differences likely stem from the steric influence of the ethyl group on the P1, C1, C2, N1 ring, influencing indirectly also the P1, C7, C8, N2 chelate. Strong absorptions are observed in the far-IR spectrum of **4** around 329 cm^{-1} which are probably associated with stretching vibrations of the chloride ligands.

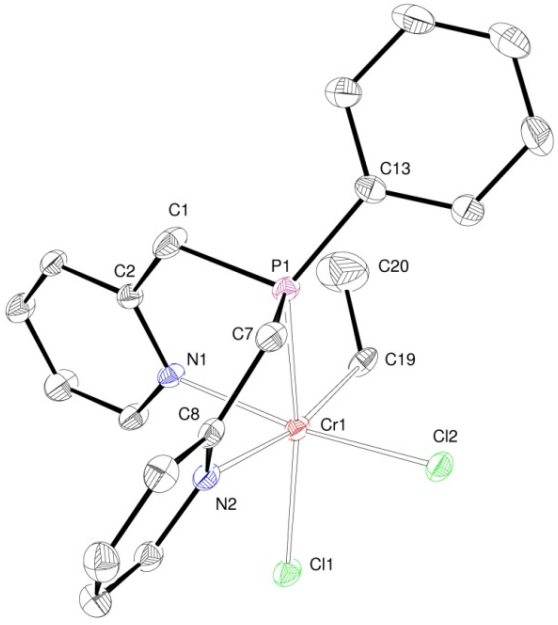

Figure 3. ORTEP of the molecular structure of **4**. Ellipsoids at 30% probability level. Hydrogen atoms omitted for clarity. Selected distances (Å) and angles (deg): Cr1-P1 2.3801(9), Cr1-N1 2.128(2), Cr1-N2 2.269(3), Cr1-Cl1 2.3534(8), Cr1-Cl2 2.3361(9), Cr1-C19 2.134(3); N1-Cr1-P1 81.44(7), N2-Cr1-P1 75.21(6), N1-Cr1-N2 84.45(9), Cl1-Cr1-P1 168.00(4), N1-Cr1-Cl2 169.12(7), N2-Cr1-C19 168.81(10).

for references, see page 132

When complex **1** was treated with 10 equiv. of $EtAlCl_2$ in a toluene/CH_2Cl_2 (1:1) mixture, the crystalline tricationic, dinuclear complex [{*fac*-Cr(NPN)}$_2$(μ-Cl)$_3$][$AlCl_4$]$_3$ (**5**·[$AlCl_4$]$_3$) was obtained in 74% yield. Its structure was determined by X-ray diffraction (Figure 4) and establishes that three chloride ligands symmetrically bridge the chromium atoms in a tricationic complex. Each metal center is further facially coordinated by a tridentate NPN ligand, through the P and N atoms, resulting in a distorted octahedral environment for the metals. The Cr-N distances are significantly shorter than those observed in **2** and **4**, consistent with a weaker *trans* influence of the chlorides and with the charge of the complex. There is a crystallographic plane of symmetry, which contains the atoms Cl1, Cl2 and Cl3. The longest Cr-Cl distance corresponds to that in *trans* position to the P donors. Three [$AlCl_4$]$^-$ counterions are present, relatively far from the metal centers. Only few chromium complexes triply bridged by halide ligands have been reported,[96,126-129] and complex **5** appears to be the first such complex containing tertiary phosphine ligands.

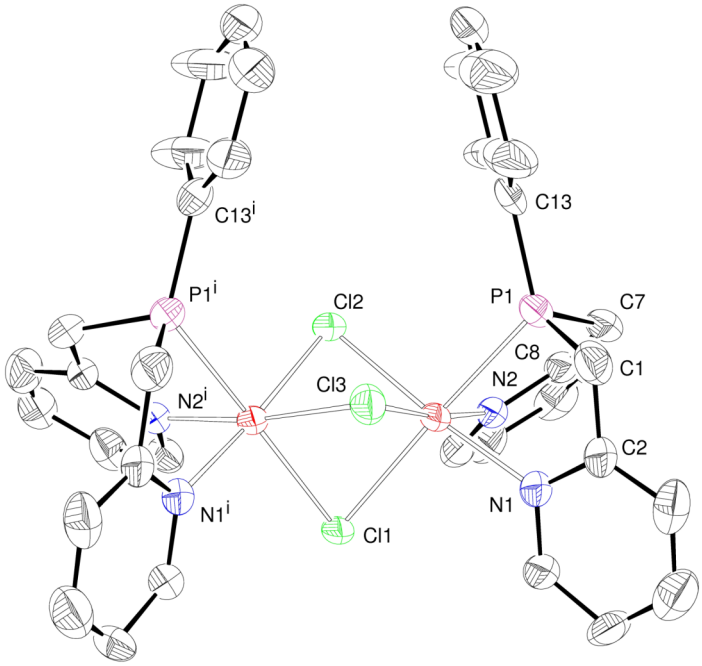

Figure 4. ORTEP of the molecular structure of **5** in **5**·[$AlCl_4$]$_3$. Ellipsoids at 30% probability level. Hydrogen atoms and [$AlCl_4$]$^-$ anions omitted for clarity. Selected distances (Å) and angles (deg): Cr1-P1 2.3476(19), Cr1-N1 2.049(5), Cr1-N2 2.047(6), Cr1-Cl1 2.3954(18), Cr1-Cl2 2.361(2), Cr1-Cl3 2.349(2); N1-Cr1-P1 78.04(17), N2-Cr1-P1 83.25(16), N2-Cr1-N1 89.8(2), Cl1-Cr1-P1 174.3(1), N1-Cr1-Cl2 175.15(17), N2-Cr1-Cl3 173.07(17), Cr1-Cl1-Cr1 74.92(7), Cr1-Cl2-Cr1 76.19(9), Cr1-Cl3-Cr1 76.67(9).

A notable aspect of this study is that the reactivity of different Al-based activators was evaluated toward the same Cr(III) precursor *fac*-[Cr(NPN)Cl_3] (**1**) and this allows a comparison to be made of their respective role. The crystallographic analysis of the reaction products helped clarify some functions of these commonly used Al-based cocatalysts. The latter were on purpose used in moderate excess with the hope to appreciate better their discriminating role and also for economical reasons in case an upscaling would be considered. In our case and under the conditions described, MAO and

for references, see page 132

$AlEt_3$ acted as alkylation agents, while $AlMe_3$ and $EtAlCl_2$ resulted in cationization. We are well aware of the fact that different results could possibly be obtained if a large excess of Al reagents was used, in particular in the case of MAO because of the various compounds it contains in variable proportions, including $AlMe_3$. We have no direct explanation why $AlMe_3$ and $AlEt_3$ behaved so differently. All the alkylated and cationic complexes we isolated were of trivalent chromium. For comparison, we attempted to synthesize Cr(II) complexes by reacting $CrCl_2$ or $[CrCl_2(THF)_2]$ with the NPN ligand. However, only the Cr(III) complex **1** was isolated by crystallization, possibly because of the instability of a hypothetical NPN Cr(II) complex. Interestingly, the PNP (PNP = $Ph_2PN(Cy)PPh_2$) ligand did not react with $[CrCl_2(THF)_2]$ to give the corresponding Cr(II) complex, but cationization by the Al cocatalyst and acquisition of a second ligand and a bridging $ClAlMe_3$ anion stabilized a Cr(II)-PNP complex.[69] Moreover, reaction of the SNS ligand (SNS = $PhSCH_2PyCH_2SPh$) with $[CrCl_2(THF)_2]$ afforded a Cr(III)-SNS complexas a result of disproportionation.[81]

8.3.2 Catalytic reactions.

Complexes **1-5** have been evaluated as pre-catalysts for the oligomerization of ethylene at 10 bar ethylene pressure. Following activation with MAO, these complexes formed active catalysts for the production of linear, short chain oligomers (Table 1). At room temperature, the **1**/MAO system was only weakly active (840 $g \cdot g\ (Cr)^{-1} \cdot h^{-1}$) and mostly polymers were formed. However, when the temperature was raised to 80 °C, not only the activity (2900 $g \cdot g\ (Cr)^{-1} \cdot h^{-1}$) but also the selectivity for α-olefins increased. Although the mononuclear complexes **1**, **2**, **4** and dinuclear **3**, **5** exhibit similar catalytic properties under comparable conditions (Figure 5), some interesting differences were observed concerning the chain length distribution of the oligomers. In particular, a higher percentage of 1-octene was produced by the **2**/MAO system, while the major oligomer produced using the **4**/MAO system was 1-decene. The analysis of the C_{10+} oligomers obtained by the **4**/MAO system closely fits a Schulz-Flory distribution (K = 0.57, K = (mol of C_{14})/(mol of C_{12})) (Figure 6). However, analysis of the C_4-C_{10} fraction reveals a significant deviation from a Schulz-Flory distribution. A similar phenomenon was observed for Cr-NHC ethylene oligomerization catalysts which operate via a metallacyclic mechanism.[93] Notwithstanding the fact that when considering both activity and selectivity, catalytic systems based on chromium complexes bearing PP, PNP or PPP ligands still dominate,[11-12] we provide here a new catalytic system for ethylene oligomerization, especially for the production of 1-decene. Notably, complexes **2** and **4** containing an alkyl group were inactive as single component catalysts, probably because of the absence of a readily available *cis* vacant coordination site for coordination of ethylene. On the basis of their characteristic C-H and C=C absorption bands, the waxes formed were found to contain mostly highly linear α-olefins. This was confirmed by ^1H and ^{13}C NMR spectroscopy. The resonances around δ 139.3 (CH=) and 114.5 (CH_2=) ppm are typical for a vinyl-unsaturated chain end.[130-131] Small amounts of branched olefins were detected by GC, most likely because of the secondary incorporation of α-olefins first formed into the metallacyclic

for references, see page 132

mechanism.[93,108] When $EtAlCl_2$ was used as cocatalyst for **1**, polyethylene was obtained without any significant detection of oligomers. The melting points of the polyethylene were found around 130 °C by DSC analysis and its infrared analysis was consistent with linear polyethylene.

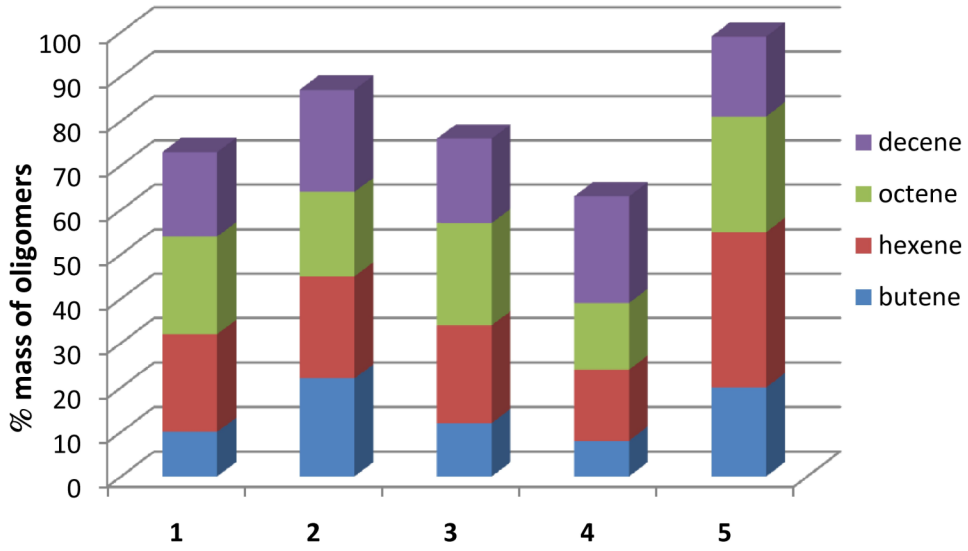

Figure 5. Oligomer distribution (C_4-C_{10}) with pre-catalysts **1-5** using MAO as cocatalyst.

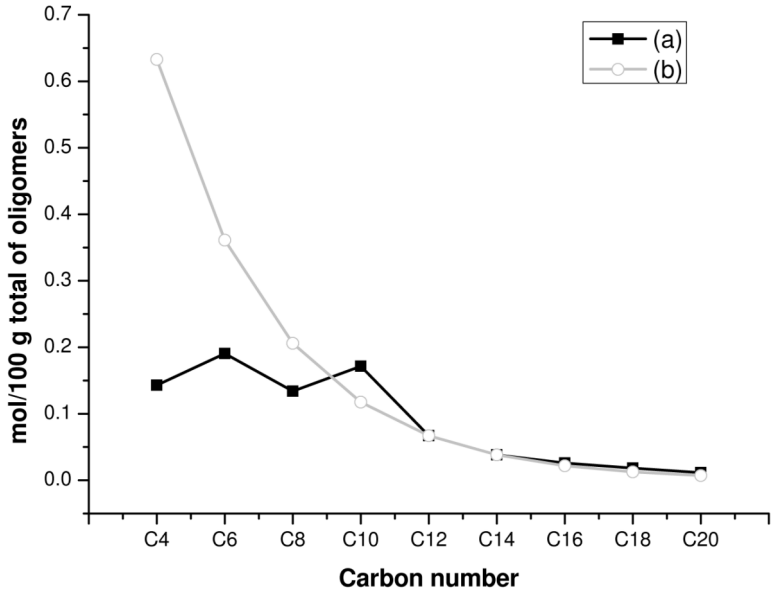

Figure 6. Plot of the molar amount of oligomers formed versus carbon number (C_4-C_{20}) for (a) the distribution obtained by the **4**/MAO system using the analysis method II (see Experimental section) (black line); (b) the calculated distribution for a *K* value of 0.57 (gray line)

for references, see page 132

Table 1. Oligomerization of ethylene with 1-5/MAO[a]

	oligomer mass distribution (%)[b]					activity	oligomers	waxes
	C_4(α-C_4)	C_6(α-C_6)	C_8(α-C_8)	C_{10}(α-C_{10})	C_{10+}	(g C_2H_4/(g Cr·h))	(wt%)	(wt%)
1[c,d]	29(55)	33(59)	21(60)	16(33)	-	840	27	83
1[e]	10(99)	22(88)	22(87)	19(82)	27	2700	78	22
2[e]	11(99)	23(92)	19(87)	23(49)	23	2800	76	24
3[e]	12(99)	22(92)	23(91)	19(84)	24	2700	62	38
4[e]	8(99)	16(90)	15(87)	24(46)	36	2800	82	18
5[d]	20(99)	35(90)	26(87)	18(71)	-	2800	57	43

[a] Conditions: T = 80 °C, 10 bar of C_2H_4, 90 min, 4×10^{-5} mol Cr, solvent 12 mL chlorobenzene and 8 mL of MAO toluene solution (total volume 20 mL). [b] Based on the oligomers formed. [c] T = room temperature. [d] Determined by GC according to method I (see Experimental section). [e] Determined by GC according to method II (see Experimental section).

8.4 Conclusions

Although it is well known that the nature and quantities used of catalyst activator (or cocatalyst) play a decisive role on the performances of a catalytic system, a detailed knowledge of the nature of the active species formed *in situ* during catalysis remains challenging and is rarely available. With this in mind, the reactions between the Cr(III) complex *fac*-[Cr(NPN)Cl_3] (**1**) and several typical aluminum activators, such as MAO, $AlMe_3$, $AlEt_3$ and $EtAlCl_2$ have been carried out with the hope to isolate new organometallic complexes resulting from their mutual interactions. The Cr methyl and ethyl complexes **2** and **4**, respectively, and the cationic dinuclear complexes **3** and **5** were isolated and crystallographically characterized. With MAO, methylation of **1** was only partial and produced **2**, while $AlEt_3$ completely alkylated **1** to afford **4**. Treatment of **1** with $AlMe_3$ in toluene, followed by recrystallization from non-coordinating solvents (toluene/CH_2Cl_2/pentane) or from a coordinating solvent (THF) afforded a Cl-bridged dinuclear dication **3** or an alkyl complex **6**, respectively. This typical alkylating reagent thus behaves under these circumstances as a cationization agent. The tricationic, dinuclear complex **5** was obtained from reaction of **1** with $EtAlCl_2$ and represents, to the best of our knowledge, the first dinuclear Cr complex containing tertiary phosphine ligands and three halide bridges. Our results illustrate the various functions exerted by different Al-based activators, which opens the possibility to better explain the diverse catalytic properties of a single pre-catalyst in the presence of different Al-based cocatalysts. The catalytic system **4**/MAO produced mostly decenes (1-decene dominating) whereas the other catalysts favored the production of C_6 and C_8 fractions.

for references, see page 132

8.5 Experimental Section

8.5.1 General Considerations

All operations were carried out using standard Schlenk techniques under inert atmosphere. Solvents were dried, degassed, and freshly distilled prior to use. Et_2O and THF were dried over sodium/benzophenone. Pentane and toluene were dried over sodium. CH_2Cl_2 was distilled from CaH_2. Acetonitrile and chlorobenzene were distilled from P_2O_5. Methylaluminoxane (MAO, 1.46 mol·L^{-1} in toluene) was purchased from Akzo Corp (USA). Trimethylaluminum (2 mol·L^{-1} in toluene) was purchased from Acros Chemicals. Triethylaluminum (93%) was purchased from Strem Chemicals (USA). Ethylaluminum dichloride (pure) was purchased from Aldrich Chemical Company. Other chemicals were commercially available and used without further purification unless otherwise stated. Bis(2-picolyl)phenylphosphine[117] and *fac*-[Cr(NPN)Cl_3] (**1**)[97] were prepared according to literature methods. IR spectra in the range 4000-650 cm^{-1} were recorded on a Thermo Nicolet 6700 instrument, equipped with SMART Orbit Diamond ATR accessory and in the 600-100 cm^{-1} range on a Nicolet 300 FT-IR instrument. Elemental analyses were performed by the "Service de microanalyse", Université de Strasbourg. Gas chromatographic analyses were performed on a Thermoquest GC8000 Top Series gas chromatograph using a HP Pona column (50 m, 0.2 mm diameter, 0.5 μm film thickness). DSC traces and melting points of polyethylene were obtained from the second scanning run on a Perkin-Elmer DSC-7 instrument, which was initially calibrated for the melting point of an indium standard at a heating rate of 10 °C min^{-1}.

8.5.2 Synthesis of *fac*-[Cr(NPN)$Cl_{2.23}Me_{0.77}$] (2)

To a suspension of *fac*-[Cr(NPN)Cl_3] (**1**) (0.451 g, 1.00 mmol) in toluene (10 mL) was added a toluene solution of MAO (6.7 mL, 1.46 mol·L^{-1}, 10 mmol) and the mixture was stirred at 20 °C for 1 h to give a green suspension. The volatiles were removed under vacuum and the resultant green solid was dissolved in THF and stored at -30 °C for one day. Green crystals were isolated from the solution and their crystal structure analysis revealed the average composition *fac*-[Cr(NPN)$Cl_{2.23}Me_{0.77}$] (0.240 g, 0.56 mmol, 56%). On the basis of this Cl/Me disorder, one can say that of the 56% isolated yield, 23% was unreacted **1** and 77% was [Cr(NPN)Cl_2Me] which cocrystallized. Selected IR absorptions (pure, diamond orbit): 3072w, 2963s, 2890s, 1610s, 1571w, 1485s, 1439s, 1385m, 1319w, 1165w, 1119w, 1065s, 1021m, 898w, 871m, 823m, 757s, 697m, 483m, 333s, 314s, 217m cm^{-1}. Anal. Calcd for $C_{18.77}H_{19.31}Cl_{2.23}CrN_2P$: C, 51.95; H, 4.49; N, 6.46. Found: C, 50.57; H, 4.71; N, 6.13. No better analyses could be obtained but we recall that the calculated values correspond to the best fit of the crystallographic model.

8.5.3 Synthesis of [{*fac*-Cr(NPN)Me(μ-Cl)}$_2$][$AlMe_xCl_{4-x}$]$_2$ (3·[$AlMe_xCl_{4-x}$]$_2$)

for references, see page 132

To a suspension of *fac*-[Cr(NPN)Cl_3] (0.451 g, 1.00 mmol) in toluene (10 mL) was added a toluene solution of $AlMe_3$ (5 ml, 2 mol·L^{-1}, 10 mmol) and the mixture was stirred at 20 °C for 1 h to give a green solution and then 10 mL CH_2Cl_2 was added. Greenish-brown crystals of [{*fac*-Cr(NPN)Me(μ-Cl)}$_2$][$AlMe_xCl_{4-x}$]$_2$ (0.280 g, 0.27 mmol, 54%, x = 1.95) were isolated by layering pentane on the above toluene/CH_2Cl_2 solution. Selected IR absorptions (pure, diamond orbit): 2930m, 2883w, 1603s, 1565w, 1482s, 1435s, 1392m, 1312m, 1177m, 1161m, 1108m, 1059m, 1026w, 1015m, 867m, 819m, 807m, 744s, 668m, 478s, 420mw, 381m, 358m, 317s, 277w cm^{-1}. Complex **3** was too air- and moisture-sensitive to give satisfactory elemental analysis.

8.5.4 Synthesis of *fac*-[Cr(NPN)Cl_2Et] (4)

To a suspension of *fac*-[Cr(NPN)Cl_3] (0.451 g, 1.00 mmol) in toluene (10 mL) was added a toluene solution of $AlEt_3$ (10 mL, 1 mol·L^{-1}, 10 mmol) and the mixture was stirred at 20 °C for 1 h to give a green solution. After concentration and filtration, green crystals of analytically pure *fac*-[Cr(NPN)Cl_2Et] (0.373 g, 0.84 mmol, 84%) were isolated from the solution at -30 °C for one day. Selected IR absorptions (pure, diamond orbit): 3111w, 3072w, 2948w, 2904w, 1608s, 1566m, 1486s, 1437s, 1376m, 1315m, 1265m, 1163m, 1112m, 1063m, 1023m, 866m, 745m, 690m, 329vs, 218m cm^{-1}. Anal. Calcd for $C_{20}H_{22}Cl_2CrN_2P$: C, 54.07; H, 4.99; N, 6.31. Found: C, 53.90; H, 4.50; N, 6.29.

8.5.5 Synthesis of [*fac*-{Cr(NPN)}$_2$(μ-Cl)$_3$][$AlCl_4$]$_3$ (**5**·[$AlCl_4$]$_3$)

To a suspension of *fac*-[Cr(NPN)Cl_3] (0.451 g, 1.00 mmol) in CH_2Cl_2 (10 mL) was added a toluene solution of $EtAlCl_2$ (10 mL, 1 mol·L^{-1}, 10 mmol) and the mixture was stirred at 20 °C for 10 min to give a red solution, which was kept at room temperature for one day to give red crystals. Complex **5**·[$AlCl_4$]$_3$ was isolated as red crystals by removing the mother liquor and washing with 5 mL toluene (0.475 g, 0.37 mmol, 74%). Selected IR absorptions (pure, diamond orbit): 2946w, 2897w, 2879w, 1632s, 1610s, 1566w, 1485s, 1440s, 1382s, 1317m, 1263m, 1166m, 1108s, 1066m, 1031m, 999w, 896w, 859m, 822m, 764w, 737w, 684w, 477s, 346m, 254mw, 178s cm^{-1}. Anal. Calcd for $C_{36}H_{34}Al_3Cl_{15}Cr_2N_4P_2$: C, 33.40; H, 2.65; N, 4.33. Found: C, 33.17; H, 2.92; N, 3.70.

8.5.6 Catalytic oligomerization of ethylene

All catalytic reactions were carried out in a magnetically stirred (900 rpm) 145 mL stainless steel autoclave. A 125 mL glass container was used to protect the inner walls of the autoclave from corrosion. The preparation of the catalytic solution of the pre-catalyst is dependent on the nature and the amount of the cocatalyst.

With MAO, 4 × 10^{-5} mol of Cr complex was dissolved in 12 mL in chlorobenzene and injected into the reactor under an ethylene flux. Then 8 mL of a cocatalyst toluene solution, corresponding to 300 equiv. of MAO, was added to the reactor to reach a total volume of 20 mL with the pre-catalyst solution.

for references, see page 132

With $EtAlCl_2$, 4 × 10^{-5} mol of Cr complex was dissolved in 10 mL of cholorobenzene and injected into the reactor under an ethylene flux. Then 5 mL of a cocatalyst toluene solution, corresponding to 10 equiv. of $EtAlCl_2$, was added to the reactor to reach a total volume of 15 mL with the pre-catalyst solution.

For reactions carried out without cocatalyst, 4 × 10^{-5} mol of Cr complex was dissolved in 15 mL of cholorobenzene and injected in the reactor under an ethylene flux.

All catalytic tests were started between 20 and 25 °C. After injection of the catalytic solution and of the cocatalyst under a constant low flow of ethylene, the reactor was pressurized to 10 bar. The temperature was kept at room temperature or heated to reach 80 °C using a loop-water bath. The 10 bar working pressure was maintained during the experiments through a continuous feed of ethylene from a reserve bottle placed on a balance to allow continuous monitoring of the ethylene uptake. At the end of each test (90 min) a dry ice bath was used to rapidly cool down the reactor, thus stopping the reaction. When the inner temperature reached 0 °C the dry ice bath was removed allowing the temperature to slowly rise to 18 °C. The gaseous phase was then transferred into a 10 L polyethylene tank filled with water. An aliquot of this gaseous phase was transferred into a Schlenk flask, previously evacuated, for GC analysis. For comparison, the workup of the non-gazeous products was performed in two different ways.

Method I: The solution was hydrolyzed *in situ* by the addition of ethanol (10 mL), transferred into a Schlenk flask, and separated from the metal complexes by trap-to-trap evaporation (20 °C, 0.8 mbar) into a second Schlenk flask previously immersed in liquid nitrogen in order to avoid any loss of product. An aliquot of the liquid fraction was used for GC analysis of the portion of C_4-C_{20}. The wax remaining in the first Schlenk tube was treated with 5% hydrochloric acid, washed with ethanol and dried under vacuum at 60 °C to constant weight.

Method II: The reactor was opened and a small amount of the catalytic mixture was collected and immediately quenched by addition of commercial 35% aqueous hydrogen chloride at 0 °C. The supernatant was analyzed by GC to determine the distribution of oligomers obtained (C_4-C_{20+}). The remaining solution was then quenched with HCl-acidified ethanol (5%), and the precipitated solid was filtered, washed with ethanol, and dried under vacuum at 60 °C to constant weight.

8.5.7 X-ray data collection, structure solution and refinement for 2, 3·[$AlMe_xCl_{4-x}]_2$, 4 and 5·[$AlCl_4]_3$

Suitable crystals for the X-ray analysis of **2**, **3**·[$AlMe_xCl_{4-x}]_2$, **4** and **5**·[$AlCl_4]_3$ were obtained as described below. The intensity data were collected at 173(2) K on a Kappa CCD diffractometer[132] (graphite monochromated MoKα radiation, λ = 0.71073 Å). Crystallographic and experimental details for the structure are summarized in Table 2. The structures were solved by direct methods (SHELXS-97) and refined by full-matrix least-squares procedures (based on F^2, SHELXL-97)[133] with anisotropic thermal parameters for all the non-hydrogen atoms. The hydrogen atoms were introduced into the

for references, see page 132

geometrically calculated positions (SHELXS-97 procedures) and refined *riding* on the corresponding parent atoms. In **2**, a chlorine and the methyl were found occupying the same site with a refined occupancy factor of 0.23/0.77, respectively. These atoms (C,Cl) were refined with restrained anisotropic parameters. In **3**·$[AlMe_xCl_{4-x}]_2$, The anion was found disordered. Two sites of terminal groups bound to Al are occupied by both a chorine and a methyl. Their mutual occupancy factors (0.75/0.25 for Cl2/C21 and 0.3/0.7 for Cl4/C22) were determined on the isotropic model and these atoms were refined with restrained anisotropic parameters. In **4**, the ethyl group was found disordered in two very close positions with the metallated C in common. It was not possible to refine the disorder and the CH_3 carbon was refined with restrained anisotropic parameters. In **5**·$[AlCl_4]_3$, one of the $[AlCl_4]^-$ anions and an acetonitrile molecule were found disordered over multiple positions with no atoms in common. Any attempt to give a reasonable model of this disorder (seriously affecting the model quality) failed. A PLATON SQUEEZE procedure was applied,[134] using a complete anisotropic model containing **5**·$[AlCl_4]_2$, resulting in an improved model quality (277 missing electron per cell, consistent with the 244 required for $[AlCl_4]^-$·MeCN). The quality of the crystals of **6**·THF, isostructural with **2**·THF, was poor and prevented a detailed description of the structure. Similarly to **2**, one coordination site is occupied by both a chloride and a methyl, in a refined occupancy factor of 0.5/0.5. These atoms were refined with restrained anisotropic parameters. CCDC 817399–817403 (complexes **2**·THF – **6**·THF) contain the supplementary crystallographic data for this paper that can be obtained free of charge from the Cambridge Crystallographic Data Center via www.ccdc.cam.ac.uk/data_request/cif.

for references, see page 132

Table 2. Data collection and refinement data for **2**·THF, **3**·$[AlMe_xCl_{4-x}]_2$, **4** and **5**·$[AlCl_4]_3$.

Compound reference	**2**·THF	**3**·$[AlMe_xCl_{4-x}]_2$	**4**	**5**·$[AlCl_4]_3$
Chemical formula	$C_{18.77}H_{19.31}Cl_{2.23}CrN_2P$·$C_4H_8O$	$C_{38}H_{40}Cl_2Cr_2N_4P_2$·$(C_{1\cdot95}H_{5\cdot85}AlCl_{2\cdot05})_2$	$C_{20}H_{22}Cl_2CrN_2P$	$C_{36}H_{34}Cl_3Cr_2N_4P_2$·$[AlCl_4]_3$
Formula Mass	507.45	1047.52	444.27	1132.52
Crystal system	Orthorhombic	Triclinic	Monoclinic	Monoclinic
a/Å	15.9497(6)	9.7268(6)	11.8957(7)	12.6248(12)
b/Å	15.6097(8)	11.9913(8)	12.4712(9)	14.1844(10)
c/Å	19.1905(9)	12.0343(7)	15.7046(8)	16.4790(16)
α/°	90.00	66.117(4)	90.00	90.00
β/°	90.00	85.239(4)	120.514(3)	90.715(3)
γ/°	90.00	76.112(4)	90.00	90.00
V/Å^3	4777.9(4)	1245.78(13)	2007.2(2)	2950.8(5)
T/K	173(2)	173(2)	173(2)	173(2)
Space group	*Pbca*	*P*-1	*P*21/*c*	*P*21/*m*
Z	8	1	4	2
μ/mm^{-1}	0.815	0.896	0.922	0.977
Meads. reflections	8365	6982	6681	9564
independent reflect.	4431	4630	3937	5394
R_{int}	0.0451	0.0278	0.0304	0.0425
Final R_1 ($I > 2\sigma(I)$)	0.0681	0.0580	0.0460	0.0858
Final $wR(F^2)$ ($I > 2\sigma(I)$)	0.1475	0.1558	0.1149	0.2287
Final R_1 (all data)	0.1182	0.0948	0.0688	0.1248
Final $wR(F^2)$ (all data)	0.1628	0.1741	0.1229	0.2447
S on F^2	1.042	1.028	1.072	1.095

Acknowledgment

We thank the Centre National de la Recherche Scientifique (CNRS), the Ministère de l'Enseignement Supérieur et de la Recherche (Paris) and the Université de Strasbourg for support, the French Embassy in Beijing for a doctoral grant to S. L. and Professor Wen-Hua Sun (Institute of Chemistry, Chinese Academy of Sciences, Beijing) for support. We are grateful to Marc Mermillon-Fournier for technical assistance and to the referees for insightful comments.

Supporting Information Available

Crystallographic and experimental details for the structures **2**·THF, **3**·$[AlMe_xCl_{4-x}]_2$, **4** and **5**·$[AlCl_4]_3$.and their CIF files giving X-ray crystal structural data. These materials are available free of charge via the Internet at http://pubs.acs.org.

for references, see page 132

References

1. Hogan, J. P.; Banks, R. L. Phillips Petroleum Co.; Belg. Pat. 530617, 1955; U.S. Pat. 2825721, 1958.
2. Hogan, J. P. *J. Polym. Sci.* **1970**, *8*, 2637-2652.
3. Karapinka, G. L. U.S. Pat. 3709853, 1973.
4. Karol, F. J.; Karapinka, G. L.; Wu, C.; Dow , A. W.; Johnson, R. N.; Garrick, W. L. *J. Polym. Sci.* **1972**, *10*, 2621-2637.
5. Groppo, E.; Lamberti, C.; Bordiga, S.; Spoto, G.; Zecchina, A. *Chem. Rev.* **2005**, *105*, 115-183.
6. Böhm, L. L. *Angew. Chem., Int. Ed.* **2003**, *42*, 5010-5030.
7. Wilke, G. *Angew. Chem., Int. Ed.* **2003**, *42*, 5000-5008.
8. McDaniel, M. P. *Adv. Catal.* **1985**, *33*, 47-98.
9. Britovsek, G. J. P.; Gibson, V. C.; Wass, D. F. *Angew. Chem., Int. Ed.* **1999**, *38*, 428-447.
10. Gibson, V. C.; Spitzmesser, S. K. *Chem. Rev.* **2003**, *103*, 283-315.
11. Dixon, J. T.; Green, M. J.; Hess, F. M.; Morgan, D. H. *J. Organomet. Chem.* **2004**, *689*, 3641-3668.
12. Wass, D. F. *Dalton Trans.* **2007**, 816-819.
13. Theopold, K. H. *Chem. Tech.* **1997**, *27*, 26-32.
14. Theopold, K. H. *Eur. J. Inorg. Chem.* **1998**, 15-24.
15. Gibson, V. C.; Newton, C.; Redshaw, C.; Solan, G. A.; White, A. J. P.; Williams, D. J. *J. Chem. Soc., Dalton Trans.* **2002**, 4017-4023.
16. Rüther, T.; Braussaud, N.; Cavell, K. J. *Organometallics* **2001**, *20*, 1247-1250.
17. MacAdams, L. A.; Buffone, G. P.; Incarvito, C. D.; Rheingold, A. L.; Theopold, K. H. *J. Am. Chem. Soc.* **2005**, *127*, 1082-1083.
18. Klemps, C.; Buchard, A.; Houdard, R.; Auffrant, A.; Mézailles, N.; Le Goff, X. F.; Ricard, L.; Saussine, L.; Magna, L.; Le Floch, P. *New J. Chem.* **2009**, *33*, 1748-1752.
19. Albahily, K.; Al-Baldawi, D.; Gambarotta, S.; Duchateau, R.; Koç, E.; Burchell, T. J. *Organometallics* **2008**, *27*, 5708-5711.
20. Albahily, K.; Koç, E.; Al-Baldawi, D.; Savard, D.; Gambarotta, S.; Burchell, T. J.; Duchateau, R. *Angew. Chem., Int. Ed.* **2008**, *47*, 5816-5819.
21. Huang, Y. B.; Jin, G.-X. *Dalton Trans.* **2009**, 767-769.
22. MacAdams, L. A.; Kim, W. K.; Liable-Sands, L. M.; Guzei, I. A.; Rheingold, A. L.; Theopold, K. H. *Organometallics* **2002**, *21*, 952-960.
23. Licciulli, S.; Thapa, I.; Albahily, K.; Korobkov, I.; Gambarotta, S.; Duchateau, R.; Chevalier, R.; Schuhen, K. *Angew. Chem., Int. Ed.* **2010**, *49*, 9225-9228.
24. Rüther, T.; Cavell, K. J.; Braussaud, N. C.; Skelton, B. W.; White, A. H. *J. Chem. Soc., Dalton Trans.* **2002**, 4684-4693.
25. Köhn, R. D.; Haufe, M.; Mihan, S.; Lilge, D. *Chem. Commun.* **2000**, 1927-1928.
26. Köhn, R. D.; Haufe, M.; Kociok-Köhn, G.; Grimm, S.; Wasserscheid, P.; Keim, W. *Angew. Chem., Int. Ed.* **2000**, *39*, 4337-4339.
27. Tomov, A. K.; Chirinos, J. J.; Long, R. J.; Gibson, V. C.; Elsegood, M. R. J. *J. Am. Chem. Soc.* **2006**, *128*, 7704-7705.
28. Esteruelas, M. A.; López, A. M.; Méndez, L.; Oliván, M.; Oñate, E. *Organometallics* **2003**, *22*, 395-406.
29. Carney, M. J.; Robertson, N. J.; Halfen, J. A.; Zakharov, L. N.; Rheingold, A. L. *Organometallics* **2004**, *23*, 6184-6190.
30. Zhang, W.; Sun, W.-H.; Zhang, S.; Hou, J.; Wedeking, K.; Schultz, S.; Fröhlich, R.; Song, H. *Organometallics* **2006**, *25*, 1961-1969.
31. Small, B. L.; Carney, M. J.; Holman, D. M.; O'Rourke, C. E.; Halfen, J. A. *Macromolecules* **2004**, *37*, 4375-4386.
32. Esteruelas, M. A.; López, A. M.; Méndez, L.; Oliván, M.; Oñate, E. *New J. Chem.* **2002**, *26*, 1542-1544.
33. Sugiyama, H.; Aharonian, G.; Gambarotta, S.; Yap, G. P. A.; Budzelaar, P. H. M. *J. Am. Chem. Soc.* **2002**, *124*, 12268-12274.
34. Junges, F.; Kuhn, M. C. A.; dos Santos, A.; Rabello, C. R. K.; Thomas, C. M.; Carpentier, J. F.; Casagrande, O. L. *Organometallics* **2007**, *26*, 4010-4014.
35. Vidyaratne, I.; Scott, J.; Gambarotta, S.; Duchateau, R. *Organometallics* **2007**, *26*, 3201-3211.
36. Zhang, J.; Li, A. F.; Hor, T. S. A. *Dalton. Trans.* **2009**, 9327-9333.
37. Zhang, J.; Li, A. F.; Hor, T. S. A. *Organometallics* **2009**, *28*, 2935-2937.
38. Kilpatrick, A. F. R.; Kulangara, S. V.; Cushion, M. G.; Duchateau, R.; Mountford, P. *Dalton Trans.* **2010**, *39*, 3653-3664.
39. Crewdson, P.; Gambarotta, S.; Djoman, M. C.; Korobkov, I.; Duchateau, R. *Organometallics* **2005**, *24*, 5214-5216.
40. Nenu, C. N.; Weckhuysen, B. M. *Chem. Commun.* **2005**, 1865-1867.

for references, see page 132

41. Hurtado, J.; Carey, D. M. L.; Muñoz-Castro, A.; Arratia-Pérez, R.; Quijada, R.; Wu, G.; Rojas, R.; Valderrama, M. *J. Organomet. Chem.* **2009**, *694*, 2636-2641.
42. Tenza, K.; Hanton, M. J.; Slawin, A. M. Z. *Organometallics* **2009**, *28*, 4852-4867.
43. Zhang, M.; Wang, K.; Sun, W.-H. *Dalton Trans.* **2009**, 6354-6363.
44. Xiao, L.; Zhang, M.; Sun, W.-H. *Polyhedron* **2010**, *29*, 142-147.
45. Gao, R.; Liang, T.; Wang, F.-S.; Sun, W.-H. *J. Organomet. Chem.* **2009**, *694*, 3701-3707.
46. Chen, Y.; Zuo, W.; Hao, P.; Zhang, S.; Gao, K.; Sun, W.-H. *J. Organomet. Chem.* **2008**, *693*, 750-762.
47. Amolegbe, S. A.; Asma, M.; Zhang, M.; Li, G.; Sun, W.-H. *Aust. J. Chem.* **2008**, *61*, 397-403.
48. Zhang, S.; Jie, S.; Shi, Q.; Sun, W.-H. *J. Mol. Catal. A: Chem.* **2007**, *276*, 174-183.
49. Arif, A. M.; Hefner, J. G.; Jones, R. A.; Whittlesey, B. R. *Inorg. Chem.* **1986**, *25*, 1080-1084.
50. Askham, F. R.; Maverick, A. W.; Stanley, G. G. *Inorg. Chem.* **1987**, *26*, 3963-3966.
51. Wu, F.-J.; Rouge, B. *US 5811618 (Amoco Corporation)*, 1995.
52. Baker, R. J.; Edwards, P. G. *J. Chem. Soc., Dalton Trans.* **2002**, 2960-2965.
53. Elowe, P. R.; McCann, C.; Pringle, P. G.; Spitzmesser, S. K.; Bercaw, J. E. *Organometallics* **2006**, *25*, 5255-5260.
54. Kuhlmann, S.; Dixon, J. T.; Haumann, M.; Morgan, D. H.; Ofili, J.; Spuhl, O.; Taccardi, N.; Wasserscheid, P. *Adv. Synth. Catal.* **2006**, *348*, 1200-1206.
55. Agapie, T.; Day, M. W.; Henling, L. M.; Labinger, J. A.; Bercaw, J. E. *Organometallics* **2006**, *25*, 2733-2742.
56. Schofer, S. J.; Day, M. W.; Henling, L. M.; Labinger, J. A.; Bercaw, J. E. *Organometallics* **2006**, *25*, 2743-2749.
57. Overett, M. J.; Blann, K.; Bollmann, A.; de Villiers, R.; Dixon, J. T.; Killian, E.; Maumela, M. C.; Maumela, H.; McGuinness, D. S.; Morgan, D. H.; Rucklidge, A.; Slawin, A. M. Z. *J. Mol. Catal. A: Chem.* **2008**, *283*, 114-119.
58. Jiang, T.; Zhang, S.; Jiang, X. L.; Yang, C. F.; Niu, B.; Ning, Y. N. *J. Mol. Catal. A: Chem.* **2008**, *279*, 90-93.
59. Bowen, L. E.; Haddow, M. F.; Orpen, A. G.; Wass, D. F. *Dalton Trans.* **2007**, 1160-1168.
60. McGuinness, D. S.; Overett, M.; Tooze, R. P.; Blann, K.; Dixon, J. T.; Slawin, A. M. Z. *Organometallics* **2007**, *26*, 1108-1111.
61. Carter, A.; Cohen, S. A.; Cooley, N. A.; Murphy, A.; Scutt, J.; Wass, D. F. *Chem. Commun.* **2002**, 858-859.
62. Bollmann, A.; Blann, K.; Dixon, J. T.; Hess, F. M.; Killian, E.; Maumela, H.; McGuinness, D. S.; Morgan, D. H.; Neveling, A.; Otto, S.; Overett, M.; Slawin, A. M. Z.; Wasserscheid, P.; Kuhlmann, S. *J. Am. Chem. Soc.* **2004**, *126*, 14712-14713.
63. Overett, M. J.; Blann, K.; Bollmann, A.; Dixon, J. T.; Hess, F.; Killian, E.; Maumela, H.; Morgan, D. H.; Neveling, A.; Otto, S. *Chem. Commun.* **2005**, 622-624.
64. Blann, K.; Bollmann, A.; Dixon, J. T.; Hess, F. M.; Killian, E.; Maumela, H.; Morgan, D. H.; Neveling, A.; Otto, S.; Overett, M. J. *Chem. Commun.* **2005**, 620-621.
65. Agapie, T.; Schofer, S. J.; Labinger, J. A.; Bercaw, J. E. *J. Am. Chem. Soc.* **2004**, *126*, 1304-1305.
66. Hey, T. W.; Wass, D. F. *Organometallics* **2010**, *29*, 3676-3678.
67. Klemps, C.; Payet, E.; Magna, L.; Saussine, L.; Le Goff, X. F.; Le Floch, P. *Chem. Eur. J.* **2009**, *15*, 8259-8268.
68. Dulai, A.; Bod, H.; Hanton, M. J.; Smith, D. M.; Downing, S.; Mansell, S. M.; Wass, D. F. *Organometallics* **2009**, *28*, 4613-4616.
69. Jabri, A.; Crewdson, P.; Gambarotta, S.; Korobkov, I.; Duchateau, R. *Organometallics* **2006**, *25*, 715-718.
70. Rucklidge, A. J.; McGuinness, D. S.; Tooze, R. P.; Slawin, A. M. Z.; Pelletier, J. D. A.; Hanton, M. J.; Webb, P. B. *Organometallics* **2007**, *26*, 2782-2787.
71. Weng, Z. Q.; Teo, S. H.; Hor, T. S. A. *Dalton Trans.* **2007**, 3493-3498.
72. Peitz, S.; Peulecke, N.; Aluri, B. R.; Hansen, S.; Müller, B. H.; Spannenberg, A.; Rosenthal, U.; Al-Hazmi, M. H.; Mosa, F. M.; Wöhl, A.; Müller, W. *Eur. J. Inorg. Chem.* **2010**, 1167-1171.
73. Aluri, B. R.; Peulecke, N.; Peitz, S.; Spannenberg, A.; Müller, B. H.; Schulz, S.; Drexler, H. J.; Heller, D.; Al-Hazmi, M. H.; Mosa, F. M.; Wöhl, A.; Müller, W.; Rosenthal, U. *Dalton Trans.* **2010**, *39*, 7911-7920.
74. McGuinness, D. S.; Wasserscheid, P.; Keim, W.; Hu, C. H.; Englert, U.; Dixon, J. T.; Grove, C. *Chem. Commun.* **2003**, 334-335.
75. Bluhm, M. E.; Walter, O.; Döring, M. *J. Organomet. Chem.* **2005**, *690*, 713-721.
76. McGuinness, D. S.; Wasserscheid, P.; Morgan, D. H.; Dixon, J. T. *Organometallics* **2005**, *24*, 552-556.
77. McGuinness, D. S.; Brown, D. B.; Tooze, R. P.; Hess, F. M.; Dixon, J. T.; Slawin, A. M. Z. *Organometallics* **2006**, *25*, 3605-3610.
78. Shin, R. Y. C.; Tan, G. K.; Koh, L. L.; Goh, L. Y.; Webster, R. D. *Organometallics* **2005**, *24*, 1401-1403.
79. Temple, C.; Jabri, A.; Crewdson, P.; Gambarotta, S.; Korobkov, I.; Duchateau, R. *Angew. Chem., Int. Ed.* **2006**, *45*, 7050-7053.

for references, see page 132

80. McGuinness, D. S.; Wasserscheid, P.; Keim, W.; Morgan, D.; Dixon, J. T.; Bollmann, A.; Maumela, H.; Hess, F.; Englert, U. *J. Am. Chem. Soc.* **2003**, *125*, 5272-5273.
81. Temple, C. N.; Gambarotta, S.; Korobkov, I.; Duchateau, R. *Organometallics* **2007**, *26*, 4598-4603.
82. Jabri, A.; Temple, C.; Crewdson, P.; Gambarotta, S.; Korobkov, I.; Duchateau, R. *J. Am. Chem. Soc.* **2006**, *128*, 9238-9247.
83. Zhang, J.; Braunstein, P.; Hor, T. S. A. *Organometallics* **2008**, *27*, 4277-4279.
84. Liu, J.-Y.; Li, Y.-S.; Liu, J.-Y.; Li, Z.-S. *J. Mol. Catal. A: Chem.* **2006**, *244*, 99-104.
85. Jones, D. J.; Gibson, V. C.; Green, S. M.; Maddox, P. J. *Chem. Commun.* **2002**, 1038-1039.
86. Xu, T. Q.; Mu, Y.; Gao, W.; Ni, J. G.; Ye, L.; Tao, Y. C. *J. Am. Chem. Soc.* **2007**, *129*, 2236-2237.
87. Huang, Y. B.; Yu, W. B.; Jin, G.-X. *Organometallics* **2009**, *28*, 4170-4174.
88. Jie, S.; Pattacini, R.; Rogez, G.; Loose, C.; Kortus, J.; Braunstein, P. *Dalton Trans.* **2009**, 97-105.
89. Jones, D. J.; Gibson, V. C.; Green, S. M.; Maddox, P. J.; White, A. J. P.; Williams, D. J. *J. Am. Chem. Soc.* **2005**, *127*, 11037-11046.
90. Zhang, W.; Sun, W.-H.; Tang, X.; Gao, T.; Zhang, S.; Hao, P.; Chen, J. *J. Mol. Catal. A: Chem.* **2007**, *265*, 159-166.
91. Kirillov, E.; Roisnel, T.; Razavi, A.; Carpentier, J. F. *Organometallics* **2009**, *28*, 2401-2409.
92. McGuinness, D. S.; Gibson, V. C.; Wass, D. F.; Steed, J. W. *J. Am. Chem. Soc.* **2003**, *125*, 12716-12717.
93. McGuinness, D. S.; Suttil, J. A.; Gardiner, M. G.; Davies, N. W. *Organometallics* **2008**, *27*, 4238-4247.
94. McGuinness, D. S.; Gibson, V. C.; Steed, J. W. *Organometallics* **2004**, *23*, 6288-6292.
95. McGuinness, D. S. *Organometallics* **2009**, *28*, 244-248.
96. Kreisel, K. A.; Yap, G. P. A.; Theopold, K. H. *Organometallics* **2006**, *25*, 4670-4679.
97. Liu, S.; Peloso, R.; Pattacini, R.; Braunstein, P. *Dalton Trans.* **2010**, *39*, 7881-7883.
98. He, L. P.; Liu, J. Y.; Pan, L.; Wu, J. Q.; Xu, B. C.; Li, Y. S. *J. Polym. Sci., Part A: Polym. Chem.* **2009**, *47*, 713-721.
99. Agapie, T.; Labinger, J. A.; Bercaw, J. E. *J. Am. Chem. Soc.* **2007**, *129*, 14281-14295.
100. Rozenel, S. S.; Chomitz, W. A.; Arnold, J. *Organometallics* **2009**, *28*, 6243-6253.
101. Chomitz, W. A.; Mickenberg, S. F.; Arnold, J. *Inorg. Chem.* **2008**, *47*, 373-380.
102. Briggs, J. R. *J. Chem. Soc., Chem. Commun.* **1989**, 674-675.
103. Emrich, R.; Heinemann, O.; Jolly, P. W.; Krüger, C.; Verhovnik, G. P. J. *Organometallics* **1997**, *16*, 1511-1513.
104. Jabri, A.; Mason, C. B.; Sim, Y.; Gambarotta, S.; Burchell, T. J.; Duchateau, R. *Angew. Chem., Int. Ed.* **2008**, *47*, 9717-9721.
105. Vidyaratne, I.; Nikiforov, G. B.; Gorelsky, S. I.; Gambarotta, S.; Duchateau, R.; Korobkov, I. *Angew. Chem., Int. Ed.* **2009**, *48*, 6552-6556.
106. Thapa, I.; Gambarotta, S.; Korobkov, I.; Duchateau, R.; Kulangara, S. V.; Chevalier, R. *Organometallics* **2010**, *29*, 4080-4089.
107. Walsh, R.; Morgan, D. H.; Bollmann, A.; Dixon, J. T. *Appl. Catal., A* **2006**, *306*, 184-191.
108. Overett, M. J.; Blann, K.; Bollmann, A.; Dixon, J. T.; Haasbroek, D.; Killian, E.; Maumela, H.; McGuinness, D. S.; Morgan, D. H. *J. Am. Chem. Soc.* **2005**, *127*, 10723-10730.
109. Wöhl, A.; Müller, W.; Peulecke, N.; Müller, B. H.; Peitz, S.; Heller, D.; Rosenthal, U. *J. Mol. Catal. A: Chem.* **2009**, *297*, 1-8.
110. Arlamn, E. J.; Cossee, P. J. *J. Catal.* **1964**, *3*, 99-104.
111. Cossee, P. J. *J. Catal.* **1964**, *3*, 80-88.
112. Manyik, R. M.; Walker, W. E.; Wilson, T. P. *J. Catal.* **1977**, *47*, 197-209.
113. McGuinness, D. S. *Chem. Rev.* **2011**, *111*, 2321-2341.
114. Tomov, A. K.; Chirinos, J. J.; Jones, D. J.; Long, R. J.; Gibson, V. C. *J. Am. Chem. Soc.* **2005**, *127*, 10166-10167.
115. Peitz, S.; Aluri, B. R.; Peulecke, N.; Müller, B. H.; Wöhl, A.; Müller, W.; Al-Hazmi, M. H.; Mosa, F. M.; Rosenthal, U. *Chem. Eur. J.* **2010**, *16*, 7670-7676.
116. Gibson, V. C.; Mastroianni, S.; Newton, C.; Redshaw, C.; Solan, G. A.; White, A. J. P.; Williams, D. J. *J. Chem. Soc., Dalton Trans.* **2000**, 1969-1971.
117. Kermagoret, A.; Tomicki, F.; Braunstein, P. *Dalton Trans.* **2008**, 2945-2955.
118. Lindner, E.; Rauleder, H.; Hiller, W. *Z. Naturforsch., B: Chem. Sci.* **1983**, *38*, 417-425.
119. Hung-Low, F.; Renz, A.; Klausmeyer, K. K. *Eur. J. Inorg. Chem.* **2009**, 2994-3002.
120. Objartel, I.; Pott, N. A.; John, M.; Stalke, D. *Organometallics* **2010**, *29*, 5670-5675.
121. Liu, S.; Peloso, R.; Braunstein, P. *Dalton Trans.* **2010**, *39*, 2563-2572.
122. Klausmeyer, K. K.; Hung, F. *Acta Crystallogr. Sect. E: Struct. Rep. Online* **2006**, *E62*, M2415-M2416.
123. Heinemann, O.; Jolly, P. W.; Krüger, C.; Verhovnik, G. P. J. *J. Organomet. Chem.* **1998**, *553*, 477-479.
124. Thomas, B. J.; Noh, S. K.; Schulte, G. K.; Sendlinger, S. C.; Theopold, K. H. *J. Am. Chem. Soc.* **1991**, *113*, 893-902.
125. Thomas, B. J.; Theopold, K. H. *J. Am. Chem. Soc.* **1988**, *110*, 5902-5903.

for references, see page 132

126. Peitz, S.; Peulecke, N.; Müller, B. H.; Spannenberg, A.; Rosenthal, U. *Acta Crystallogr., Sect. E: Struct. Rep. Online* **2009**, *65*, M1574.
127. Kreisel, K. A.; Yap, G. P. A.; Theopold, K. H. *Inorg. Chem*. **2008**, *47*, 5293-5303.
128. Wei, P. R.; Stephan, D. W. *Organometallics* **2003**, *22*, 1712-1717.
129. Morse, D. B.; Rauchfuss, T. B.; Wilson, S. R. *J. Am. Chem. Soc.* **1990**, *112*, 1860-1864.
130. Kokko, E.; Lehmus, P.; Leino, R.; Luttikhedde, H. J. G.; Ekholm, P.; Näsman, J. H.; Seppälä, J. V. *Macromolecules* **2000**, *33*, 9200-9204.
131. Galland, G. B.; Quijada, R.; Rojas, R.; Bazan, G.; Komon, Z. J. A. *Macromolecules* **2002**, *35*, 339-345.
132. Bruker-Nonius, *Kappa CCD Reference Manual*, Nonius BV, The Netherlands, 1998.
133. Sheldrick, G. M. *SHELXL-97*; Program for crystal structure refinement; University of Göttingen: Germany, 1997.
134. Spek, A. L. *J. Appl. Crystallogr*. **2003**, *36*, 7-13.

for references, see page 132

CHAPITRE IX

General Conclusions

The search for new pre-catalysts that tolerate a variety of functional groups is far from being over. In our ongoing research on the coordination chemistry and catalytic behavior of metal complexes bearing heterotopic ligands, we have synthesized a series of N^O, N^N^N or N^N^O multidentate ligands, and their Ti(IV) complexes were obtained and structurally characterized. All the titanium complexes are catalytically active for ethylene polymerization, and the results indicated that the complexes bearing a tridentate ligand show higher thermal stability and prolonged catalytic live-times, while the complexes bearing bidentate ligands show better performances for copolymerization of ethylene with higher α-olefins. Our results also indicate that the structure of the ligands, including electronic and steric effects, as well as the catalytic conditions, such as activators, temperature, time, etc., affect the catalytic performances.

We synthesized a range of new Pd(II) complexes bearing bis(2-picolyl)phenylphosphine ($N_{py}PN_{py}$) ligand. The solid-state structures of the palladium compounds point out the versatility of the $N_{py}PN_{py}$ molecule, which can act as *N,P*-chelating ligand (in $[PdCl_2(N_{py}PN_{py}$-*N,P*)] and *cis*-$[Pd(N_{py}PN_{py}$-*N,P*)$_2](BF_4)_2$), *N,P,N-mer*-chelating ligand (in $[PdCl(N_{py}PN_{py}$-*N,P,N*)]PF_6 and $[Pd(N_{py}PN_{py}$-*N,P,N*)(NCMe)]$(PF_6)_2$), (*N,P*)-*N* bridging ligand (in $[Pd_2Cl_2(\mu$-$N_{py}PN_{py})_2](PF_6)_2$). On the basis of NMR experiments in DMSO-d_6, the hemilability of $N_{py}PN_{py}$ in $[PdCl_2(N_{py}PN_{py}$-*N,P*)] has been demonstrated, the two pyridine moieties being involved in a dynamic exchange in the coordination sphere of the metal. Dynamic processes in DMSO solution have also been observed for complex $[PdCl(N_{py}PN_{py}$-*N,P,N*)]PF_6 and an equilibrium between the species $[PdCl(N_{py}PN_{py}$-*N,P,N*)$]^+$ and $[PdCl(N_{py}PN_{py}$-*N,P*)(DMSO)$]^+$ has been inferred.

We also synthesized the Cr(III) complex *fac*-$[Cr(NPN)Cl_3]$ which represents a rare example of Cr-NPN system active for ethylene oligomerization in the presence of MAO as co-catalyst. Reaction of this complex with 1 equiv. of $TlPF_6$ unexpectedly afforded a novel Cr(III)/Tl(I) complex ion in which the unusual interactions involving the Tl^+ cation are of possible relevance to catalyst activation steps. The reactions between the Cr(III) complex *fac*-$[Cr(NPN)Cl_3]$ and several typical aluminum activators, such as MAO, $AlMe_3$, $AlEt_3$ and $EtAlCl_2$ have been carried out in order to gain a deeper insight into the nature of the active species possibly formed *in situ* during catalysis. The Cr alkyl complexes *fac*-$[Cr(NPN)Cl_{2.23}Me_{0.77}]$ and *fac*-$[Cr(NPN)Cl_2Et]$ and the cationic complexes $[\{$*fac*-$Cr(NPN)Me(\mu$-$Cl)\}_2][AlMe_xCl_{4-x}]_2$ and $[\{$*fac*-$Cr(NPN)\}_2(\mu$-$Cl)_3][AlCl_4]_3$ were isolated and crystallographically characterized. Our results illustrate the various functions exerted by different Al-based activators, which opens the possibility to better explain the diverse catalytic properties of a single pre-catalyst in the presence of different Al-based co-catalysts.